



IntechOpen

Alkenes

Edited by Reza Davarnejad and Baharak Sajjadi



ALKENES

Edited by **Reza Davarnejad**
and **Baharak Sajjadi**

Alkenes

<http://dx.doi.org/10.5772/65566>

Edited by Reza Davarnejad and Baharak Sajjadi

Contributors

Jaime Galvez, Marcos G. Alberti, Alejandro Enfedaque, Frederic Lefebvre, Yassine Bouhoute, Kai Szeto, Nicolas Merle, Aimery De Mallmann, Régis Gauvin, Mostafa Taoufik, Takeo Sasaki, Thies Thiemann, Fatima Merza, Ahmed Taha, Lyudmila Parfenova, Tatyana Tyumkina, Pavel Kovyazin, Leonard Khalilov, Usein Dzhemilev, Nina I. Kuznetsova, Lidia I. Kuznetsova, Bair S. Balzhinimaev, Olga A. Yakovina

© The Editor(s) and the Author(s) 2018

The moral rights of the and the author(s) have been asserted.

All rights to the book as a whole are reserved by INTECH. The book as a whole (compilation) cannot be reproduced, distributed or used for commercial or non-commercial purposes without INTECH's written permission.

Enquiries concerning the use of the book should be directed to INTECH rights and permissions department (permissions@intechopen.com).

Violations are liable to prosecution under the governing Copyright Law.



Individual chapters of this publication are distributed under the terms of the Creative Commons Attribution 3.0 Unported License which permits commercial use, distribution and reproduction of the individual chapters, provided the original author(s) and source publication are appropriately acknowledged. If so indicated, certain images may not be included under the Creative Commons license. In such cases users will need to obtain permission from the license holder to reproduce the material. More details and guidelines concerning content reuse and adaptation can be found at <http://www.intechopen.com/copyright-policy.html>.

Notice

Statements and opinions expressed in the chapters are those of the individual contributors and not necessarily those of the editors or publisher. No responsibility is accepted for the accuracy of information contained in the published chapters. The publisher assumes no responsibility for any damage or injury to persons or property arising out of the use of any materials, instructions, methods or ideas contained in the book.

First published in Croatia, 2018 by INTECH d.o.o.

eBook (PDF) Published by IN TECH d.o.o.

Place and year of publication of eBook (PDF): Rijeka, 2019.

IntechOpen is the global imprint of IN TECH d.o.o.

Printed in Croatia

Legal deposit, Croatia: National and University Library in Zagreb

Additional hard and PDF copies can be obtained from orders@intechopen.com

Alkenes

Edited by Reza Davarnejad and Baharak Sajjadi

p. cm.

Print ISBN 978-953-51-3766-5

Online ISBN 978-953-51-3767-2

eBook (PDF) ISBN 978-953-51-3982-9

We are IntechOpen, the first native scientific publisher of Open Access books

3,300+

Open access books available

107,000+

International authors and editors

113M+

Downloads

151

Countries delivered to

Our authors are among the
Top 1%

most cited scientists

12.2%

Contributors from top 500 universities



WEB OF SCIENCE™

Selection of our books indexed in the Book Citation Index
in Web of Science™ Core Collection (BKCI)

Interested in publishing with us?
Contact book.department@intechopen.com

Numbers displayed above are based on latest data collected.
For more information visit www.intechopen.com



Meet the editor



Dr. Reza Davarnejad was born in 1978 (Arak, Iran). He received his PhD degree from the Universiti Sains Malaysia (Penang, Malaysia) in 2010. He joined the Department of Chemical Engineering at the Arak University (Arak, Iran) as an assistant professor in 2010. His researches are presently being conducted on the environmental engineering (water and wastewater treatment) through advanced oxidation processes such as electro-Fenton and adsorption. He is a consultant of some industries (local and international ones) as well. He currently has more than 80 publications and research activities. Furthermore, he has been as deputy (educational & research) of Mahallat Institute of Higher Education (Mahallat, Iran) since 2017. At present, he is an associate professor in Chemical Engineering at the Arak University.



Dr. Baharak Sajjadi was born in Iran in 1984. She graduated in Chemical Engineering in 2008 from the Arak University (Iran) and received her master degree, ranked as the first-best student in 2010, from the same university. She completed her PhD degree in the area of biochemical processing in 2015 from the University of Malaya. Her other interests include computational fluid dynamic (CFD) simulation, energy and environment, bioenergy and biofuels and Sono-Physics. Till date, she has published more than 40 papers in high-impact research journals. She joined the University of Mississippi in the United States in early 2017 as a postdoctoral researcher and is currently a research assistant professor working on transformational solar chemical looping and photo-ultrasonic renewable biomass refinery.

Contents

Preface XI

Section 1 Alkene Synthesis 1

- Chapter 1 **Tandem-, Domino- and One-Pot Reactions Involving Wittig- and Horner-Wadsworth-Emmons Olefination 3**
Fatima Merza, Ahmed Taha and Thies Thiemann

Section 2 Alkene Functionalization 41

- Chapter 2 **Alkene and Olefin Functionalization by Organoaluminum Compounds, Catalyzed with Zirconocenes: Mechanisms and Prospects 43**
Lyudmila V. Parfenova, Pavel V. Kovyazin, Tatyana V. Tyumkina, Leonard M. Khalilov and Usein M. Dzhemilev

Section 3 Alkene Metathesis 65

- Chapter 3 **Olefin Metathesis by Group VI (Mo, W) Metal Compounds 67**
Frédéric Lefebvre, Yassine Bouhoute, Kai C. Szeto, Nicolas Merle, Aimery de Mallmann, Régis Gauvin and Mostafa Taoufik

Section 4 Oxidation of the Simplest Conjugated Diolefin 97

- Chapter 4 **Reactivity of a Simplest Conjugated Diolefin in Liquid-Phase Oxidation: Mechanisms and Products 99**
Nina I. Kuznetsova, Lidia I. Kuznetsova, Olga A. Yakovina and Bair S. Bal'zhinimaev

Section 5 Polyolefins 119

Chapter 5 **Poly(olefin sulfone)s 121**

Takeo Sasaki, Khoa Van Le and Yumiko Naka

Chapter 6 **Polyolefin Fibres for the Reinforcement of Concrete 145**

Marcos G. Alberti, Alejandro Enfedaque and Jaime C. Gálvez

Preface

Ethylene, the first stable member of the alpha- or 1-*olefin* family, was discovered in 1795 by four Dutch chemists: Deimann, Van Troostwick, Bondt, and Louwrenburgh. Since that time, ethylene was known as olefin gas. Other *olefins*, including propylene, isobutylene, and pentene, were gradually discovered and studied in the nineteenth century. Because C_2H_4 had one hydrogen less than C_2H_5 ethyl, the Greek suffix of “ene” was added to its sequel in the mid-nineteenth century, and olefin gas was known as ethylene till 1852. In 1866, German chemist, Huffman, established the hydrocarbon naming systems based on alkanes. In this system, each hydrocarbon with two hydrogen atoms less than the corresponding alkanes was named as “**Alkene.**”

About a century after the discovery of ethylene, alkenes, which are known as olefins too, gained attention. However, alkenes’ markets rose significantly when the polyolefins (polyalkenes) were developed after World War II. Today, more than 200 years after the discovery of ethylene, alkenes are used as intermediates and feedstock for manufacturing many industrial chemicals in large quantities, and polyolefin is the world’s most widely used synthetic polymer. The global market for alpha-alkene is expected to reach USD 12.58 billion by 2025. The drivers for this market are the increasing demand for fuels, plastics, lubricants, and oilfield chemicals, as well as the recent discoveries of shale gas. In addition, the other driving force of this market is the growing applications of polyalpha-alkene-based lubricants as these compounds possess highly desirable characteristics such as high thermal stability, viscosity index, oxidative stability, low toxicity, and compatibility with mineral oils to the final product.

Due to the increasing quantity of alkenes produced worldwide and *the importance of these compounds* in the industry, it is therefore essential to have broadened knowledge on the technology of alkene production and consumption and its corresponding reactions. These and the most recent advances in synthetic aspects of alkenes are covered in the current book *Alkenes*. Emphasis is given to synthesis process, the efficient new catalysts for synthesis, reactions, and the most recent applications of alkenes. Furthermore, new developments in metathesis of alkenes (“metathesis” means “changes of position” in Greek) are covered. There are many other textbooks on the basic concepts related to alkenes or alkene-corresponded issues. We have omitted those repeating concepts and have just focused on the most recent advances; however, those aspects that are required to understand each chapter have been extensively explained. The book *Alkenes* includes five main chapters. The first chapter focuses on alkene synthesis through Wittig reaction, which allows the preparation of an alkene by the reaction of an aldehyde or a ketone. The second chapter covers the functionalization of alkenes by organoaluminum compounds with particular focus on modern concepts of the alkene hydro-, carbo-, and cycloaluminum mechanisms. The third chapter explains the alkene metathesis that entails the redistribution of fragments of alkenes. Analy-

sis of various routes of oxidation of the simplest conjugated diolefin, 1,3-butadiene (BD), is the main objective of the fourth chapter, followed by the *polyolefins* in the fifth chapter. In this last chapter, two different types of polyolefins are considered, polyolefin fibers and polyolefin sulfone, along with their applications in photodegradable plastics and reinforcement of concrete, respectively. We hope that *Alkenes* will benefit the readers.

Dr. Reza Davarnejad

Associate Professor of Chemical Engineering Department,
Arak University,
Arak, Iran

Baharak Sajjadi

Research Assistant Professor,
Department of Chemical Engineering,
University of Mississippi, U.S.A

Alkene Synthesis

Tandem-, Domino- and One-Pot Reactions Involving Wittig- and Horner-Wadsworth-Emmons Olefination

Fatima Merza, Ahmed Taha and Thies Thiemann

Additional information is available at the end of the chapter

<http://dx.doi.org/10.5772/intechopen.70364>

Abstract

The Wittig olefination utilizing phosphoranes and the related Horner-Wadsworth-Emmons (HWE) reaction using phosphonates transform aldehydes and ketones into substituted alkenes. Because of the versatility of the reactions and the compatibility of many functional groups towards the transformations, both Wittig olefination and HWE reactions are a mainstay in the arsenal of organic synthesis. Here, an overview is given on Wittig- and Horner-Wadsworth-Emmons (HWE) reactions run in combination with other transformations in one-pot procedures. The focus lies on one-pot oxidation Wittig/HWE protocols, Wittig/HWE olefinations run in concert with metal catalyzed cross-coupling reactions, Domino Wittig/HWE—cycloaddition and Wittig-Michael transformations.

Keywords: Wittig olefination, one-pot reactions, Domino reactions, tandem reactions, Horner-Wadsworth-Emmons olefination

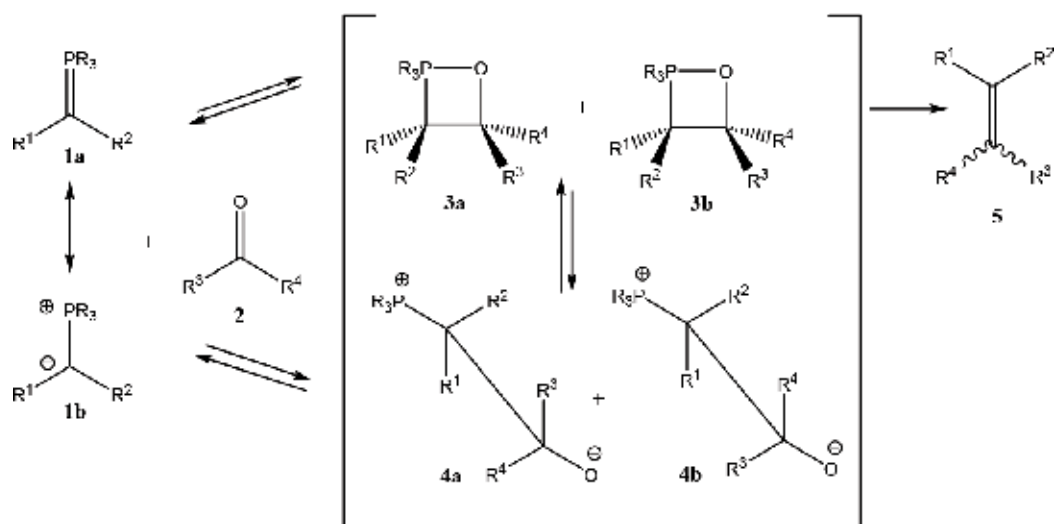
1. Introduction

The Wittig olefination utilizing phosphoranes and the related Horner-Wadsworth-Emmons (HWE) reaction using phosphonates transform aldehydes and ketones into substituted alkenes. Because of the versatility of the reactions and the compatibility of many functional groups in the transformations, both Wittig olefination and HWE reactions are a mainstay in the arsenal of organic synthesis. The mechanism of the Wittig olefination has been the subject of intense debate [1]. While initially it was supposed that all Wittig olefination reactions lead via 1,2-addition to betaine structures **4** as zwitterionic intermediates that would form oxaphosphetane **3** with a final release of alkene and phosphine oxide by ring opening (*syn*-cycloreversion process), it has been seen more recently that especially under salt-free, aprotic conditions, many ylides undergo

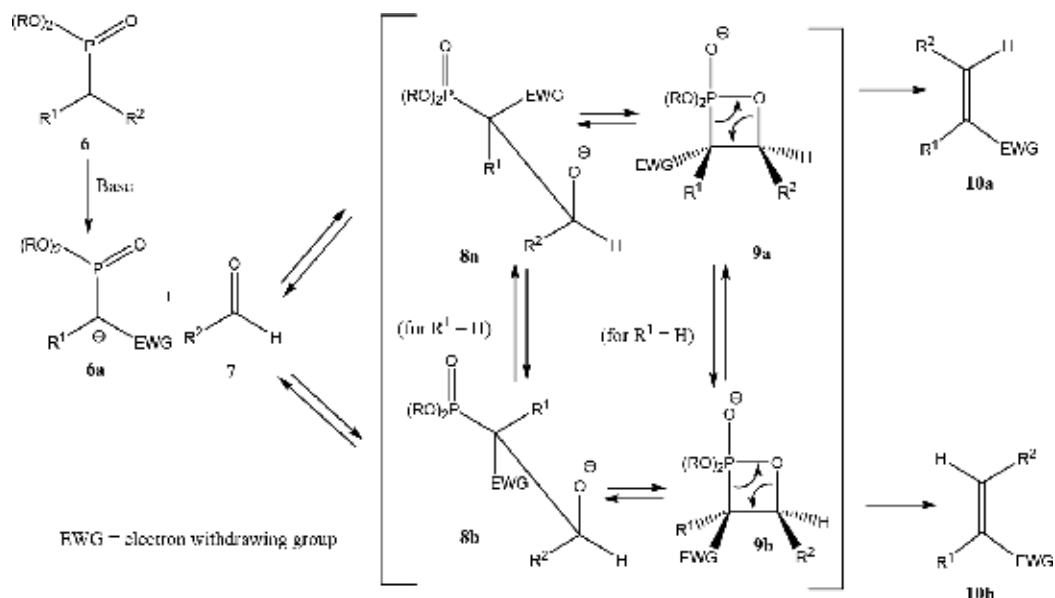
a π^2s/π^2a [2+2]-cycloaddition with the carbonyl component leading to the oxaphosphetane **3** directly [2], which in certain cases can be in equilibrium with betaine structures **4** (**Scheme 1**). In HWE reactions, the deprotonated phosphonate **6a** undergoes a nucleophilic addition to the carbonyl compound (e.g., **7**), which usually is the rate limiting step [3]. The elimination to the final products proceeds through oxaphosphetane **9** (**Scheme 2**). The Wittig olefination has been used industrially in the synthesis of terpenoids [4]. Recently, a one-pot synthesis of the vasodilator and anti-platelet agent Beraprost sodium, a prostacyclin analog, was communicated with the HWE reaction as the key transformation with the idea of using the approach in an industrial synthesis of the pharmaceutical [5].

For years after the discovery of the Wittig olefination [6, 7], most Wittig transformations were carried out under inert atmosphere using dry solvents such as THF [8], DME [9], diethyl ether [10] and benzene [11]. Later it was realized that stabilized and semi-stabilized Wittig reagents can be reacted in non-de-aerated solvents, where the solvents need not be dried specifically. Most of these conjugated Wittig reagents are thermally stable and tolerate water, air and mild oxidants, while maintaining reactivity towards aldehydes and often also towards ketones. This allows for a plethora of reaction conditions for many Wittig olefination reactions such as obviating solvents altogether [12, 13] or running the reactions in aqueous solutions [14, 15] or in mixed solvents [16]. Also, it permits one-pot transformations of Wittig olefinations in combination with other reactions, also because the stabilized and to some extent the semi-stabilized phosphoranes are inert to mild oxidizing and reducing agents. However, also with non-stabilized phosphoranes, where reactions have to be performed under the exclusion of air and moisture, Wittig reactions can be performed in conjunction with further transformations [17].

This chapter is to give an insight into the types of transformations that can be combined with Wittig- and Horner-Wadsworth-Emmons olefinations in Domino-, tandem and one-pot



Scheme 1. Schematic presentation of the reaction mechanism of the Wittig olefination.



Scheme 2. General reaction mechanism of the HWE reaction.

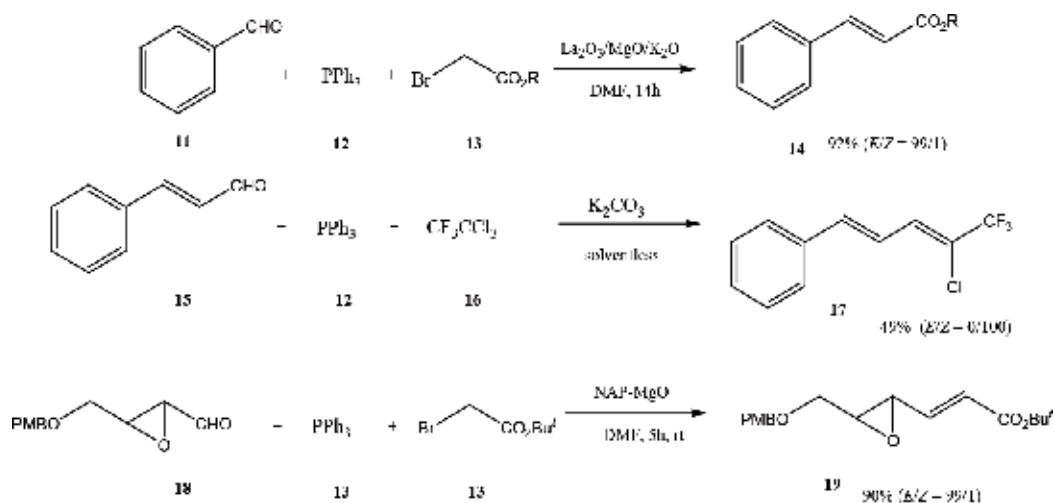
reaction strategies. These include the preparation of phosphoranes and their reaction *in situ*, one-pot oxidation of alcohols to aldehydes and Wittig-olefination, *in situ*-recycling of phosphine oxides and catalytic Wittig reactions, one-pot Wittig-olefination metal catalyzed C–C bond forming reactions such as Suzuki-Miyaura, Sonogashira- and Heck reactions, Wittig and Horner-Emmons reactions in combination with polar cyclizations, Wittig-reactions carried out in combination with electrocyclic reactions, one-pot Wittig and Horner Emmons-addition reactions; cascade reactions featuring (triphenylphosphoranylidene)-ethenone and similar phosphoranes.

2. Wittig and Horner-Wadsworth-Emmons (HWE) olefination reactions with phosphoranes and phosphonates prepared *in situ*

Primarily, phosphoranes as Wittig reagents are prepared by the reaction of a triarylphosphine, usually triphenylphosphine, or, more seldom, a trialkylphosphine, and an alkyl halide with subsequent dehydrohalogenation of the triaryl(alkyl)alkylphosphonium halide produced. Non-stabilized Wittig reagents are not stable enough to be stored over longer periods of time; therefore, it is the norm that the Wittig-ylide is formed *in situ* from the oftentimes stable phosphonium salt, usually with a strong base, and then reacted directly with the carbonyl compound. In the case of stabilized phosphoranes, they are often stable enough to store, and the dehydrohalogenation necessitates only a weak base such as sodium carbonate or even sodium bicarbonate [18]. Nevertheless, this likewise allows the preparation of the phosphorane and the subsequent Wittig olefination in one pot [19], where even protic solvents can be used, such

as water. Similarly, semi-stabilized phosphoranes can be obtained *in situ* from their respective phosphonium salts, also even in aqueous medium, where LiCl promotes the Wittig olefination and suppresses the decomposition of the phosphoranes [14, 15]. Furthermore, all the catalytic Wittig reactions (see below) rely on the fact that the phosphorane is produced *in situ*.

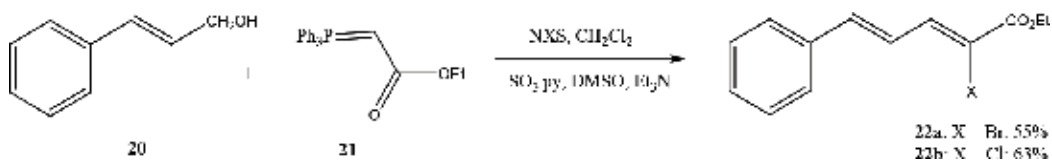
Perhaps more interesting is the one-pot reaction of an alkyl halide, a phosphine and a carbonyl compound (**Scheme 3**). This can be achieved by consecutive addition of the components, when one or more of the components are sensitive, or by mixing of all components simultaneously. A consecutive addition of components in one pot was pursued by McNulty and Das who reacted air-sensitive triethylphosphine with benzyl bromides to the respective benzyltriethylphosphonium bromides, which were transformed to the phosphoranes with aq. NaOH, before being reacted with benzaldehydes to give (*E*)-stilbenes in an aqueous Wittig olefination [20]. Here, the triethylphosphine oxide by-product is water soluble. This reaction procedure has been diversified further by a one-pot preparation of benzyltriethylphosphonium bromides from the air-stable triethylphosphine hydrobromide and benzyl alcohols and subsequent Wittig olefination with aromatic aldehydes in aqueous medium [21]. Simultaneous mixing of alkyl halide such as α -haloesters (e.g., **13**), α -halonitriles, α -halocarbonyl compounds and α -alkyl- α -halocarbonyl compounds, triphenylphosphine (**12**), and carbonyl compound (e.g., **11**, **15**, **18**) in the presence either of a base [17, 22–26] or an alkene [27] was shown to give α,β -unsaturated esters [17, 22–27] (e.g., **14**, **17**, **19**), α,β -unsaturated nitriles [23, 26] and enones [27], respectively (**Scheme 3**). Epoxides are stable under these reaction conditions as can be seen in the transformation of **18** to **19** (**Scheme 1**). A one-pot, fluoride catalyzed Wittig-olefination has also been devised, where ethyl bromoacetate is reacted with carbaldehydes in the presence of tri-*n*-butylphosphine and tetrabutylammonium fluoride (Bu_4NF) to give (*E*)-configured α,β -unsaturated esters in good yield [28]. The synthesis of α,β -unsaturated esters has also been achieved from their alkyl halide and aldehyde constituents using tributylarsine [29] or a substituted triarylsarsine instead of triphenylphosphine [30]. The use of tributylarsine in the presence triphenyl phosphite [29] led to the creation of a catalytic system which was



Scheme 3. *In situ* preparation of phosphoranes and subsequent Wittig olefination.

developed further with one-pot transformations that were managed with catalytic amounts (2 mol%) of poly(ethylene glycol) and (PEG)-supported tellurides in the presence of K_2CO_3 as base [31–34]. Also, micellar reaction systems such as micellar solutions of sodium dodecyl sulfate (SDS) in water have been used, in which Wittig olefinations were carried out between aldehydes and phosphoranes, synthesized *in situ* [35, 36]. A. Galante has performed Wittig reactions in the fluorous phase with *in situ* pre-formed perfluorinated ylides [37].

Traditionally, stabilized halophosphoranes have been prepared by the halogenation of the nonhalogenated parent phosphoranes and a subsequent dehydrohalogenation of the halogenated phosphonium salt obtained. Karama et al. have combined this *in situ* halogenation: dehydrohalogenation step with the Wittig reaction itself. Additionally, an *in situ* alcohol oxidation to provide the aldehyde starting material was integrated into many of these reaction sequences (**Scheme 4**) [38–42].

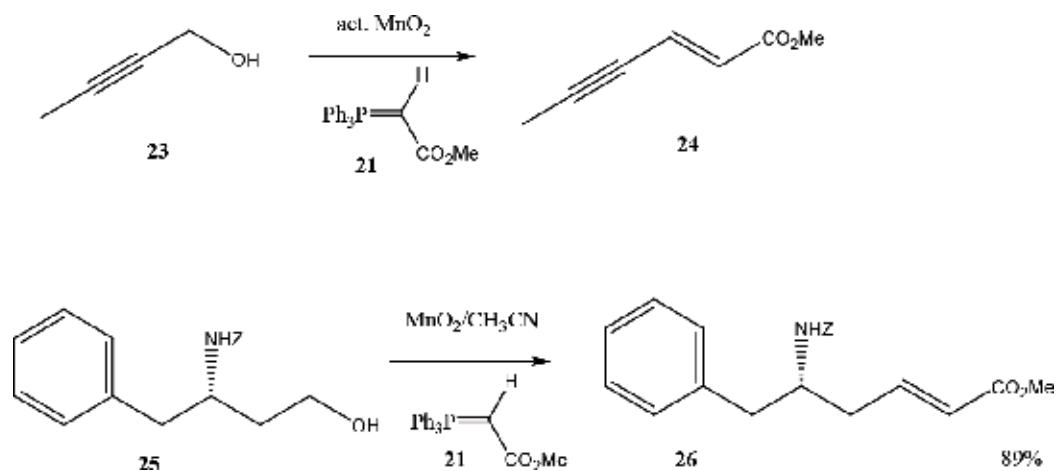
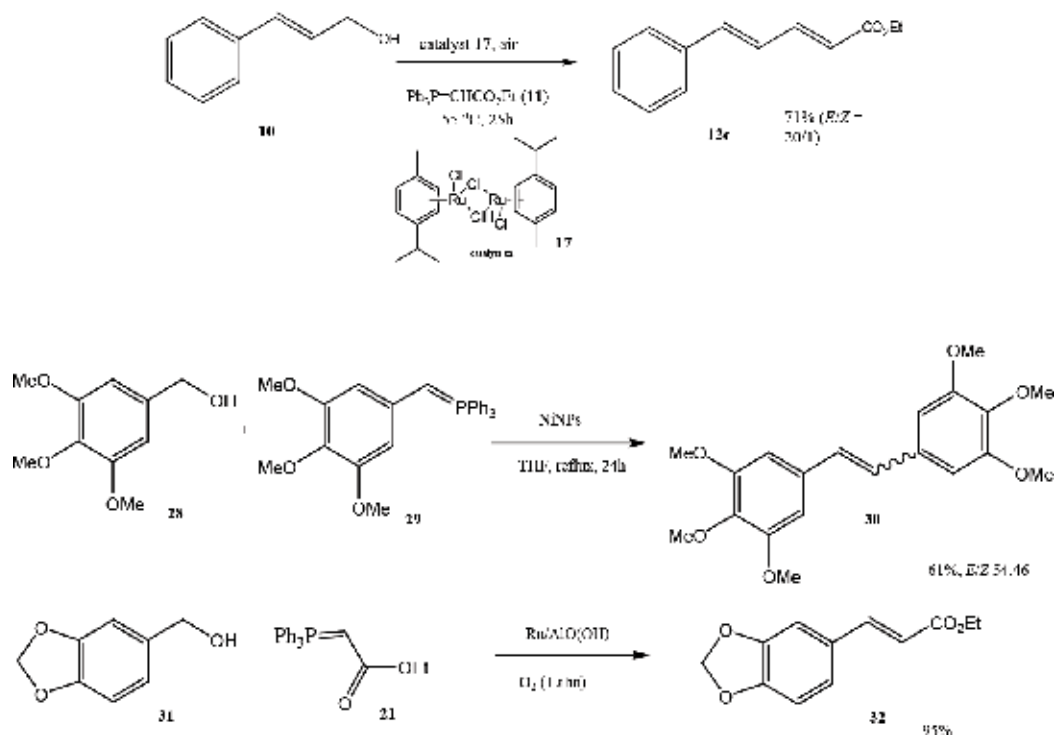


Scheme 4. One-pot oxidation, halogenation, and Wittig reaction to 2-haloacrylates.

3. *In situ* alcohol oxidation – Wittig/HWE reactions; other *in situ* aldehyde preparations run with subsequent Wittig/HWE sequences in one pot

The tolerance of stabilized phosphoranes towards mild oxidants allows for the oxidation of an alcohol to an aldehyde and its Wittig reaction in one-pot (**Schemes 5** and **6**). As oxidants, activated MnO_2 [43–46], barium permanganate [47, 48], tetra-*n*-propylammonium perruthenate (TPAP)/*N*-methylmorpholine *N*-oxide (NMO) [49–54] and TPAP/*N,N,N',N'*-tetramethylethylenediamine dioxide (TMEDA O_2) [55], *o*-iodoxybenzoic acid (IBX) [56–58], Dess-Martin periodinane [59–61], DMSO-oxalyl chloride (Swern conditions) [62–64], DMSO- SO_3 -pyridine (Parikh-Doering oxidation) [38, 39] or DMSO- SO_3 -triethylamine [65], pyridinium chlorochromate (PCC) or PCC/celite [66–69] as well as pyridinium dichromate (PDC) [70] such as PDC encapsulated in sol gel [71] have been used. In addition, metal catalyzed aerobic oxidation reactions of aldehydes with concomitant olefination reactions are known, where [(*eta-p*-cymene) $RuCl_2$] $_2$ (27) [72], nanoparticulate ruthenium supported on highly porous aluminum oxyhydroxide [73] or on silica gel [74], and nickel nanoparticles [75, 76] (**Scheme 6**) have been used as catalyst in the case of a concomitant Wittig reaction and gold/palladium bimetallic nanoparticles in the case of a concomitant Horner-Wadsworth-Emmons (HWE) reaction [77], Cu(I)-phenanthroline as a catalyst in an oxidation: HWE: sequential procedure [78].

Taylor et al. give a good overview of the tandem oxidation-Wittig processes developed until 2005, focusing especially on the tandem oxidation process (TOP) developed by his group [43–46],

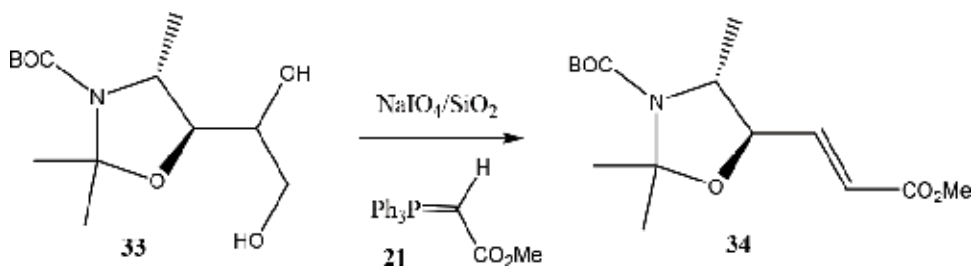
Scheme 5. One-pot MnO_2 -mediated oxidation—Wittig olefination.

Scheme 6. One-pot metal catalyzed oxidation of alcohols utilizing oxygen—Wittig reaction.

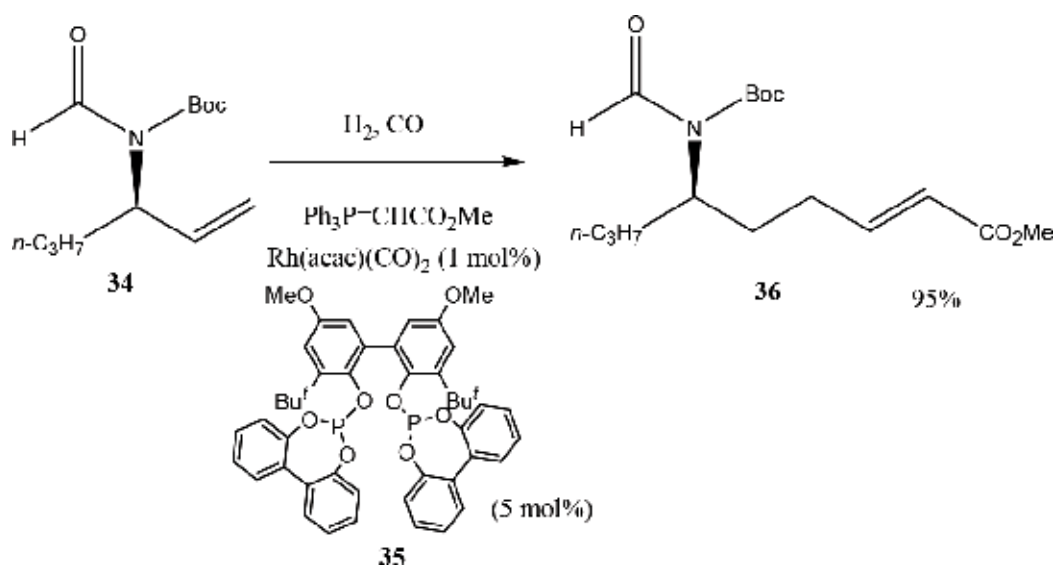
using activated MnO_2 [79]. Over the years, this process has been used more often [40, 80–97] than the other processes shown above. Recently, also MnO_2 derived molecular sieve material such as OMS-2 [$\text{KMn}^{4+}\text{Mn}^{3+}\text{O}_{16} \cdot n\text{H}_2\text{O}$] has been used with success in aerobic, catalytic one-pot oxidation Wittig reactions of benzylic and allylic alcohols to the respective cinnamates [98]. Overall, the

Wittig transformations of the aldehydes produced *in situ* allows for the manipulation of aldehydes that are inherently instable such as of silyl substituted aldehydes, propargyl aldehyde [97], and chiral γ -aminoaldehydes, the latter without loss of stereochemical integrity (**Scheme 5**) [89]. In the case of Wittig transformations of chiral α -aminoaldehydes, β -aminoalcohols were oxidized to α -aminoaldehydes with NaOCl in the presence of AcNH-TEMPO, where the crude α -aminoaldehydes gained from the oxidation were subjected directly to olefination to give Wittig products without loss of stereochemical integrity [99–101].

Other preparation methods of aldehydes in conjunction with Wittig olefinations or HWE reactions have been reported. Thus, an oxidative cleavage of a glycol can be carried out in combination with a subsequent Wittig-olefination [102–105] (**Scheme 7**). Also a one-pot carboxylic acid to aldehyde reduction and Wittig reaction is known [106]. Finally, a Domino hydroformylation/Wittig olefination procedure has been developed, starting from allylamines (**Scheme 8**). The aldehyde is not isolated [107]. Domino/hydroformylation/Wittig olefination protocols have been introduced with other olefinic starting materials, also [108–110].



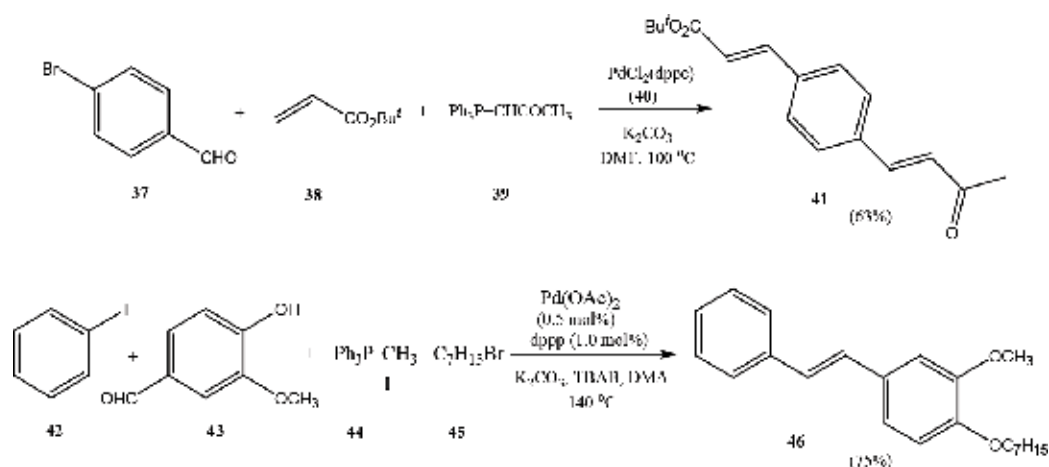
Scheme 7. Oxidative glycol cleavage—Wittig reaction.



Scheme 8. Hydroformylation—Wittig reaction.

4. Wittig- and HWE reactions and C–C-coupling reactions in one-pot procedures

Wittig- and Horner-Wadsworth-Emmons reactions can be combined with C–C-coupling reactions such as Suzuki cross-coupling [111–113], Mizoroki-Heck reaction [113–118] and Sonogashira-reaction [119]. Initially, it was observed that conjugated phosphoranes were stable under reaction conditions used for Heck- or Suzuki reactions (**Scheme 9**). Thus, phosphoranes themselves could be functionalized by Suzuki- [120], Mizoroki-Heck- [121], or Sonogashira-type [119] cross-coupling reactions, either in solution or when polymer-bound [122]. These phosphoranes could then be subjected to normal Wittig-olefination reactions with ketones or aldehydes [120–122]. The one-pot Wittig-Heck-reaction strategy can be extended to include an *O*-alkylation, where the Wittig reaction of a *p*-hydroxybenzaldehyde (**43**) with methylenetriphenylphosphorane, obtained *in situ* from phosphonium salt **44** provides the *p*-hydroxystyrene as the olefin component in the Mizoroki-Heck reaction in the presence of an alkyl bromide (e.g., **45**), which *O*-alkylates the phenoxy-function to give alkoxy stilbenes **46** (**Scheme 9**) [123].

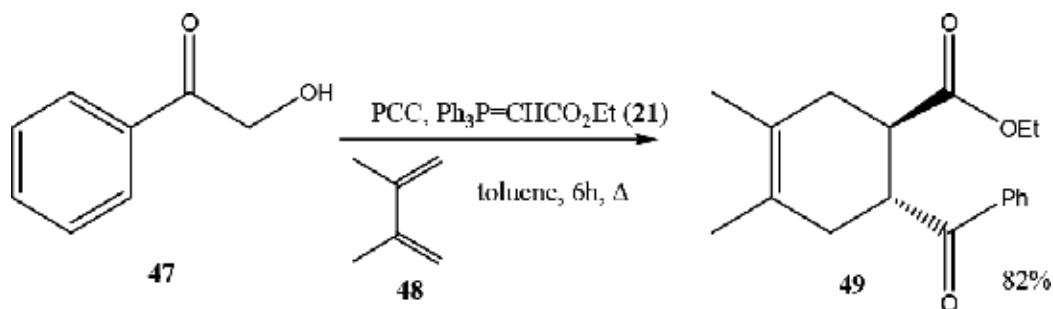


Scheme 9. One-pot Heck cross-coupling/Wittig reaction.

5. One-pot Wittig- and HWE olefination/cycloaddition reaction

One can easily visualize that an alkene prepared by a Wittig olefination can easily be used as a 2-pi component in cycloaddition reactions, in one pot (**Scheme 10**). A typical such cycloaddition is [4+2]-cycloaddition, such as the classical Diels Alder reaction, which can be performed both inter-[69, 124] and intramolecularly [125–132] in tandem with a Wittig-reaction.

Hilt and Hengst have published a cobalt(I)-catalyzed Diels Alder reaction of alkylnyltriphenylphosphonium and 1,3-dienes with a consecutive Wittig reaction of the cycloadduct with

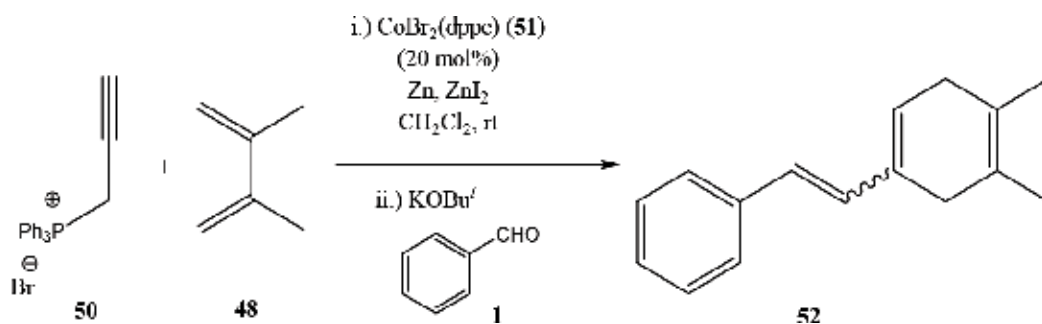


Scheme 10. Oxidation—Wittig-olefination—Diels-Alder reaction sequence.

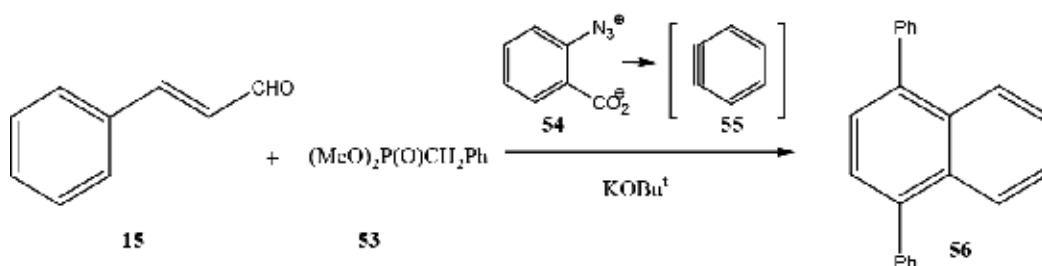
various aldehydes in one pot that lead after a further dehydrogenative step to substituted stilbenes and styrenes (Scheme 11) [133].

Interesting is the cycloaddition of *in situ* produced benzyne (55) to 1,4-diphenylbutadiene, prepared *in situ* by HWE reaction from cinnamaldehyde, (15) give 1,4-diphenylnaphthalene (56) (Scheme 12) [134].

The transformation sequence Diels-Alder/Wittig can be part of a more complex reaction chain. Thus, Ramachary and Barbas III [135] have forwarded a Domino Wittig/Knoevenagel/



Scheme 11. Cobalt (I)-catalyzed Diels Alder reaction—Wittig reaction.

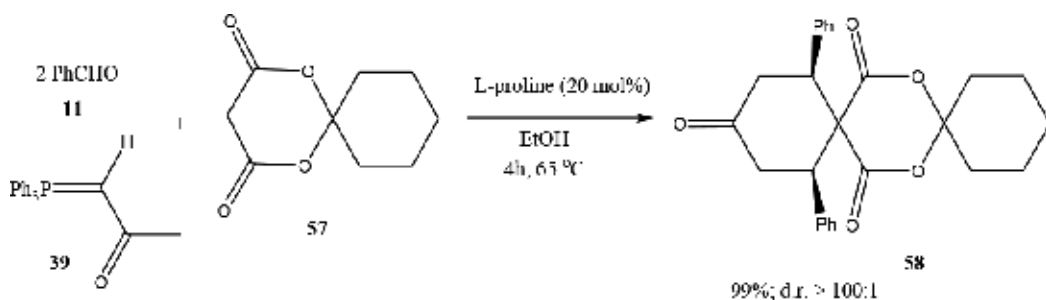


Scheme 12. One-pot HWE reaction—cycloaddition of *in situ* produced benzyne.

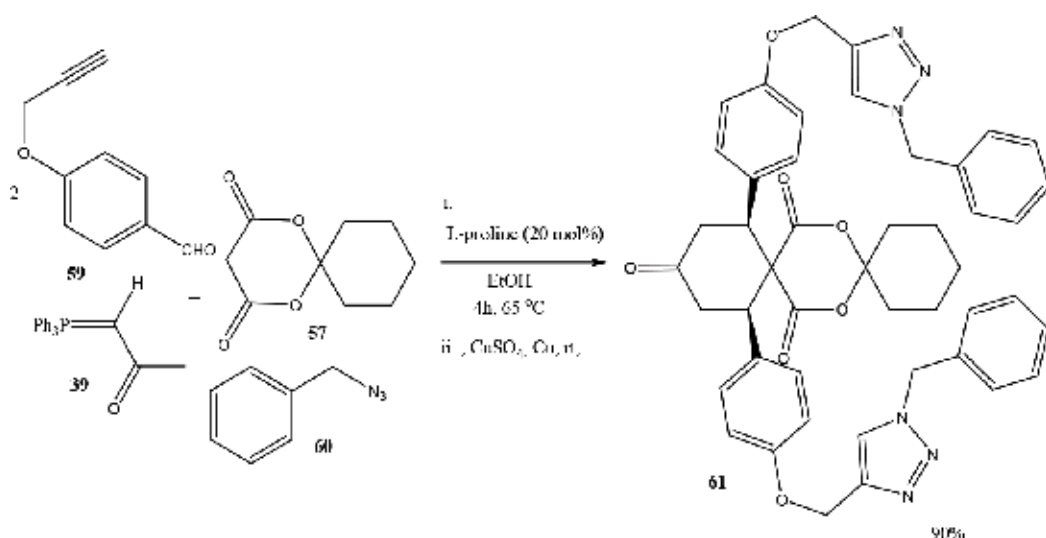
Diels-Alder sequence to spirotriones **58** (**Scheme 13**) and a Wittig/Knoevenagel/Diels-Alder/Huisgen cycloaddition sequence to polysubstituted triazoles **61** (**Scheme 14**).

Oxidation of benzyl alcohols to benzaldehydes can be incorporated into a Wittig-Diels Alder sequence [69]. Also, hetero-Diels-Alder reactions can be run in tandem with a Wittig olefination as shown by Ramachary et al. in their synthesis of tetrahydropyrans **64** (**Scheme 15**) [136]. Here, diamine **63** is used as a catalyst. The reaction, however, gives the product only in low enantiomeric excess (**Scheme 15**).

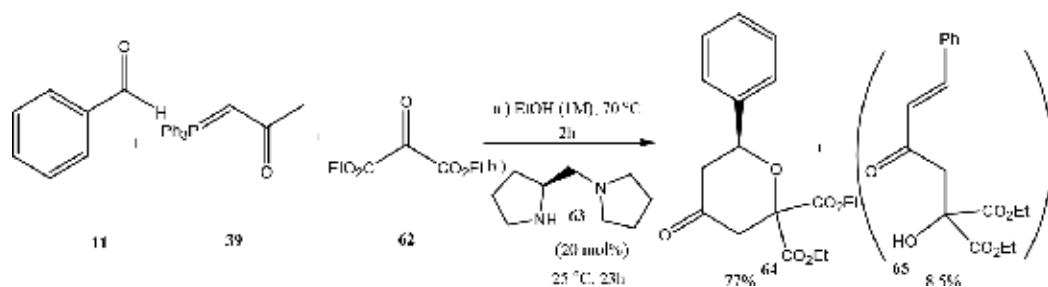
Huisgen type [3+2]-cycloaddition reactions can be run also in a simple tandem process rather than incorporated in a more complex reaction chain (see above). A typical example is shown in **Scheme 16**, where azidoethyl-tetrahydro-hydroxyfuran **66** is treated with phosphorane **21** to give triazoline **68** alongside diazoamine **69** [137]. Further such approaches are known [138, 139].



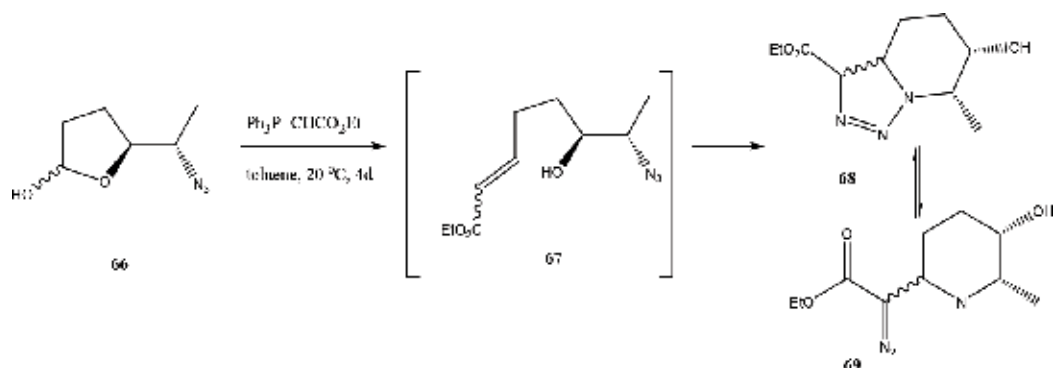
Scheme 13. Domino Wittig/Knoevenagel/Diels-Alder sequence.



Scheme 14. Wittig/Knoevenagel/Diels-Alder/Huisgen cycloaddition sequence.



Scheme 15. Wittig-reaction/hetero-Diels Alder reaction.

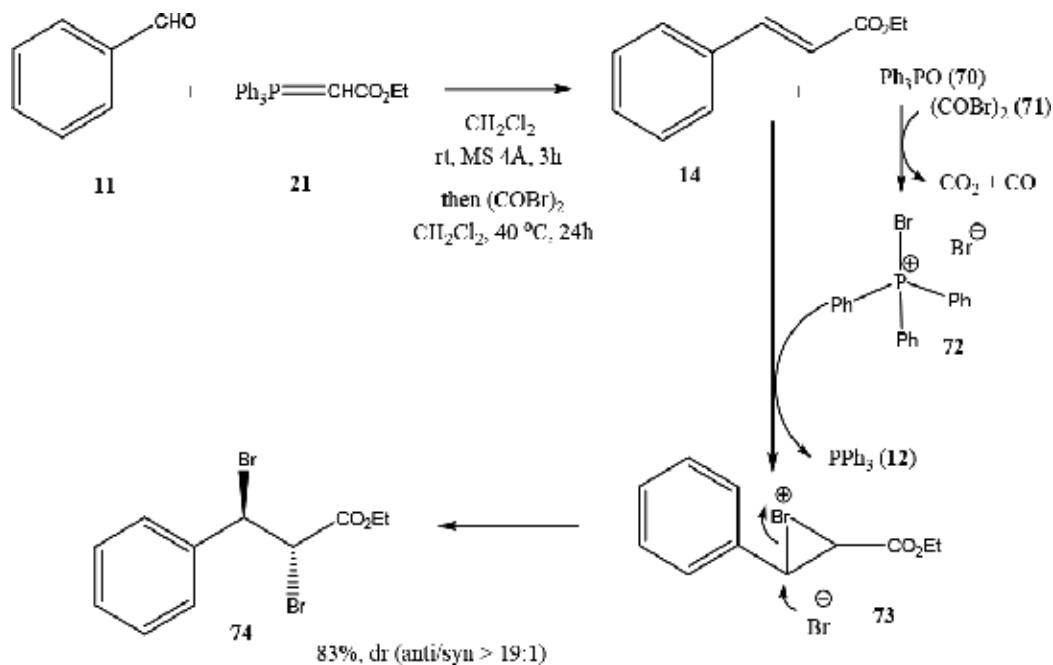
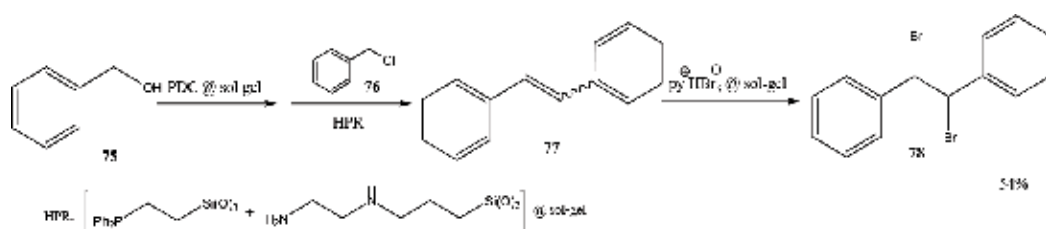


Scheme 16. Wittig reaction—intramolecular Huisgen type [3+2]-cycloaddition.

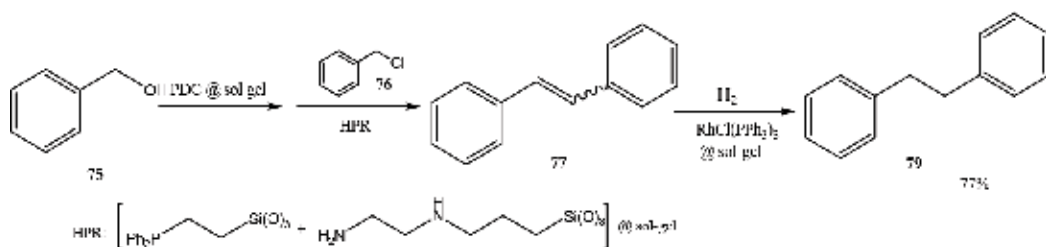
6. One-pot Wittig- and HWE olefination/addition reaction

Electrophiles can be added to the alkene function obtained, in a one-pot reaction with the Wittig olefination. A typical example is the stereoselective bromination of the Wittig product with oxalyl bromide (71), where triphenylphosphine oxide (70) as side product of the olefination step acts as a catalyst in the bromination (**Scheme 17**) [140]. Hamza and Blum have developed a sol-gel entrapped tertiary phosphine by co-polycondensation of tetramethoxysilane, 2-diphenyl(phosphino)ethyltri(ethoxy)silane and *N*-2-(aminoethyl)-3-aminopropyltri(methoxy)silane. This could be reacted in a Wittig type olefination with benzyl chlorides (e.g., 76) and benzaldehydes, prepared *in situ* from benzyl alcohols (e.g., 75). The strategy allows for the combination of the process with a bromination step in one pot by addition of sol-gel-bound pyridinium hydrobromide perbromide after completion of the Wittig reaction (**Scheme 18**) [71].

Alternatively, the process can be combined with a hydrogenation step by the addition of hydrogen in the presence of an added heterogenized Wilkinson catalyst (**Scheme 19**) [141]. A further Wittig olefination—hydrogenation sequence was developed by Zhou et al. who obtained α -CF₃- γ -ketoesters 82 by adding trichlorosilane to the reaction mixture where triphenylphosphine oxide (again as side product of the Wittig olefination) acts as a Lewis base and activates the silane as hydrogenating agent (**Scheme 20**) [142]. The routine was expanded to other aldehydes including alkanals as educts [143]. This reaction was also carried out with

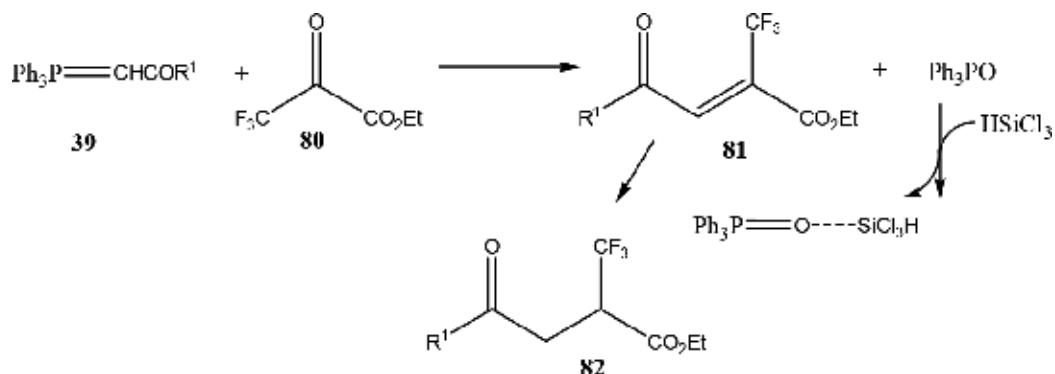
Scheme 17. Wittig olefination— Ph_3PO -catalyzed addition of bromine.

Scheme 18. Wittig olefination—addition of bromine.

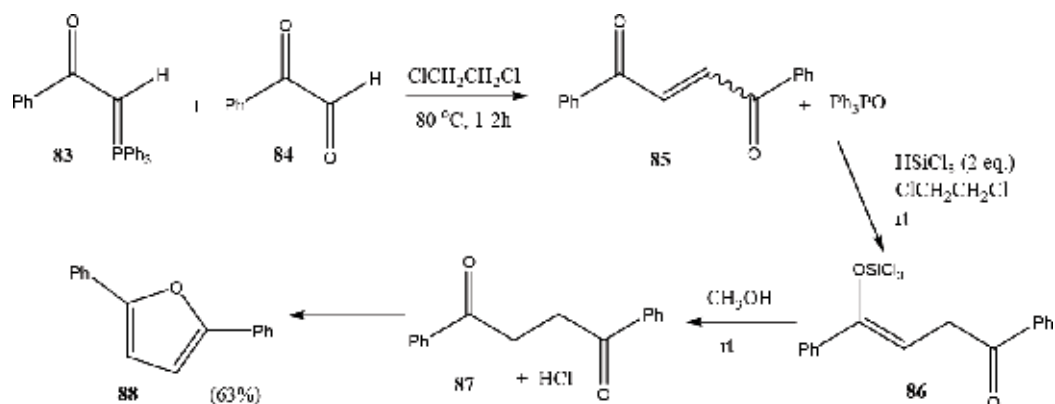


Scheme 19. Wittig olefination—hydrogenation.

glyoxal derivatives **84** as starting materials, where after conjugate addition of trichlorosilane a few drops of methanol were added to the solution resulting in conversion of the trichlorosilylenol ether (**86**) to the keto compound **87** while at the same time generating HCl, which then promoted a Paal-Knorr reaction of **87** to the furan **88** (Scheme 21) [144].



Scheme 20. Wittig reaction—triphenylphosphine oxide catalyzed hydrogenation.

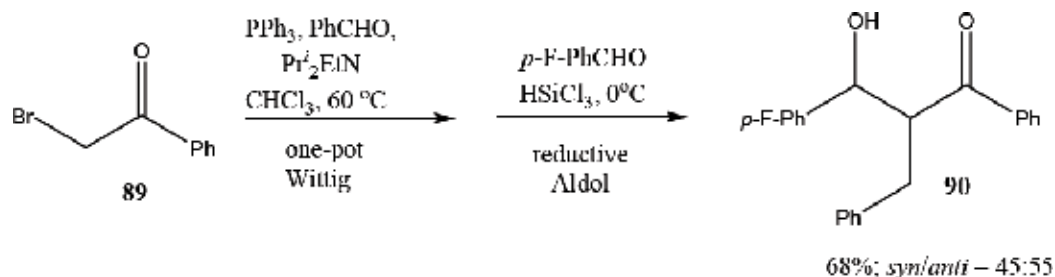


Scheme 21. Furan synthesis by one-pot Wittig olefination—hydrogenation—Paal-Knorr reaction.

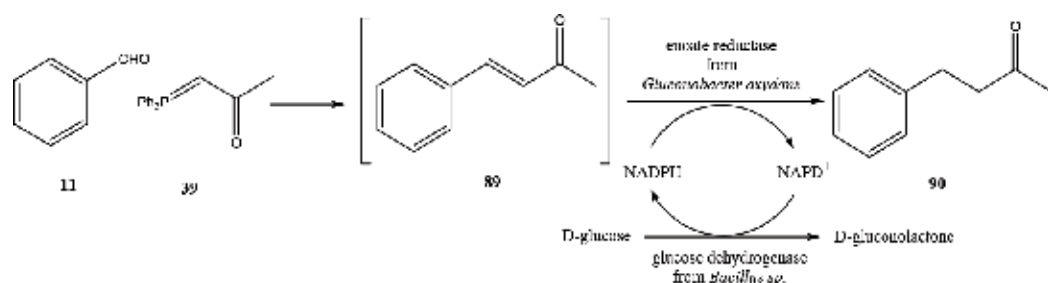
Lu and Toy showed that the Wittig-olefination—trichloromethylsilane conjugate addition sequence can be coupled with the initial preparation of the phosphorane in one pot [145]. The conjugate addition to furnish the silyl enol ether can be combined with a reductive Aldol reaction, where for the Wittig reaction and for the reductive Aldol reaction two separate aldehydes can be used (**Scheme 22**) [145]. The reactions above can be run with a triarylphosphine-tertiary amine bifunctional polymeric reagent (Rasta-Resin- $\text{PPh}_3\text{-NBn}^i\text{Pr}_2$), where the polymer bound triarylphosphine oxide also exerts a catalyzing effect on the addition of Cl_3SiH while making it possible to recycle the polymer [146].

As many Wittig olefinations can be performed in aqueous medium, it is possible to combine the reaction with an enzymatic step. One such sequence is the enzymatic reduction of the olefinic moiety by a recombinant enoate reductase from *Gluconobacter oxydans*, carried out with an enzyme-coupled *in situ* cofactor regeneration with a glucose dehydrogenase as enzyme component and D-glucose as co-substrate (**Scheme 23**) [147].

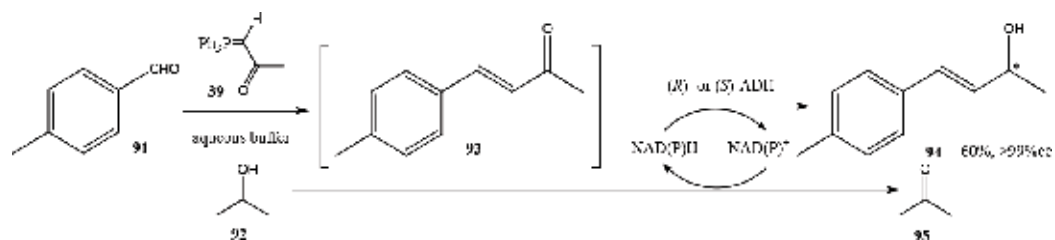
Interestingly, a Wittig reaction can also be run in combination with an enzymatic reduction, where the *in situ* prepared enone **93** is transformed to the alkenol **94** (**Scheme 24**) [148].



Scheme 22. Wittig olefination—reductive Aldol reaction.

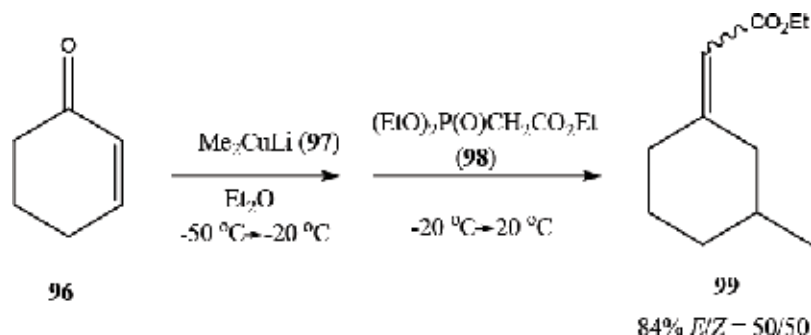


Scheme 23. Wittig-olefination—enzymatic ene-hydrogenation.

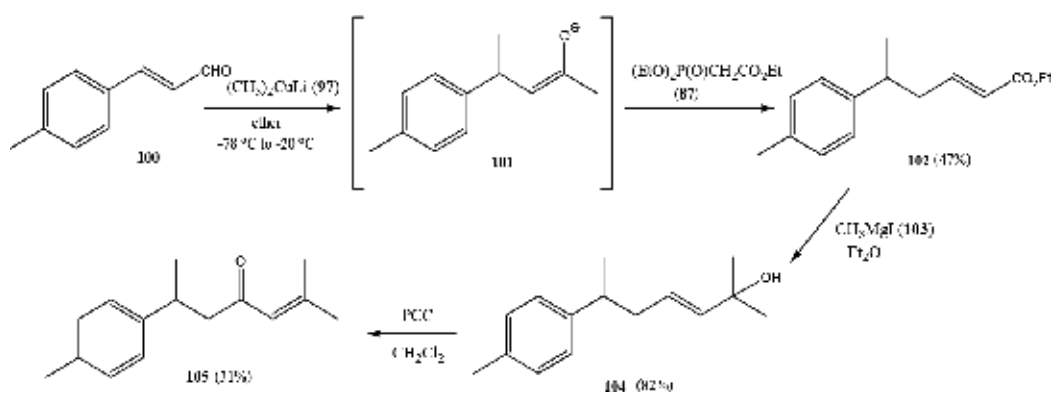


Scheme 24. Wittig-olefination—enzymatic keto-reduction.

The possibility of a combination of a Wittig/HWE olefination and a Michael addition has been studied by a number of research groups. Thus, Piva and Comesse have added phosphonoesters to copper enolates derived from the 1,4 addition of cuprates **97** to enones **96** with the idea that the enolate would deprotonate the phosphonoester **98** producing the reactive ketone and phosphonate, which undergo HWE reaction. Products **99** of the tandem Michael-HWE reaction are produced in acceptable yield (Scheme 25) [149, 150]. This strategy was used with *p*-methylcinnamaldehyde (**100**) as carbonyl component in the total synthesis of (\pm)-*ar*-turmerone (**105**), a bisabolane-type natural product found in *Zingiber* and *Curcuma* species (Scheme 26) [151].



Scheme 25. One-pot Michael addition—HWE reaction.

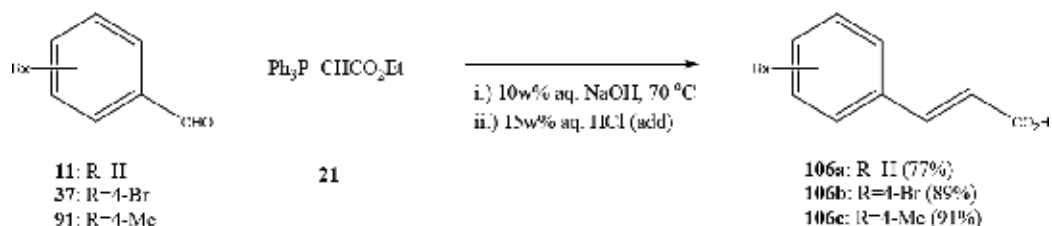


Scheme 26. Synthetic route to utilizing a one-pot Michael addition—HWE reaction.

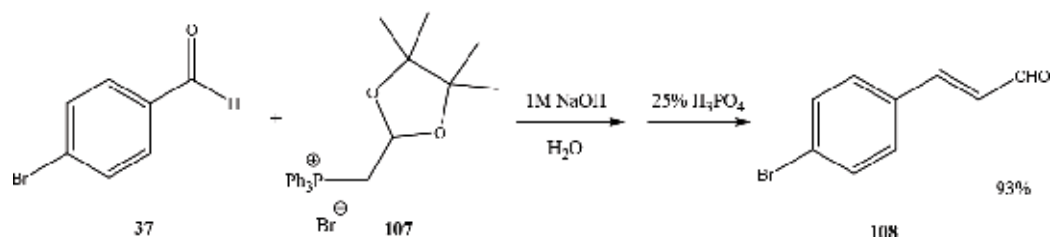
7. One-pot Wittig-olefination/functional group interconversion

Wittig reactions can be performed with alkoxy carbonylmethylidetriphenylphosphorane (**21**) in aq. NaOH, where the cinnamates formed are hydrolysed *in situ* to cinnamic acids **106** (**Scheme 27**) [152]. After completion of the reaction, triphenylphosphine oxide can be filtered off from the strongly basic, aqueous solution, and the cinnamic acids are isolated by simple filtration after acidification of the filtrate. Pinacol-acetal tripropylphosphonium salt **107** has been reacted in aq. 1 M NaOH with different benzaldehydes **37**; the cinnamaldehyde *O,O*-pinacol acetal can be hydrolyzed directly to the cinnamaldehydes **108** with 25w% aq. H₃PO₄ (**Scheme 28**) [153].

This procedure provides a nice alternative to the reaction of benzaldehydes with triphenylphosphoranylidenacetaldehyde, which often produces dienals and trienals as side-products. A tandem Wittig-cyanosilylation was developed by Zhou et al., where again Ph₃P=O as side product of the Wittig olefination acts as Lewis base to catalyze TMSCN in the cyanosilylation step. Chiral salen



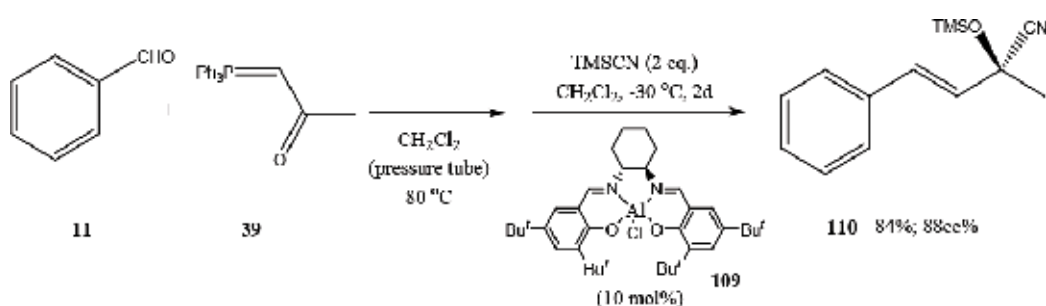
Scheme 27. One-pot Wittig reaction—ester hydrolysis.



Scheme 28. One-pot Wittig reaction—acetal hydrolysis.

aluminum catalyst **109** was used as Lewis acid to activate the keto function in the cyanosilylation. Products were obtained with high enantioselectivity [68–93%ee]. TMSCN and chiral catalyst **109** were added after completion of the Wittig reaction, albeit in one pot (Scheme 29) [143].

As Wittig reactions can be carried out in aqueous medium, enzymatic reactions can be integrated into the process (*vide supra*). In this regard, M. Krauß et al. showed that 4-phenylbut-3-en-2-ones (**93**), obtained by Wittig olefination, are reduced to the corresponding 4-phenylbut-3-en-2-ols (**94**) in >99 ee(%) using (*S*)-alcohol dehydrogenase [(*S*)-ADH] from *Rhodococcus* sp. or (*R*)-ADH from *Lactobacillus kefir* [148].



Scheme 29. Wittig reaction—cyanosilylation.

8. One-pot Wittig- and HWE olefination/cyclization

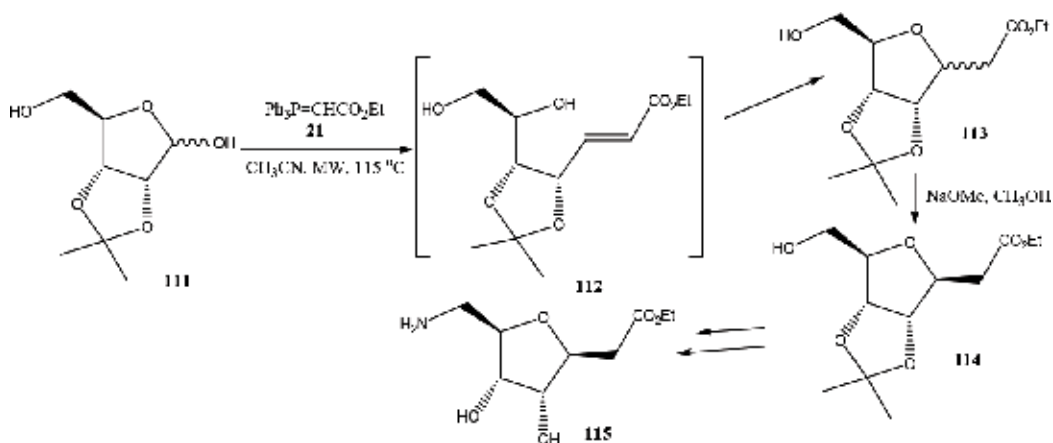
Michael type cyclization—cyclic hemiacetals can be used efficiently as substrates in Wittig olefination reactions with stabilized Wittig reagents. After the Wittig reaction, the tethered alcohol

function induces a cyclization through a Michael reaction. This reaction sequence has been used especially in the construction of functionalized C-glycosides such as in the stereospecific synthesis of ω -amino- β -D-furanoribosylacetic acid derivative **115** (Scheme 30) [154].

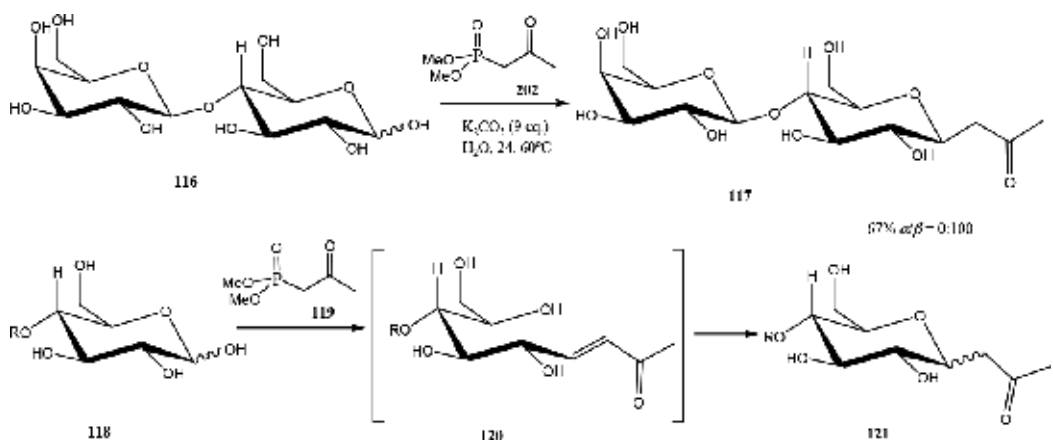
In their synthesis to C-glycoside amphiphiles, Ranoux et al. followed a similar strategy, reacting non-protected sugars with HWE reagents in aqueous or solventless conditions, leading to C-glucosides **117** and **121** (Scheme 31) [155].

A different mechanism to C-glucosides operates when 5,6-dideoxy-5,6-anhydro-6-nitro-D-glucufuranose **122** is reacted with an excess of phosphorane **21**. Here, **21** acts as a base and **122** experiences an anion driven ring opening to **123**, which undergoes an oxy-Michael addition to **124** with concomitant Wittig reaction, resulting in C-vinyl glycoside **125** (Scheme 32) [156].

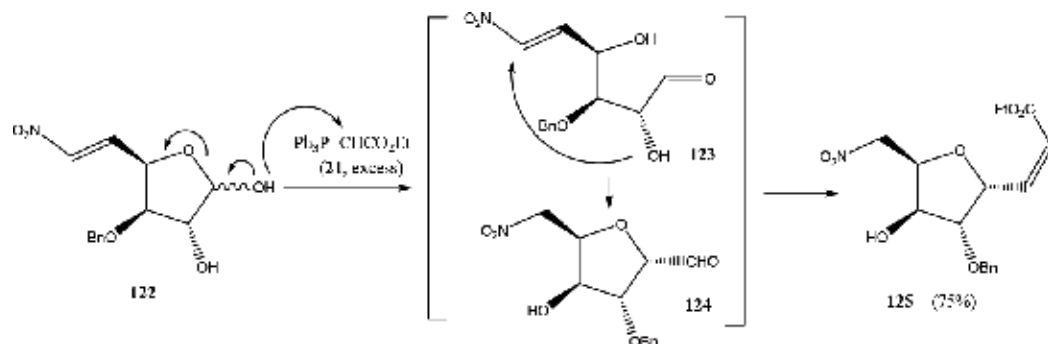
A highly stereoselective tandem Wittig-reaction-Michael addition has been developed by Liu et al. [157] when reacting 3-carboxy-2-oxopropylidene)triphenylphosphorane **126** with



Scheme 30. Synthesis of ω -amino- β -D-furanoribosylacetic acid derivative **115** utilizing a Wittig olefination-ring closure reaction en route.



Scheme 31. Synthesis of C-glucosides with a HWE-ring closure reaction.

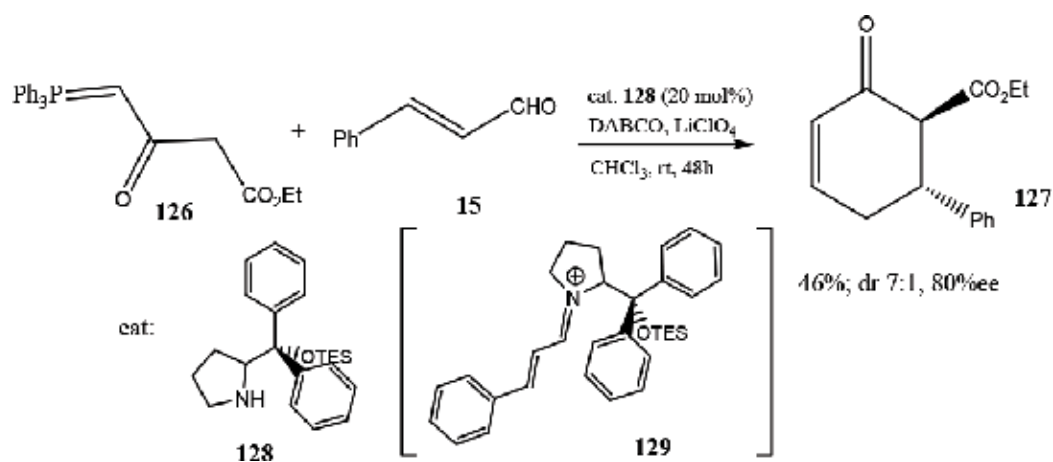


Scheme 32. Tandem oxy-Michael addition–Wittig reaction.

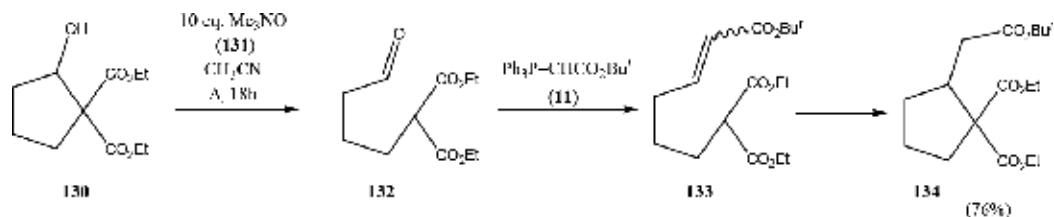
aldehydes (e.g., **15**), using a chiral pyrrolidine-based catalyst such as **128** (**Scheme 33**). Most likely, the asymmetric Michael addition proceeds by the reaction of **15** with the iminium compound **129** (**Scheme 33**), formed from **15** with catalyst **128**.

Beltrán-Rodil et al. have elaborated a retro-aldol initiated Wittig-olefination-Michael addition sequence leading to an exchange of the hydroxyl function in **130** for a carbalkoxymethyl group in **134**. The retro-aldol reaction is effected by the commercially available trimethylamine *N*-oxide (TMAO, **131**) [158] (**Scheme 34**).

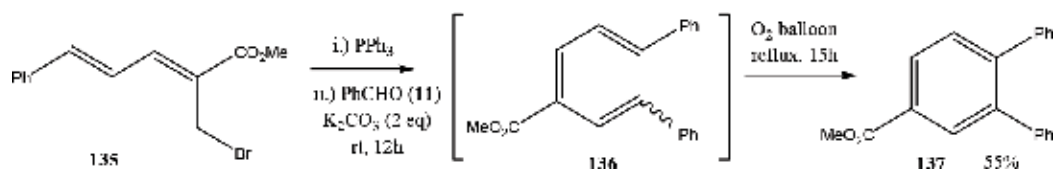
Electrocyclizations, incl. photocyclizations, and pericyclic reactions: Electrocyclization can be run in concert with Wittig reactions. One such example is shown in **Scheme 35**, where allylic bromide **135**, the product of a Morita-Baylis-Hillman transformation, is converted with triphenylphosphine to the corresponding phosphonium salt, which is reacted with benzaldehyde (**11**) to give triene **136**. **136**, heated under aeration, undergoes a 6π -electrocyclization–base catalyzed aerobic oxidation to *o*-terphenyl derivative **137** (**Scheme 35**) [159].



Scheme 33. Asymmetric Michael-addition-Wittig-olefination.



Scheme 34. Retro-aldol-Wittig-olefination-Michael addition cascade.



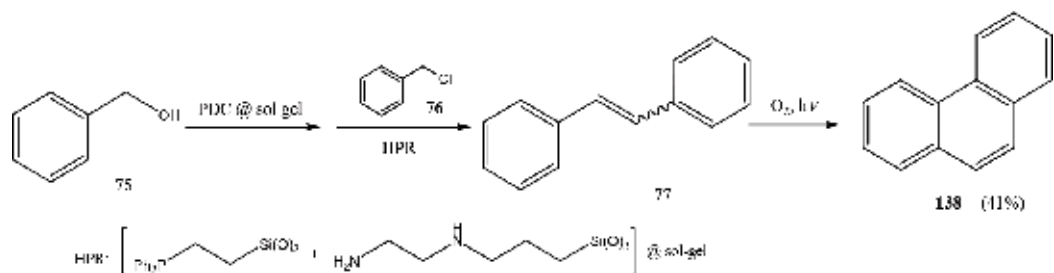
Scheme 35. One-pot phosphorane synthesis—Wittig-reaction—6 π -electrocyclization—oxidative dehydrogenation.

Similarly, Hamza and Blum [71], who developed a Wittig olefination with a sol-gel entrapped tertiary phosphine derived phosphorane (*vide supra*, **Schemes 18** and **19**) showed that the Wittig reaction can be run in concert with a photochemical cyclization under aerobic conditions to produce phenanthrene (**138**) (**Scheme 36**) [71].

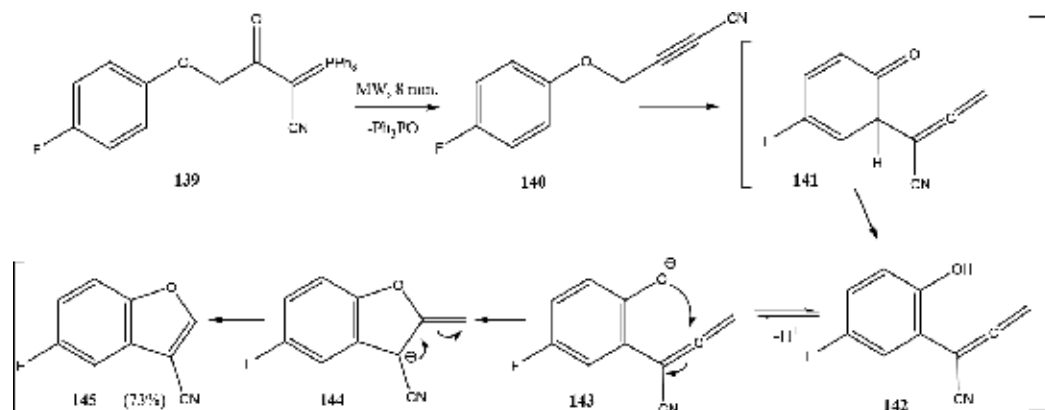
A number of tandem Wittig/HWE reaction—Claisen/Cope rearrangements have been reported [160–173]. A typical example is shown in **Scheme 37**, where neat (4-fluorophenoxyacetyl)cyanomethylene)triphenylphosphorane **139** is subjected to microwave irradiation at 450 W in a sealed tube to undergo an intramolecular Wittig reaction—Claisen rearrangement to furnish benzofuran **134** (**Scheme 37**) [173].

Mali et al. achieved the synthesis of seselin and angelicin derivatives (e.g., **148** and **150**) by a tandem Wittig-olefination—Claisen rearrangement from propargyl and chloroalkyl ethers of 2,4-dihydroxybenzaldehyde and 2,4-dihydroxyacetophenone (e.g., **146** and **149**) (**Scheme 38**) [164].

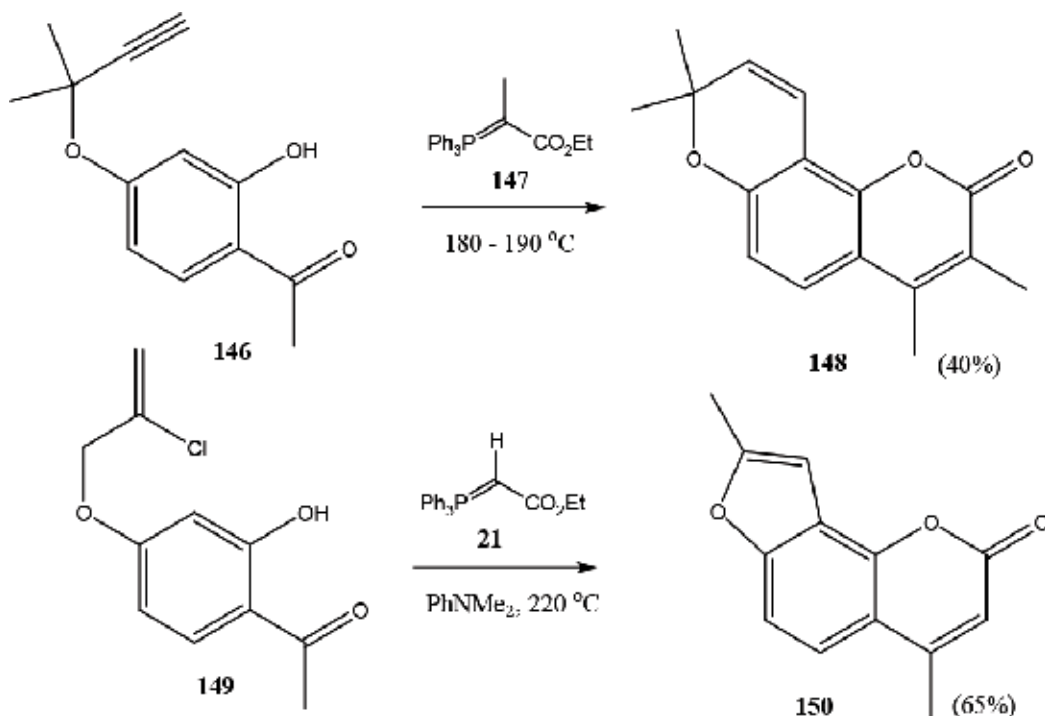
Nevertheless, sometimes, these reactions are not easy to control. Thus, a cascade of Wittig reaction and double Claisen and Cope rearrangements starting from 2,4-prenyloxybenzaldehyde



Scheme 36. Wittig olefination—photocyclization—oxidative dehydrogenation.



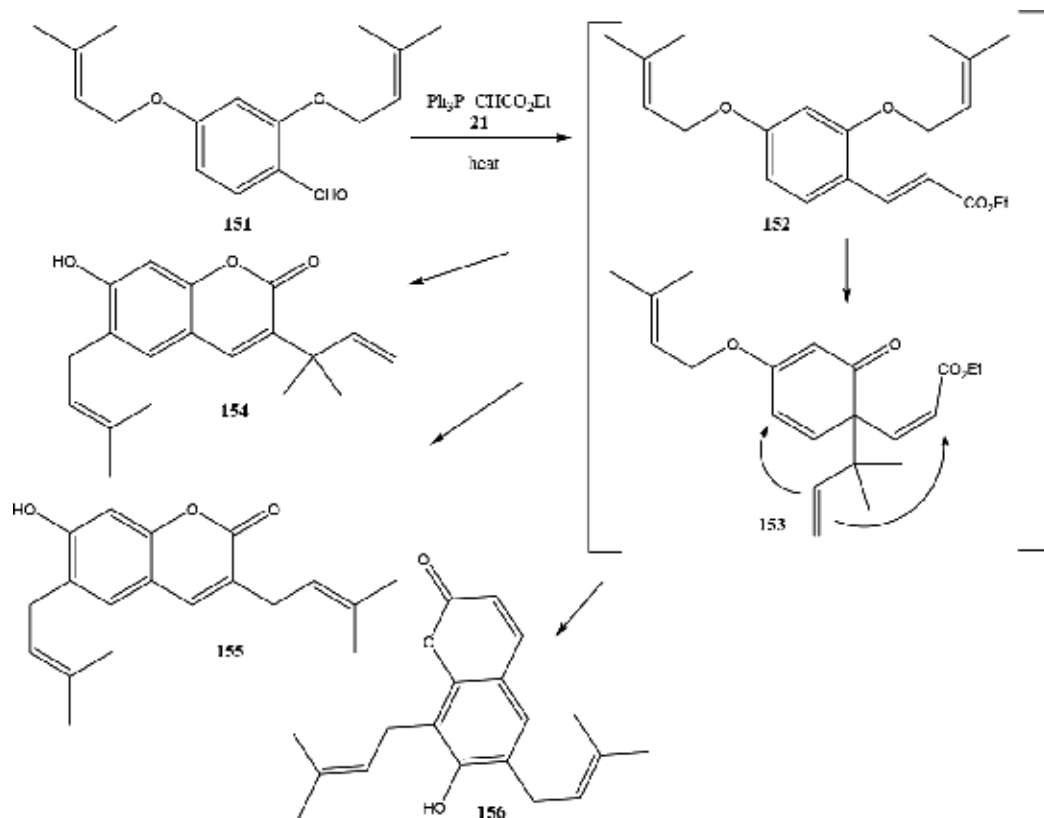
Scheme 37. Intramolecular Wittig reaction—Claisen rearrangement.



Scheme 38. One-pot syntheses of seselin and angelicin derivatives.

151 leads to a plethora of products through the range of reactions that are possible with the intermediate **153**, itself produced through the Wittig reaction and a first Claisen rearrangement. The final products found include gravelliferone (**154**, 10%), balsamiferone (**155**, 5%), and 6,8-diprenylumbelliferone (**156**, 15%) (Scheme 39) [169].

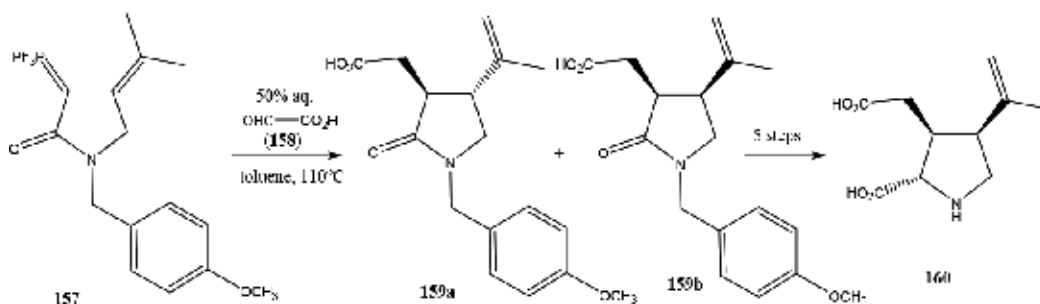
Less common is the tandem Wittig and ene reaction. Tilve et al. have published such a combination of Wittig and ene reaction in their total synthesis of (\pm)-kainic acid (**160**), an amino



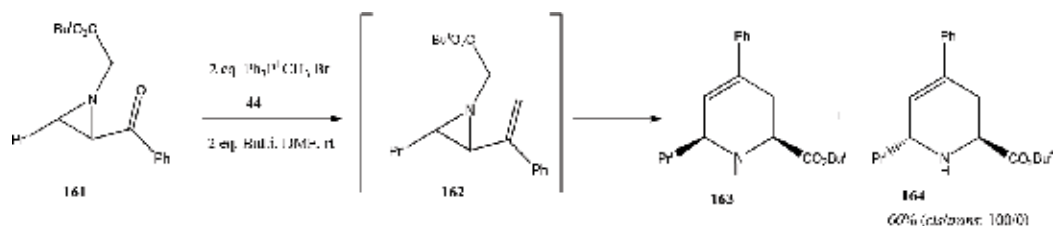
Scheme 39. Wittig reaction—double Claisen and cope rearrangements.

acid found in different species of red algae [174]. Here, the product was formed in 65% yield as a mixture of diastereoisomers **1598a/159b** in a ratio of 1:5. Previously, the authors had synthesized (\pm)-kainic acid (**160**) utilizing a Wittig—Michael reaction as the key step (Scheme 40) [175].

Finally, the possibility of a tandem Wittig-olefination—aza-Wittig rearrangement should be mentioned—this combination was carried out on 2-benzoylaziridine **161** to give stereoisomeric dehydropiperidines **163/164** (Scheme 41) [176].



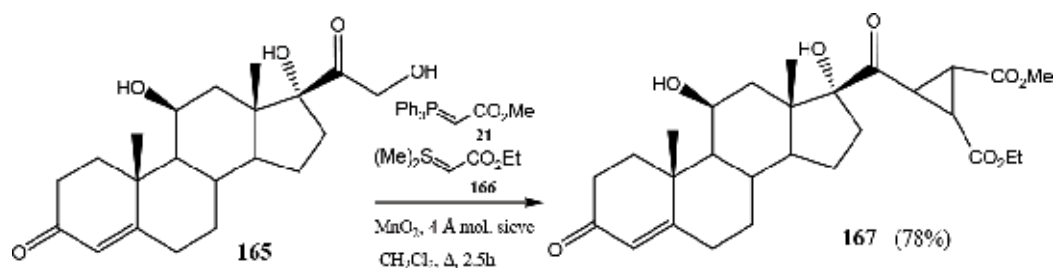
Scheme 40. Wittig-ene cascade as a key step towards the synthesis of kainic acid (**160**).



Scheme 41. Tandem Wittig-olefination—aza-Wittig-rearrangement.

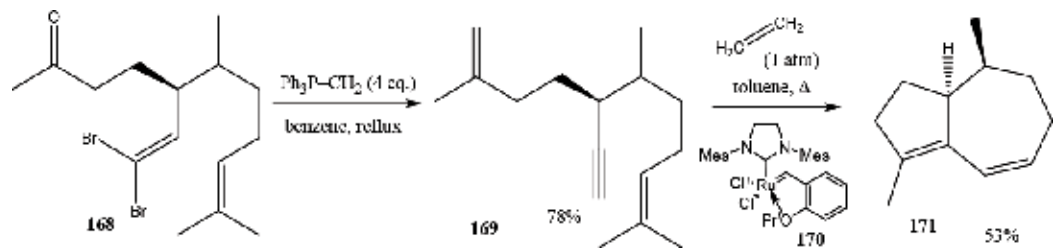
9. Other transformations

A wealth of further transformations have been found to be possible in combination with Wittig/HWE reactions. Thus, cyclopropanation of alkenes using sulfur-ylide reagent **166** can be run in tandem with a Wittig reaction with a conjugated phosphorane such as **21**. This combination of reactions can be performed with the preparation of the aldehyde as the Wittig substrate by oxidation of the corresponding alcohol **165** with MnO_2 in one pot (Scheme 42) [177].



Scheme 42. One-pot oxidation—Wittig-olefination—cyclopropanation.

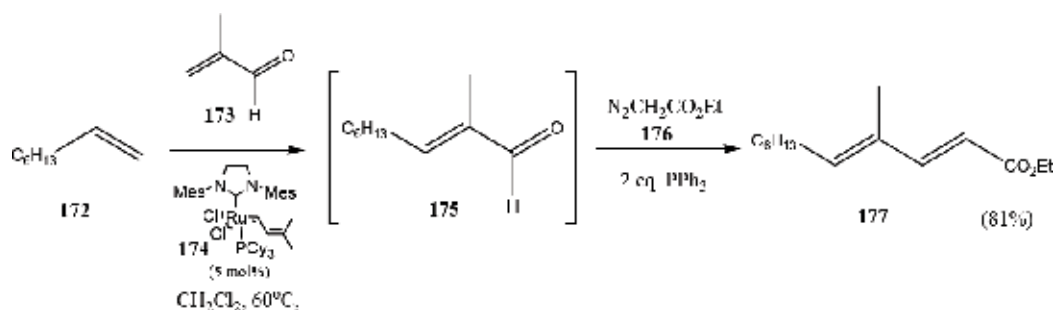
Generally, non-stabilized phosphoranes are basic. This basicity has been used by Knüppel et al. in the transformation of α,α -dibromoone **168** with excess methylenetriphenylphosphorane, where the phosphorane induces a Corey-Fuchs-reaction-type dehydrobromination/debromination to generate a terminal alkyne, which together with the concomitantly run Wittig-olefination delivers **169**, an intermediate to the trisnorsesquiterpene (–)-clavukerin A (**171**) (Scheme 43)



Scheme 43. Wittig-olefination—Corey-Fuchs-reaction-type dehydrobromination/debromination.

[178]. A metathesis reaction completes the sequence to **171**. In this case, the metathesis reaction is not run in one pot with the previous transformations.

Nevertheless, one-pot Wittig—metathesis reactions are well known from the literature [179–181]. A typical example is shown in **Scheme 44**, where catalyst **174** serves both as a catalyst for the metathesis as well as for the Wittig olefination, when the *in situ* produced aldehyde **175** is treated with triphenylphosphine and ethyl diazoacetate (**176**) in one pot (**Scheme 44**).

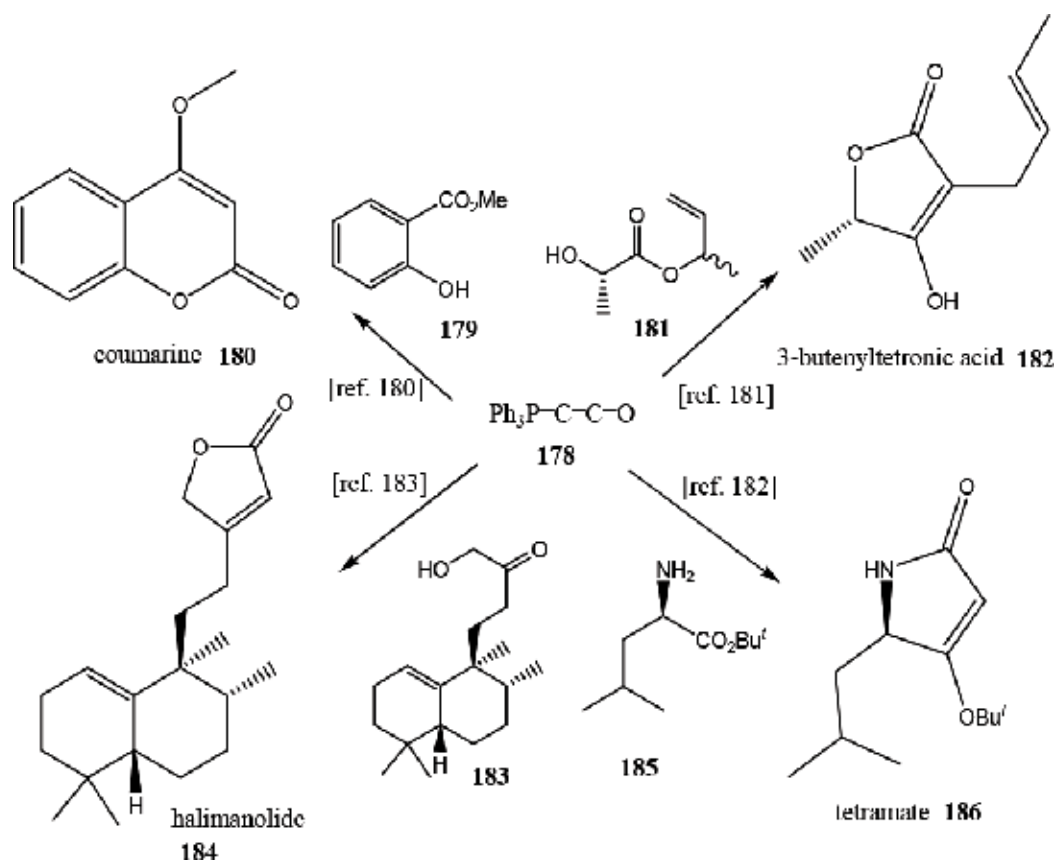


Scheme 44. One-pot Wittig—Metathesis reaction.

10. Conclusion

Due to the fact that phosphoranes and phosphonates are stable under more diverse conditions than was initially realized, it has become possible to perform reaction cascades and one-pot reactions with Wittig- and HWE reactions as an integral part of the reaction sequence. Frequently, Wittig olefination reactions are carried out with *in situ* prepared phosphonium salts and phosphoranes [17, 22–27]. One-pot oxidation—Wittig olefination reactions are also quite common [40, 43–110], especially when the carbonyl component is labile [89, 97]. Often, the oxidant of choice is MnO_2 [40, 43–46, 79–97], although a number of reactions are known where transformations were carried with air oxygen using metals and metal oxides as catalysts [72–78]. As many Wittig- and HWE reactions tolerate metal catalysts, this allows the running of Wittig/HWE reactions in combination with metal catalyzed cross coupling reactions and olefinations such as Heck [114–123], Suzuki [111–113], Sonogashira [119–121], and metathesis reactions [179–181]. The alkenes gained in the olefination reactions can be submitted to cycloaddition reactions, including Diels Alder reactions [69]. Furthermore, the alkenes lend themselves to 1,2-addition reactions [71, 140] in one-pot procedures. In cases where enones or enaldehydes are produced in the olefination reaction, a 1,4-addition becomes a possibility; this includes the Michael addition [149–151]. Also, the combination of ring opening of cyclic hemiacetals or acetals, olefination reaction and a 1,4-addition leading to ring closure is quite common [154–156]. The outcome of one-pot sequences of olefination reaction—electrocyclic rearrangement can be predicted less easily. Nevertheless, one-pot Wittig olefination—Claisen- [173], Wittig olefination—Cope- [169], and Wittig olefination—aza Wittig [176] rearrangement reactions have been published. Lastly, Wittig olefination and HWE reactions have been combined with functional group transformations, including the hydrolysis of an ester function [152] and the reduction of a carbonyl group [148].

The prospects of multi-step, one-pot reactions and reaction cascades incorporating Wittig reagents can be seen in the rich chemistry of ketylidetriphenylphosphorane (**178**) (Scheme 45) [182–185], which has been reviewed earlier [182, 186, 187]. Lastly, catalytic Wittig reactions can be seen as a subset of tandem reactions involving phosphoranes. Further research in specifically this area will help make the Wittig olefination more atom-economical and environmentally sustainable, so that this reliable alkene forming reaction will remain a competitive olefination strategy of choice.



Scheme 45. Cascade reactions with ketylidetriphenylphosphorane (**178**).

Author details

Fatima Merza¹, Ahmed Taha² and Thies Thiemann^{1*}

*Address all correspondence to: thies@uaeu.ac.ae

1 Department of Chemistry, College of Science, United Arab Emirates

2 UAEU Libraries, United Arab Emirates University, Al Ain, United Arab Emirates

References

- [1] Maryanoff BE, Reitz AB. The Wittig olefination reaction and modifications involving phosphoryl stabilized carbanions, stereochemistry, mechanism, and selected synthetic aspects. *Chemical Reviews*. 1989;**89**:863-927
- [2] Vedejs E, Marth CF. Mechanism of the Wittig reaction: The role of substituents at phosphorus. *Journal of the American Chemical Society*. 1988;**110**:3948-3958
- [3] Larsen EO, Aksnes G. Kinetic studies of the Horner reaction I. *Phosphorus Silicon*. 1983;**15**:219-228
- [4] Pommer H. The Wittig reaction in industrial practice. *Angewandte Chemie (International Ed. in English)*. 1977;**16**:423-429
- [5] Wang Y, Hou DL, Hu HZ, Zhang BZ, Wang ES. Efficient synthesis of beraprost sodium. *Chemical Research in Chinese Universities*. 2016;**32**:581-585
- [6] Wittig G, Schöllkopf U. Über Triphenylphosphinmethylene als olefinbildende Reagenzien (1. Mitteil.). *Chemische Berichte*. 1954;**87**:1318-1330
- [7] Wittig G, Haag W. Ueber Triphenylphosphinmethylene als olefinbildende Reagenzien (2. Mitteil.). *Chemische Berichte*. 1955;**88**:1654-1666
- [8] Taber C, Nelson CG. Potassium hydride in paraffin: A useful base for organic synthesis. *The Journal of Organic Chemistry*. 2006;**71**:8973-8974
- [9] Corey EJ, Clark DA, Goto G, Marfat A, Mioskowski C, Samuelsson B, Hammerström B. Stereospecific total synthesis of a "slow reacting substance" of anaphylaxis, leukotriene C-1. *Journal of the American Chemical Society*. 1980;**192**:1436-1439
- [10] Wittig G, Schöllkopf U. Methylene cyclohexane. *Organic Syntheses*. 1960;**40**:66-66
- [11] Aksnes G, Berg TJ, Gramstad T. Temperature and solvent effects in Wittig reactions. *Phosphorus, Sulfur, and Silicon*. 1995;**106**:79-84
- [12] Thiemann T, Watanabe M, Tanaka Y, Mataka S. Solvent-free Wittig olefination with stabilized phosphoranes—scope and limitations. *New Journal of Chemistry*. 2004;**28**:578-584
- [13] Thiemann T. Solventless Wittig reactions with fluorinated benzaldehydes. *Journal of Chemical Research*. 2007;**31**:336-341
- [14] Wu J, Zhang D, Wei S. Wittig reactions of stabilized phosphorus ylides with aldehydes in water. *Synthetic Communications*. 2005;**35**:1213-1222
- [15] Wu J, Zhang D. Aqueous Wittig reactions of aldehydes with *in situ* formed semistabilized phosphorus ylides. *Synthetic Communications*. 2005;**35**:2543-2551
- [16] Watanabe M, Ribeiro Morais G, Mataka S, Ideta K, Thiemann T. Two variations of solvent-reduced Wittig olefination reactions—comparison of solventless Wittig reactions to Wittig reactions under ultrasonication with minimal work-up. *Zeitschrift für Naturforschung B*. 2005;**60**:909-915

- [17] Parvartur PT, Torney PS, Tilve SG. Recent developments of Wittig reaction in organic synthesis through tandem or sequential processes. *Current Organic Synthesis*. 2013;**10**: 288-317
- [18] Kelly MJB, Fallot LB, Gustaffson JL, Bergdahl BM. Water mediated Wittig reactions of aldehydes in the teaching laboratory: Using sodium bicarbonate for the in situ formation of stabilized ylides. *Journal of Chemical Education*. 2016;**93**:1631-1636
- [19] Al Jasem Y, El-Esawi R, Thiemann T. Wittig- and Horner-Wadsworth-Emmons (HWE) olefination reactions with stabilized and semi-stabilized phosphoranes and phosphonates under non-classical conditions. *Journal of Chemical Research*. 2014;**38**:453-463
- [20] McNulty J, Das P. Highly stereoselective and general synthesis of (*E*)-stilbenes and alkenes by means of an aqueous Wittig reaction. *European Journal of Organic Chemistry*. 2009;4031-4035
- [21] McNulty J, Das P, McLeod D. Microwave-assisted, aqueous Wittig reactions: Organic-solvent- and protecting-group-free chemoselective synthesis of functionalized alkenes. *European Journal of Chemistry*. 2010;**16**:6756-6760
- [22] El-Batta A, Jiang C, Zhao W, Anness R, Cooksy AL, Bergdahl M. Wittig reactions in water media employing stabilized ylides with aldehydes. Synthesis of α,β -unsaturated esters from mixing aldehydes, α -bromoesters, and Ph_3P in aqueous NaHCO_3 . *The Journal of Organic Chemistry*. 2007;**72**:5244-5259
- [23] Wu J, Yue C. One-pot Wittig reactions in aqueous media: A rapid and environmentally benign synthesis of α,β -unsaturated carboxylic esters and nitriles. *Synthetic Communications*. 2006;**36**:2939-2947
- [24] Westman J. An efficient combination of microwave dielectric heating and the use of solid-supported triphenylphosphine for Wittig reactions. *Organic Letters*. 2001;**3**:3745-3747
- [25] Choudhary BM, Mahendar K, Kantam ML, Ranganath KVS, Athar T. The one-pot Wittig reaction: A facile synthesis of α,β -unsaturated esters and nitriles by using nanocrystalline magnesium oxide. *Advanced Synthesis and Catalysis*. 2006;**348**:1977-1985
- [26] Kantam ML, Kumar KBS, Balasubramanyam V, Venkanna GT, Figueras F. One-pot Wittig reaction for the synthesis of α,β -unsaturated esters using highly basic magnesium/lanthanum mixed oxide. *Journal of Molecular Catalysis A: Chemical*. 2010;**321**:10-14
- [27] Liu D-N, Tian S-K. Stereoselective synthesis of polysubstituted alkenes through a phosphine-mediated three-component system of aldehydes, α -halo carbonyl compounds, and terminal alkenes. *Chemistry – A European Journal*. 2009;**15**:4538-4542
- [28] Fumagalli T, Sello G, Orsini F. One-pot, fluoride promoted Wittig reaction. *Synthetic Communications*. 2009;**39**:2178-2195
- [29] Shi L, Wang W, Wang Y, Huang Y. The first example of a catalytic Wittig-type reaction. Tri-*n*-butylarsine catalysed olefination in the presence of triphenyl phosphite. *The Journal of Organic Chemistry*. 1989;**54**:2027-2028

- [30] Wang C, Yang L, Zhou R, Mei G. Solvent-free, one-pot synthesis of α,β -unsaturated esters in the presence of a C3-symmetric arsine. *Synthetic Communications*. 2016;**46**:1074-1079
- [31] Huang Z-Z, Ye S, Xia W, Yu Y-H, Tang Y. Wittig-type olefination catalysed by PEG-telluride. *The Journal of Organic Chemistry*. 2002;**67**:3096-3103
- [32] Huang Z-Z, Ye S, Xia W, Tang Y. A practical catalytic Wittig-type reaction. *Journal of the Chemical Society, Chemical Communications*. 2001;1384-1385
- [33] Huang Z-Z, Tang Y. Unexpected catalyst for Wittig-type and dehalogenation reactions. *The Journal of Organic Chemistry*. 2002;**67**:5320-5326
- [34] Tang Y, Ye S, Huang Z-Z, Huang Y-Z. Telluronium ylides in cyclopropanation and catalytic olefination. *Heteroatom Chemistry*. 2002;**13**:463-466
- [35] Orsini F, Sello G, Fumigalli T. One-pot Wittig reactions in water and in the presence of a surfactant. *Synlett*. 2006;1717-1718
- [36] Agarkar SV, Pathan RU. Green synthesis of morpholino cinnamides using sodium lauryl sulphate and water. *Chemical Science Review and Letters*. 2014;**4**:1-3
- [37] Galante A, Lhoste P, Sinou D. Wittig reaction using perfluorinated ylides. *Tetrahedron Letters*. 2001;**42**:5425-5427
- [38] Karama U, Mahfouz R, Al-Othman Z, Warad I, Almansoor A. One-pot combination of the Wittig olefination with bromination and oxidation reactions. *Synthetic Communications*. 2013;**43**:893-898
- [39] Karama U, Alshamari H, Abdelall H, Sultan MA. A facile one-pot synthesis of (Z)- α -chloro- α,β -unsaturated esters from alcohols. *Arabian Journal of Chemistry*. in press
- [40] Karama U, Al-Othman Z, Al-Majid A, Almansour A. A facile one-pot synthesis of α -bromo- α,β -unsaturated esters from alcohols. *Molecules*. 2010;**15**:3276-3280
- [41] Karama U. One-pot synthesis of (E)- α -chloro- α,β -unsaturated esters. *Journal of Chemical Research*. 2009;405-406
- [42] Karama U. One-pot approach to the conversion of alcohols into α -iodo- α,β -unsaturated esters. *Synthetic Communications*. 2010;**40**:3447-3451
- [43] Wei X, Taylor RJK. *In situ* oxidation – Wittig reactions. *Tetrahedron Letters*. 1998;**39**:1815-3818
- [44] Blackburn L, Wei X, RJK T. Manganese oxide can oxidize unactivated alcohols under in situ oxidation-Wittig conditions. *Journal of the Chemical Society, Chemical Communications*. 1999;1337-1338
- [45] Wei X, Taylor RJK. In situ manganese dioxide alcohol oxidation – Wittig reactions: Preparation of bifunctional dienyl building blocks. *The Journal of Organic Chemistry*. 2000;**65**:616-620

- [46] Taylor RJK, Campbell L, McAllister GD. (\pm)-trans-3,3'-(1,2-cyclopropanediyl)bis-2-(*E*)-propenoic acid, diethyl ester: Tandem oxidation procedure (TOP) using MnO₂ oxidation – Stabilized phosphorane trapping. *Organic Syntheses*. 2008;**85**:15-26
- [47] Shuto S, Niizuma S, Matsuda S. One-pot conversion of α,β -unsaturated alcohols into the corresponding carbon-elongated dienes with a stable phosphorus-ylide – BaMnO₄ system. Synthesis of 6'-methylene derivatives of neplanocin A as potential antiviral nucleosides. New neplanocin analogues. 11. *The Journal of Organic Chemistry*. 1998;**63**:4489-4493
- [48] Gholinejad M, Firouzabadi H, Bahrami M, Nájera C. Tandem oxidation – Wittig reaction using nanocrystalline barium manganate (BaMnO₄): An improved one-pot protocol. *Tetrahedron Letters*. 2016;**57**:3773-3775
- [49] MacCoss RN, Balkus EP, Ley SV. A sequential tetra-*n*-propylammonium perruthenate (TPAP)-Wittig oxidation olefination protocol. *Tetrahedron Letters*. 2003;**44**:7779-7781
- [50] Hoshi M, Kaneko O, Nakajima M, Arai S, Nishida A. Total synthesis of \pm -lundurine B. *Organic Letters*. 2014;**16**:768-771
- [51] Lagouette R, Šebesta P, Jiroš P, Kalinová B, Jirošová A, Straka J, Černá K, Šobotník J, Cvačka J, Jahn U. Total synthesis, proof of absolute configuration, and biosynthetic origin of stylopsal, the first isolated sex pheromone of *Strepsiptera*. *Chemistry – A European Journal*. 2013;**19**:8515-8524
- [52] Candy M, Tomas L, Parat S, Hernan V, Bienaymé H, Pons J-M, Bressy C. A convergent approach to (-)-calystatin A based on local symmetry. *Chemistry – A European Journal*. 2012;**18**:14267-14271
- [53] Matovic NJ, Hayes PY, Penman K, Lehmann RP, De Voss JJ. Polyunsaturated alkyl amides from *Echinacea*: Synthesis of diynes, enynes, and dienes. *The Journal of Organic Chemistry*. 2011;**76**:4467-4481
- [54] Boyer A, Isono N, Lackner S, Lautens M. Domino rhodium(I)-catalysed reactions for the efficient synthesis of substituted benzofurans and indoles. *Tetrahedron*. 2010;**66**:6468-6482
- [55] Read CDG, Moore PW, Williams CM. *N,N,N',N'*-Tetramethylenediamine dioxide (TMEDA O₂) facilitates atom economical/open atmosphere Ley-Griffith (TPAP) tandem oxidation – Wittig reactions. *Green Chemistry*. 2015;**17**:4537-4540
- [56] Crich D, Mo X-S. One pot selective 5'-oxidation/olefination of 2'-deoxynucleosides. *Synlett*. 1999;67-68
- [57] Maiti A, Yadav JS. One-pot oxidation and Wittig olefination of alcohols using *o*-iodoxybenzoic acid and stable Wittig ylide. *Synthetic Communications*. 2001;**31**:1499-1506
- [58] Chen J, Fu X-G, Zhou L, Zhang J-T, Qi X-L, Cao X-P. A convergent route for the total synthesis of malynamides O, P, Q, and R. *The Journal of Organic Chemistry*. 2009;**74**:4149-4157

- [59] Huang CC. Synthesis of C-14 labelled 1-(4-methoxybenzoyl)-5-oxo-2-pyrrolidinepropanoic acid (CI-933). *Journal of Labelled Compounds and Radiopharmaceuticals*. 1987;**24**:676-681
- [60] Barrett AGM, Hamprecht D, Ohkubo M. Dess-Martin periodinane oxidation of alcohols in the presence of stabilized phosphorus ylides: A convenient method for the homologation of alcohols via unstable aldehydes. *The Journal of Organic Chemistry*. 1997;**62**:9376-9378
- [61] Mori K. Pheromone synthesis. Part 257: Synthesis of methyl (2*E*,4*Z*,7*Z*)-2,4,7-decatrienoate and methyl (*E*)-2,4,5-tetradecatrienoate, the pheromone components of the male dried bean beetle, *Acanthoscelides obtectus* (Say). *Tetrahedron*. 2015;**71**:5589-5596
- [62] Ireland RE, Norbeck DW. Application of the Swern oxidation to the manipulation of highly reactive carbonyl compounds. *The Journal of Organic Chemistry*. 1985;**50**:2198-2200
- [63] Salgado A, Mann E, Sanchez-Sancho F, Herradon B. Synthesis of heterocyclic γ -amino- α,β -unsaturated acid derivatives and peptide-heterocycle hybrids. *Heterocycles*. 2003;**60**:57-71
- [64] Lin S, Deiana L, Tseggai A, Córdova A. Concise total synthesis of dihydrocorynanthenol, Protoemetinol, protoemetine, 3-*epi*-protoemetinol and emetine. *European Journal of Organic Chemistry*. 2012;398-408
- [65] Crisóstomo FRP, Carrillo R, Martín T, García-Tellado F, Martín VS. A convenient one-pot oxidation/Wittig reaction for the C2-homologation of carbohydrate-derived glycols. *The Journal of Organic Chemistry*. 2005;**70**:10099-10101
- [66] Bressette AR, Glover IV LC. A convenient one-pot PCC oxidation Wittig reaction of alcohols. *Synlett* 2004:738-740.
- [67] Shet J, Desai V, Tilve S. Domino primary alcohol oxidation-Wittig reaction: Total synthesis of ABT-418 and (*E*)-4-oxonon-2-enoic acid. *Synthesis*. 2004;1859-1863
- [68] Majik MS, Parameswaran PS, Tilve SG. Total synthesis of (-)- and (+)-tedanalactam. *The Journal of Organic Chemistry*. 2009;**74**:6378-6381
- [69] Harris GH, Graham AE. Efficient oxidation-Wittig olefination-Diels-Alder multicomponent reactions of α -hydroxyketones. *Tetrahedron Letters*. 2010;**51**:6890-6892
- [70] Dhumaskar KL, Bhat C, Tilve SG. PDC-mediated tandem oxidative Wittig olefination. *Synthetic Communications*. 2014;**44**:1501-1506
- [71] Hamza K, Blum J. One-pot combination of the Wittig olefination with oxidation, hydrogenation, bromination and photocyclization reactions. *Tetrahedron Letters*. 2007;**48**:293-295
- [72] Kim G, Lee DG, Chang S. *In situ* aerobic alcohol oxidation-Wittig reactions. *Bulletin of the Korean Chemical Society*. 2001;**22**:943-944

- [73] Lee EY, Kim Y, Lee JS, Park J. Ruthenium-catalyzed, one-pot alcohol oxidation-Wittig reaction producing α,β -unsaturated esters. *European Journal of Organic Chemistry*. 2009;2943-2946
- [74] Carillo AI, Schmidt LC, Marín ML, Scaiano JC. Mild synthesis of mesoporous silica supported ruthenium nanoparticles as heterogeneous catalysts in oxidative Wittig coupling reactions. *Catalysis Science & Technology*. 2014;4:435-440
- [75] Alonso F, Riente P, Yus M. Wittig-type olefination of alcohols promoted by nickel nanoparticles: Synthesis of polymethoxylated and polyhydroxylated stilbenes. *European Journal of Organic Chemistry*. 2009;6034-6042
- [76] Alonso F, Riente P, Yus M. One-pot synthesis of stilbenes from alcohols through a Wittig-type olefination reaction promoted by nickel nanoparticles. *Synlett*. 2009;1579-1582
- [77] Miyamura H, Suzuki A, Yasukawa T, Kobayashi S. Integrated process of aerobic oxidation-olefination-asymmetric C-C bond formation catalysed by robust heterogeneous gold/palladium and chirally modified rhodium nanoparticles. *Advanced Synthesis and Catalysis*. 2015;357:3815-3819
- [78] Reddy AGK, Mahendar L, Satyanarayana G. Simple copper(I)-catalysed oxidation of benzylic/allylic alcohols to carbonyl compounds: Synthesis of functionalized cinnamates in one pot. *Synthetic Communications*. 2014;44:2076-2087
- [79] Taylor RJK, Reid M, Foot J, Raw SA. Tandem oxidation processes using manganese dioxide. *Accounts of Chemical Research*. 2005;38:851-869
- [80] MacDonald G, Alcaraz L, Wei X, Lewis NJ, Taylor RJK. Unsaturated amides derived from 2-amino-3-hydroxycyclopentenone: A Stille approach to Asuka mABA, 2880-II, and limocrocin. *Tetrahedron*. 1998;54:9823-9836
- [81] Alcaraz L, Macdonald G, Ragot J, Lewis NJ, Taylor RJK, Manumycin A. Revision of structure and synthesis of the (+)-enantiomer. *The Journal of Organic Chemistry*. 1998;63:3526-3527
- [82] Alcaraz L, Macdonald G, Ragot J, Lewis NJ, Taylor RJK. Synthetic approaches to the manumycin A, B, and C antibiotics: The first total synthesis of (+)-manumycin-A. *Tetrahedron*. 1999;55:3707-3716
- [83] Zeng F, Negishi E. A highly efficient, selective, and general method for the synthesis of conjugated (all-*E*)-oligoenes of the $(\text{CH}=\text{CH})_n$ type via iterative hydrozirconation-palladium-catalysed cross-coupling. *Organic Letters*. 2002;4:703-706
- [84] Petrowski RJ. Straightforward preparation of (2*E*,4*Z*)-2,4-heptadien-1-ol and (2*E*,4*Z*)-2,4-heptadienal. *Synthetic Communications*. 2003;33:3233-3241
- [85] Nicolaou KC, Li Y, Fylaktakidou KC, Monenschein H, Li Y, Weyershausen B, Mitchell HJ, Wei H-X, Guntupalli P, Hepworth D, Sugita K. Total synthesis of apopotolidin. *Journal of the American Chemical Society*. 2003;125:15433-15442

- [86] Aitken DJ, Faure S, Roche S. Synthetic approaches to the southern part of cyclotheonamide C. *Tetrahedron Letters*. 2003;**44**:8827-8830
- [87] Mladenova M, Tavlinova M, Momchev M, Alami M, Ourévitch M, Brion JD. An iterative procedure for the synthesis of conjugated omega-chlorotrienoic and -tetraenoic esters and related derivatives. *European Journal of Organic Chemistry*. 2003;2713-2718
- [88] Phillips DJ, Pillinger KS, Li W, Taylor AE, Graham AE. Desymmetrization of diols by a tandem oxidation/Wittig olefination reaction. *Journal of the Chemical Society, Chemical Communications*. 2006;2280-2282
- [89] Davies SB, McKerverey MA. Convenient in-situ synthesis of nonracemic N-protected β -amino aldehydes from β -amino acids. Applications in Wittig reaction and heterocycle synthesis. *Tetrahedron Letters*. 1999;**40**:1229-1232
- [90] Lang S, Taylor RJK. Tandem oxidation-Wittig-Wittig sequences for the preparation of functionalized dienolates. *Tetrahedron Letters*. 2006;**47**:5489-5492
- [91] Blackburn L, Pei C, Taylor RJK. *In situ* alcohol oxidation-Wittig reactions using non-stabilized phosphoranes. *Synlett*. 2002;215-218
- [92] Blackburn L, Kanno H, Taylor RJK. *In situ* alcohol oxidation-Wittig reactions using *N*-methoxy-*N*-methyl-2-(triphenylphosphoranylidene)acetamide: Application to the synthesis of a novel analogue of 5-oxo-eicosatetraenoic acid. *Tetrahedron Letters*. 2003;**44**:115-118
- [93] Runcie KA, Taylor RJK. The *in situ* oxidation-Wittig reaction of α -hydroxyketones. *Journal of the Chemical Society, Chemical Communications*. 2002;974-975
- [94] Quesada E, Raw SA, Reid M, Roman E, Taylor RJK. One-pot conversion of activated alcohols into 1,1-dibromoalkenes and terminal alkynes using tandem oxidation processes with manganese dioxide. *Tetrahedron*. 2006;**62**:6673-6680
- [95] McAllister GA, Oswald MF, Paxton RJ, Raw SA, Taylor RJK. The direct preparation of functionalized cyclopropanes from allylic alcohols or α -hydroxyketones using tandem oxidation processes. *Tetrahedron*. 2006;**62**:6681-6694
- [96] Raw SA, Reid M, Roman E, Taylor RJK. A tandem oxidation procedure for the conversion of alcohols into 1,1-dibromoalkenes. *Synlett*. 2004;819-822
- [97] Pavlakos E, Georgiou T, Tofi M, Montagnon T, Vassilikogiannakis G. γ -Spiroketal γ -lactones from 2-(γ -hydroxyalkyl)furans: Syntheses of epi-pyrenolides D and crassalactone D. *Organic Letters*. 2009;**11**:4556-4559
- [98] Kona J, King'ondo CK, Howell AR, Suib SL. OMS-2 for aerobic, catalytic, one-pot alcohol oxidation-Wittig reactions: Efficient access to α,β -unsaturated esters. *ChemCatChem*. 2014;**6**:749-752
- [99] Loukas V, Noula C, Kokotos G. Efficient protocol for the synthesis of enantiopure gamma-amino acids with proteinogenic side chains. *Journal of Peptide Science*. 2003;**9**:312-319

- [100] Loukas V, Markidis T, Kokotos G. Amino acid based synthesis of chiral long chain diamines and tetramines. *Molecules*. 2002;**7**:767-776
- [101] Magrioti V, Antonopoulou G, Pantoleon E, Kokotos G. Synthesis of 2-amino alcohols and unnatural amino acids from serine. *ARKIVOC*. 2002;**Xiii**:51-55
- [102] Dunlap NK, Mergo W, Jones JM, Carrick JD. A general procedure for a one-pot oxidative cleavage/Wittig reaction of glycols. *Tetrahedron Letters*. 2002;**43**:3923-3925
- [103] Terrell LR, Ward JS II, Maleczka RE Jr. Synthetic studies toward amphidinolide A: A synthesis of fully functionalized subunits. *Tetrahedron Letters*. 1999;**40**:3097-3100
- [104] Ray PC, Roberts SM, Juliá-Colonna SM. Stereoselective epoxidation of some α,β -unsaturated enones possessing a stereogenic centre at the γ -position: Synthesis of a protected galactonic acid derivative. *Journal of the Chemical Society, Perkin Transactions 1*. 2001;**149**:149-153
- [105] Outram HS, Raw SA, Taylor RJK. *In situ* oxidative diol cleavage-Wittig process. *Tetrahedron Letters*. 2002;**43**:6185-6187
- [106] Duan Y, Yao P, Du Y, Feng J, Wu Q, Zhu D. Synthesis of α,β -unsaturated esters via a chemo-enzymatic chain elongation approach by combining carboxylic acid reduction and Wittig reaction. *Beilstein Journal of Organic Chemistry*. 2015;**11**:2245-2251
- [107] Farwick A, Helmchen G. Stereoselective synthesis of β -proline derivatives from allylamines via Domino hydroformylation/Wittig olefination and Aza-Michael addition. *Advanced Synthesis and Catalysis*. 2010;**352**:1023-1032
- [108] Ruan Q, Zhou L, Breit B. New phosphorus self-assembling ligands for the tandem hydroformylation-Wittig olefination reaction of homoallylic alcohols—A key step for stereoselective pyran synthesis. *Catalysis Communications*. 2014;**53**:87-90
- [109] Breit B, Zahn SK. Domino hydroformylation-Wittig reactions. *Angewandte Chemie, International Edition*. 1999;**38**:969-971
- [110] Wong GW, Landis CR. Iterative asymmetric hydroformylation/Wittig olefination sequence. *Angewandte Chemie, International Edition*. 2013;**52**:1564-1567
- [111] Thiemann T, Watanabe M, Tanaka Y, Mataka S. One-pot Wittig-olefination/Suzuki-reaction—The compatibility of conjugated phosphoranes in Pd(0) catalysed C-C-bond forming reactions. *New Journal of Chemistry*. 2006;**30**:359-369
- [112] Thiemann T, Watanabe M, Tanaka Y, Mataka S. One pot Suzuki coupling—Wittig olefination reactions. *Journal of Chemical Research*. 2004;**28**:723-727
- [113] Chaudhary AR, Bedekar AV. 1-(α -aminobenzyl)-2-naphthol as phosphine-free ligand Pd-catalysed Suzuki and one-pot Wittig-Suzuki reaction. *Applied Organometallic Chemistry*. 2012;**26**:430-437
- [114] Burmester C, Mataka S, Thiemann T. Synthesis of non-symmetric Divinylarenes by a Heck/Wittig reaction combination. *Synthetic Communications*. 2010;**40**:3196-3208

- [115] Saiyed AS, Bedekar AV. One-pot synthesis of stilbenes by dehydrohalogenation–Heck olefination and multicomponent Wittig–Heck reaction. *Tetrahedron Letters*. 2010;**51**:6227-6231
- [116] Saiyed AS, Patel KN, Kamath BV, Bedekar AV. Synthesis of stilbene analogues by one-pot oxidation-Wittig and oxidation-Wittig–Heck reaction. *Tetrahedron Letters*. 2012;**53**:4692-4696
- [117] Patel HA, Patel AL, Bedekar AV. Polyaniline-anchored palladium catalyst-mediated Mizoroki-Heck and Suzuki-Miyaura reactions and one-pot Wittig-Heck and Wittig-Suzuki reactions. *Applied Organometallic Chemistry*. 2015;**29**:1-6
- [118] Patel KN, Bedekar AV. One-pot synthesis and study of spectroscopic properties of oligo(phenylenevinylene)s. *Tetrahedron Letters*. 2015;**56**:6617-6621
- [119] Watanabe M, Mataka S, Thiemann T. One pot Sonogashira-coupling/Wittig olefination procedures. *Journal of Chemical Research*. 2005;**29**:636-639
- [120] Thiemann T, Umeno K, Ohira D, Inohae E, Sawada T, Mataka S. Suzuki-Kumada coupling with Bromoaryl methylidene phosphoranes. *New Journal of Chemistry*. 1999;**23**:1067-1070
- [121] Thiemann T, Umeno K, Inohae E, Mataka S. Novel elongated Phosphoranes by Heck-reaction and Pd(0)-catalysed Alkynylation and their use in C-7 group functionalisation in Estrones. *The Reports of Institute of Advanced Material Study, Kyushu University*. 2000;**14**(1):17-29 *Chem. Abstr.* 2000;133:335380w
- [122] Thiemann T, Umeno K, Wang J, Arima K, Watanabe M, Tabuchi Y, Tanaka Y, Gorohmaru H, Mataka S. Elongated phosphoranes by C-C coupling of haloaryl methylidene phosphoranes—Synthesis and applications. *Journal of the Chemical Society, Perkin Transactions 1*. 2002;2090-2110
- [123] Patel KN, Kamath BV, Bedekar AV. Synthesis of alkoxy stilbenes by one-pot *O*-alkylation-Wittig and *O*-alkylation Wittig-Heck reaction sequence. *Tetrahedron Letters*. 2013;**54**:80-84
- [124] Thiemann T, Ohira D, Li YQ, Sawada T, Mataka S, Rauch K, Noltemeyer M, de Meijere A. [4+2]-Cycloaddition of Thiophene-S-monoxides onto activated Methylene-cyclopropanes. *Journal of the Chemical Society, Perkin Transactions 1*. 2000;**17**:2968-2976
- [125] Jarosz S, Szewczyk K. Stability of regioisomeric sugar allyltins. Cleavage of the carbon-oxygen bond under radical conditions. *Tetrahedron Letters*. 2001;**42**:3021-3024
- [126] Jarosz S, Kozłowska E, Jeżewski A. Intramolecular Diels-Alder reaction of chiral, highly oxygenated trienoates derived from sugar allyltins. *Tetrahedron*. 1997;**53**:10775-10782
- [127] Jarosz S, Skóra S. A convenient route to enantiomerically pure highly oxygenated decalins from sugar allyltin derivatives. *Tetrahedron: Asymmetry*. 2000;**11**:1433-1448

- [128] Jarosz S. Tandem Wittig-Diels-Alder reaction between sugar-derived phosphoranes and sugar aldehydes. An easy route to optically pure highly oxygenated decalins. *Journal of the Chemical Society, Perkin Transactions 1*. 1997;3579-3580
- [129] Tilve SG, Torney PS, Patre RE, Kamat DP, Srinivasan BR, Zubkov FI. Domino Wittig-Diels Alder reaction: Synthesis of carbazole lignans. *Tetrahedron Letters*. 2016;57:2266-2268
- [130] Torney P, Patre R, Tilve S. A rapid assembly of furo[3,4-b]- and pyrrolo[3,4-b]carbazolones by Domino Wittig Diels Alder reaction. *Synlett*. 2011;639-642
- [131] Wu J, Sun L, Dai W-M. Microwave-assisted tandem Wittig-intramolecular Diels-Alder cycloaddition. Product distribution and stereochemical assignment. *Tetrahedron*. 2006;62:8360-8372
- [132] Wu J, Jiang X, Xu J, Dai W-M. Tandem Wittig-intramolecular Diels-Alder cycloaddition of ether-tethered 1,3,9-decatrienes under microwave heating. *Tetrahedron*. 2011;67:179-192
- [133] Hilt G, Hengst C. A concise synthesis of substituted stilbenes and styrenes from propargylic phosphonium salts by a cobalt-catalysed Diels-Alder/Wittig olefination reaction sequence. *The Journal of Organic Chemistry*. 2007;72:7337-7342
- [134] Chen Z, Shou W, Wang Y. One-pot synthesis of 1,4-diarylnaphthalenes via a Wittig-Horner reaction/[4+2]-cycloaddition/dehydrogenation sequence. *Synthesis*. 2009;1075-1080
- [135] Ramachary DB, Barbas CF. Towards organo-click chemistry: Development of organocatalytic multicomponent reactions through combinations of Aldol, Wittig, Knoevenagel, Michael, Diels-Alder and Huisgen cycloaddition reactions. *Chemistry—A European Journal*. 2004;10:5323-5331
- [136] D. B. Ramachary, R. Mondal, S. Jain, Direct organocatalytic Wittig/hetero-Diels-Alder reactions in one-pot: Synthesis of highly-substituted tetrahydropyranes. *ARKIVOC* 2016;ii:98-115.
- [137] Herdeis C, Schiffer T. Synthesis of nonracemic 2,3,6-trisubstituted piperidine derivatives from sugar lactones via tandem Wittig [2+3] cycloaddition reaction. A novel entry to prosopis and cassia alkaloids. *Tetrahedron*. 1999;55:1043-1056
- [138] Herdeis C, Telsler J. A stereoselective synthesis of nonracemic (+)-desoxoprosophylline by a tandem Wittig [2+3]-cycloaddition reaction. *European Journal of Organic Chemistry*. 1999;1407-1414
- [139] Herdeis C, Schiffer T. Synthesis of chiral nonracemic homo-1-deoxyzasugars with D-talo- and L-allo-configuration via tandem Wittig [2+3] cycloaddition reaction. *Tetrahedron*. 1999;52:14745-14756
- [140] Yu T-Y, Wei H, Luo Y-C, Wang Y, Wang Z-Y, Xu P-F. PPh_3O as an activating reagent for one-pot stereoselective syntheses of di- and polybrominated esters from simple aldehydes. *The Journal of Organic Chemistry*. 2016;81:2730-2736

- [141] Gelman F, Blum J, Avnir D. One-pot reactions with opposing reagents: Sol-gel entrapped catalyst and base. *Journal of the American Chemical Society*. 2000;**122**:11999-12000
- [142] Chen L, Shi T-D, Zhou J. Waste as catalyst: Tandem Wittig/conjugate addition reduction sequence to α -CF₃ γ -keto esters that uses Ph₃PO as catalyst for the chemoselective conjugate reduction. *Chemistry, An Asian Journal*. 2013;556-559
- [143] Cao J-J, Zhou F, Zhou J. Improving the atom efficiency of the Wittig reaction by a "waste as catalyst/co-catalyst" strategy. *Angewandte Chemie, International Edition*. 2010;**49**:4976-4980
- [144] Chen L, Du Y, Zeng X-P, Shi T-D, Zhou F, Zhou J. Successively recycle waste as catalyst: A one-pot Wittig/1,4-reduction/Paal-Knorr sequence for modular synthesis of substituted furans. *Organic Letters*. 2015;**17**:1557-1560
- [145] Lu J, Toy PH. Tandem one-pot Wittig/reductive aldol reactions in which the waste from one catalyzes a subsequent reaction. *Chemistry, An Asian Journal*. 2011;**6**:2251-2254
- [146] Teng Y, Lu J, Toy PH. Rasta resin-PPh₃-NBnPr₂ and its use in one-pot Wittig cascades. *Chemistry, An Asian Journal*. 2012;**7**:351-359
- [147] Krauß M, Winkler T, Richter N, Dommer S, Fingerhut A, Hummel W, Gröger H. Combination of C=C bond formation by Wittig reaction and enzymatic C=C bond reduction in a one-pot process in water. *ChemCatChem*. 2011;**3**:293-296
- [148] Krauß M, Hummel W, Gröger H. Enantioselective one-pot two-step synthesis of hydrophobic allylic alcohols in aqueous medium through the combination of a Wittig reaction and an enzymatic ketone reduction. *European Journal of Organic Chemistry*. 2007;5175-5179
- [149] Piva O, Comesse S. Tandem Michael-Wittig-Horner reaction: One-pot synthesis of δ -substituted α,β -unsaturated esters. *Tetrahedron Letters*. 1997;**38**:7191-7194
- [150] Piva O, Comesse S. Tandem Michael-Wittig-Horner reaction: One-pot synthesis of δ -substituted α,β -unsaturated carboxylic acid derivatives – Application to a concise synthesis of (Z)- and (E)-octodec-1-ol. *European Journal of Organic Chemistry*. 2000;2417-2424
- [151] Chuzel O, Piva O. Tandem Michael-Wittig-Horner reaction: Application to the synthesis of bisabolenes. *Synthetic Communications*. 2003;**33**:393-402
- [152] Thiemann T, Elshorbagy MW, Salem M, Ahmadani SAN, Al-Jasem Y, Al Azani M, Al-Sulaibi M, Al-Hindawi B. Facile, direct reaction of benzaldehydes to 3-arylprop-2-enoic acids and 3-arylprop-2-ynoic acids in aqueous medium. *International Journal of Organic Chemistry*. 2016;**6**:26-141
- [153] McNulty J, Zepeda-Velazquez C, McLeod D. Development of a robust reagent for the two-carbon homologation of aldehydes to (E)- α,β -unsaturated aldehydes. *Green Chemistry*. 2013;**15**:3146-3149

- [154] Ma D, Li X, Hao L, Zhang P, Chen H, Zhao Y. Stereospecific synthesis of ω -amino- β -D-furanoribosyl acetic acid based on microwave assisted Wittig-Michael tandem reaction. *Chemical Journal of Chinese Universities*. 2014;**35**:959-964
- [155] Ranoux A, Lemiègre L, Benoit M, Guégan J-P, Benvegu T. Horner-Wadsworth-Emmons reaction of unprotected sugars in water or in the absence of any solvent: One-step access to C-glycoside amphiphiles. *European Journal of Organic Chemistry*. 2010;**32**:1314-1323
- [156] Kumar RS, Karthikeyan K, Kumar BVNP, Muralidharan D, Perumal PT. Synthesis of densely functionalized C-glycosides by a tandem oxy Michael addition-Wittig olefination pathway. *Carbohydrate Research*. 2010;**345**:457-461
- [157] Liu Y-K, Ma C, Jiang K, Liu T-Y, Chen Y-C. Asymmetric tandem Michael addition – Wittig reaction to cyclohexenone annulation. *Organic Letters*. 2009;**11**:2848-2851
- [158] Beltrán-Rodil S, Donald JR, Edwards MG, Raw SA, Taylor RJK. Tandem retro-aldol/Wittig/Michael and related cascade processes. *Tetrahedron Letters*. 2009;**50**:3378-3380
- [159] Lim CH, Kim SH, Kim KH, Kim JN. An efficient synthesis of *o*-terphenyls from Morita-Baylis-Hillman adducts of cinnamaldehydes: A consecutive bromination, Wittig reaction, 6π -electrocyclization, and an aerobic oxidation process. *Tetrahedron Letters*. 2013;**54**:2476-2479
- [160] Quesada E, Taylor RJK. Tandem Horner-Wadsworth-Emmons olefination/Claisen rearrangement/hydrolysis sequence: Remarkable acceleration in water with microwave irradiation. *Synthesis*. 2005;3193-3195
- [161] Ajmeri AA, Rao SSM. Studies in synthesis and characterization of tandem Wittig and Claisen reactions of cinnamylated and prenylated 2, 4-dihydroxybenzaldehyde. *Indian Journal of Heterocyclic Chemistry*. 2014;**24**:175-180
- [162] Mali RS, Sandhu PK. One-pot Wittig reaction and Claisen rearrangement of 2-hydroxy-4-prenyloxybenzaldehyde and 2-hydroxy-4-prenyloxyacetophenone: Synthesis of 2',3',3'-trimethyl-2',3'-dihydroangelicins. *Journal of Chemical Research (S)*. 1996;148-149
- [163] Mali RS, Joshi P. Useful syntheses of prenylated and pyrano-3-aryl coumarins. *Synthetic Communications*. 2001;**31**:2883-2891
- [164] Mali RS, Pandhare NA, Sindkhedkar MD. Convenient two-step syntheses of seselin and angelicin derivatives. *Tetrahedron Letters*. 1995;**36**:7109-7110
- [165] Mali RS, Walture AS, Babu KN. Synthesis of 7-desoxy-8-allyl coumarins. *Organic Preparations and Procedures International*. 1996;**28**:217-221
- [166] Mali RS, Joshi PP, Sandhu PK, Manekar-Tilve A. Efficient syntheses of 6-prenyl coumarins and linear pyranocoumarins: Total synthesis of suberosin, toddaculin, O-methylapigravin (O-methylbrosiperin), O-methylbalsamiferone, dihydroxanthyletin, xanthyletin, and luvangetin. *Journal of the Chemical Society, Perkin Transactions 1*. 2002;371-376

- [167] Rehman H, Rao JM. Tandem intramolecular Wittig and Claisen rearrangement reactions in the thermolysis of 2-methyl-2-phenoxypropionylcyanomethylenetriphenylphosphoranes: Synthesis of substituted 2H-1-benzopyrans and benzofurans. *Tetrahedron*. 1987;**43**:5335-5340
- [168] Yadla R, Rao JM. Thermolysis of phenoxyacetylcyanomethylenetriphenylphosphoranes – Tandem intramolecular Wittig and Claisen rearrangement reactions. *Heterocycles*. 1987;**26**:329-331
- [169] Patre RE, Shet JB, Parameswaran PS, Tilve SG. Cascade Wittig reaction-double Claisen and Cope rearrangements: One-pot synthesis of diprenylated coumarins gravelliferone, balsamiferone, and 6,8-diprenylumbelliferone. *Tetrahedron Letters*. 2009;**50**:6488-6490
- [170] Schmidt B, Riemer M. Synthesis of allyl- and prenylcoumarins via microwave-promoted tandem Claisen rearrangement/Wittig olefination. *Synthesis*. 2016;**48**:141-149
- [171] Kawasaki T, Terashima R, Sakaguchi K-e, Sekiguchi H, Sakamoto M. A short route to “reverse-prenylated” pyrrolo[2,3-*b*]indoles via tandem olefination and Claisen rearrangement of 2-(3,3-dimethylallyloxy)indol-3-ones: First total synthesis of flustramine C. *Tetrahedron Letters*. 1996;**37**:7525-7528
- [172] Rama Rao VVVNS, Reddy GV, Yadla R, Narsaiah B, Rao PS. Synthesis of fluorine containing 3-cyano/ethoxycarbonyl-2-ethyl-benzo[*b*]furans via microwave assisted tandem intramolecular Wittig and Claisen rearrangement. *ARKIVOC*. 2005;**3**:211-220
- [173] Rama Rao VVVNS, Reddy GV, Maitraie D, Ravikanth S, Yadla R, Narsaiah B, Rao PS. One-pot synthesis of fluorine containing 3-cyano/ethoxycarbonyl-2-methylbenzo[*b*]furans. *Tetrahedron*. 2004;**60**:12231-12237
- [174] Majik MS, Parameswaran PS, Tilve SG. Tandem Wittig-Ene reaction approach to Kainic acid. *The Journal of Organic Chemistry*. 2009;**74**:3591-3594
- [175] Bhat C, Tilve SG. Tandem approach for the synthesis of functionalized pyrrolidones: Efficient routes toward allokainic acid and kainic acid. *Tetrahedron Letters*. 2013;**54**:245-248
- [176] Coldham I, Collis AI, Mould RJ, Rathmell RE. Synthesis of 4-phenylpiperidines by tandem Wittig Olefination – aza- Wittig rearrangement of 2-benzoylaziridines. *Journal of the Chemical Society, Perkin Transactions 1*. 1995;**2739**-2745
- [177] Huang WH, Wang LL. One-pot synthesis of cyclopropane derivatives with a *cis/trans* stereoselectivity by Wittig olefination - sulfur ylide cyclopropanation sequence. *Journal of Chemical Research*. 2013;**380**-384
- [178] Knüppel S, Rogachev VO, Metz P. A concise catalytic route to the marine sesquiterpenoids (-)-clavukerin A and (-)-isoclavukerin A. *European Journal of Organic Chemistry*. 2010;**(32)**:6145-6148
- [179] Sirasani G, Paul T, Andrade RB. Sequencing cross-metathesis and non-metathesis reactions to rapidly access building blocks for synthesis. *Tetrahedron*. 2011;**67**:2197-2205

- [180] Paul T, Andrade RB. Sequential cross-metathesis/phosphorus-based olefination: Stereoselective synthesis of 2,4-dienoates. *Tetrahedron Letters*. 2007;**48**:5367-5370
- [181] Murelli RP, Snapper ML. Ruthenium-catalyzed tandem cross-metathesis/Wittig olefination: Generation of conjugated dienoic esters from terminal olefins. *Organic Letters*. 2007;**9**:1749-1752
- [182] Schobert R, Gordon GJ. Bioactive heterocycles from Domino Wittig-pericyclic reactions. *Current Organic Chemistry*. 2002;**6**:1181-1196
- [183] Schobert R, Löffler J, Siegfried S. Phosphacumulene ylides as versatile C₂ building blocks: New pathways to tetronates, coumarins and azacycles. *Targets in Heterocyclic Systems*. 1999;**3**:245
- [184] Schobert R, Dietrich M, Mullen G, Urbina-Gonzalez J-M. Phosphorus ylide based functionalizations of tetronic and tetramic acids. *Synthesis*. 2006;3902-3914
- [185] Marcos IS, Pedrero AB, Sexmero MJ, Diez D, Basabe P, Hernandez FA, Urones JG. Synthesis and absolute configuration of three natural *ent*-halimanoilides with biological activity. *Tetrahedron Letters*. 2003;**44**:369-372
- [186] Schobert R. Domino syntheses of bioactive tetronic and tetramic acids. *Naturwissenschaften*. 2007;**94**:1-11
- [187] Schobert R, Hölzl C. Heterocycles from unsaturated phosphorus ylides. *Topics in Heterocyclic Chemistry*. 2008;**12**:193-218

Alkene Functionalization

Alkene and Olefin Functionalization by Organoaluminum Compounds, Catalyzed with Zirconocenes: Mechanisms and Prospects

Lyudmila V. Parfenova, Pavel V. Kovyazin,
Tatyana V. Tyumkina, Leonard M. Khalilov and
Usein M. Dzhemilev

Additional information is available at the end of the chapter

<http://dx.doi.org/10.5772/intechopen.69319>

Abstract

Alkene and olefin functionalization via addition of electro- or nucleophilic reagents is one of the convenient synthetic methods for the insertion of heteroatoms into organic molecules. The use of organometallic reagents in these reactions in combination with the specific catalysts provides high substrate conversion and process selectivity. The introduction of this approach into the chemistry of organoaluminum compounds leads to the development of chemo-, regio- and stereoselective catalytic methods of alkene and olefin functionalization. The chapter focuses on the modern concepts of the alkene hydro-, carbo- and cycloaluminum mechanisms, that is, the experimental and theoretical data on the intermediate structures involved in the product formation, the effects of the catalyst and organoaluminum compound structure, reaction conditions on the activity and selectivity of the bimetallic systems. The prospects of the development of enantioselective methods using these catalytic systems for the alkene and olefin transformations are considered.

Keywords: hydrometalation, carbometalation, cyclometalation, zirconocenes, organoaluminum compounds, reaction mechanism, asymmetric catalysis

1. Introduction

Insertion of various functional groups into the molecules is one of the central problems of organic chemistry. In this regard, alkene and olefin double bonds are often considered as possible

reactive centers for the construction of C-heteroatom fragments. The classic functionalization methods are based on the addition reaction of electro- or nucleophilic reagents toward the unsaturated substrates, for example, halogenation, oxidation, hydrohalogenation, hydroboration, hydroamination, hydrosilylation, hydro- and carbometalation, etc. (**Table 1**).

Each type of functionalization goes under specific conditions and involves various reagents and catalysts, which obviously affects the mechanisms of the processes and product structure. Thus, this chapter is focused on the reactions of alkenes with organometallic compounds as the effective routes for the synthesis of numerous classes of organic compounds.

Reactions of alkenes with organometallic reagents run with high substrate conversion and selectivity due to the generation of active intermediates with C-metal bonds (**Table 1**), further modification of which provides a wide range of products. The organoaluminum compounds (OACs) occupied a strong position in the chemistry of alkenes and olefins [1–11]. The acyclic and cyclic products bearing organoaluminum moiety obtained as a result of hydro-, carbo- and cycloaluminum require no further separation and could be readily modified to alcohols,

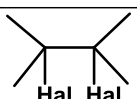
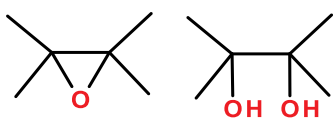
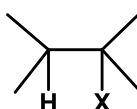
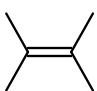
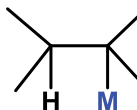
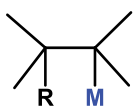
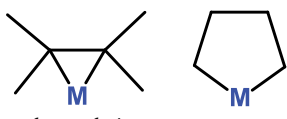
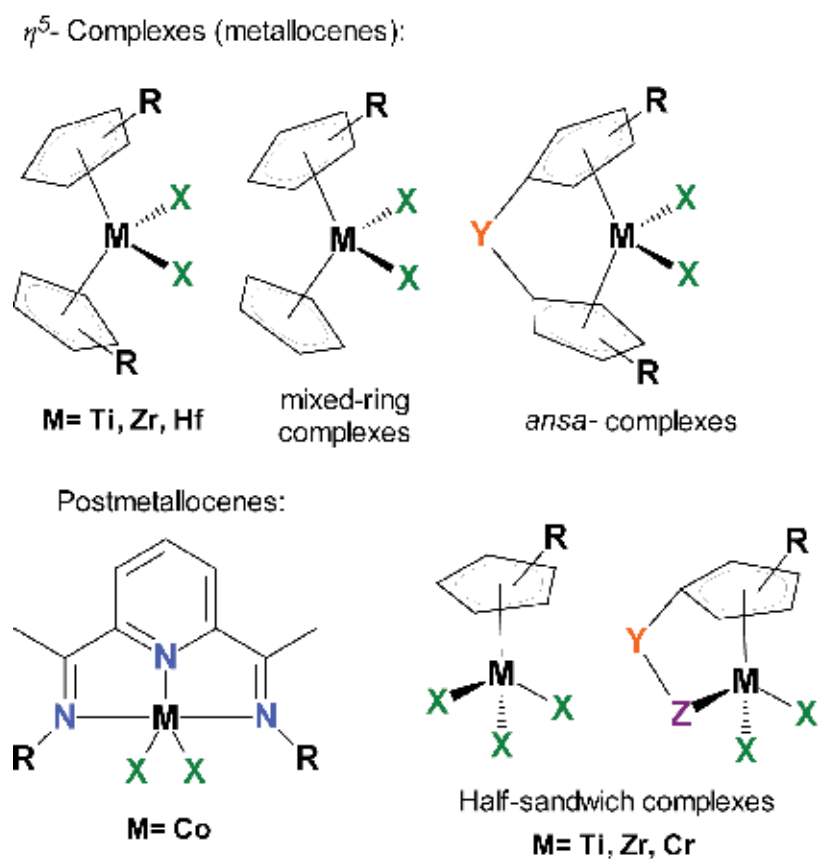
Substrate	Reagent	Product	
	Hal ₂		
	[O]		
	H-X X = Hal, OH, SO ₄ , NR ₂ , BR ₂ , SiR ₃ , PO(OR) ₂ , etc.		
	M-H M = Li, Mg, Al, Zn, Zr, etc. Catalysts: [Ti], [Zr], [Co], [Ni]	 hydrometalation	Section 2.1. M = Al (OAC) Catalysts: (η ⁵ -L) ₂ ZrCl ₂
	M-R M = Li, Mg, Al, Zn, Zr, etc. R = Alk, Ar, Allyl Catalysts: [Cu], [Ti], [Zr], [Ni], [Fe], [Co]	 carbometalation	Sections 2.2, 3 M = Al (OAC) Catalysts: (η ⁵ -L) ₂ ZrCl ₂
	M-R M = Mg, Al, Zr etc. R = Alk, Alkenyl Catalysts: [Ti], [Zr], [Hf]	 cycloaluminum	Sections 2.2, 3 M = Al (OAC) Catalysts: (η ⁵ -L) ₂ ZrCl ₂

Table 1. Alkene and olefin functionalization via addition reactions.

halides, heterocycles, carbocycles and others [9, 12–18]. For example, the well-known Ziegler-Alfol process for the synthesis of higher and linear primary alcohols from ethylene [12] has been realized in the industrial scale.

The application of transition metal complexes as catalysts enables the reactions of OAC and alkenes to proceed under mild conditions with chemo- and stereoselectivity control. Among the complexes Group IV transition metals played a significant role in the development of alkene functionalization methods using OAC. Structural types of catalysts can be varied from metal salts to metallocenes and postmetallocenes (**Scheme 1**). The special milestone in this research is the discovery of metallocene catalysis, which serves as an effective tool for the stereochemistry regulation via η^5 -ligand structure variation and provides an opportunity to a comprehensive study of the reaction mechanisms.

The future development of these methods needs understanding the reaction mechanisms: how the OAC nature, reaction conditions, catalyst and alkene structure regulate the substrate conversion, chemo- and enantioselectivity; what kinds of intermediates define the process pathways. Among the mechanistic studies much attention has been paid to the catalytic systems



Scheme 1. Structural types of transition metal complexes applied as catalysts in alkene hydro-, carbo- and cycloaluminum.

based on zirconocenes due to several reasons. First, a broad range of catalytic reactions can be implemented in these systems, from hydro-, carbo- and cyclometalation to polymerization of unsaturated compounds. Second, these systems are convenient for fundamental investigations, since η^5 -ligands bound to zirconium atoms act like magnetic probes indicating the electronic state of the transition metal atom and reflecting the molecule symmetry. Third, the reaction times and intermediate lifetimes appear to be convenient for nuclear magnetic resonance (NMR) monitoring, which is the most informative method for the studies of homogeneous catalytic reactions. Moreover, the systems are substantially free of paramagnetic species, which, for example, in the case of titanium complexes, preclude observation of the genesis of intermediates due to pronounced NMR signal broadening.

Thus, the chapter presents the results on the experimental and theoretical studies of the mechanisms of alkene hydro-, carbo- and cyclometalation by organoaluminum compounds (AlR_3 and XAlBu^i), catalyzed with zirconium η^5 -complexes. The factors that determine the intermediate reactivity and, consequently, the activity of the catalytic systems, reaction pathway and enantioselectivity are considered. The prospects of the development of stereoselective methods using these catalytic systems for the alkene and olefin transformations are discussed.

2. Mechanisms of alkene functionalization, catalyzed by zirconium η^5 -complexes

2.1. Mechanism of zirconocene catalysis in alkene hydroalumination

The catalytic alkene hydroalumination has found wide application as an efficient regio- and stereoselective method for the double and triple bond reduction providing important synthons for organic and organometallic chemistry [4, 13–15]. Various transition metal complexes can be used as the catalysts of the reaction, however, the compounds based on the metals with no vacant d orbital show much less activity in the reaction (e.g., Cu, Zn vs. Ti, Zr, Co, Ni) [16–21]. Moreover, the significant effect of the OAC nature and ligand structure on the hydrometalation product yield has been shown [22, 23].

Studies on the catalytic activity of the systems $\text{L}_2\text{ZrCl}_2\text{-XAlBu}^i$ ($\text{L} = \text{C}_5\text{H}_5, \text{C}_5\text{H}_4\text{Me}, \text{Ind}, \text{C}_5\text{Me}_5$; $\text{L}_2 = \text{rac-Me}_2\text{C}(2\text{-Me-4-Bu}^t\text{-C}_5\text{H}_2)_2, \text{meso-Me}_2\text{C}(2\text{-Me-4-Bu}^t\text{-C}_5\text{H}_2)_2, \text{rac-Me}_2\text{C}(3\text{-Bu}^t\text{-C}_5\text{H}_3)_2, \text{rac-Me}_2\text{C}(\text{Ind})_2, \text{rac-Me}_2\text{Si}(\text{Ind})_2$ and $\text{rac-C}_2\text{H}_4(\text{Ind})_2$; $\text{X} = \text{H}, \text{Cl}, \text{Bu}^i$) in the alkene hydroalumination [22, 23] showed that the most active catalytic systems are those based on the Zr complexes with sterically hindered ligands in combination with HAlBu^i_2 (**Figure 1**). Catalysts with less bulky ligands are most active in the reaction of alkenes with AlBu^i_3 or ClAlBu^i_2 .

The reaction mechanism (e.g., see [16–21]) implies the generation of transition metal hydride L_nMH formed upon σ -ligand exchange; then this species coordinates alkene to give an alkyl derivative. In the last step, as a result of the transmetalation of alkyl fragment from M to Al, the organoaluminum product is formed and the transition metal hydride is recovered (**Scheme 2**).

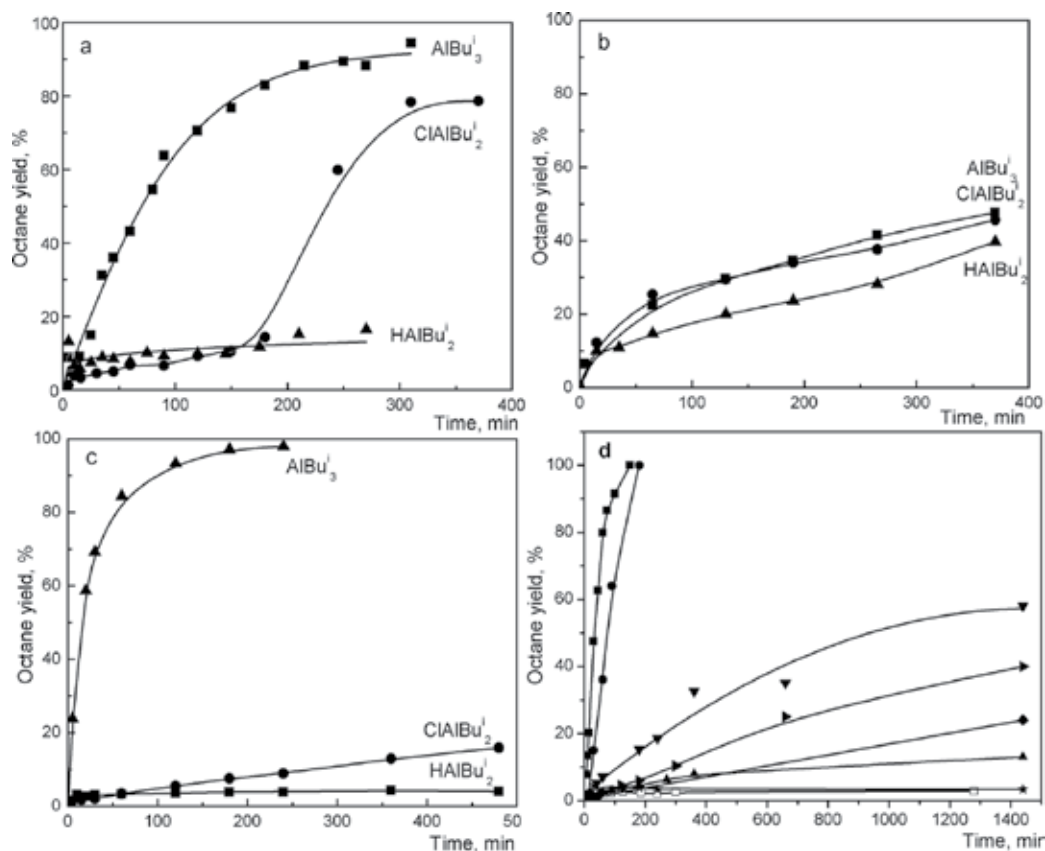
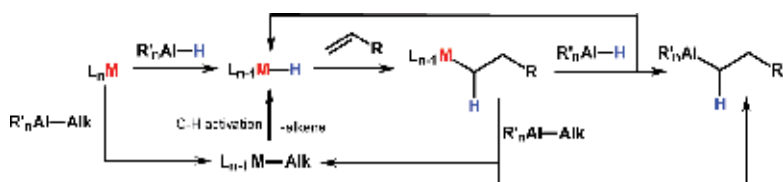


Figure 1. The effect of η^5 -ligand and OAC structure on octane yield in the reaction of 1-octene hydroalumination (molar ratio L_2ZrCl_2 :AOC:alkene 1:60:50, C_8H_{16} , $t = 20^\circ C$). (a) $L = Cp$; (b) $L = Ind$; (c) $L = CpMe_3$; (d) $rac-Me_2C(2-Me-4-Bu^t-C_5H_2)_2ZrCl_2 + HAIBu_2$ (■), $rac-Me_2C(3-Bu^t-C_5H_3)_2ZrCl_2 + HAIBu_2$ (●), $rac-C_2H_4(Ind)_2ZrCl_2 + HAIBu_2$ (▼), $rac-Me_2C(Ind)_2ZrCl_2 + HAIBu_2$ (►), $rac-Me_2Si(Ind)_2ZrCl_2 + HAIBu_2$ (◆), $rac-Me_2C(2-Me-4-Bu^t-C_5H_2)_2ZrCl_2 + AlBu_3$ (□), $rac-C_2H_4(Ind)_2ZrCl_2 + AlBu_3$ (*), $meso-Me_2C(2-Me-4-Bu^t-C_5H_2)_2ZrCl_2 + HAIBu_2$ (▲).

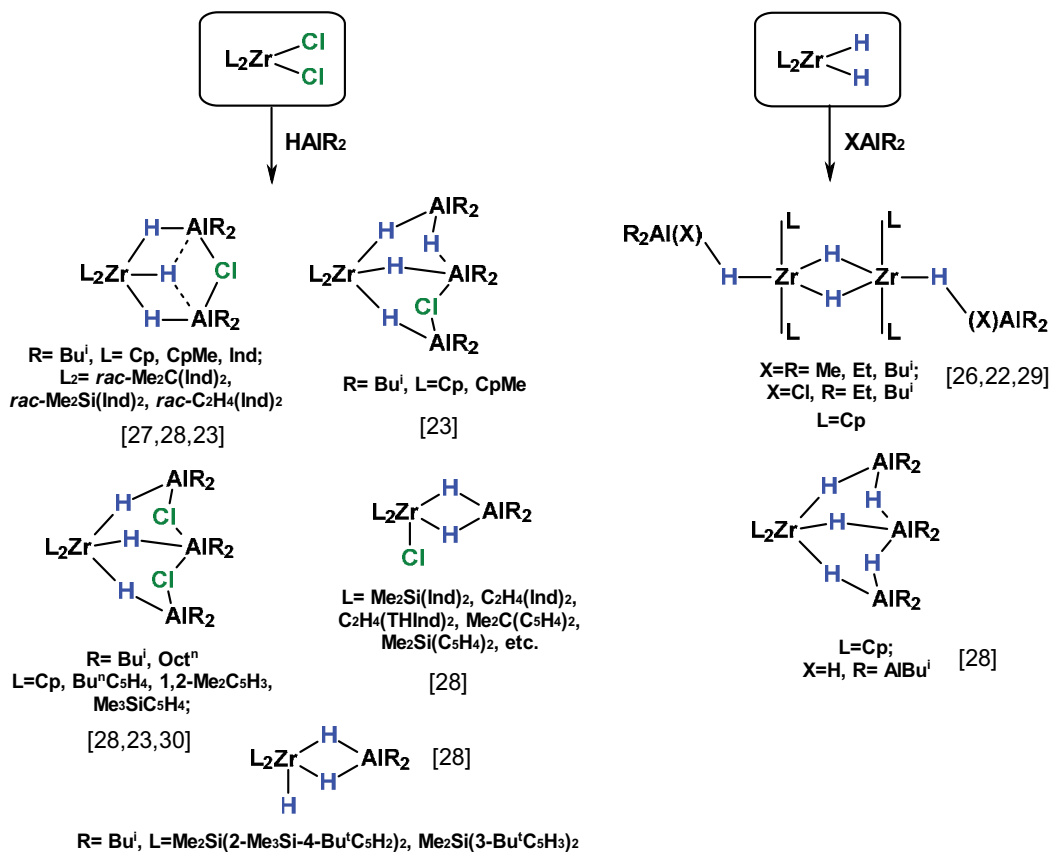


Scheme 2. Generalized scheme of catalytic alkene hydrometalation.

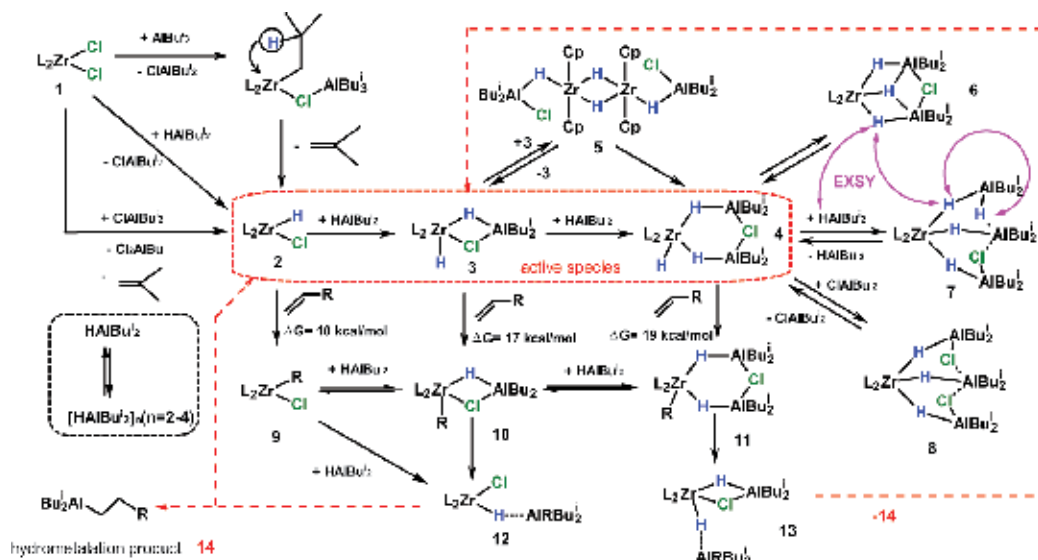
Furthermore, a large number of various bimetallic hydride complexes were identified in reactions of metal chlorides, hydrides and alkyl derivatives with OAC (see, e.g., reviews [24, 25]) that gave an idea on the involvement of such a type of complexes as key intermediates in the hydrometalation reaction. The structural types of the hydride Zr, Al-complexes, which could

be observed in the reactions of zirconocenes with aluminum hydrides or alkylaluminums, are presented in **Scheme 3**.

Our studies on the olefin hydroalumination by $XAlBu^i_2$ ($X = H, Cl, Bu^i$), catalyzed with Zr η^5 -complexes, using the quantum chemical methods [31, 32], chemical kinetics [33] and NMR [22, 23], showed that the reaction is a complex multi-step process (**Scheme 4**). The use of zirconocenes with less electron-donating and sterically hindered ligands provides the stable Zr, Al-hydride clusters $L_2Zr(\mu-H)_3(AlBu^i_2)_2(\mu-Cl)$ (**6**) ($L = Cp, CpMe, Ind$; $L_2 = rac-Me_2C(Ind)_2, rac-Me_2Si(Ind)_2, rac-C_2H_4(Ind)_2$), $L_2Zr(\mu-H)_3(AlBu^i_2)_3(\mu-Cl)(\mu-H)$ (**7**), $L_2Zr(\mu-H)_3(AlBu^i_2)_3(\mu-Cl)_2$ (**8**) ($L = Cp, CpMe$), which tend to form bridging Zr–H–Al bonds, and, hence, these complexes have low activity in the reaction with alkene. Moreover, intra- and intermolecular exchange between the hydride atoms in these clusters and $[HAlBu^i_2]_n$ oligomers were found. Thus, the complexes exist in equilibrium with each other and $HAlBu^i_2$ self-associates, while the intermolecular exchange involves the OAC monomer and occurs via dissociation of bimetallic complexes



Scheme 3. Structural types of some hydride Zr, Al-complexes [22, 23, 26–30].



Scheme 4. Mechanism of alkene hydroalumination by $XAlBu_2$ ($X = H, Cl, Bu$), catalyzed with $Zr \eta^5$ -complexes.

(**Figure 2**). Increasing of the $[HAIBu_2]_n$ concentration, that is, realization the catalytic conditions, shifts the equilibrium toward low active large clusters into which the alkene insertion is hampered due to their competing intermolecular exchange with OAC oligomers.

Reaction of Cp_2ZrCl_2 with $AlBu_3$ goes via alkyl chloride exchange and isobutylene elimination, which give the intermediates $Cp_2Zr(\mu-H)_3(AlBu_2)(AlBu_3)$ and $Cp_2Zr(\mu-H)_3(AlBu_2)_2(\mu-Cl)$. The absence of fast exchange between these hydride clusters increases the lifetime of the active sites with free $Zr-H$ bond, and this is responsible for the high activity of the $Cp_2ZrCl_2-AlBu_3$ catalytic system toward alkene [23].

High yields of hydroalumination products in the reactions of alkenes with $HAIBu_2$, catalyzed by Zr complexes with bulky ligands ($L = CpMe_5$, $rac-Me_2C(2-Me-4-Bu^t-C_5H_2)_2$, $rac-Me_2C(3-Bu^t-C_5H_3)_2$) are caused by the formation of Zr, Al -bimetallic active sites (**4**) containing a $[L_2ZrH_3]$ moiety with a free $Zr-H$ bond, in which the steric hindrance in the ligand prevents the formation of

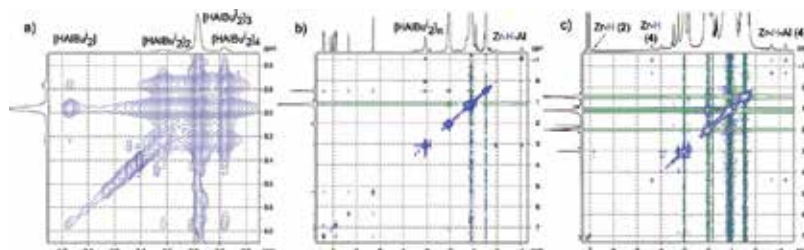


Figure 2. EXSY spectra of (a) $HAIBu_2$ in C_6D_6 (3.3 mol/L, 300 K, $\tau = 0.3$ s); (b) system $Ind_2ZrCl_2-HAIBu_2(1:12)$ in d_8 -toluene at 275 K ($\tau = 0.3$ s); (c) system $(CpMe_5)_2ZrCl_2-HAIBu_2(1:26)$ in d_8 -toluene at 265 K ($\tau = 0.3$ s). Diagonal and cross-peaks of the same phase demonstrate the existence of chemical exchange.

low-active intermediates. The *meso*-isomer of the sterically hindered cyclopentadienyl complex $\text{Me}_2\text{C}(2\text{-Me-4-Bu}^t\text{-C}_5\text{H}_2)_2\text{ZrCl}_2$ gives the intermediate with the shielded free Zr–H bond, which makes the catalytic system inactive [23].

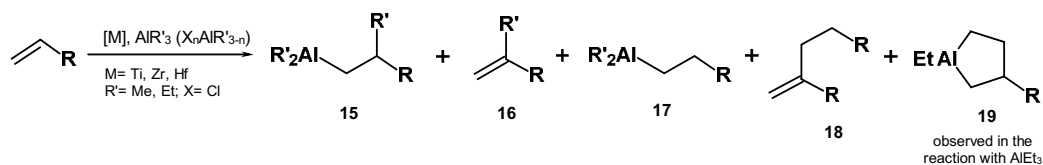
Thus, the $\text{L}_2\text{ZrCl}_2\text{-XAlBu}^i$ systems provide Zr, Al-hydride complexes with Zr–H–Zr and Zr–H–Al-bridged bonds in which intra- and intermolecular hydride exchange between Zr and Al, controlled by the steric factor of the η^5 -ligand, OAC nature and by the reaction conditions (reactant ratio), plays the key role in the catalytic process. The energy of cleavage of these bridging bonds and the ability of the complex to have initially a free Zr–H bond are the factors determining the activity of Zr, Al-hydride intermediates in the alkene hydroalumination.

2.2. Mechanisms of zirconocene catalysis in alkene carbo- and cycloalumination

Catalytic alkene and acetylene carbo- and cycloalumination are convenient one-pot synthetic routes to the acyclic and cyclic OACs that could be converted into alcohols, halides, heterocycles, carbocycles and others [2–11]. The using of enantiomerically pure complexes as the catalysts affords the asymmetric induction in the reactions. Thus, the method of Zr-catalyzed asymmetric carboalumination of alkenes-ZACA-reaction has been developed [7–11, 34], which was applied to the synthesis of a number of biologically active compounds. The involvement of methylaluminoxane (MAO) [35–38] or other Lewis acidic cocatalysts [39] substantially increases the activity of the catalytic systems providing alkene dimers, oligomers and polymers.

Summarizing the information on the study of the reaction of alkenes with alkylaluminums ($\text{R} = \text{Me}, \text{Et}$) in the presence of metal complexes [40–46], it should be noted that the process can give various products depending on the reagent nature, catalyst structure and reaction conditions (**Scheme 5**): saturated and unsaturated alkylated products (**15** and **16**), hydrometalation products (**17**), dimers (**18**) and cyclic OACs (**19**). As shown in **Tables 2** and **3** [46], the use of chlorinated solvent altogether with Zr catalysts, which contain bulky ligand (CpMe_3), increases the yield of carbometalation products **15**. The dimers **18** predominate in the reaction of alkenes with AlMe_3 , catalyzed by zirconocenes with Cp and CpMe ligands. The maximal yields of cyclic OAC **19** were observed in the reaction that runs in hydrocarbon solvent and in the presence of Zr complexes substituted with Cp, CpMe , CpMe_3 and Ind ligands.

Obviously, the reaction pathways are determined by the catalytically active sites of a definite type. Thus, bimetallic Zr, Al-alkyl complexes $\text{L}_2\text{ZrR}(\mu\text{-Cl})\text{AlR}_n\text{Cl}_{3-n}$ in the reaction of zirconocenes with alkylaluminums were found [47–52] and the complexes were suggested as key intermediates of olefin β -alkylation (**Scheme 6**). Using of strong Lewis acids, for example, MAO or perfluoroaryl boranes enhances the catalytic system productivity by several orders



Scheme 5. Reaction of alkenes with AlR_3 ($\text{R} = \text{Me}, \text{Et}$) in the presence of metal complexes.

L ₂ ZrCl ₂	Solvent	Hexene-1 conversion, %	Product yield, %			
			15	16	17	18
Cp ₂ ZrCl ₂	CH ₂ Cl ₂	92	3	14	7	68
	C ₆ H ₅ CH ₃	69	3	21	7	38
(CpMe) ₂ ZrCl ₂	CH ₂ Cl ₂	84	11	14	7	52
	C ₆ H ₅ CH ₃	39	9	9	9	12
(CpMe ₃) ₂ ZrCl ₂	CH ₂ Cl ₂	68	53	8	7	-
	C ₆ H ₅ CH ₃	44	15	14	14	1
Ind ₂ ZrCl ₂	CH ₂ Cl ₂	87	28	18	8	33
	C ₆ H ₅ CH ₃	70	38	14	10	8

Table 2. Effect of catalyst structure and solvent on the product yields in the reaction of hexene-1 with AlMe₃, catalyzed by L₂ZrCl₂ (mole ratio AlMe₃:alkene:L₂ZrCl₂ = 60:50:1, reaction time 24 h, 22°C).

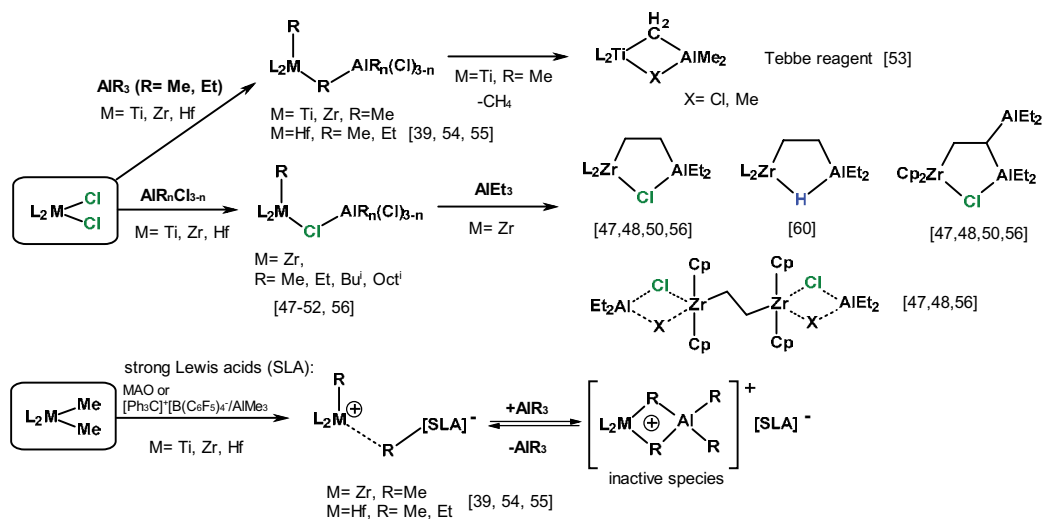
due to the generation of highly active cationic species, which are formed as a result of the ionic pair dissociation [39, 54, 55].

Further transformations of the neutral alkyl bimetallic complexes via α -C-H (Ti) or β -C-H (Zr) activation gives the stable structures with M-CH₂-Al, M-CH₂CHR-Al or M-CH₂CH₂-M bridges. Five-membered bimetallic complex L₂ZrCH₂CH₂(μ -Cl)AlEt₂ was found to be the intermediate that is responsible for the cycloalumination pathway [50, 56, 57].

The Me-group exchange between Zr and Al atoms in the complexes L₂ZrMe(μ -Cl)AlMe₃ has been observed by the means of dynamic 2D NMR spectroscopy [58, 59] (**Figure 3a**). Moreover, the exchange between the magnetically nonequivalent hydrogens, which belong to the opposite parts of *ansa*-ligand in the complex Me₂SiInd₂ZrMe(μ -Cl)AlMe₃, was found (**Figure 3b**). This dynamic picture could be explained by the intermolecular exchange

L ₂ ZrCl ₂	Solvent	Hexene-1 conversion, %	Product yield, %				
			15	16	17	18	19
Cp ₂ ZrCl ₂	CH ₂ Cl ₂	96	16	16	13	<1	51
	C ₆ H ₆	91	24	2	2	-	63
(CpMe) ₂ ZrCl ₂	CH ₂ Cl ₂	98	16	9	10	-	62
	C ₆ H ₆	97	6	10	12	-	69
(CpMe ₃) ₂ ZrCl ₂	CH ₂ Cl ₂	99	48	13	10	7	21
	C ₆ H ₆	96	15	2	5	-	74
Ind ₂ ZrCl ₂	CH ₂ Cl ₂	93	36	3	7	2	45
	C ₆ H ₆	99	25	-	<1	<1	74

Table 3. Effect of catalyst structure and solvent on the product yields in the reaction of hexene-1 with AlEt₃, catalyzed by L₂ZrCl₂ (mole ratio AlEt₃:alkene:L₂ZrCl₂ = 60:50:1, reaction time 24 h, 22°C).



Scheme 6. Bimetallic Zr, Al-intermediates in the reaction of zirconocenes with alkylaluminums [39, 47–56].

between the diastereomers of the complex, containing a stereogenic center on the transition metal atom, via $\text{Me}_2\text{SiInd}_2\text{ZrCl}_2$.

On the basis of these investigations, we proposed the mechanism, where the alkyl chloride bimetallic complex associated with the AlR_3 molecule is the starting point of the several catalytic cycles, carbo-, cyclometalation, hydrometalation and dimerization (**Scheme 7**). The zirconocenes with more electron-deficient η^5 -ligands in combination with chlorinated solvents provide a greater concentration of a key intermediate, which speeds up all the pathways, ensuring the high conversion of a substrate. The steric hindrances in η^5 -ligand and solvation by chlorine containing solvents delay the processes of C–H activation in the methylalkyl substituted intermediate increasing the carbometalation product yield.

As shown in **Figure 4**, dynamic processes are also characteristic to the five-membered bimetallic complex $\text{L}_2\text{ZrCH}_2\text{CH}_2(\mu\text{-Cl})\text{AlEt}_2$. Thus, we found intermolecular exchange by

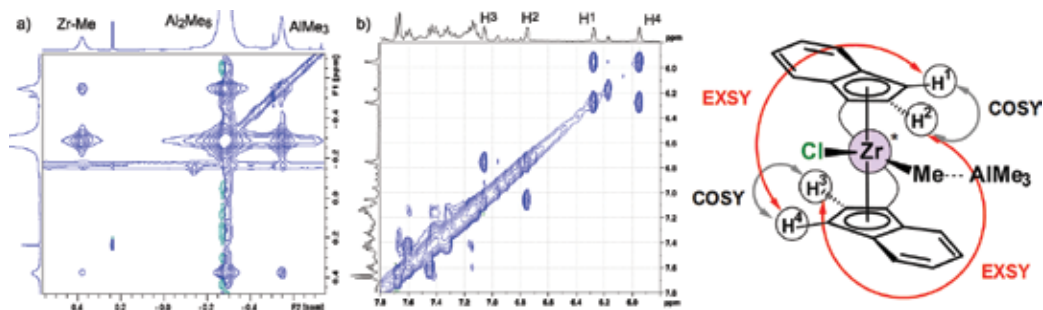


Figure 3. EXSY spectra of (a) system $\text{Cp}_2\text{ZrCl}_2-(\text{AlMe}_3)_2$ in CD_2Cl_2 at 300 K ($\tau = 0.3$ s); (b) system $\text{Me}_2\text{SiInd}_2\text{ZrCl}_2-(\text{AlMe}_3)_2$ in CD_2Cl_2 at 300 K ($\tau = 0.3$ s).

hydrogens in the pairs H¹-H⁴ and H²-H³ of *ansa*-ligand, as well as between the H-atoms of Zr-CH₂ and Al-CH₂ groups. The exchange may exist due to the equilibrium between the five-membered complex diastereomers, which apparently goes via the zirconacyclopentane structure.

Another evidence of the zirconacyclopentane generation in the systems L₂ZrCl₂-AlEt₃ could be the observation of diastereomeric five-membered bimetallic complexes CpCp'ZrCH₂CH₂(μ-H)AlEt₂(Cp' = η⁵-(1-neomenthyl-4,5,6,7-tetrahydroindenyl)) [60], the formation is possible due to realization of two parallel stages—two types of β-C-H activation in L₂ZrEt₂ (**Scheme 7**): (i) elimination of ethane to give zirconacyclopentane and (ii) formation of Et₂AlH from Et₃Al and L₂ZrHEt with loss of ethylene.

Moreover, our density functional theory (DFT) calculations showed that equilibrium between zirconacyclopentane (**23**) and bimetallic five-membered Zr, Al-complex (**22**) is thermodynamically probable; however, it is shifted toward the bimetallic intermediate [61]. Analysis of the reactions between the complexes and olefins demonstrated that zirconacyclopentane is more reactive toward the substrate than the intermediate **22** (**Scheme 7**). The insertion of olefin into **22** is accompanied by removal of the ClAlEt₂ molecule from the zirconium coordination sphere. The interaction of olefins with zirconacyclopentane and bimetallic five-membered Zr, Al-complex provides zirconacyclopentane structures, which is involvement in the cyclometalation process, has been proposed earlier [62, 63]. Transmetalation of zirconacyclopentane

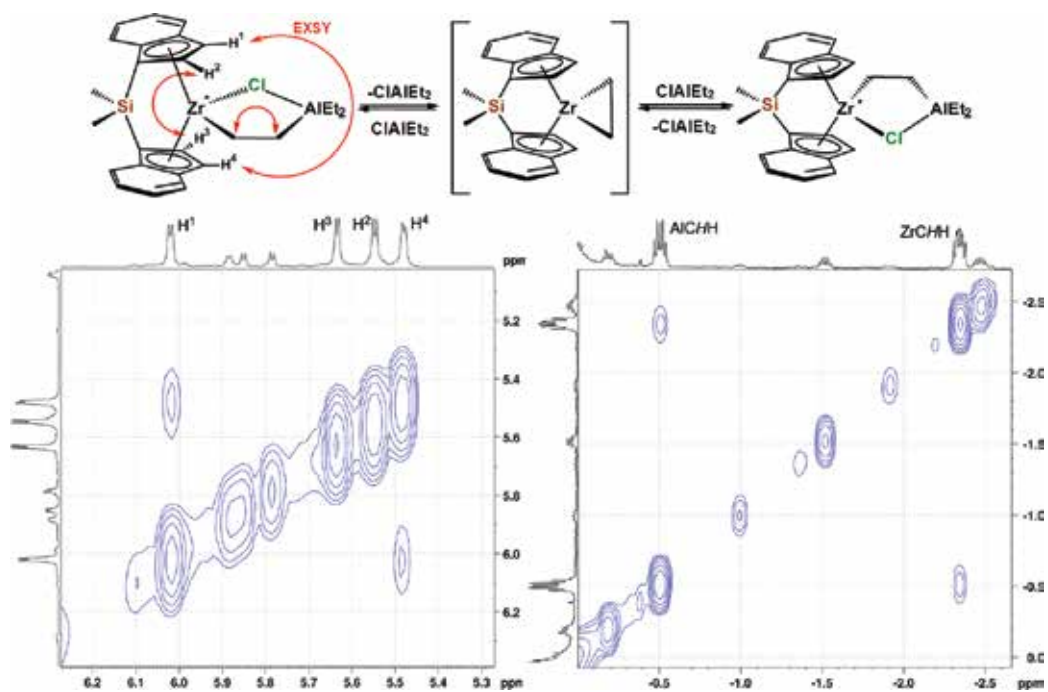
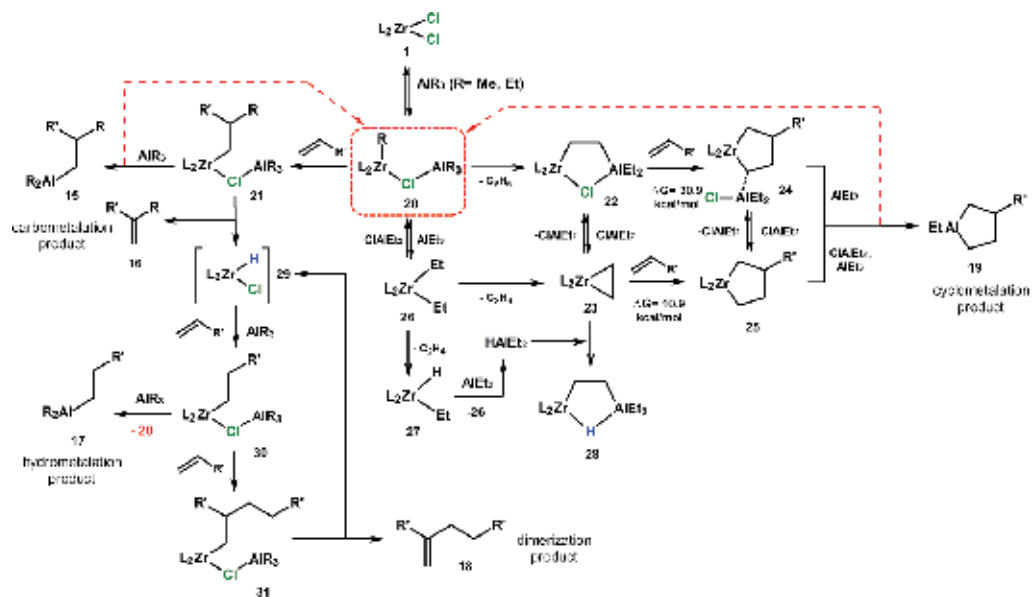


Figure 4. EXSY spectra of system Me₂SiInd₂ZrCl₂-(AlEt₂)₂ in d₈-toluene at 305 K (τ = 0.3 s).



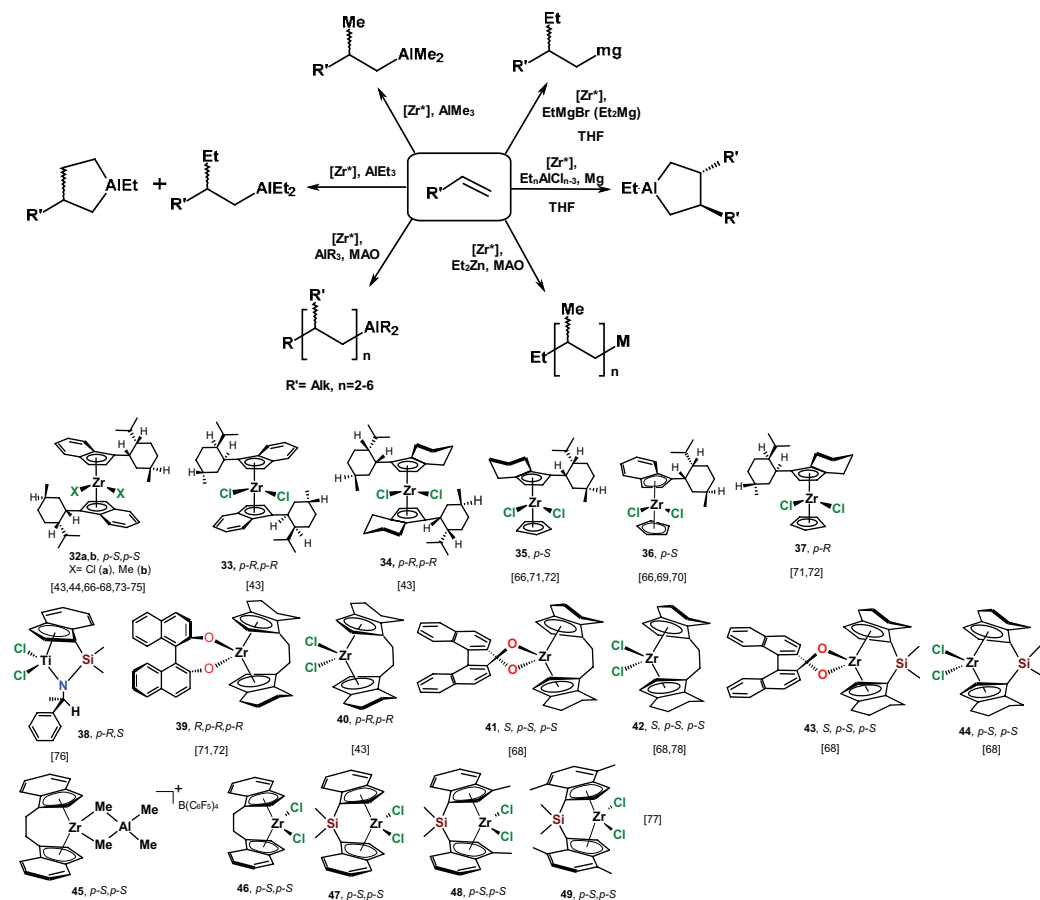
Scheme 7. Mechanisms of reactions of alkenes with AlR_3 ($\text{R} = \text{Me, Et}$), catalyzed with $\text{Zr} \eta^5$ -complexes.

by OACs goes via several stages and gives alumolanes. The probability of this process was shown experimentally using low temperature NMR spectroscopy [56].

3. Asymmetric alkene carbo- and cycloalumination, catalyzed by enantiomerically pure Group IV metallocenes

The development of stereoselective catalytic methods for the synthesis of cyclic and acyclic OAC using chiral transition metal η^5 -complexes is an actual field of chemistry. Among these, chiral Ti and Zr complexes found application in the enantioselective functionalization of alkenes with organomagnesium and -aluminum compounds [7–11, 34, 64, 65].

Thus, in the reaction of alkenes with organoaluminum compounds C_2 - and C_1 -symmetric conformationally labile (32–37) and rigid (38–49) enantiomerically pure complexes were used as catalysts (**Scheme 8**). Thus, the high enantioselectivity (up to 95%*ee*) of alkene carbometallation by AlR_3 ($\text{R} = \text{Me, Et}$) was achieved in the reactions, catalyzed by conformationally labile complex 32a in chlorinated solvents [43, 44]. Later, it was demonstrated that the replacement of AlMe_3 by AlEt_3 in the reaction catalyzed by complex 32a results in the *R* to *S* change of the absolute configuration of the β -stereogenic center in the carboalumination products [66–68]. Furthermore, the cycloalumination of terminal alkenes gives aluminacyclopentanes with 24–57%*ee* [44, 66, 67, 69]; the maximum enantioselectivity (~57%*ee*) in cycloalumination was found in the reaction of vinyl-substituted hydrocarbons with AlEt_3 , conducted in CH_2Cl_2 [67].



Scheme 8. Enantiomerically pure Zr and Ti complexes as catalysts in the reactions of alkenes with AlR₃ (R = Me, Et) [43, 44, 66–78].

Study on the olefin carboalumination with AlMe₃ in the presence of conformationally rigid *ansa*-zirconocenes **45–49** showed that the highest enantioselectivity (about 80%*ee*) was achieved in the styrene methylalumination, catalyzed by the [Ph₃C][B(C₆F₅)₄]-activated complex **45** [71]. The reaction of alkenes with AlMe₃ catalyzed by **44** in the presence of MAO gave methylalumination products in 66% yield and with enantiomeric purity of 65%*ee* [68]. Using of complexes **42**, **44** in the alkene carboalumination with AlEt₃ afforded 2-ethyl-substituted derivatives with enantiomeric excess of 50–51%*ee*. The reaction provided optically active diastereomerically pure functionally substituted alkylated alkene dimers as well [68]. The strategy of all-syn deoxypropionate motif construction, found in a number of natural products, by the asymmetric oligomerization of propylene in the presence of **42** with both stereoselectivity and chain-end functionalizability has been presented in Ref. [72].

Thus, the chemo- and enantioselectivity of these reactions are substantially affected by the catalyst and alkene structures, OAC nature and reaction conditions (temperature, reactant ratio

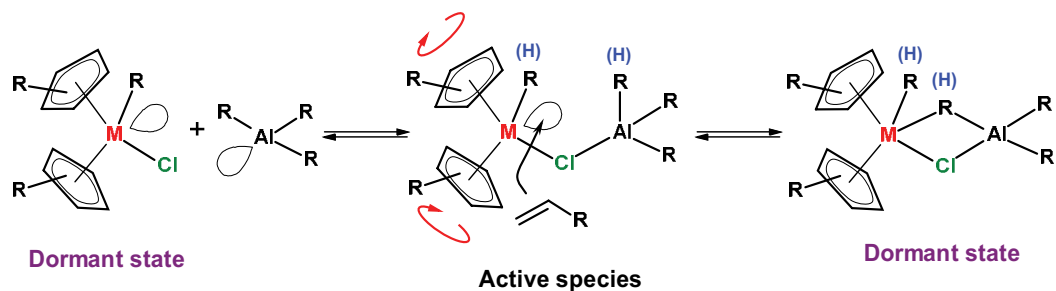
and solvent). Presumably, the key factor determining the dependence of enantioselectivity on the solvent nature and OAC structure is the conformational behavior of the η^5 -ligands in bimetallic Zr, Al-intermediates, which control the reaction pathways. The effect of a solvent nature on the rate of intramolecular exchange between conformers of neomenthyl-substituted zirconocenes **32a**, **35** and **36**, which are formed as a result of the rotation of the indenyl fragments relative to $[\text{ZrCl}_2]$, has been shown by the means of dynamic nuclear magnetic resonance (DNMR) spectroscopy [68]. Comparison of the conformer composition and dynamics of the complexes with their activity and stereoselectivity in the reactions of OACs with alkenes led to the conclusion that the enantioselectivity of the reactions is determined by the kinetic factor, namely, by the rate of interaction in a pair: conformer of catalytically active center-substrate. Thus, in order to achieve high enantioselectivity in the studied reactions, the catalyst molecule should have a specific conformational mobility for the formation of a suitable rotamer, which lifetime will be sufficient for the alkene insertion.

In this connection, further optimization of the ligand environment, namely the search for appropriate conformers that could be formed via either introduction of suitable substituents into the indenyl ligand or upon binding of ligands could advance these studies toward the design of more efficient catalysts for alkene functionalization by organomagnesium and -aluminum reagents.

4. Conclusions

Thus, the catalytic alkene hydro-, carbo- and cycloaluminum are complex multi-step processes, in which a large number of intermediate bimetallic Zr, Al-complexes are involved. Studies of the reaction mechanisms allow to understand the chemistry of the processes on a deeper level and to narrow the search for new catalytic systems.

Finally, the next remarks should be sound. First, the initial OACs exist as self-associated structures in the solutions, where the exchange between hydride atoms or alkyl groups could run via dissociation on monomers, which represents the Lewis acids and which effective concentration influences on the stages of key intermediates formation. Second, since the catalyst (IV group transition metals) is a Lewis acid too due to a free nonbonding orbital, then it disturbs the above balance, making the system more dynamic. Thus, one of the important roles of the catalyst besides the formation of active species is to accelerate the exchange through the dissociation with the release of the active OAC monomer. Third, the interaction of alkyl or hydride complex with the monomer gives active species—bimetallic intermediates, which reactivity depends on the availability of the free nonbonding orbital (**Scheme 9**). The active species should be coordinatively unsaturated, where at least one of the bridge bond is broken. In the case of bimetallic hydride complexes, there is the tendency to form inactive bridge bonds, whereas bimetallic alkyl substituted intermediates are inclined to the dissociation. Therefore, the activity of intermediates depends on the living time of active species, in which the electrophilicity of the metal center could be increased via η^5 -ligand, thereby accelerating the process of alkene introduction. However, there is a danger of another process—C—H activation in the products, which could be prevented by using more bulky ligands or more polar solvents.



Scheme 9. Exchange processes in bimetallic intermediates as factors that determine the properties of catalytic systems.

Fourth, the activity of catalytic systems and the degree of asymmetric induction in catalytic alkene functionalization by OACs is substantially affected by the intramolecular ligand mobility and conformational composition of the bimetallic intermediates.

Thus, the regulation of activity, chemo- and stereoselectivity of the studied systems is the problem of fine tuning of the catalytically active center, in which should be a balance between electronic and steric factors of the catalyst, OAC and the substrate.

Acknowledgements

The authors thank the Russian Foundation of Basic Research for financial support.

Author details

Lyudmila V. Parfenova*, Pavel V. Kovyazin, Tatyana V. Tyumkina, Leonard M. Khalilov and Usein M. Dzhemilev

*Address all correspondence to: luda_parfenova@mail.ru

Institute of Petrochemistry and Catalysis, Russian Academy of Sciences, Ufa, Russian Federation

References

- [1] Woodward S, Dagorne S, editors. *Modern Organoaluminum Reagents. Preparation, Structure, Reactivity and Use*. Berlin Heidelberg: Springer-Verlag; 2013. p. 312. DOI: 10.1007/978-3-642-33672-0
- [2] Tolstikov GA, Dzhemilev UM, Tolstikov AG. *Aluminiyorganicheskie soedineniya v organicheskom sinteze (Organoaluminum compounds in organic synthesis)*. Novosibirsk: Akad. izd. GEO; 2009. p. 645. ISBN 978-5-9747-0147-4

- [3] Ibragimov AG, Dzhemilev UM. Metal complex catalysis in the synthesis of organo-aluminium compounds. *Russian Chemical Reviews*. 2000;**69**(2):121-135. DOI: 10.1070/RC2000v069n02ABEH000519
- [4] Dzhemilev UM, Ibragimov AG. Hydrometallation of unsaturated compounds. In: Andersson PG, Munslow IJ, editors. *Modern Reduction Methods*. Weinheim: Wiley-VCH Verlag GmbH & Co. KGaA; 2008. pp. 447-490. Chapter 18. DOI: 10.1002/9783527622115.ch18
- [5] Dzhemilev UM, Ibragimov AG. Catalytic cyclometalation reaction of unsaturated compounds in synthesis of magna- and aluminacarbocycles. *Journal of Organometallic Chemistry*. 2010;**695**(8):1085-1110. DOI: 10.1016/j.jorganchem.2010.01.002
- [6] D'yakonov VA. Dzhemilev Reaction in Organic and Organometallic Synthesis. *Chemistry Research and Applications Series*. New York: Nova Science Publishers; 2010. p. 96. ISBN: 978-1-60876-683-3
- [7] Negishi E. Asymmetric carbometallations. In: Ojima I, editor. *Catalytic Asymmetric Synthesis*. 2nd ed. New York, USA: John Wiley & Sons, Inc.; 2005. pp. 165-190. Chapter 4. DOI: 10.1002/0471721506.ch5
- [8] Negishi E, Huo S. Zirconium-catalyzed enantioselective carboalumination of "unactivated" alkenes as a new synthetic tool for asymmetric carbon-carbon bond formation. *Pure and Applied Chemistry*. 2002;**74**(1):151-157. DOI: 10.1351/pac200274010151
- [9] Negishi E. Transition metal-catalyzed organometallic reactions that have revolutionized organic synthesis. *Bulletin of the Chemical Society of Japan*. 2007;**80**(2):233-257. DOI: 10.1246/bcsj.80.233
- [10] Negishi E. Bimetallic catalytic systems containing Ti, Zr, Ni, and Pd. Their applications to selective organic syntheses. *Pure and Applied Chemistry*. 1981;**53**(12):2333-2356. DOI: 10.1351/pac198153122333
- [11] Xu S, Negishi E. Zirconium-catalyzed asymmetric carboalumination of unactivated terminal alkenes. *Accounts of Chemical Research*. 2016;**49**(10):2158-2168. DOI: 10.1021/acs.accounts.6b00338
- [12] Ziegler K, Krupp F, Zosel K. Eine einfache synthese primärer Alkohole aus Olefinen. *Angewandte Chemie*. 1955;**67**:425-426. DOI: 10.1002/ange.19550671609
- [13] Guiry PJ, Coyne AG, Carroll AM. 10.19 – C–E bond formation through hydroboration and hydroalumination. In: Crabtree RH, Mingos DMP, editors. *Comprehensive Organometallic Chemistry III*. Elsevier Ltd.; Oxford. 2007. pp. 839-869. DOI: 10.1016/B0-08-045047-4/00141-2
- [14] Zaidlewicz M, Wolan A, Budny M. 8.24 Hydrometallation of C=C and C≡C bonds. Group 3. In: Knochel P, Molander GA, editors. *Comprehensive Organic Synthesis II*. 2nd ed. Elsevier Ltd.; Amsterdam. 2014. pp. 877-963. DOI: 10.1016/B978-0-08-097742-300826-0
- [15] Joseph J, Jaroschik F, Harakat D, Radhakrishnan KV, Vasse JL, Szymoniak J. Titanium-catalyzed hydroalumination of conjugated dienes: Access to fulvene-derived allylaluminium

reagents and their diastereoselective reactions with carbonyl compounds. *Chemistry – A European Journal*. 2014;**20**(18):5433-5438. DOI: 10.1002/chem.201304775

- [16] Sato F, Sato S, Sato M. Addition of lithium aluminium hydride to olefins catalyzed by zirconium tetrachloride: A convenient route to alkanes and 1-haloalkanes from 1-alkenes. *Journal of Organometallic Chemistry*. 1976;**122**(2):C25-C27. DOI: 10.1016/S0022-328X(00)80622-1
- [17] Sato F, Sato S, Kodama H, Sato M. Reactions of lithium aluminum hydride or alane with olefins catalyzed by titanium tetrachloride or zirconium tetrachloride. A convenient route to alkanes, 1-haloalkanes and terminal alcohols from alkenes. *Journal of Organometallic Chemistry*. 1977;**142**(1):71-79. DOI: 10.1016/S0022-328X(00)91817-5
- [18] Ashby EC, Noding SA. Hydrometalation. 3. Hydroalumination of alkenes and dienes catalyzed by transition metal halides. *Journal of Organic Chemistry*. 1979;**44**(24):4364-4371. DOI: 10.1021/jo01338a025
- [19] Ashby EC, Noding SA. Hydrometalation. 5. Hydroalumination of alkenes and alkynes with complex metal hydrides of aluminum in the presence of bis(cyclopentadienyl) dichlorotitanium. *Journal of Organic Chemistry*. 1980;**45**(6):1035-1041. DOI: 10.1021/jo01294a023
- [20] Negishi E, Yoshida T. A novel zirconium-catalyzed hydroalumination of olefins. *Tetrahedron Letters*. 1980;**21**(16):1501-1504. DOI: 10.1016/S0040-4039(00)92757-6
- [21] Welianje NM, McGuinness DS, Gardinera MG, Patel J. Cobalt-bis(imino)pyridine complexes as catalysts for hydroalumination–isomerisation of internal olefins. *Dalton Transactions*. 2016;**45**:10842-10849. DOI: 10.1039/c6dt01113f
- [22] Parfenova LV, Pechatkina SV, Khalilov LM, Dzhemilev UM. Mechanism of Cp₂ZrCl₂-catalyzed olefin hydroalumination by alkylalanes. *Russian Chemical Bulletin, International Edition*. 2005;**54**:316-327. DOI: 10.1007/s11172-005-0254-z
- [23] Parfenova LV, Kovyazin PV, Nifant'ev IE, Khalilov LM, Dzhemilev UM. Role of Zr, Al-hydride intermediate structure and dynamics in alkene hydroalumination by XAlBui₂ (X= H, Cl, Bui), catalyzed with Zr η⁵-Complexes. *Organometallics*. 2015;**34**(14):3559-3570. DOI: 10.1021/acs.organomet.5b003
- [24] Parfenova LV, Khalilov LM, Dzhemilev UM. Mechanisms of reactions of organoaluminum compounds with alkenes and alkynes catalyzed by Zr complexes. *Russian Chemical Reviews*. 2012;**81**(6):524-548. DOI: 10.1070/RC2012v081n06ABEH004225
- [25] Butler MJ, Crimmin MR. Magnesium, zinc, aluminium and gallium hydride complexes of the transition metals. *Chemical Communications*. 2017;**53**:1348-1365. DOI: 10.1039/c6cc05702k
- [26] Wailes PC, Weigold H, Bell AP. Reaction of dicyclopentadieny zirconium dihydride with trimethylaluminum. Formation of a novel hydride containing both Zr-H-Zr and Zr-H-Al. *Journal of Organometallic Chemistry*. 1972;**43**:C29-C31. DOI: 10.1016/S0022-328X(00)81589-2

- [27] Shoer LL, Gell KI, Schwartz G. Mixed-metal hydride complexes containing Zr-H-Al bridges. Synthesis and relation to transition-metal-catalyzed reactions of aluminum hydrides. *Journal of Organometallic Chemistry*. 1977;**136**:c19-c22. DOI: 10.1016/S0022-328X(00)82126-9
- [28] Baldwin SM, Bercaw JE, Brintzinger HH. Alkylaluminum-complexed zirconocene hydrides: Identification of hydride-bridged species by NMR Spectroscopy. *Journal of the American Chemical Society*. 2008;**130**:17423-17433. DOI: 10.1021/ja8054723
- [29] Parfenova LV, Vildanova RF, Pechatkina SV, Khalilov LM, Dzhemilev UM. New effective reagent [Cp₂ZrH₂-CIAIEt₂]₂ for alkene hydrometallation. *Journal of Organometallic Chemistry*. 2007;**692**:3424-3429. DOI: 10.1016/j.jorganchem.2007.04.007
- [30] Weliange NM, McGuinness DS, Gardinera MG, Patel J. Insertion and isomerisation of internal olefins at alkylaluminium hydride: Catalysis with zirconocene dichloride. *Dalton Transactions*. 2015;**44**:20098-20107. DOI: 10.1039/c5dt03257a
- [31] Pankratyev EY, Tyumkina TV, Parfenova LV, Khalilov LM, Khursan SL, Dzhemilev UM. DFT study on mechanism of olefin hydroalumination by XAlBui₂ in the presence of Cp₂ZrCl₂ catalyst. I. Simulation of intermediate formation in reaction of HAlBui₂ with Cp₂ZrCl₂. *Organometallics*. 2009;**28**:968-977. DOI: 10.1021/om800393j
- [32] Pankratyev EY, Tyumkina TV, Parfenova LV, Khalilov LM, Khursan SL, Dzhemilev UM. DFT and ab initio study on mechanism of olefin hydroalumination by XAlBui₂, in the presence Cp₂ZrCl₂ catalyst. II. Olefin interaction with catalytically active centers. *Organometallics*. 2011;**30**:6078-6089. DOI: 10.1021/om200518h
- [33] Parfenova LV, Balaev AV, Gubaidullin IM, Pechatkina SV, Abzalilova LR, Spivak SI, Khalilov LM, Dzhemilev UM. Kinetic model of olefin hydroalumination by HAlBui₂ and AlBui₃ in presence of Cp₂ZrCl₂ catalyst. *International Journal of Chemical Kinetics*. 2007;**39**(6):333-339. DOI: 10.1002/kin.20238
- [34] Negishi E. Discovery of ZACA reaction – Zr-catalyzed asymmetric carboalumination of alkenes. *Archive for Organic Chemistry*. 2011;(8):34-53. DOI: 10.3998/ark.5550190.0012.803
- [35] Sinn H, Kaminsky W, Vollmer HJ, Woldt R. Lebende Polymere bei Ziegler-Katalysatoren extremer Produktivität. *Angewandte Chemie*. 1980;**92**(5):396-402. DOI: 10.1002/ange.19800920517
- [36] Sinn H, Kaminsky W, Vollmer HJ, Woldt R. "Living polymers" on polymerization with extremely productive ziegler catalysts. *Angewandte Chemie International Edition*. 1980;**19**(5):390-392. DOI: 10.1002/anie.198003901
- [37] Sinn H, Kaminsky W. Ziegler-Natta catalysis. *Advances in Organometallic Chemistry*. 1980;**18**:99-149. DOI: 10.1016/S0065-3055(08)60307-X
- [38] Kaminsky W, editor. Polyolefins: 50 years after Ziegler and Natta II. Polyolefins by Metallocenes and Other Single-Site Catalysts. Berlin Heidelberg: Springer-Verlag; 2013. p. 366. DOI: 10.1007/978-3-642-40805-2

- [39] Chen EY-X, Marks TJ. Cocatalysts for metal-catalyzed olefin polymerization: Activators, activation processes, and structure–activity relationships. *Chemical Reviews*. 2000; **100**(4):1391-1434. DOI: 10.1021/cr980462j
- [40] Dzhemilev UM, Vostrikova OS, Tolstikov GA, Ibragimov AG. New method for inserting ethyl group in β -position of higher α -olefins using diethylaluminum chloride. *Russian Chemical Bulletin*. 1979;**28**:2441-2442. DOI: 10.1007/BF00951739
- [41] Dzhemilev UM, Ibragimov AG, Vostrikova OS, Tolstikov GA, Zelenova LM. New method of β -alkylation of α -olefins using dialkylaluminum chlorides with catalytic amounts of Ti, Zr, and Hf complexes. *Russian Chemical Bulletin*. 1981;**30**:281-284. DOI: 10.1007/BF00953581
- [42] Dzhemilev UM, Ibragimov AG, Vostrikova OS., Tolstikov GA. Carbalumination of higher α -olefins catalyzed by titanium and zirconium complexes. *Russian Chemical Bulletin*. 1985;**34**:196-197. DOI: 10.1007/BF01157356
- [43] Kondakov DY, Negishi E. Zirconium-catalyzed enantioselective methylalumination of monosubstituted alkenes. *Journal of the American Chemical Society*. 1995;**117**:10771-10772. DOI: 10.1021/ja00148a031
- [44] Kondakov DY, Negishi E. Zirconium-catalyzed enantioselective alkylalumination of monosubstituted alkenes proceeding via noncyclic mechanism. *Journal of the American Chemical Society*. 1996;**118**:1577-1578. DOI: 10.1021/ja953655m
- [45] Christoffers J, Bergman RG. Zirconocene-alumoxane (1:1) – a catalyst for the selective dimerization of α -olefins. *Inorganica Chimica Acta*. 1998;**270**:20-27. DOI: 10.1016/S0020-1693(97)05819-2
- [46] Parfenova LV, Gabdrakhmanov VZ, Khalilov LM, Dzhemilev UM. On study of chemoselectivity of reaction of trialkylalanes with alkenes, catalyzed with Zr π -complexes. *Journal of Organometallic Chemistry*. 2009;**694**:3725-3731. DOI: 10.1016/j.jorganchem.2009.07.037
- [47] Kaminsky W, Sinn H. Mehrfach durch Metalle Substituierte Athane. *Liebigs Annalen der Chemie*. 1975;(3):424-437. DOI: 10.1002/jlac.197519750307
- [48] Kaminsky W, Vollmer HJ. Kernresonanzspektroskopische Untersuchungen an den Systemen Dicyclopentadienyl zircon (IV) und Organoaluminium. *Liebigs Annalen der Chemie*. 1975;(3):438-448. DOI: 10.1002/jlac.197519750308
- [49] Yoshida T, Negishi E. Mechanism of the zirconium-catalyzed carboalumination of alkynes. Evidence for direct carboalumination. *Journal of the American Chemical Society*. 1981;**103**:4985-4987. DOI: 10.1021/ja00406a071
- [50] Negishi E., Kondakov DY, Choueiri D, Kasai K, Takahashi T. Multiple mechanistic pathways for zirconium-catalyzed carboalumination of alkynes. Requirements for cyclic carbometallation processes involving C-H activation. *Journal of the American Chemical Society*. 1996;**118**:9577-9588. DOI: 10.1021/ja9538039

- [51] Beck S, Brintzinger HH. Alkyl exchange between aluminium trialkyls and zirconocene dichloride complexes—a measure of electron densities at the Zr center. *Inorganica Chimica Acta*. 1998;**270**:376-381. DOI: 10.1016/S0020-1693(97)05871-4
- [52] Tritto I, Zucchi D, Destro M, Sacchi MC, Dall’Occo T, Galimberti M. NMR investigations of the reactivity between zirconocenes and β -alkyl-substituted aluminoxanes. *Journal of Molecular Catalysis A Chemical*. 2000;**160**:107-114. DOI: 10.1016/S1381-1169(00)00237-5
- [53] Tebbe FN, Parshall GW, Reddy GS. Olefin homologation with titanium methylene compounds. *Journal of the American Chemical Society*. 1978;**100**:3611-3613. DOI: 10.1021/ja00479a061
- [54] Bochmann M, Lancaster SJ. Cationic group IV metal alkyl complexes and their role as olefin polymerization catalysts: The formation of ethyl-bridged dinuclear and heterodinuclear zirconium and hafnium complexes. *Journal of Organometallic Chemistry*. 1995;**497**:55-59. DOI: 10.1016/0022-328X(95)00109-4
- [55] Rocchigiani L, Busico V, Pastore A, Macchioni A. Comparative NMR study on the reactions of Hf(IV) organometallic complexes with Al/Zn alkyls. *Organometallics*. 2016;**35**:1241-1250. DOI: 10.1021/acs.organomet.6b00088
- [56] Khalilov LM, Parfenova LV, Rusakov SV, Ibragimov AG, Dzhemilev UM. Synthesis and conversions of metallocycles. 22. NMR studies of the mechanism of Cp₂ZrCl₂-catalyzed cycloalumination of olefins with triethylaluminum to form aluminacyclopentanes. *Russian Chemical Bulletin*. 2000;**49**:2051-2058. DOI: 10.1023/A:1009536328369
- [57] Balaev AV, Parfenova LV, Gubaidullin IM, Rusakov SV, Spivak SI, Khalilov LM, Dzhemilev UM. The mechanism of Cp₂ZrCl₂-Catalyzed alkene cycloalumination with triethylaluminum to give alumacyclopentanes. *Doklady Physical Chemistry*. 2001;**381**:279-282. DOI: 10.1023/A:1012900227841
- [58] Gabdrakhmanov VZ. Mechanism of catalytic olefin carboalumination by trialkylalanes in the presence of Zr η^5 -complexes [dissertation]. Ufa; 2010. p. 112
- [59] Kovyazin PV, Permyakov VK, Parfenova LV, Nifant’ev IE, Khalilov LM, Dzhemilev UM. Zirconium ansa-complexes as catalysts in reactions of trialkylalanes with alkenes. In: *Book of Abstracts of International Symposium «Modern trends in Organometallic Chemistry and Catalysis»* (devoted to 90th Anniversary of Academician M.E. Volpin); June 3-7; Moscow. 2013. p. P48
- [60] Parfenova LV, Berestova TV, Molchankina IV, Khalilov LM, Whitby RJ, Dzhemilev UM. Stereocontrolled monoalkylation of mixed-ring complex CpCp’ZrCl₂ (Cp’ = 1-neomenthyl-4,5,6,7-tetrahydroindenyl) by lithium, magnesium and aluminum alkyls. *Journal of Organometallic Chemistry*. 2013;**726**:37-45. DOI: 10.1016/j.jorganchem.2012.12.004
- [61] Tyumkina TV, Islamov DN, Parfenova LV, Whitby RJ, Khalilov LM, Dzhemilev UM. Mechanistic aspects of chemo- and regioselectivity in Cp₂ZrCl₂-catalyzed alkene cycloalumination by AlEt₃. *Journal of Organometallic Chemistry*. 2016;**822**:135-143. DOI: 10.1016/j.jorganchem.2016.08.019

- [62] Dzhemilev UM, Ibragimov AG. Regio- and stereoselective synthesis for a novel class of organoaluminium compounds — substituted aluminacyclopentanes and aluminacyclopentenes assis. *Journal of Organometallic Chemistry*. 1994;**466**:1-4. DOI: 10.1016/0022-328X(94)88022-0
- [63] Dzhemilev UM. Catalytic replacement of transition metal atoms in metallocarbycles by the atoms of nontransition metals. *Mendeleev Communications*. 2008;**18**:1-5. DOI: 10.1016/j.mencom.2008.01.001
- [64] Hoveyda AH, Morken JP. Enantioselective C-C and C-H bond formation mediated or catalyzed by chiral ebthi complexes of titanium and zirconium. *Angewandte Chemie International Edition*. 1996;**35**:1263-1284. DOI: 10.1002/anie.199612621
- [65] Hoveyda AH. Chiral zirconium catalysts for enantioselective synthesis. In: Marek I, editor. *Titanium and Zirconium in Organic Synthesis*. Weinheim, Germany: Wiley-VCH Verlag GmbH & Co. KgaA; 2002. pp. 180-229. Chapter 6. DOI: 10.1002/3527600671.ch6
- [66] Parfenova LV, Berestova TV, Tyumkina TV, Kovyazin PV, Khalilov LM, Whitby RJ, Dzhemilev UM. Enantioselectivity of chiral zirconocenes as catalysts in alkene hydro-, carbo- and cycloaluminum reactions. *Tetrahedron Asymmetry*. 2010;**21**:299-310. DOI: 10.1016/j.tetasy.2010.01.001
- [67] Parfenova LV, Kovyazin PV, Tyumkina TV, Makrushina AV, Khalilov LM, Dzhemilev UM. Catalytic enantioselective ethylaluminum of terminal alkenes: Substrate effect and absolute configuration assignment. *Tetrahedron Asymmetry*. 2015;**26**:124-135. DOI: 10.1016/j.tetasy.2014.11.019
- [68] Parfenova LV, Zakirova IV, Kovyazin PV, Karchevsky SG, Istomina GP, Khalilov LM, Dzhemilev UM. Intramolecular mobility of η^5 -ligands in chiral zirconocene complexes and enantioselectivity of alkene functionalization by organoaluminum compounds. *Dalton Transactions*. 2016;**45**:12814-12826. DOI: 10.1039/c6dt01366j
- [69] Parfenova LV, Kovyazin PV, Tyumkina TV, Berestova TV, Khalilov LM, Dzhemilev UM. Asymmetric alkene cycloaluminum by AlEt₃, catalyzed with neomenthylindenyl zirconium η^5 -complexes. *Journal of Organometallic Chemistry*. 2013;**723**:19-25. DOI: 10.1016/j.jorganchem.2012.10.021
- [70] Parfenova LV, Berestova TV, Kovyazin PV, Yakupov AR, Mesheryakova ES, Khalilov LM, Dzhemilev UM. Catalytic cyclometallation of allylbenzenes by EtAlCl₂ and Mg as new route to synthesis of dibenzyl butane lignans. *Journal of Organometallic Chemistry*. 2014;**772-773**:292-298. DOI: 10.1016/j.jorganchem.2014.09.033
- [71] Bell L, Whitby RJ, Jones RVH, Standen MCH. Catalytic asymmetric carbomagnesian of unactivated alkenes. A new, effective, active, cheap and recoverable chiral zirconocene. *Tetrahedron Letters*. 1996;**37**:7139-7142. DOI: 10.1016/0040-4039(96)01561-4
- [72] Bell L, Brookings DC, Dawson GJ, Whitby RJ, Jones RVH, Standen MCH. Asymmetric ethylmagnesian of alkenes using a novel zirconium catalyst. *Tetrahedron*. 1998;**54**:14617-14634. DOI: 10.1016/S0040-4020(98)00920-X

- [73] Shaughnessy H, Waymouth RM. Enantio- and diastereoselective catalytic carboalumination of 1-Alkenes and α , ω -dienes with cationic zirconocenes: Scope and mechanism. *Organometallics*. 1998;**17**:5728-5745. DOI: 10.1021/om9807811
- [74] Wipf P, Ribe S. Water/MAO acceleration of the zirconocene-catalyzed asymmetric methylalumination of α -olefins. *Organic Letters*. 2000;**2**:1713-1716. DOI: 10.1021/ol005865w
- [75] Wipf P, Ribe S. Water-accelerated tandem Claisen rearrangement-catalytic asymmetric carboalumination. *Organic Letters*. 2001;**3**:1503-1505. DOI: 10.1021/ol015816z
- [76] Millward DB, Cole AP, Waymouth RM. Catalytic carboalumination of olefins with cyclopentadienyl amidotitanium dichloride complexes. *Organometallics*. 2000;**19**:1870-1878. DOI: 10.1021/om990707y
- [77] Petros RA, Camara JM, Norton JR. Enantioselective methylalumination of α -olefins. *Journal of Organometallic Chemistry*. 2007;**692**:4768-4773. DOI: 10.1016/j.jorganchem.2007.06.028
- [78] Ota Y, Murayama T, Nozaki K. One-step catalytic asymmetric synthesis of all-syn deoxypropionate motif from propylene: Total synthesis of (2R,4R,6R,8R)-2,4,6,8-tetramethyldecanoic acid. *Proceedings of the National Academy of Sciences*. 2016;**113**:2857-2861. DOI: 10.1073/pnas.1518898113

Alkene Metathesis

Olefin Metathesis by Group VI (Mo, W) Metal Compounds

Frédéric Lefebvre, Yassine Bouhoute, Kai C. Szeto,
Nicolas Merle, Aimery de Mallmann,
Régis Gauvin and Mostafa Taoufik

Additional information is available at the end of the chapter

<http://dx.doi.org/10.5772/intechopen.69320>

Abstract

Olefin metathesis is an important reaction not only in petroleum chemistry but also in fine chemistry. Professors Grubbs, Schrock, and Chauvin obtained the Nobel Prize in 2005 for the development of this reaction (determination of the mechanism and synthesis of homogeneous catalysts). This reaction can be described as the redistribution of carbon chains of olefins via a breaking of their C=C double bonds. It is catalyzed by metal carbenes and the catalytic cycle passes through a metallacyclobutane. The purpose of this chapter is to give an overview of catalysts based on tungsten or molybdenum active for this reaction. Numerous tungsten and molybdenum organometallic complexes displaying a carbene functionality were synthesized. Some of them are highly active in olefin metathesis. Industrially, tungsten oxide on silica is used as a precursor of the propene production by olefin metathesis of but-2-ene and ethylene. However, the active sites are not well known but they can be modeled by grafting, via surface organometallic chemistry, perhydrocarbyl complexes of molybdenum or tungsten on oxide surfaces. After a review of the complexes used in homogeneous catalysis, a review of the industrial catalysts and their models will be given.

Keywords: olefin metathesis, molybdenum, tungsten, heterogeneous catalysis

1. Introduction

Olefin metathesis can be described as the redistribution of the two fragments obtained by breaking the double bond of an olefin (**Figure 1**). This reaction is of great interest not only for industry (for example, for the production of propene from ethylene and butene) but also for organic chemistry, mainly for the formation of cycles [1].

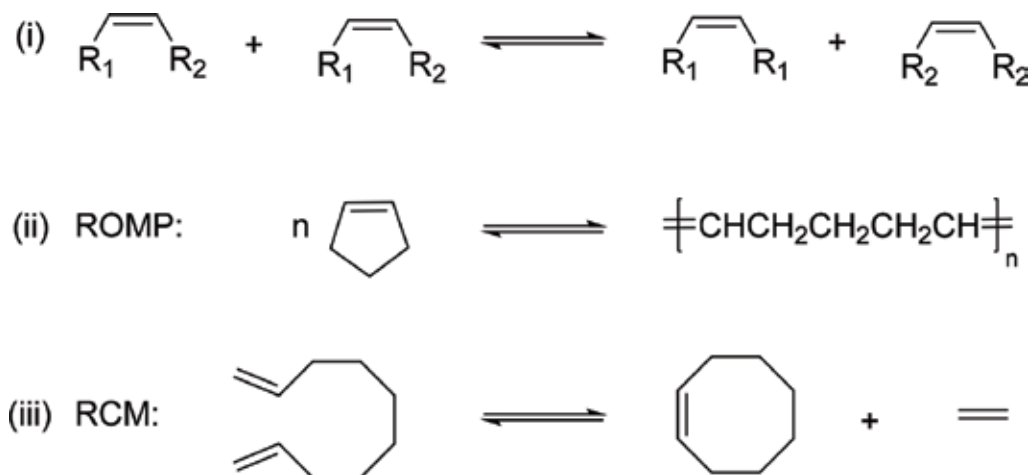


Figure 1. The three olefin metathesis reactions.

Historically, the reaction was not recognized as a metathesis reaction. At the end of the 1950s, there were many studies in industrial laboratories on the catalytic effects of systems containing transition metal ions on unsaturated hydrocarbons. These works had been initiated partly by the results of Ziegler and Natta in the field of ethylene and propene polymerization and partly by those obtained by Phillips and Standard Oil in ethylene polymerization by heterogeneous systems. Many observations were made which could not be explained by the reactions known at this period. Finally, it was really Calderon and Ofstead, at Goodyear, who obtained the first conclusive results, which led to the formulation of metathesis as a general principle of reversible scission and recombination of carbon-carbon double bonds.

The olefin metathesis reaction can be divided into three different reactions (**Figure 1**): (i) the homo-metathesis and the cross-metathesis which involve the exchange of fragments of acyclic olefins; (ii) the ring opening metathesis polymerization (ROMP), which involves the opening of a cyclic olefin, and (iii) the ring closing metathesis (RCM), which corresponds to the formation of a cyclic olefin by reaction of a diene. Three other classes of olefin metathesis are (iv) ring-opening metathesis polymerization, (v) acyclic diene metathesis, and (vi) ethenolysis.

The mechanism of the olefin metathesis reaction remained unknown for several years and various intermediates were postulated. In 1968, Calderon proposed a cyclobutane coordinated to the metal as an intermediate species (**Figure 2**) [2]. Pettit proposed the formation of a tetramethylene complex [3], while Grubbs postulated the formation of a metallacyclopentane [4].

Finally, Chauvin proposed the now admitted and experimentally proved mechanism of the olefin metathesis reaction and obtained the Nobel Prize in 2005 with Grubbs and Schrock for this discovery [5]. This mechanism necessitates the presence of a metallocarbene species which can coordinate an olefin, leading to the formation of a metallacyclobutane. Upon rearrangement this cycle will lead to the formation of a new olefin and restore the metal carbene species (**Figure 3**).

This mechanism implies that the reactions are equilibrated and the metallacyclobutane can lead to new products (productive metathesis) or to the starting olefins (degenerative metathesis).

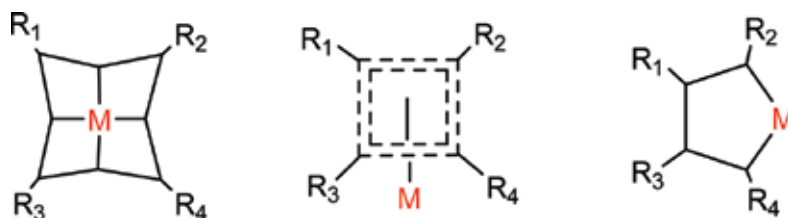


Figure 2. Intermediates proposed for the olefin metathesis reaction.

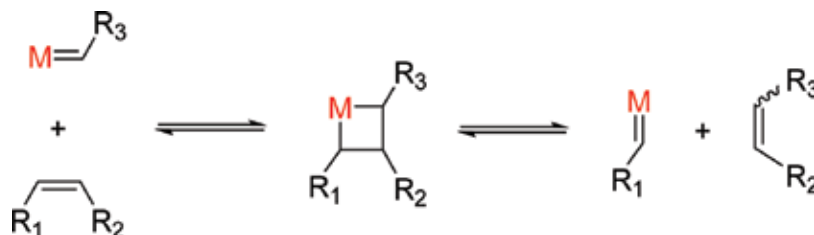


Figure 3. Mechanism of the olefin metathesis reaction.

This mechanism has been confirmed by the synthesis of homogeneous complexes containing a nucleophilic carbenic function and the formation of a metallacyclobutane by their reaction with an olefin [6, 7]. These species display a good activity in the olefin metathesis reaction, in agreement with a mechanism involving them. In addition, numerous complexes with metallacyclobutane intermediates were isolated and gave additional proofs to the Chauvin's mechanism [8, 9]. During last years, the development of highly active homogeneous and heterogeneous catalysts made the olefin metathesis reaction a powerful tool in numerous domains such as petrochemistry, polymers synthesis, fine chemistry, and synthesis of natural products.

Usually, olefin metathesis catalysts contain elements from groups 6 to 8, typically molybdenum, tungsten, rhenium, and ruthenium. While catalysts based on ruthenium are widely used in organic synthesis at the laboratory scale, molybdenum and tungsten are used industrially at a larger scale. Systems based on rhenium were developed but their use remains marginal.

Due to the importance of catalysts based on group (VI) elements, this review will be limited to them, with the aim to have a better understanding of the nature of the active sites in the industrial systems.

2. Group VI complexes used in homogeneous catalysis

The first homogeneous catalytic systems using group VI metals (W or Mo) were ill-defined Ziegler-Natta type compounds, formed *in situ* by contacting a precatalyst and a cocatalyst [10]. The first example of olefin metathesis was described in 1955 by Anderson and Merckling who observed the formation of polynorbornene during the reaction of norbornene and $\text{TiCl}_4/\text{LiAl}(\text{heptyl})_4$ [11]. Two other catalytic systems based on quite the same elements ($\text{WCl}_6/\text{AlEt}_3$

and $\text{MoCl}_5/\text{AlEt}_3$) were described by Natta et al. in 1964 [12]. Depending on the catalytic system used, trans- or cis-polymers were obtained by polymerization of cyclopentene and tungsten leading to the trans compound. Later, various catalysts based on tungsten combined to an alkylating agent were described such as $\text{WCl}_6/\text{EtOH}/\text{EtAlCl}_2$, $\text{WCl}_6/\text{SnBu}_4$, or $(\text{ArO})_4\text{WCl}_2/\text{SnMe}_4$ and are active for the metathesis of internal olefins such as cis-pent-2-ene [13–15]. Systems based on the combination of nitrosyl complexes of molybdenum or tungsten with alkylaluminum species were developed for the metathesis of terminal olefins (pent-1-ene, oct-1-ene) [16–19]. In parallel, many academic researchers tried to synthesize metal alkylidene species which should be active for olefin metathesis as proposed by Chauvin. Casey et al. isolated in 1973 the first electrophilic metal alkylidene, $[(\text{CO})_5\text{W}=\text{C}(\text{C}_6\text{H}_5)_2]$, which is of the Fisher type and is active in olefin metathesis at room temperature without any cocatalyst [20]. After 1980, Schrock has prepared all a family of molybdenum and tungsten complexes with nucleophilic carbene functions. The general formula of these complexes, which are highly active in olefin metathesis, is $[\text{M}(\text{=CHCMe}_2\text{Ph})(\text{=N-Ar})(\text{OR}')_2]$ where R' and Ar are sterically encumbered groups. The structure of some of these complexes is depicted in **Figure 4**.

As these complexes are not very sensitive to functional groups, their use was then extended to fine chemistry [21, 22], oleochemistry [23], and to the synthesis of functional polymers [24] while during many years olefin metathesis was confined to nonfunctional olefins. In these complexes, the metal is surrounded by the carbene moiety and by various electro-attractor and/or sterically encumbered ligands allowing a good stability in solution and good activity, selectivity, and stability. For example, complex **6**, which contains an imido group and a binaphthyl

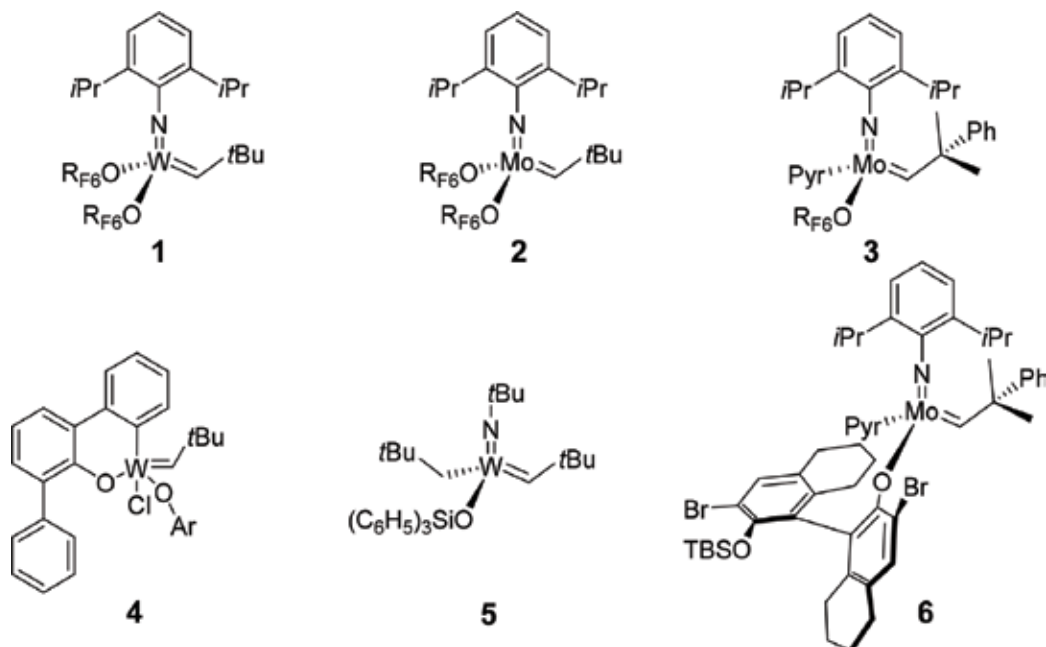


Figure 4. Some W(VI) and Mo(VI) complexes bearing imido, aryloxy, and carbenic functions highly active in olefin metathesis.

ligand, is able to perform the cross-metathesis of methyl oleate with ethylene (**Figure 5**) with a good yield (Turnover number (TON) = 4750) [23]. The reaction products, dec-1-ene and methyl decen-9-oate, are important intermediates in the chemical industry and are used for the preparation of polyolefins, surfactants, and lubricating compounds. The TON can be considerably increased (up to 50,000) upon addition of $\text{Al}(\text{octyl})_3$ [25].

Osborn et al. have developed another family of complexes where the imido group is replaced by an oxo ligand. For that purpose, they prepared oxo alkyl complexes of molybdenum and tungsten. The idea was that these species were not stable, due to the small energy of the metal-carbon bond, and should lead to the formation of the carbenic complex upon α -H abstraction. Oxo complexes of molybdenum and tungsten with neopentyl and/or neosilyl ligands were prepared (**Figure 6**) [26] and are active in the metathesis of linear, cyclic, and functional olefins, but in presence of Lewis acids such as AlCl_3 , SnCl_4 , or GaCl_3 [27, 28].

Later, Schrock et al. have synthesized pentacoordinated complexes of tungsten(VI) with oxo and alkylidene groups stabilized by phosphine ligands (**Figure 7**) [29, 30]. These systems are active in metathesis of terminal and internal olefins in presence of a Lewis acid such as AlCl_3 [31].

Complex **9**, which contains two chloro ligands, has been used as a precursor for the preparation of numerous oxo carbenic complexes where chlorine was replaced by other ligands such as phenoxide, pyrrolidyl, thiophenoxide, or siloxide. By this way, Schrock et al. have studied the effect of the modification of the coordination sphere of this complex on its activity and selectivity in metathesis of terminal olefins and ROMP of norbornene derivatives. For example, $\text{W}(=\text{O})(\text{CHCMe}_2\text{Ph})-(\text{Me}_2\text{Pyr})(\text{OAr})$ (Me_2Pyr = 2,5-dimethylpyrrolide, OAr = aryloxy) **13** is active in ROMP of 2,3-dicarbomethoxynorbornadiene (DCMNBD) and leads selectively to the cis syndiotactic polymer while complex $\text{W}(=\text{O})(\text{CHCMe}_2\text{Ph})(\text{OR})_2$ **10** leads selectively to the cis isotactic polymer [32]. Addition of a Lewis acid such as $\text{B}(\text{C}_6\text{F}_5)_3$ leads to a considerable increase of both the activity and the selectivity.

Complexes with thiophenoxide ligands were also prepared and their activity in metathesis of oct-1-ene and polymerization of DCMNBD was compared to that of the corresponding

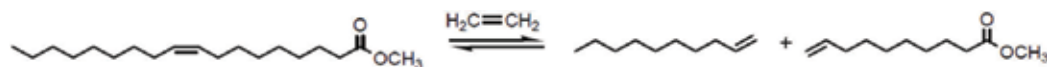


Figure 5. Cross-metathesis of ethylene and methyl oleate.

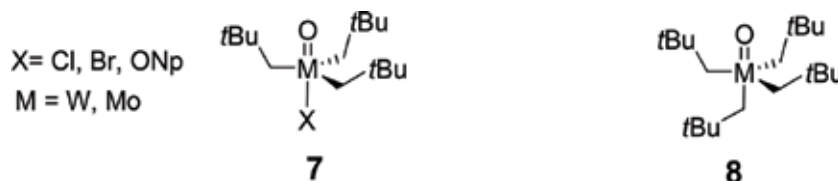


Figure 6. Oxo alkyl complexes synthesized by Osborn et al.

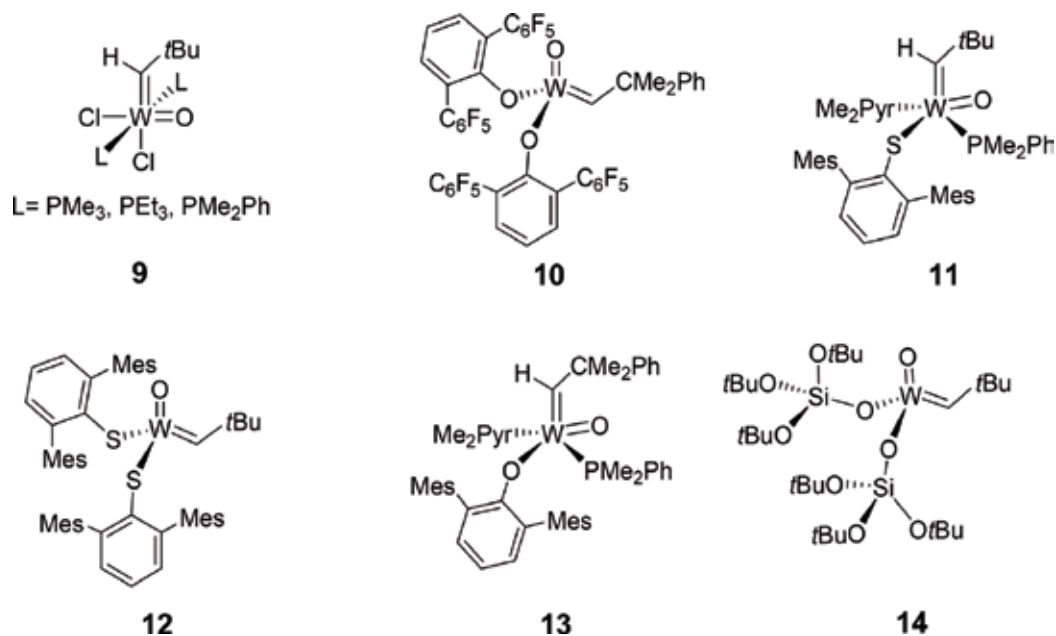
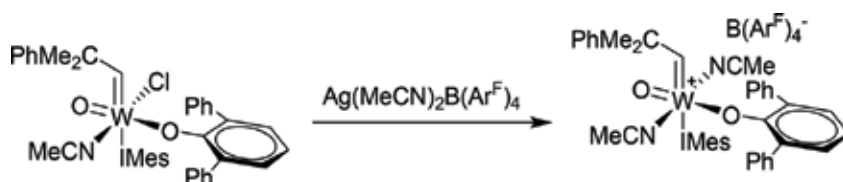


Figure 7. Oxo carbenic complexes synthesized by Schrock et al.



phenoxide complexes. They are less active and less selective. This was attributed to a higher electronic density around the metal, due to a stronger σ -donor effect of thiophenoxides compared to phenoxides [33]. The bis-siloxy oxo alkylidene tungsten complex **14** has been described recently. However, it displays a low initial activity (Turnover frequency (TOF) = 12 min⁻¹) in metathesis of cis oct-4-ene at 80°C. This low activity has been explained by the low thermal stability of this complex in absence of phosphine ligands [34].

Buchmeiser et al. have increased the catalytic activity of these oxo complexes by increasing the electrophilicity of the metal by transforming them into cationic species. They have reported recently the synthesis and X-ray structure of the first stable cationic complex of tungsten by removing chlorine of the W–Cl bond by reaction with Ag(MeCN)₂B(ArF)₄ (**Figure 8**). This complex is highly active (the TONs can reach 10,000) in metathesis of olefins functionalized by nitrile, sec-amine, or thioether groups [35].

3. Solids containing group VI (Mo, W) metal ions used in heterogeneous catalysis

Oxides of group VI (molybdenum and tungsten) and group VII (rhenium) are often used in industrial processes when they are supported on silica or alumina. The triolefin process, developed by Phillips (**Figure 9**), was the first commercial application using WO_3 supported on silica for olefin metathesis [36]. Initially, this process was developed in order to convert propene into ethylene and but-2-ene. Later, due to the increasing request of propene for the synthesis of numerous chemicals (polypropylene, acrylonitrile, propene oxide, cumene, and acetone), new processes were developed for the production of propene.

Actually, the propene production by metathesis is mainly made by use of the OCT (Olefins Conversion Technology) process, developed by ABB Lummus Technology at Houston. This reaction is the reverse of the triolefin process, with quite the same catalyst [37, 38]. It produces ca. 6% of the world production (6.5 Mtons/year in 2014). The SHOP (Shell Higher Olefins Process) is one of the main industrial processes using olefin metathesis for the production of α -olefins, which are precursors for plasticizers and detergents [37, 39]. The catalyst is based on $\text{MoO}_3/\text{Al}_2\text{O}_3$ or WO_3/SiO_2 , the production ability being ca. 1.2 Mtons/year [37]. Another industrial process using olefin metathesis is the synthesis of neohexene from di-isobutene and ethylene (**Figure 10**). Neohexene is mainly used for perfumes where it is a starting material for the obtention of synthetic musks [40].

The main application of these heterogeneous systems is in petrochemistry and their use in other domains such as organic synthesis, oleochemistry, or polymerization remains very limited, mainly due to the drastic conditions which are required and to their intolerance of functional groups. The most often used catalyst is WO_3/SiO_2 due to the following reasons: (i) it is resistant to poisoning by oxygenated and sulfided compounds due to the high reaction temperature (more than 350°C) [41, 42]; (ii) even if the coke formation is important at high temperature, the catalyst can be regenerated easily by calcination in air [42], without decomposition of the active sites, in

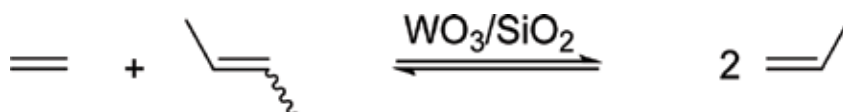


Figure 9. The Triolefin process developed by Phillips.

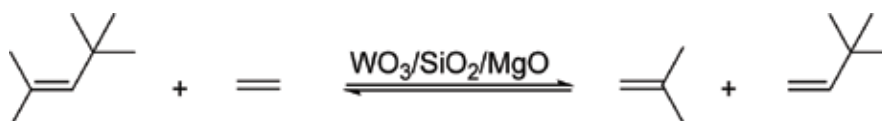


Figure 10. Synthesis of neohexene by olefin metathesis.

contrast to other systems such as $\text{MoO}_3/\text{Al}_2\text{O}_3$ or $\text{Re}_2\text{O}_7/\text{Al}_2\text{O}_3$; and (iii) its preparation is easy, by impregnation of a high surface area silica by an aqueous solution of ammonium metatungstate $[(\text{NH}_4)_6\text{H}_2\text{W}_{12}\text{O}_{40} \cdot x\text{H}_2\text{O}]$.

A lot of studies were made on the WO_3/SiO_2 system, before and after activation by propene, by using various spectroscopic methods such as Raman, UV-visible, EPR, XANES, and EXAFS. The first studies were made by Raman and led to the conclusion that the active site was an isolated surface complex of tungsten but of unknown structure [43]. The first postulated surface species was a pentacoordinated tungsten complex but no experimental justification was given [44].

In 1991, Basrur et al. have proposed that the active species of the WO_3/SiO_2 catalyst was a bis-oxo bis-siloxy tungsten complex $[(\equiv\text{SiO})_2\text{W}(=\text{O})_2]$ and that the activation by propene led to a reduction of tungsten and formation of acetone or to a transformation of the $\text{W}=\text{O}$ double bond into a metal-carbene bond with liberation of acetaldehyde [45]. A characterization by EXAFS at room temperature of WO_3/SiO_2 has shown that polytungstic species are present on the surface of silica [46]. By using a combination of Raman and UV-visible spectroscopies *in situ*, Wachs et al. have shown that, at room temperature, the tungsten oxide phase is composed of nanoparticles of WO_3 and of polyoxotungstate clusters $(\text{W}_{12}\text{O}_{39})^{6-}$, **17** (**Figure 11**). After dehydration at 450°C under air, these polyoxotungstate clusters evolve into bis-oxo bis-siloxy tungsten species **15** and mono-oxo tetra-siloxy tungsten species **16** while the nanoparticles remain unchanged [47, 48].

Some authors have studied propene metathesis on WO_3/SiO_2 and have shown that the reaction rate is linearly dependent on the propene partial pressure [49]. It has also been reported that the amount of surface tungsten and the treatment of the catalyst by an inert gas (nitrogen, argon, helium) [45] or by hydrogen [50] have a significant effect on the catalytic activity.

Recently, Wachs et al. have studied the effect of the WO_3 amount on silica on the catalytic activity in propene metathesis at 300°C . The results are depicted in **Figure 12**. The catalytic activity increases with the amount of WO_3 until a value of ca. 8 wt.% and then remains quite constant. These results were explained as follows: At low coverage ($\text{WO}_3 < 8$ wt.%) the catalytic activity is proportional to the amount of isolated mono-oxo and di-oxo species (which are all assumed to be active in olefin metathesis). At high coverage, the reaction rate is not dependent on the tungsten loading, due to the formation of WO_3 crystallites which are inactive [51]. There is also an effect of the WO_3 loading on the amount to ethylene and butenes.



Figure 11. Proposed molecular structures for WO_3/SiO_2 .

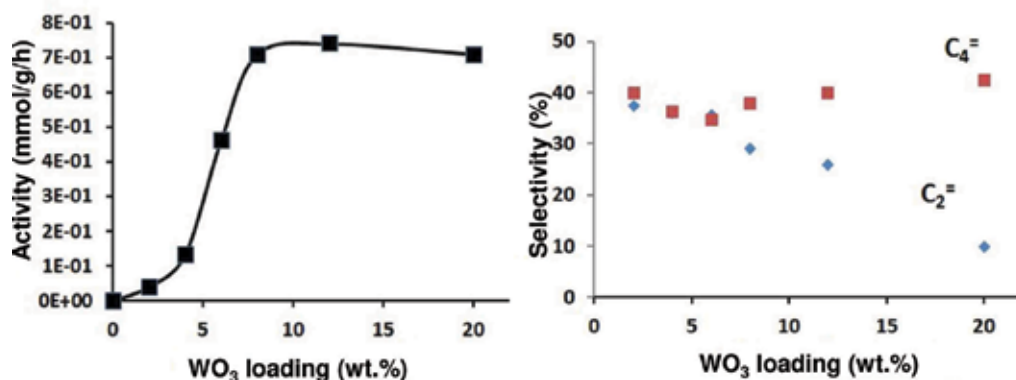


Figure 12. Conversion and ethylene/butene ratio as a function of the WO₃ loading during propene metathesis at 300°C.

At low coverage, the ethylene/butene ratio is equal to ca. 1 as expected while at high coverage it decreases strongly, due to the formation of C₄–C₆ alkanes. This was interpreted as due to the presence of Brønsted acid sites on the WO₃ crystallites (or nanoparticles), which led to oligomerization and cracking [51].

Recently operando methods (UV-Vis, Raman, XANES/EXAFS) were used in order to characterize the catalyst during its pretreatment and in presence of propene, the aim being to establish a structure-activity relationship. Wachs et al. studied by Raman the effect of the pretreatment in air on a WO₃/SiO₂ catalyst as a function of the oxide loading [51]. For low coverages, the Raman spectrum shows new bands at 1016 and 958 cm⁻¹, which were attributed to the symmetric vibrations of di-oxo and mono-oxo species, respectively. The di-oxo species displays also an asymmetric vibration band at 968 cm⁻¹. The absence of the W–O–W band at 200–300 cm⁻¹ confirms the absence, at low coverage, of WO₃ aggregates. These results are in agreement with the UV-visible results. When the tungsten amount is higher than 0.6%, the Raman peak at 990 cm⁻¹ increases with the amount of tungsten. At high loadings, three new bands appear at 270, 720, and 805 cm⁻¹, characteristic of tungsten oxide nanoparticles. The main conclusion of this study is that tungsten is well dispersed on the silica surface for WO₃ loadings below 8 wt.%.

The catalyst containing 4 wt.% was also studied by operando Raman spectroscopy during the metathesis reaction of propene (1% in argon) at 300°C. The bands characteristics of the mono-oxo and di-oxo species (which are the sole species on the solid) decrease simultaneously with time and disappear after 100 minutes [51]. This proves that the two species were activated by propene and led to the formation of carbene species with elimination of oxygen from the coordination sphere of tungsten (Figure 13). After reoxidation by an O₂/Ar mixture, the initial bands of the tungsten oxide species are restored with their intensity and no formation of nanoparticle is detected by Raman. For catalysts with high loadings (8 wt.% WO₃), the activation under propene leads to a strong decrease of the bands characteristic of the nanoparticles with formation of oxygenates such as formaldehyde or acetaldehyde but no acetone is formed. In addition, a study by ESR and UV-visible spectroscopy has shown that tungsten is mainly in the +VI oxidation state.

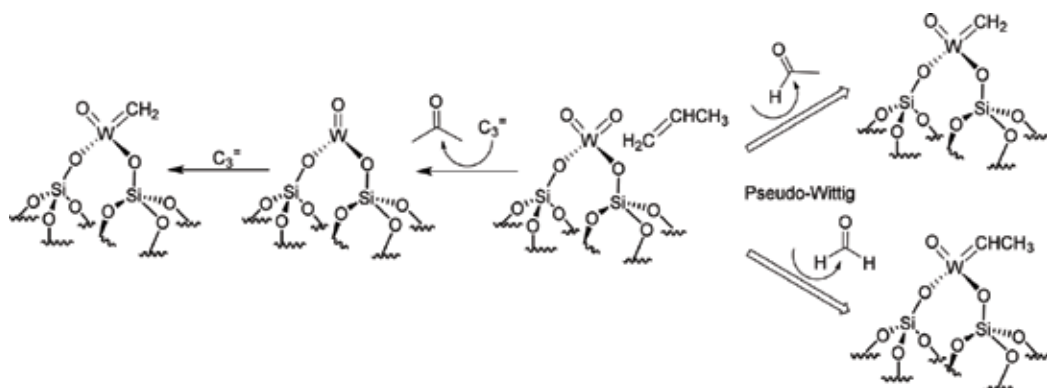


Figure 13. Possible mechanisms for the activation of the di-oxo tungsten species by propene.

However, Bell et al. [52] have recently shown by an *in situ* XANES study that there is a reduction of W(VI) to W(IV) during the activation of WO_3/SiO_2 at 500°C . This result is in agreement EXAFS data and with the formation of acetone during the activation (**Figure 13**). The amount of evolved acetone shows that for a catalyst containing 5.4 wt. only 5% of tungsten atoms are active in olefin metathesis. This value is similar to what had been reported for MoO_3 supported on silica [53] and that proposed by Wachs et al. for WO_3 on silica [51]. Unfortunately, no mechanism was proposed to explain the transformation of the mono-oxo tungsten (IV) species into the bis-oxo-oxo-carbene $(=\text{SiO})_2(\text{O})\text{W}=\text{CHR}$ ($\text{R} = \text{H}, \text{CH}_3$). Very recently Stair et al. have observed, during a Temperature Programmed Reduction (TPR) study of WO_3/SiO_2 in presence of propene, the formation of a mixture of methane, carbon monoxide, and hydrogen [54]. They proposed that the activation at 700°C is made via a pseudo-Wittig reaction with evolution of aldehydes, not stable at high temperature and which decompose into small molecules (**Figure 13**).

EXAFS spectra of a pretreated 5.4 wt.% WO_3/SiO_2 catalyst show the presence of mono-oxo and di-oxo tungsten species with contributions in the Fourier transform at 0.12 nm ($\text{W}=\text{O}$) and 0.16 nm ($\text{W}-\text{O}$) (the true distances take into account a phase correction and are slightly larger by 0.04 nm than those deduced from the Fourier transform). After treatment at 600°C under inert gas (helium), Bell et al. observed a decrease of the peak at 0.16 nm [52]. This decrease was attributed to the transformation of the mono-oxo species into the di-oxo one (**Figure 14**). This increase of the di-oxo concentration could explain the higher activity of this system compared to that obtained after activation under air.

Stair et al. reported recently that a pretreatment at high temperature of the WO_3/SiO_2 catalyst by a gas containing propene increased by two to three orders of magnitude its activity at low temperature [54]. Surprisingly, these catalysts can be regenerated by a treatment under nitrogen at high temperature.

Even if some tentative structure-activity relationships were made for the MO_3/SiO_2 ($\text{M} = \text{Mo}, \text{W}$) catalysts, the structure of the true active species is not really known up to now. The main problem is due to the low amount of active sites. Spectroscopic methods such as in-operando Raman,

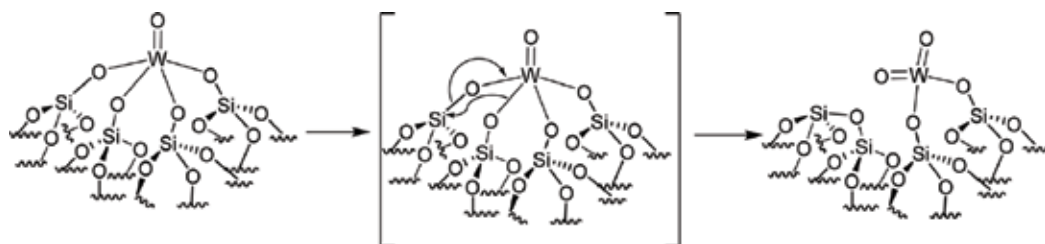


Figure 14. Conversion of the mono-oxo tungsten(VI) species into the di-oxo one.

UV-Vis, XANES, or EXAFS show all surface species, not only those which are active in olefin metathesis. As a consequence, it is very difficult to understand the activation mechanism of the catalyst (and also its deactivation).

The preparation of systems containing a higher amount of active sites could lead to more active (and easily regenerated) systems and could allow a better characterization and mechanistic study of the initiation and deactivation steps and their rationalization in terms of classical organometallic chemistry. Surface organometallic chemistry (SOMC) is a choice method for the preparation of silica supported complexes. Numerous tungsten complexes with a variety of ligands (alkyl, carbene, carbyne, oxo, imido, aryloxy, etc.) were immobilized on oxide supports in order to obtain single site species which can be applied for the valorization of hydrocarbons via various reactions (alkane or alkene metathesis, methane coupling, etc.) [55, 56]. These materials can be characterized by the same spectroscopic methods than the conventional catalysts (solid-state NMR, EXAFS, DRIFT, ESR, UV-Vis, etc.).

4. Supported tungsten catalysts prepared by SOMC

SOMC can be considered as a bridge between homogeneous and heterogeneous catalysis [55–57]. Its aim is to graft organometallic complexes on oxide surfaces (silica, alumina, titania, zirconia, etc.) or on metal surfaces. In the case of oxides, the complex can be linked to the support by one or more bonds with surface oxygen atoms. When the support has been previously functionalized, the bonding can be made via other atoms such as P, N, Si, etc. As it is the case in homogeneous catalysis, these surface organometallic species can be defined by their ligands around the metal. Two types of ligands can be considered, those which will be involved in the catalytic cycle and those which are only spectators (such as oxo, alkoxo, amido, or imido groups). The modification of both types of ligands can have a drastic effect on the activity and selectivity of a given catalytic reaction, allowing to establish structure-activity relationships. For example, pretreatment of the support at different temperatures will lead to the synthesis of surface complexes with one, two, or three bonds with the surface. This new approach has many advantages:

- The catalyst can be easily separated from the reaction products and recycled.
- The catalysts are single sites, as in homogeneous catalysis.

- The metal complexes have a limited mobility on the surface, avoiding the bimolecular decomposition reactions which are often observed in homogeneous catalysis [58].
- The catalysts can be characterized easily by use of spectroscopic methods, as all species are identical.
- The good knowledge of the structure of the active site allows to propose a reasonable catalytic cycle and to determine how deactivation and regeneration will proceed.

A lot of organometallic complexes of groups 4–8 were grafted on a variety of surfaces such as amorphous inorganic oxides [55], zeolites [59], or metals [60, 61]. This methodology led to numerous applications in fine chemistry and/or petrochemistry including reactions which were not known up to now. This is mainly due to a combination of organometallic synthesis and surface science. The catalytic efficiency of the materials prepared by this way depends on the coordination sphere around the metal, on the number, and the character (ionic or covalent) of the bonds with the support and on the nature of the oxide support (silica, alumina, silica-alumina, etc.).

In the case of tungsten SOMC, the choices of the organometallic precursor and of the support are mainly dependent on the expected catalytic reaction and on the intermediates involved in the postulated catalytic cycle. The high oxidation state of tungsten (VI) allows the possibility of a number of ligands in the coordination sphere leading to both spectators and reactive species in the catalytic cycle. The reactive species will be hydrides, alkyl, carbenes, and carbynes. During the last few years, many studies were made with such surface complexes in olefin metathesis. We will review here only those containing the oxo ligand as they could be considered as models of the industrial heterogeneous catalysts. There are two principal methodologies which have been developed to achieve well-defined tungsten oxo species on oxide: (i) grafting of a reactive tungsten carbyne complex followed by transfer of oxygen from the support and (ii) grafting of an organometallic complex bearing oxo ligand.

4.1. Supported tungsten complexes with oxo and hydride ligands

The first carbynic complex of tungsten(VI), $[W(\equiv C tBu)(CH_2 tBu)_3]$, was synthesized in 1978 by Clark and Schrock [62]. Later, various complexes of the same type were synthesized, for example, $[W(\equiv C tBu)X_3]$ ($X = Cl, OtBu, N^iPr_2$) [63, 64]. Some of these complexes (mainly those with a pronounced electrophilic character such as $[W(\equiv C tBu)(OtBu)_3]$) displayed a moderate activity in alkynes metathesis. Unfortunately, these systems deactivated rapidly by a bimolecular reaction leading to a dinuclear tungsten complex with a $W \equiv W$ triple bond [65, 66]. In order to avoid this deactivation, these complexes were heterogeneized. $[W(\equiv C tBu)X_3]$ ($X = Cl, OtBu, CH_2 tBu$) was grafted on silica partially dehydroxylated at 500°C. Weiss et al. proposed that there was formation of the carbenic species $[(\equiv SiO)W(\equiv C tBu)X_3]$ ($X = Cl, tBu$) by addition of the Si–OH bond of silica on the carbyne bond [67]. The carbenic ligand was evidenced by its reactivity with acetone via a pseudo-Wittig reaction and indirectly by the catalytic activity in olefin metathesis. $[W(\equiv C tBu)(CH_2 tBu)_3]$ was then grafted on silica, dehydroxylated at 200°C (SiO_{2-200}) and at 700°C (SiO_{2-700}). When silica was treated at 700°C the main reaction product was $[(\equiv SiO)W(\equiv C tBu)(CH_2 tBu)_2]$ **18**, while $[(\equiv SiO)_2W(\equiv C tBu)(CH_2 tBu)]$ **19** was formed on silica treated at 200°C (**Figure 15**) [68].

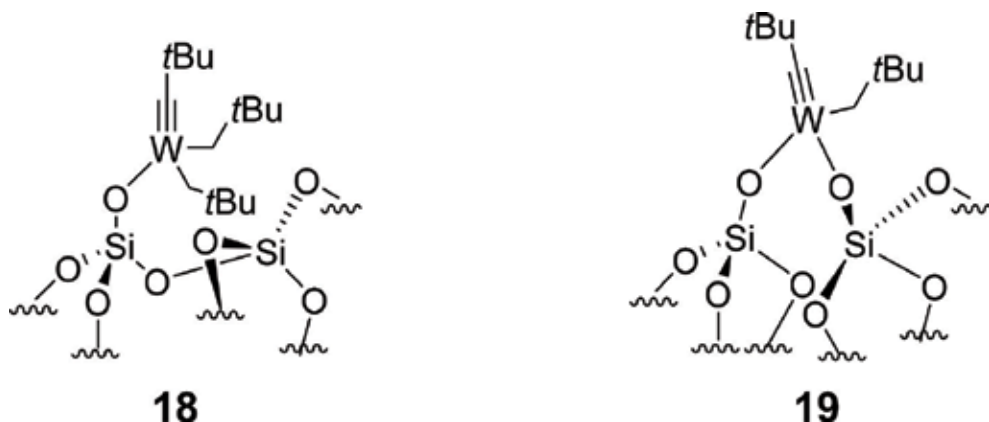


Figure 15. Species formed during the reaction of $[W(=CtBu)(CH_2tBu)_3]$ with SiO_{2-200} and SiO_{2-700} .

The structures of species **18** and **19** were confirmed by solid-state NMR (1H , ^{13}C , HETCOR, J-resolved). The interaction with the silica surface was studied by ^{17}O MAS NMR by using enriched silica [69]. This study showed the existence of interactions between protons of residual hydroxyl groups and the alkyl ligands of the supported species.

Species **18** shows a good activity in propene metathesis (initial TOF 5.5 min^{-1} , TON = 11,000 after 40 h) [68]. Two mechanisms were proposed explaining the formation of the carbene ligand. The first one is a α -H transfer from the alkyl ligand to the carbyne during the coordination of the olefin and formation of a bis-alkylidene complex [70]. The other possibility is to form directly the carbene by metathesis between the olefin and the carbyne: a metallacyclobutene is formed which decomposes into a carbene-alkenyl tungsten complex (**Figure 16**).

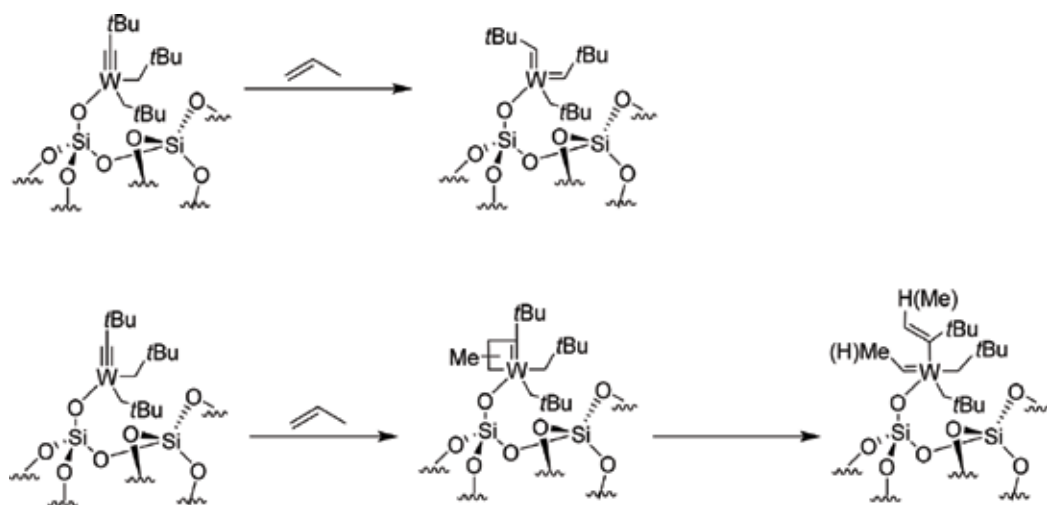


Figure 16. Possible mechanisms of formation of a carbene from the surface carbyne.

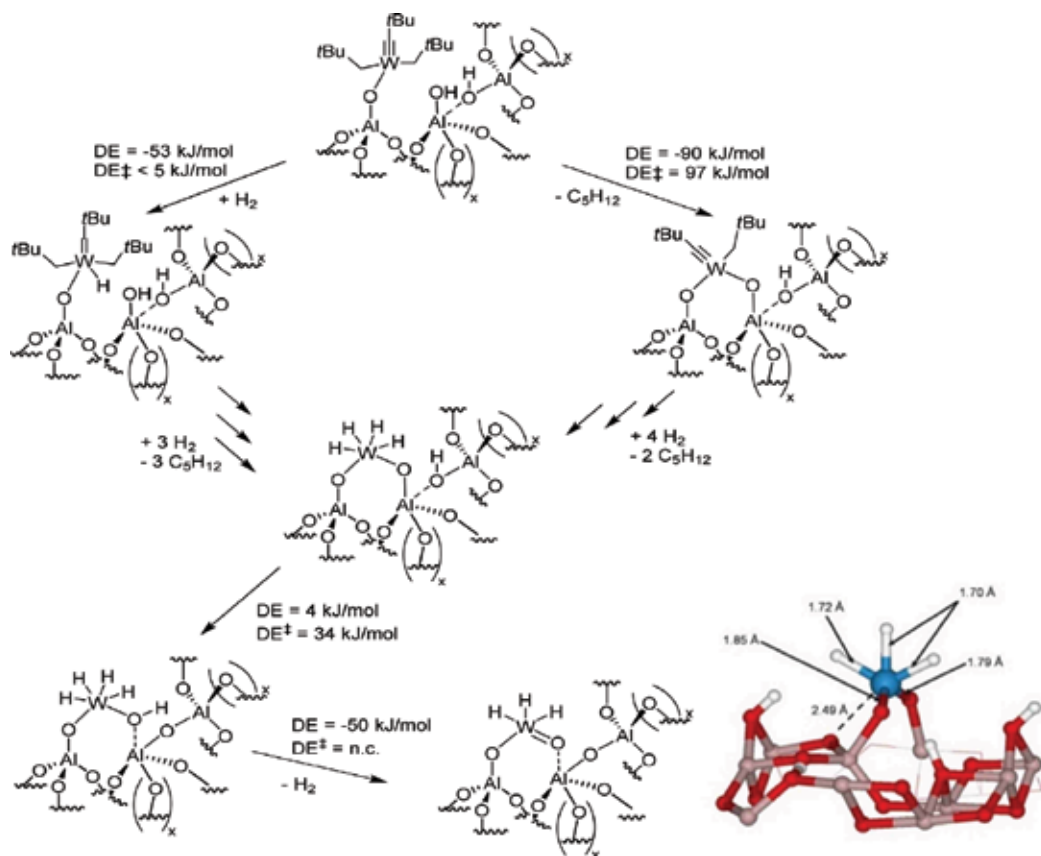


Figure 17. Mechanism proposed for the formation of the oxo hydride tungsten species on alumina.

The grafting reaction of $[W(\equiv C tBu)(CH_2 tBu)_3]$ was also studied on alumina dehydroxylated at $500^\circ C$. Alumina is a complex support as aluminum can be tetra-, penta-, or hexacoordinated and its surface hydroxyl groups can be bound to one, two, or three aluminum atoms. As a result, there is a great variety of hydroxyl groups with variable acidity. The determination of the surface complexes obtained after grafting needed the use of a variety of experimental (DRIFT, solid-state NMR, EXAFS) and theoretical (DFT calculations) methods [71]. The evolved gas (one neopentane per grafted tungsten) and microanalysis were in agreement with the formation of a complex having only one covalent bond with the surface, $[(Al_sO)W(\equiv C tBu)(CH_2 tBu)_2]$ **20**. The infrared study showed that there is a partial consumption of the hydroxyl groups and that only those linked to one tetrahedral aluminum have reacted [72]. The ^{13}C CP-MAS NMR spectrum of $[(Al_sO)W(\equiv C tBu)(CH_2 tBu)_2]$ shows only a broad signal between 50 and 110 ppm for the $W-CH_2$ -carbon atoms. DFT calculations show that this broadening is due to an interaction between these methylene groups and the residual surface aluminum groups.

In contrast to complexes **18** and **19** formed on silica, complex **20** has a good activity in propane metathesis at $150^\circ C$ with an initial TOF equal to $1.8 h^{-1}$ [73]. The mechanism of this reaction

involves three steps: dehydrogenation of the alkane, olefin metathesis, and hydrogenation of the resulting olefin. This example shows that the support can have a nonnegligible effect on the catalysis. Treatment under hydrogen at 150°C of the complexes obtained on silica and alumina leads also to completely different species. On silica sintering is observed and TEM shows that tungsten particles (size 0.1–0.2 nm) are formed [71]. On alumina no sintering is observed and a hydride species is obtained [71, 73]. This hydride species is characterized by a small peak at 10.0 ppm in ^1H MAS NMR and by two infrared bands at 1903 and 1804 cm^{-1} . The attribution of the two infrared bands was confirmed by isotopic exchange W-H/W-D upon addition of deuterium [71]. In addition, EXAFS showed the presence of a W=O double bond [74]. All these data combined to DFT calculations allowed to propose that the surface hydride is a tris-hydride oxo tungsten(VI) complex stabilized by coordination of the oxo ligand to one surface aluminum (**Figure 17**) [75].

The mechanism of formation of this surface species was elucidated by use of DFT calculations. These calculations suggested that the oxo species is formed by reaction of an unstable tungsten hydride species with one oxygen atom of the alumina surface. Such a phenomenon is prohibited on silica surfaces due to the stability of the Si-O bond. This oxo-hydride tungsten is more active than the industrial WO_3/SiO_2 catalyst for the cross-metathesis of ethylene and but-2-ene to propene. For example, at 120°C the TON can reach 9000 and at 150°C 16,000 after 48 h. At 200°C the TON increases to 22,000 but a rapid deactivation of the catalyst is observed [76].

While an excess of ethylene is needed in the case of the industrial WO_3/SiO_2 catalyst to achieve a good selectivity to propene [77], the tungsten hydride on alumina is very selective (more than 98%) even for ethylene/butene ratios lower than 1. From a mechanistic point of view, the initiation step occurs via the insertion of three ethylene molecules in the W-H bonds, leading to a tris-ethyl tungsten surface complex (the insertion of ethylene is more favorable from both thermodynamic and kinetic points of view than that of but-2-ene [78, 79]). The next step is the elimination of ethane (which can be detected by gas chromatography) by a α -H abstraction, leading to the active ethyl-ethylidene oxo tungsten complex (**Figure 18**) [76].

More interestingly, this system is also active for the direct conversion of ethylene to propene with a very good selectivity (more than 95%). The TON can reach 1120 after 120 h [80]. The

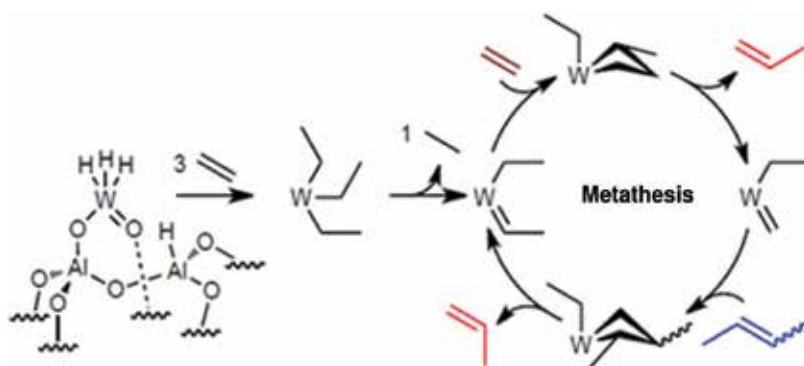


Figure 18. Formation of the active species from tungsten hydride and catalytic cycle for ethylene/but-2-ene cross-metathesis.

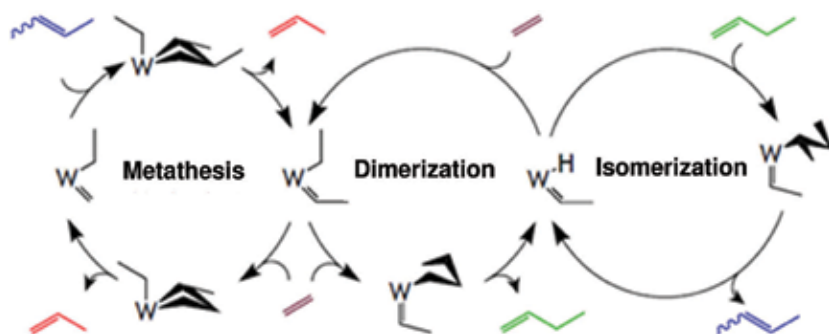


Figure 19. Proposed mechanism for the direct conversion of ethylene to propene.

mechanism of this reaction passes probably via the same ethyl ethylidene oxo tungsten complex than above as ethane is also detected at the first stages of the reaction. This complex can then convert ethylene to propene via three successive reactions: (i) dimerization of ethylene to but-1-ene; (ii) isomerization of but-1-ene to but-2-ene; and (iii) cross-metathesis between ethylene and but-2-ene (**Figure 19**).

This hydride species displays also a good activity in the metathesis of isobutene into 2,3-dimethylbutenes with a relative selectivity reaching 92% [81, 82]. It is the first example of use of a supported tungsten complex for this reaction, which is very difficult, due to the high steric hindrance in the gem-tetra-substituted metallocyclobutane intermediate. All these works show the beneficial effect of the oxo ligand (even if it is only spectator) in the coordination sphere of tungsten for metathesis of olefins. In this case, the oxo ligand was formed by extraction from the surface of alumina toward the xophilic tungsten center after its reduction under hydrogen.

4.2. Supported oxo-alkyl and oxo-carbene tungsten complexes

As shown above, the industrial WO_3/SiO_2 catalyst contains only a very small amount of really active sites, rendering their characterization by spectroscopic methods very difficult. However, it has been proposed by several authors that the active site is a tungsten(VI) complex with the formula $[(\equiv\text{Si}-\text{O})_2\text{W}(=\text{O})(=\text{CHR})]$ and containing two siloxy ligands, one oxo ligand and a carbene. However, oxo alkylidene tungsten complexes are very unstable and there are only few reports on them. The first supported tungsten oxo alkyl species active in olefin metathesis was achieved by grafting reaction of the complexes synthesized by Osborn et al. (**Figure 6**) [26]. Upon α -H abstraction, these complexes can lead to supported oxo-alkylidene species. The first oxo-alkyl complex of tungsten supported on silica was prepared by reaction of $\text{W}(=\text{O})(\text{CH}_2t\text{Bu})_4$ with silica dehydroxylated at 700°C [83]. The reaction occurs via breaking of a $\text{W}-\text{C}$ bond and leads selectively to $[(\equiv\text{SiO})(\text{W}=\text{O})(\text{CH}_2t\text{Bu})_3]$ **22** (**Figure 20**). This complex has been fully characterized by DRIFT, Raman spectroscopy, solid-state NMR, and EXAFS. The Raman spectrum displays a band at 935 cm^{-1} which is characteristic of the $\text{W}=\text{O}$ bond. EXAFS indicates that the supported complex has a bipyramidal trigonal structure with the oxo ($d(\text{W}=\text{O}) = 0.171\text{ nm}$) and siloxy ligands ($d(\text{W}-\text{O}) = 0.197\text{ nm}$) in axial position while the

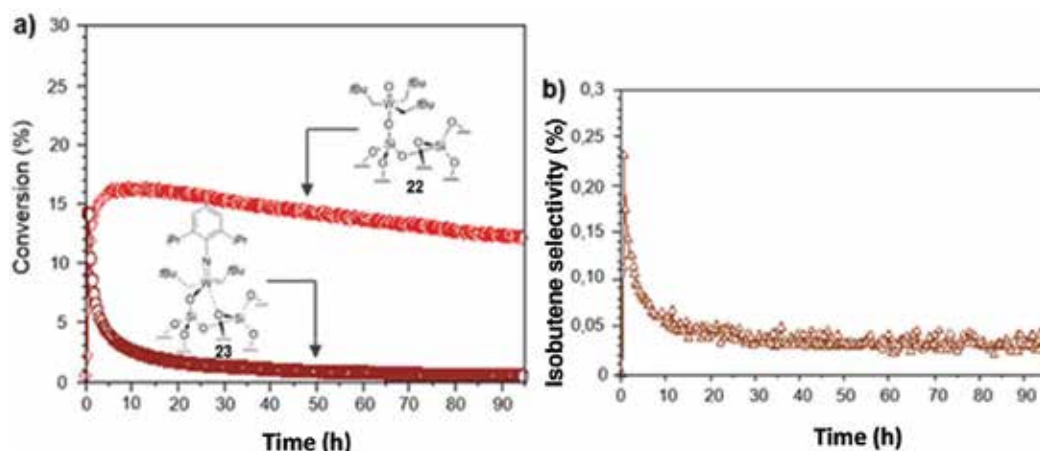


Figure 22. Metathesis of propene catalyzed by complexes **22** and **23**: (a) Conversion as a function of time; (b) isobutene selectivity as a function of time for complex **23**.

meta-allyl-tungsten hydride. This hydride is then converted into an inactive tungsten(IV) species with the evolution of isobutene by reductive elimination (**Figure 23**) [83].

The variation of the isobutene selectivity is quite the same than that of the conversion (**Figure 22a** and **b**) in agreement with a deactivation mechanism implying isobutene. This result shows also that the oxo ligand has a nonnegligible effect on the activity and stability of the tungsten catalysts. Recently, Eisenstein et al. performed DFT calculations on these compounds and found that replacement of the imido ligand by an oxo one increases the energy barrier of the β -H transfer in the mechanism of **Figure 23** and so stabilizes the catalyst [84]. $[(\equiv\text{SiO})\text{W}(=\text{O})(\text{CHtBu})_3]$ was the first reported model of the WO_3/SiO_2 industrial catalyst. The latter surface compound is monopodally anchored to the surface, which is different from the proposed active site in the industrial WO_3/SiO_2 catalyst precursor. However, the real model for the industrial catalyst (being a bipodal tungsten oxo carbene species) was not achieved with the former organometallic complex grafted on SiO_{2-200} (support that frequently yields bipodal species). The expected $\text{W}-\text{C}$ silanolysis step does not occur (**Figure 24**), even after thermal treatment. Such reactivity is reminiscent of tungsten aqueous organometallic chemistry described by Schrock and Lippard [85, 86]. Indeed, the coordination environment of **22**

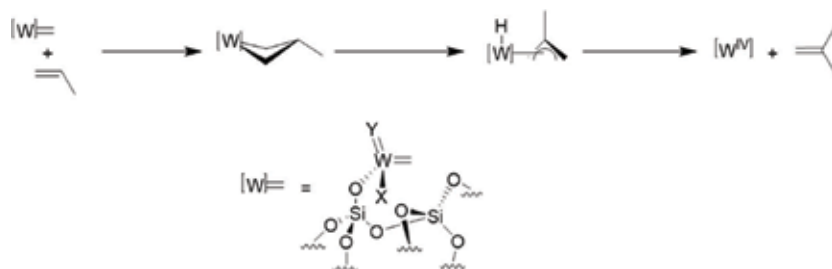


Figure 23. Mechanism of deactivation of the tungsten catalyst.

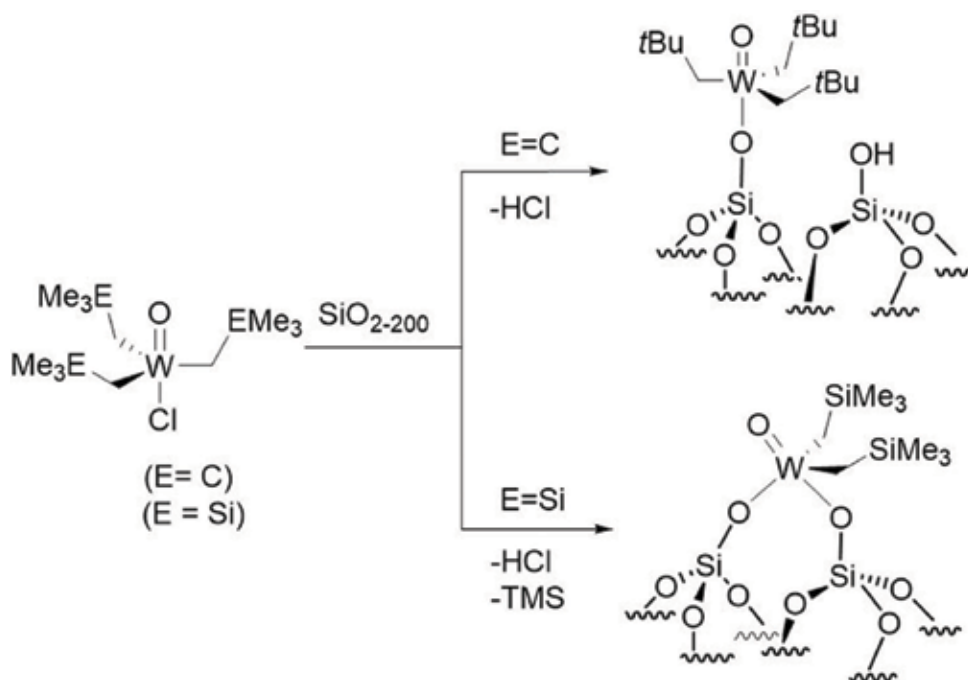


Figure 24. Reaction of $\text{W}(=\text{O})(\text{CH}_2\text{tBu})_4$ and $\text{W}(=\text{O})\text{Cl}(\text{CH}_2\text{SiMe}_3)_3$ with $\text{SiO}_2\text{-200}$.

is very similar to that of the trisoxo alkyl dinuclear complex $[\text{O}(\text{WONp}_3)_2]$ which is stable toward excess water. In order to push forward the second protonolysis step, the neopentyl ligand needs to be replaced by a more reactive fragment. Interestingly, Xue et al. have recently studied the reactivity of $[\text{W}(=\text{CSiMe}_3)(\text{CH}_2\text{SiMe}_3)_3]$ with H_2O and found a different behavior compared to $[\text{W}(=\text{CtBu})\text{Np}_3]$ [87]. When $[\text{W}(=\text{CSiMe}_3)(\text{CH}_2\text{SiMe}_3)_3]$ reacts with water, the authors observed mainly two products: tungsten bis-oxo bis-neosilyl trimer and $[\text{WO}(\text{OSiMe}_3)(\text{CH}_2\text{SiMe}_3)_3]$.

Then, the new complex $[\text{WOCl}(\text{CH}_2\text{SiMe}_3)_3]$ was obtained in 70% yield from $[\text{W}(=\text{CSiMe}_3)(\text{CH}_2\text{SiMe}_3)_3]$ by hydrolysis at -78°C with 2 eq. of H_2O in THF (resulting in the formation of the unstable intermediate $[\text{WO}(\text{OSiMe}_3)(\text{CH}_2\text{SiMe}_3)_3]$ as reported by Xue) followed by reaction with 1 eq. of $\text{Me}_3\text{SiCl}/\text{HCl}$. Thus, grafting of $[\text{WO}(\text{CH}_2\text{SiMe}_3)_3\text{Cl}]$ onto silica dehydroxylated at 200°C yields the well-defined bipodal species $[(\text{SiO}_2)_2\text{WO}(\text{CH}_2\text{SiMe}_3)_2]$ **24** via consecutive HCl and SiMe_4 release. This was demonstrated by mass balance analysis, elemental analysis, IR, advanced solid-state NMR (^1D and $2\text{D } ^1\text{H}$, ^{13}C , ^{29}Si and ^{17}O), and EXAFS. Furthermore, DFT calculations allowed understanding and rationalizing the experimental results regarding grafting selectivity of $[\text{WO}(\text{CH}_2\text{SiMe}_3)_3\text{Cl}]$ compared to its neopentyl counterpart [88].

More recently, Schrock et al. synthesized new oxo tungsten complexes bearing various ligands and studied their grafting on silica dehydroxylated at 700°C . Ligands such as 2,6-mesitylphenoxy, 2,6-diadamantyl-methylphenoxy, thio-2,6-mesitylphenoxy, or tris(tert-butoxy)siloxy were used and the corresponding carbenes were synthesized (**Figure 25**) [34, 89–91].

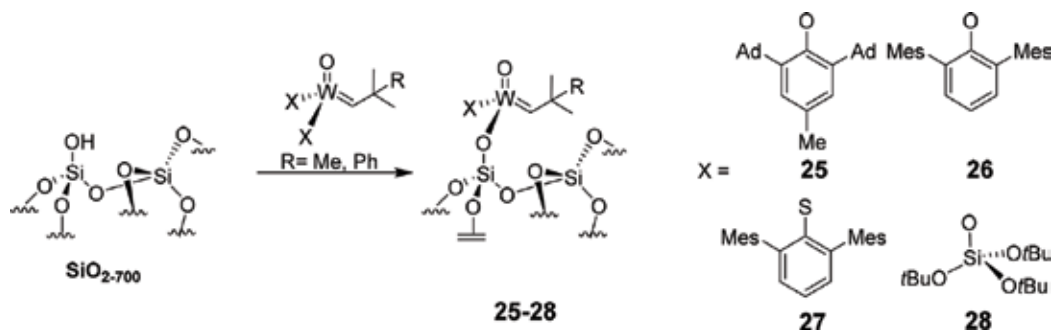


Figure 25. Grafting reaction of oxo-carbene tungsten complexes on silica.

The characterization of the grafted materials by infrared spectroscopy, chemical analysis, and solid-state NMR shows that the presence of these sterically encumbered ligands leads to a nonselective grafting reaction. For example, $[W(=O)(=CHtBu)(O-2,6\text{-mesitylphenoxide})_2]$ leads mainly (ca. 80%) to $[(\equiv SiO)W(=O)(=CHtBu)(O-2,6\text{-mesitylphenoxide})_2]$, formed by σ metathesis between the silanol group and the $W-Ar$ ligand. The minor product, $[(\equiv SiO)W(=O)(CH_2tBu)(O-2,6\text{-mesitylphenoxide})_2]$, is formed by protonation of the carbene moiety by the silanol group [90].

In order to reveal the stability and robustness of the real model of industrial catalyst **24** (being a supported bipodal tungsten oxo species active in olefin metathesis) with respect to the iso-electronic monopodal tungsten oxo aryloxo species, **25**, both materials were exposed to a continuous flow of propylene with a molar flow rate of $60 \text{ mol}_{C_3H_6} \cdot \text{mol}_W^{-1} \text{ min}^{-1}$ ($20 \text{ mL}_{C_3H_6} \text{ min}^{-1}$; 80°C , 1 bar). Both materials gave only metathesis products (equimolar amounts of ethylene and 2-butenes). **25** presents a very fast deactivation, affording a TON = 3,000 after 25 h on stream. Conversely, **24** efficiently performs propene metathesis with sustained activity over 24 h operating time (TON = 24,000). Although **24** (after activation with the olefinic substrate) and **25** have the same coordination environment and both catalysts are active in propylene metathesis, there is a remarkable difference in stability. The local structure of **24** closely resembles the proposed industrial WO_3/SiO_2 catalyst and showed a fairly stable catalytic activity with time on stream of propylene. On the other hand, **25** belongs to “model of model” rather than a true and robust catalyst, deactivated rapidly with time on stream. The huge different in the catalytic performance may be due to the importance of the bipodal nature of **24**, or the presence of a bulky organic ligand in **25**, which can gradually undergo intramolecular C–H activation with time and loss of the active tungsten alkylidene sites.

5. Conclusion

As shown above, there is a great interest to the study of olefin metathesis, not only by academics but also by industry. Indeed, this reaction can be considered as a key step in many

processes of fine chemistry, polymerization, or petrochemistry. This reaction can be catalyzed by homogeneous or heterogeneous systems.

Table 1 lists all well-defined systems reviewed in this chapter.

The homogeneous systems are well-described and structure-activity relationships were made allowing defining the best ligands and oxidation state of the metal for example. The heterogeneous systems, in contrast, are ill-defined even if they are preferred by industrials, due to their easy separation and recycling. Actually, WO_3/SiO_2 is often used by industry but the exact structure of the active species, which is in a small proportion, remains unknown even if it is generally accepted that it should be a species like $[(\equiv\text{Si}-\text{O})_2\text{W}(=\text{O})(=\text{CHR})]$. This model was then modeled by grafting organometallic complexes of tungsten containing an oxo ligand and able to give carbene species on the surface. These systems can be considered as models of the active site of WO_3/SiO_2 but their synthesis remains very complicated and up to now only few examples of such catalysts were reported, preventing the attainability of structure-activity relationships.

Catalyst	Reference
Homogeneous catalysts	
$[(\text{CO})_5\text{W}=\text{C}(\text{C}_6\text{H}_5)_2]$	Casey et al. [20], 31
$[\text{M}(=\text{CHCMe}_2\text{Ph})(=\text{N}-\text{Ar})(\text{OR})_2]$ M = Mo, W	Malcolmson et al. [21], 30; Schrock and Czekelius [22], 107; Marinescu et al. [23], 108; Schrock [24], 109
$\text{M}(=\text{O})(\text{CH}_2\text{C}(\text{CH}_3)_2)\text{X}$ M = Mo, W; X = Cl, Br, ONp, Np	Kress et al. [26], 111
$\text{W}(=\text{O})\text{Cl}_2\text{L}(\text{=CH}-t\text{Bu})$ L = PMe_3 , PEt_3 , PMe_2Ph	Wengrovius and Schrock [29], 118; Wengrovius et al. [30], 117
$\text{W}(=\text{O})(=\text{CHCMe}_2\text{Ph})-(\text{Me}_2\text{Pyr})(\text{OAr})$ (Me_2Pyr = 2,5-dimethylpyrrolide, OAr = aryloxy)	Wengrovius and Schrock [29], 118; Wengrovius et al. [30] 117
$\text{W}(=\text{O})(=\text{CHCMe}_2\text{Ph})(\text{OR})_2$	Wengrovius and Schrock [29], 118; Wengrovius et al. [30] 117
$\text{W}(=\text{O})(=\text{CHCMe}_2)(\text{OSi}(\text{OtBu})_3)_3$	Mougel and Coperet [34], 122
$[\text{W}(=\text{O})(=\text{CHCMe}_2\text{Ph})(\text{Mes})(\text{OAr})(\text{NCMe}_2)]^+$	Schowner et al. [35], 123
Heterogeneous catalysts	
$[(\equiv\text{SiO})\text{W}(=\text{C}t\text{Bu})\text{X}_3]$ (X = Cl, $t\text{Bu}$)	Weiss and Lössel [67], 61
$[(\equiv\text{SiO})\text{W}(=\text{C}t\text{Bu})(\text{CH}_2t\text{Bu})_2]$	Le Roux, 2005 [68], 62
$[(\equiv\text{SiO})_2\text{W}(=\text{C}t\text{Bu})(\text{CH}_2t\text{Bu})]$	Le Roux, 2005 [68], 62
$[(\text{Al}_s\text{O})\text{W}(=\text{C}t\text{Bu})(\text{CH}_2t\text{Bu})_2]$	Le Roux, 2005 [71], 68
$[(\equiv\text{SiO})(\text{W}=\text{O})(\text{CH}_2t\text{Bu})_2]$	Mazoyer, 2010 [74], 94
$[(\equiv\text{SiO})(\text{W}=\text{N}(2,6\text{-}i\text{PrC}_6\text{H}_3)(\text{CH}_2t\text{Bu})(=\text{CH}t\text{Bu}))]$	Mazoyer, 2010 [74], 94
$[(\equiv\text{SiO})_2\text{WO}(\text{CH}_2\text{SiMe}_2)_2]$	Grekov et al. [88], 162
$[(\equiv\text{SiO})\text{W}(=\text{O})(=\text{CH}t\text{Bu})(\text{O}-2,6\text{-mesitylphenoxide})]$	Conley et al. [90], 156

Table 1. Some representative metathesis catalysts listed in this review.

Author details

Frédéric Lefebvre^{1*}, Yassine Bouhoute¹, Kai C. Szeto¹, Nicolas Merle¹, Aimery de Mallmann¹, Régis Gauvin² and Mostafa Taoufik¹

*Address all correspondence to: frederic.lefebvre@univ-lyon1.fr

1 C2P2 (CNRS-UMR 5265), University of Lyon, ESCPE Lyon, Villeurbanne Cedex, France

2 UCCS (CNRS-UMR 8181), University of Lille, USTL, Villeneuve d'Ascq, France

References

- [1] Grubbs RH, Wenzel AG. Handbook of Metathesis: Catalyst Development and Mechanism (2). Weinheim: Wiley-VCH; 2015. 430 p
- [2] Calderon N, Ofstead EA, Ward JP, Judy WA, Scott KW. Olefin metathesis. I. Acyclic vinylenic hydrocarbons. Journal of the American Chemical Society. 1968;**90**(15):4133-4140. PubMed PMID: 1968:476241. English
- [3] Lewandos GS, Pettit R. Mechanism of the metal-catalyzed disproportionation of olefins. Journal of the American Chemical Society. 1971;**93**(25):7087-7088. PubMed PMID: 1972:33618. English
- [4] Biefeld CG, Eick HA, Grubbs RH. Crystal structure of bis(triphenylphosphine) tetramethyleneplatinum(II). Inorganic Chemistry. 1973;**12**(9):2166-2170. PubMed PMID: 1973:484430. English
- [5] Herisson JL, Chauvin Y. Catalysis of olefin transformations by tungsten complexes. II. Telomerization of cyclic olefins in the presence of acyclic olefins. Makromolekulare Chemie. 1971;**141**:161-176. PubMed PMID: 1971:477375. French
- [6] Casey CP, Burkhardt TJ. (Diphenylcarbene)pentacarbonyltungsten(0). Journal of the American Chemical Society. 1973;**95**(17):5833-5834. PubMed PMID: 1973:515701. English
- [7] Schrock RR. Alkylcarbene complex of tantalum by intramolecular α -hydrogen abstraction. Journal of the American Chemical Society. 1974;**96**(21):6796-6797. PubMed PMID: 1975:16916. English
- [8] Ivin KJ, Mol IC. Olefin Metathesis and Metathesis Polymerization. San Diego: Academic Press; 1997. p. 496
- [9] Peryshkov DV, Schrock RR. Synthesis of tungsten oxo alkylidene complexes. Organometallics. 2012;**31**(20):7278-7286. PubMed PMID: 2012:1439921. English
- [10] Hoff R, Mathers RT. Handbook of Transition Metal Polymerization Catalysts. John Wiley & Sons, Inc., Hoboken, N.J. ; 2010. p. 575

- [11] Anderson AW, Merckling NG, Inventors. Polymeric bicyclo[2.2.1]hept-2-ene. Patent 1954-4531442721189; 1955, 19540830
- [12] Natta G, Dall'Asta G, Mazzanti G. Stereospecific homopolymerization of cyclopentene. *Angewandte Chemie*. 1964;**76**(18):765-772. PubMed PMID: 1964:492706. language unavailable
- [13] Basset JM, Leconte M. Progress in olefin metathesis. *Chemtech*. 1980;**10**(12):762-767. PubMed PMID: 1981:83145. English
- [14] Calderon N, Chen HY, Scott KW. Olefin metathesis, a novel reaction for skeletal transformations of unsaturated hydrocarbons. *Tetrahedron Letters*. 1967;**34**:3327-3329. PubMed PMID: 1968:77620. English
- [15] Quignard F, Leconte M, Basset JM. Aryl oxide ligands in metathesis of olefins and olefinic esters: Catalytic behavior of $W(OAr)_2Cl_4$ complexes associated with alkyltin or alkyllead cocatalysts; alkylation of $W(OAr)_2Cl_4$ by $SnMe_4$, $SnBu_4$, $PbBu_4$, $MgNp_2$: Synthesis of $W(OAr)_2Cl_2(CHCMe_3)(OR_2)$ and $W(OAr)_2Cl(CHCMe_3)(CH_2CMe_3)(OR_2)$. *Journal of Molecular Catalysis*. 1986;**36**(1-2):13-29. PubMed PMID: 1987:196552. English
- [16] Hughes WB. Kinetics and mechanism of the homogeneous olefin disproportionation reaction. *Journal of the American Chemical Society*. 1970;**92**(3):532-537. PubMed PMID: 1970:89460. English
- [17] Seyferth K, Taube R. Complex catalysis. XXI. Formation and structure of the catalytically active complex in olefin metathesis catalysts based on nitrosylmolybdenum compounds. *Journal of Molecular Catalysis*. 1985;**28**(1-3):53-69. PubMed PMID: 1985:131474. English
- [18] Zuech EA. Homogeneous catalysts for olefin disproportionation. *Chemical Communications (London)*. 1968;**19**:1182. PubMed PMID: 1968:505786. English
- [19] Zuech EA, Hughes WB, Kubicek DH, Kittleman ET. Homogeneous catalysts for olefin disproportionations from nitrosyl molybdenum and tungsten compounds. *Journal of the American Chemical Society*. 1970;**92**(3):528-531. PubMed PMID: 1970:89487. English
- [20] Casey CP, Tuinstra HE, Saeman MC. Reactions of $(CO)_5WC(Tol)_2$ with alkenes. A Model for structural selectivity in the olefin metathesis reaction. *Journal of the American Chemical Society*. 1976;**98**(2):608-609. PubMed PMID: 1976:90260. English
- [21] Malcolmson SJ, Meek SJ, Sattely ES, Schrock RR, Hoveyda AH. Highly efficient molybdenum-based catalysts for enantioselective alkene metathesis. *Nature (London, U K)*. 2008;**456**(7224):933-937. PubMed PMID: 2008:1515283. English
- [22] Schrock RR, Czekelius C. Recent advances in the syntheses and applications of molybdenum and tungsten alkylidene and alkylidyne catalysts for the metathesis of alkenes and alkynes. *Advanced Synthesis & Catalysis*. 2007;**349**(1+2):55-77. PubMed PMID: 2007:162252. English
- [23] Marinescu SC, Schrock RR, Muller P, Hoveyda AH. Ethenolysis reactions catalyzed by imido alkylidene monoaryloxy monopyrrolide (MAP) complexes of molybdenum. *Journal of*

- the American Chemical Society. 2009;**131**(31):10840-10841. PubMed PMID: 2009:874487. English
- [24] Schrock RR. Synthesis of stereoregular polymers through ring-opening metathesis polymerization. *Accounts of Chemical Research*. 2014;**47**(8):2457-2466. PubMed PMID: 2014:939468. English
- [25] Wampler KM, Cohen SA, Frater GE, Ondi L, Varga J, Inventors. Treating natural oils prior to olefin metathesis reactions for prevention of catalyst poisoning. Patent 2014-14209686 20140275595; 2014, US20140275595 20140313
- [26] Kress JRM, Russell MJM, Wesolek MG, Osborn JA. Tungsten(VI) and molybdenum(VI) oxo alkyl species. Their role in the metathesis of olefins. *Journal of the Chemical Society, Chemical Communications*. 1980;**10**:431-432. PubMed PMID: 1981:30875. English
- [27] Kress J, Wesolek M, Le Ny JP, Osborn JA. Molecular complexes for efficient metathesis of olefins. The oxo-ligand as catalyst-cocatalyst bridge and the nature of the active species. *Journal of the Chemical Society, Chemical Communications*. 1981;**20**:1039-1040. PubMed PMID: 1982:85695. English
- [28] Kress JRM, Osborn JA, Wesolek MG, Inventors. Oxo complexes of transition metals coordinated with a Lewis acid their use as catalysts in the metathesis of olefins. Patent 1981-22932499083; 1982, FR2499083 19810204
- [29] Wengrovius JH, Schrock RR. Synthesis and characterization of tungsten oxo neopentylidene complexes. *Organometallics*. 1982;**1**(1):148-155. PubMed PMID: 1982:35460. English
- [30] Wengrovius JH, Schrock RR, Churchill MR, Missert JR, Youngs WJ. Multiple metal-carbon bonds. 16. Tungsten-oxo alkylidene complexes as olefins metathesis catalysts and the crystal structure of $W(O)(CHCMe_3)(PEt_3)Cl_2$. *Journal of the American Chemical Society*. 1980;**102**(13):4515-4516. PubMed PMID: 1980:514665. English
- [31] Peryshkov DV, Schrock RR, Takase MK, Muller P, Hoveyda AH. Z-Selective olefin metathesis reactions promoted by tungsten oxo alkylidene complexes. *Journal of the American Chemical Society*. 2011;**133**(51):20754-20757. PubMed PMID: 2011:1497530. English
- [32] Forrest WP, Axtell JC, Schrock RR. Tungsten Oxo alkylidene complexes as initiators for the stereoregular polymerization of 2,3-dicarbomethoxynorbornadiene. *Organometallics*. 2014;**33**(9):2313-2325. PubMed PMID: 2014:714355. English
- [33] Townsend EM, Hyvl J, Forrest WP, Schrock RR, Muller P, Hoveyda AH. Synthesis of molybdenum and tungsten alkylidene complexes that contain sterically demanding arene-thiolate ligands. *Organometallics*. 2014;**33**(19):5334-5341. PubMed PMID: 2014:1580814. English
- [34] Mougél V, Coperet C. Isostructural molecular and surface mimics of the active sites of the industrial WO_3/SiO_2 metathesis catalysts. *ACS Catalysis*. 2015;**5**(11):6436-6439. PubMed PMID: 2015:1556675. English

- [35] Schowner R, Frey W, Buchmeiser MR. Cationic Tungsten-Oxo-Alkylidene-N-Heterocyclic carbene complexes: Highly active olefin metathesis catalysts. *Journal of the American Chemical Society*. 2015;**137**(19):6188-6191. PubMed PMID: 2015:789653. English
- [36] Streck R. Economic and ecological aspects in applied olefin metathesis. *Journal of Molecular Catalysis*. 1992;**76**(1-3):359-372. PubMed PMID: 1992:654077. English
- [37] Mol JC. Industrial applications of olefin metathesis. *Journal of Molecular Catalysis A: Chemical*. 2004;**213**(1):39-45. PubMed PMID: 2004:189514. English
- [38] Parkinson G. Revving up for alkylation. *Chemical Engineering*. 2001;**108**(1):27. PubMed PMID: 2001:102614. English
- [39] Freitas ER, Gum CR. Shell's higher olefins process. *Chemical Engineering Progress*. 1979;**75**(1):73-76. PubMed PMID: 1979:189352. English
- [40] Banks RL, Banasiak DS, Hudson PS, Norell JR. Specialty chemicals via olefin metathesis. *Journal of Molecular Catalysis*. 1982;**15**(1-2):21-33. PubMed PMID: 1982:494379. English
- [41] Mol JC. Olefin metathesis over supported rhenium oxide catalysts. *Catalysis Today*. 1999;**51**(2):289-299. PubMed PMID: 1999:366303. English
- [42] van Schalkwyk C, Spamer A, Moodley DJ, Dube T, Reynhardt J, Botha JM, et al. Factors that could influence the activity of a WO_3/SiO_2 catalyst: Part III. *Applied Catalysis, A: General*. 2003;**255**(2):143-152. PubMed PMID: 2003:925182. English
- [43] Thomas R, Moulijn JA, De Beer VHJ, Medema J. Structure/metathesis-activity relations of silica supported molybdenum and tungsten oxide. *Journal of Molecular Catalysis*. 1980;**8**(1-3):161-174. PubMed PMID: 1981:138843. English
- [44] Van Roosmalen AJ, Koster D, Mol JC. Infrared spectroscopy of some chemisorbed molecules on tungsten oxide-silica. *Journal of Physical Chemistry*. 1980;**84**(23):3075-3079. PubMed PMID: 1980:626329. English
- [45] Basrur AG, Patwardhan SR, Vyas SN. Propene metathesis over silica-supported tungsten oxide catalyst. Catalyst induction mechanism. *Journal of Catalysis*. 1991;**127**(1):86-95. PubMed PMID: 1991:61415. English
- [46] Martin C, Malet P, Solana G, Rives V. Structural analysis of Silica-Supported tungstates. *The Journal of Physical Chemistry B*. 1998;**102**(15):2759-2768. PubMed PMID: 1998:211419. English
- [47] Kim DS, Ostromecki M, Wachs IE. Surface structures of supported tungsten oxide catalysts under dehydrated conditions. *Journal of Molecular Catalysis A: Chemical*. 1996;**106**(1-2):93-102. PubMed PMID: 1996:201271. English
- [48] Ross-Medgaarden EI, Wachs IE. Structural determination of bulk and surface tungsten oxides with UV-vis diffuse reflectance spectroscopy and raman spectroscopy. *Journal of Physical Chemistry C*. 2007;**111**(41):15089-15099. PubMed PMID: 2007:1065318. English

- [49] Luckner RC, McConchie GE, Wills GB. Initial rates of propylene disproportionation over tungsten trioxide on silica catalysts. *Journal of Catalysis*. 1973;**28**(1):63-68. PubMed PMID: 1973:34369. English
- [50] Westhoff R, Moulijn JA. Reduction and activity of the metathesis catalyst tungsten oxide/silica. *Journal of Catalysis*. 1977;**46**(3):414-416. PubMed PMID: 1977:422237. English
- [51] Lwin S, Li Y, Frenkel AI, Wachs IE. Nature of WO_x sites on SiO_2 and their molecular structure-reactivity/selectivity relationships for propylene metathesis. *ACS Catalysis*. 2016;**6**(5):3061-3071. PubMed PMID: 2016:537580. English
- [52] Howell J, Li Y-P, Bell AT. Propene metathesis over supported tungsten oxide catalysts: A study of active site formation. *ACS Catalysis*. 2016;**6**(11):7728-7738
- [53] Amakawa K, Wrabetz S, Kroehnert J, Tzolova-Mueller G, Schloegl R, Trunschke A. In situ generation of active sites in olefin metathesis. *Journal of the American Chemical Society*. 2012;**134**(28):11462-11473. PubMed PMID: 2012:860486. English
- [54] Ding K, Gulec A, Johnson AM, Drake TL, Wu W, Lin Y, et al. Highly efficient activation, regeneration, and active site identification of oxide-based olefin metathesis catalysts. *ACS Catalysis*. 2016;**6**:5740-5746. PubMed PMID: 2016:1165119. English
- [55] Basset J-M, Psaro R, Roberto D, Ugo R. *Modern Surface Organometallic Chemistry*. Weinheim: Wiley-VCH; 2009. p. 697
- [56] Coperet C, Chabanas M, Saint-Arroman RP, Basset J-M. Homogeneous and heterogeneous catalysis: Bridging the gap through surface organometallic chemistry. *Angewandte Chemie International Edition*. 2003;**42**(2):156-181. PubMed PMID: 2003:86262. English
- [57] Lefebvre F, Candy J-P, Mallmann AD, Dufaud V, Nicolai G, Santini C, et al. Organometallic surface chemistry: Fundamental aspects and applications in catalysis. *Actualite Chimique*. 1996;**7**:47-54. PubMed PMID: 1997:63237. French
- [58] Lopez LPH, Schrock RR, Mueller P. Dimers that contain unbridged W(IV)/W(IV) double bonds. *Organometallics*. 2006;**25**(8):1978-1986. PubMed PMID: 2006:223542. English
- [59] Wang X, Zhao H, Lefebvre F, Basset J-M. Surface organometallic chemistry of tin: grafting reaction of $Sn(CH_3)_4$ in HY zeolite supercage. *Chemistry Letters*. 2000;**10**:1164-1165. PubMed PMID: 2000:728329. English
- [60] Deghedi L, Basset J-M, Bergeret G, Candy J-P, Valero MC, Dalmon J-A, et al. Preparation of nanosized bimetallic Ni-Sn and Ni-Au/ SiO_2 catalysts by SOMC/M. Correlation between structure and catalytic properties in styrene hydrogenation. *Studies in Surface Science and Catalysis*. 2010;**175** (Scientific Bases for the Preparation of Heterogeneous Catalysts):617-620. PubMed PMID: 2010:1318512. English
- [61] Ryndin YA, Candy JP, Didillon B, Savary L, Basset JM. Surface organometallic chemistry on metals applied to the environment: Hydrogenolysis of $AsPh_3$ with nickel supported on alumina. *Journal of Catalysis*. 2001;**198**(1):103-108. PubMed PMID: 2001:127569. English

- [62] Clark DN, Schrock RR. Multiple metal-carbon bonds. 12. Tungsten and molybdenum neopentylidyne and some tungsten neopentylidene complexes. *Journal of the American Chemical Society*. 1978;**100**(21):6774-6776. PubMed PMID: 1979:6500. English
- [63] Schrock RR. High-oxidation-state molybdenum and tungsten alkylidyne complexes. *Accounts of Chemical Research*. 1986;**19**(11):342-348. PubMed PMID: 1987:5106. English
- [64] Schrock RR, Clark DN, Sancho J, Wengrovius JH, Rocklage SM, Pedersen SF. Tungsten(VI) neopentylidyne complexes. *Organometallics*. 1982;**1**(12):1645-1651. PubMed PMID: 1982:616382. English
- [65] Chisholm MH, Conroy BK, Eichhorn BW, Folting K, Hoffman DM, Huffman JC, et al. Reactions involving alkynes and tungsten-tungsten triple bonds supported by alkoxide ligands. *Polyhedron*. 1987;**6**(4):783-792. PubMed PMID: 1988:186780. English
- [66] Chisholm MH, Folting K, Hoffman DM, Huffman JC. Metal alkoxides: Models for metal oxides. 4. Alkyne adducts of ditungsten hexaalkoxides and evidence for an equilibrium between dimetallatetrahedrane and methylidynemetal complexes: $W_2(\mu-C_2H_2).dblharw. 2W\equiv CH$. *Journal of the American Chemical Society*. 1984;**106**(22):6794-6805. PubMed PMID: 1984:592133. English
- [67] Weiss K, Lössel G. Heterogeneous, metathesis-active Schrock-type carbene complexes by reaction of carbyne tungsten(VI) complexes with silica gel. *Angewandte Chemie International Edition*. 1989;**28**(1):62-64
- [68] Le Roux E, Taoufik M, Chabanas M, Alcor D, Baudouin A, Copéret C, et al. Well-Defined surface tungstenocarbene complexes through the reaction of $[W(:CtBu)(CH_2tBu)_3]$ with silica. *Organometallics*. 2005;**24**(17):4274-4279
- [69] Merle N, Trebosc J, Baudouin A, Rosal ID, Maron L, Szeto K, et al. 17O NMR Gives Unprecedented Insights into the structure of supported catalysts and their interaction with the silica carrier. *Journal of the American Chemical Society*. 2012;**134**(22):9263-9275. PubMed PMID: 2012:675847. English
- [70] Morton LA, Zhang X-H, Wang R, Lin Z, Wu Y-D, Xue Z-L. An unusual exchange between Alkylidyne Alkyl and Bis(alkylidene) tungsten complexes promoted by phosphine coordination: Kinetic, thermodynamic, and theoretical studies. *Journal of the American Chemical Society*. 2004;**126**(33):10208-10209
- [71] Le Roux E, Taoufik M, Copéret C, de Mallmann A, Thivolle-Cazat J, Basset J-M, et al. Development of tungsten-based heterogeneous alkane metathesis catalysts through a structure-activity relationship. *Angewandte Chemie International Edition*. 2005;**44**(41):6755-6758
- [72] Joubert J, Delbecq F, Sautet P, Le Roux E, Taoufik M, Thieuleux C, et al. Molecular understanding of alumina supported Single-Site catalysts by a combination of experiment and theory. *Journal of the American Chemical Society*. 2006;**128**(28):9157-9169. PubMed PMID: 2006:600203. English

- [73] Le Roux E, Taoufik M, Baudouin A, Coperet C, Thivolle-Cazat J, Basset J-M, et al. Silica-alumina-supported, tungsten-based heterogeneous alkane metathesis catalyst: Is it closer to a silica- or an alumina-supported system? *Advanced Synthesis & Catalysis*. 2007;**349**(1+2):231-237. PubMed PMID: 2007:162268. English
- [74] Mazoyer E. PhD Thesis, New generation of catalysts based on tungsten supported on oxides for the production of propylene (in French). Lyon; 2010
- [75] Basset J-M, Coperet C, Soulivong D, Taoufik M, Thivolle Cazat J. Metathesis of alkanes and related reactions. *Accounts of Chemical Research*. 2010;**43**(2):323-334. PubMed PMID: 2009:1306176. English
- [76] Mazoyer E, Szeto KC, Merle N, Norsic S, Boyron O, Basset J-M, et al. Study of ethylene/2-butene cross-metathesis over W-H/Al₂O₃ for propylene production: Effect of the temperature and reactant ratios on the productivity and deactivation. *Journal of Catalysis*. 2013;**301**:1-7. PubMed PMID: 2013:570955. English
- [77] Zhao Q, Chen S-L, Gao J, Xu C. Effect of tungsten oxide loading on metathesis activity of ethene and 2-butene over WO₃/SiO₂ catalysts. *Transition Metal Chemistry (Dordrecht, Neth)*. 2009;**34**(6):621-627. PubMed PMID: 2009:966795. English
- [78] Li X, Guan J, Zheng A, Zhou D, Han X, Zhang W, et al. DFT studies on the reaction mechanism of cross-metathesis of ethylene and 2-butylene to propylene over heterogeneous Mo/HBeta catalyst. *Journal of Molecular Catalysis A: Chemical*. 2010;**330**(1-2):99-106. PubMed PMID: 2010:1121562. English
- [79] Malani H, Hayashi S, Zhong H, Sahnoun R, Tsuboi H, Koyama M, et al. Theoretical investigation of ethylene/1-butene copolymerization process using constrained geometry catalyst (CpSiH₂NH)-Ti-Cl₂. *Applied Surface Science*. 2008;**254**(23):7608-7611. PubMed PMID: 2008:1116275. English
- [80] Taoufik M, Le Roux E, Thivolle-Cazat J, Basset J-M. Direct transformation of ethylene into propylene catalyzed by a tungsten hydride supported on alumina: Trifunctional Single-Site catalysis. *Angewandte Chemie International Edition*. 2007;**46**(38):7202-7205
- [81] Garron A, Stoffelbach F, Merle N, Szeto KC, Thivolle-Cazat J, Basset J-M, et al. Improved direct production of 2,3-dimethylbutenes and 3,3-dimethylbutene from 2-methylpropene on tungsten hydride based catalysts. *Catalysis Science & Technology*. 2012;**2**(12):2453-2455. PubMed PMID: 2012:1637865. English
- [82] Merle N, Stoffelbach F, Taoufik M, Le Roux E, Thivolle-Cazat J, Basset J-M. Selective and unexpected transformations of 2-methylpropane to 2,3-dimethylbutane and 2-methylpropene to 2,3-dimethylbutene catalyzed by an alumina-supported tungsten hydride. *Chemical Communications (London)*. 2009;**18**:2523-2525. PubMed PMID: 2009:482548. English
- [83] Mazoyer E, Merle N, de Mallmann A, Basset J-M, Berrier E, Delevoye L, et al. Development of the first well-defined tungsten oxo alkyl derivatives supported on silica by SOMC: Towards a model of WO₃/SiO₂ olefin metathesis catalyst. *Chemical Communications (London)*. 2010;**46**(47):8944-8946. PubMed PMID: 2010:1458482. English

- [84] Solans-Monfort X, Coperet C, Eisenstein O. Oxo vs. imido alkylidene d⁰-metal species: How and why do they differ in structure, activity, and efficiency in alkene metathesis? *Organometallics*. 2012;**31**(19):6812-6822. PubMed PMID: 2012:1398582. English
- [85] Feinstein-Jaffe I, Gibson D, Lippard SJ, Schrock RR, Spool A. A molecule containing the OWOWO unit. Synthesis, structure and spectroscopy of hexaneopentyliditungsten trioxide. *Journal of the American Chemical Society*. 1984;**106**(21):6305-6310. PubMed PMID: 1984:571435. English
- [86] Feinstein-Jaffe I, Pedersen SF, Schrock RR. Aqueous tungsten(VI) alkyl chemistry. *Journal of the American Chemical Society*. 1983;**105**(24):7176-7177. PubMed PMID: 1983:612653. English
- [87] Morton LA, Miao M, Callaway TM, Chen T, Chen S-J, Tuinman AA, et al. Reactions of d⁰ tungsten alkylidyne complexes with O₂ or H₂O. Formation of an oxo siloxy complex through unusual silyl migrations. *Chemical Communications (London)*. 2013;**49**(83):9555-9557. PubMed PMID: 2013:1517232. English
- [88] Grekov D, Bouhoute Y, Szeto KC, Merle N, De Mallmann A, Lefebvre F, et al. Silica-supported tungsten neosilyl oxo precatalysts: Impact of the podality on activity and stability in olefin metathesis. *Organometallics*. 2016;**35**:2188-2196
- [89] Conley MP, Forrest WP, Mougél V, Coperet C, Schrock RR. Bulky aryloxide ligand stabilizes a heterogeneous metathesis catalyst. *Angewandte Chemie International Edition*. 2014;**53**(51):14221-14224. PubMed PMID: 2014:2056032. English
- [90] Conley MP, Mougél V, Peryshkov DV, Forrest WP, Gajan D, Lesage A, et al. A well-defined silica-supported tungsten oxo alkylidene is a highly active alkene metathesis catalyst. *Journal of the American Chemical Society*. 2013;**135**(51):19068-19070. PubMed PMID: 2013:1916575. English
- [91] Mougél V, Pucino M, Coperet C. Strongly σ donating thiophenoxide in silica-supported tungsten oxo catalysts for improved 1-alkene metathesis efficiency. *Organometallics*. 2015;**34**(3):551-554. PubMed PMID: 2015:141437. English

Oxidation of the Simplest Conjugated Diolefin

Reactivity of a Simplest Conjugated Diolefin in Liquid-Phase Oxidation: Mechanisms and Products

Nina I. Kuznetsova, Lidia I. Kuznetsova,
Olga A. Yakovina and Bair S. Bal'zhinimaev

Additional information is available at the end of the chapter

<http://dx.doi.org/10.5772/intechopen.71259>

Abstract

Ethylene is the simplest member of olefin series, but butadiene-1,3 (BD) is the simplest conjugated diolefin. In this chapter, we describe liquid-phase oxidations of BD with an emphasis on comparison of the diolefin with monoolefins. BD interacts with oxygen to form polyperoxide, whose thermal decomposition or hydrogenation leads to the formation of 2-butene-1,4-diol, 3-butene-1,2-diol, or butanediols together with furan and acrolein. BD can be oxidized in polar solvents by radical chain route to form directly the dioxigenates. Metal catalysts are able to control the oxidation by promoting formation of 2-butene-1,4-diol, 4-hydroxybut-2-enal, and furan. PdTe/C catalyst is applied in industry to produce 2-butene-1,4-diol diacetates with selectivity of 98%. The outstanding selectivity of the catalyst is caused by combined action of components in nonradical route and esterification of final product in acetic acid. Similar reaction in methyl alcohol yields 1,4-dimethoxy-2-butene, but with lower efficiency. The nonradical mechanism is firmly established for epoxidation of BD with hydrogen peroxide catalyzed by phosphotungstates. The selectivity of BD and hydrogen peroxide conversion to 3,4-epoxy-1-butene around 100% is attained. Analysis of published information and our own studies show many similarities in oxidation of BD and light olefins, which are very useful for understanding the mechanisms.

Keywords: butadiene-1,3, olefin, oxygen, hydrogen peroxide, homogeneous catalyst, heterogeneous catalyst, liquid-phase oxidation, oxidation products, mechanism

1. Introduction

Butadiene-1,3 (BD) is diolefin containing two conjugated double bonds. In oxidation, BD exhibits properties inherent to all olefins, but higher reactivity was compared to but-1-ene and

but-2-ene. Both BD and C_4 -olefins can be a feedstock for producing valuable chemicals by gas-phase oxidation [1, 2]. The oxidation on oxide catalysts in gas phase results in the formation of maleic anhydride together with crotonaldehyde and 2,5-dihydrofuran. Centy and Trifiro suggested a simple consecutive pathway for BD oxidation over V-P-oxide catalysts [3, 4], whereas Honicke et al. proposed multiple pathways from BD to crotonaldehyde, 2,5-dihydrofuran, 2-butene-1,4-dial, 2(5H)-furanone and furan, and finally to maleic anhydride over V_2O_5 catalysts [5]. Schroeder specified the oxidation pathway on V-Mo-oxide catalysts, including 3,4-epoxy-1-butene as a primary oxidation product [6]. Epoxidation of BD occurs over Ag catalysts [7–10] used in industry for the production of ethylene oxide and intensively investigated in the oxidation of other olefins (e.g., [11, 12]). 3,4-Epoxy-1-butene is further converted into 2,3-dihydrofuran followed by hydrolysis to form 4-hydroxybutyraldehyde. The secondary transformations occur directly under epoxidation conditions on Ag catalysts promoted with B-P [13], Mo [14], and Mo-P-Sb [15] or by subsequent treatments of 3,4-epoxy-1-butene.

In the early 1980s, oxidation of n-butane has become the preferred method for manufacturing maleic anhydride [16, 17]. The invented synthesis of maleic anhydride from butane creates a competition for the gas-phase oxidation of BD since hydrogenation of maleic anhydride opens a possibility of producing various oxygenates, which produced from BD earlier. At the same time, the gas-phase oxidation of BD still suffers from formation of polymer resins, which leads to excessive consumption of raw materials and catalyst deactivation. This problem and large power consumption inherent to all gas-phase reactions are absent in the liquid-phase oxidation since the low temperature and application of appropriate solvents prevent the formation of the resins. The liquid-phase low-temperature oxidative reactions, in particular the oxidation of olefins, were intensively studied at the end of the last century [18–23]. A renewed interest in this area is growing now [24–27] and can be expected to be strengthened in the nearest future as a response to modern requirements of green chemistry to minimize power and materials consumption. In addition, the liquid-phase reactions are well applicable for the oxidation of various olefins and BD because of high reactivity of these hydrocarbons that allows the oxidation at low temperature. At the same time, BD becomes more affordable owing to permanent improvements in its manufacturing.

The title of this chapter concerns the application of green oxygen (air and hydrogen peroxide) in liquid-phase conditions. The liquid-phase oxidative reactions are an important part in chemistry of all olefins and, in particular, of the simplest representative of conjugated diolefins as they open many routes for the conversion of the hydrocarbons. We represent here an analysis of literature information concerning the oxidation of BD in liquids and references to the related reactions of olefins. In detail, we described the catalytic systems in the study of which we acquired our own experience.

2. Radical chain reactions of BD with oxygen

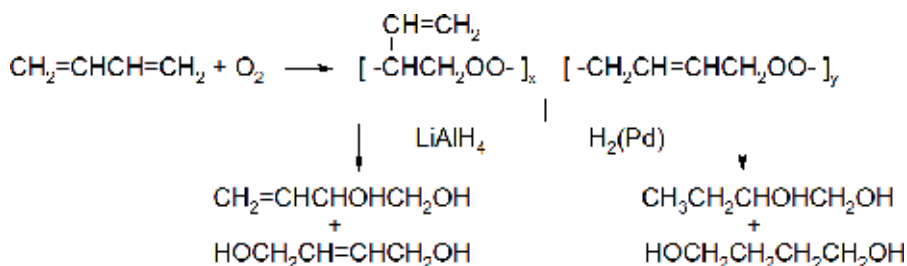
Olefins readily interact with radical species. The most susceptible to radical attack is allyl position to produce allyl oxygenates [28, 29]. In the absence of an allylic carbon atom,

one of the double bonds of BD is involved in the oxidation. Neat or dissolved in a nonpolar solvent, BD interacts with oxygen at moderate temperature according to radical chain mechanism to form oligomeric butadiene polyperoxide, $C_4H_6O_2$ [30]. The reaction is accelerated by increasing the temperature or adding free radical initiators and inhibited by adding acids. From the NMR analysis, molecular structure of the polyperoxide formed at 50°C in the presence of 37 Torr of oxygen was composed of equal amounts of 1,4- and 1,2-butadiene units separated by peroxide units [31]. The structure of the polyperoxide (the ratio of 1,4- to 1,2-butadiene units) does not depend on the reaction temperature, whereas the content of bound oxygen in the polyperoxide varies with oxygen pressure. The ratio of peroxide to hydrocarbon units is below 1 at a low oxygen partial pressure. Thermal decomposition as well as hydrogenation of polyperoxide leads to the formation of 3-butene-1,2-diol and 2-butene-1,4-diol or corresponding saturated diols, preferably 1,4-derivatives (**Scheme 1**) [30, 32–35].

Decomposition of the polyperoxide forms not only 3-butene-1,2-diol and 2-butene-1,4-diol but also side products such as formaldehyde, acrolein (from 1,2-units), and resinous insoluble material (presumably resulting from the reaction of the 1,4-units with aldehydes) [31]. Therefore, the preferred formation of 1,4-oxygenates from the thermal decomposition of polyperoxide is not a strong support of predominance of 1,4-units in the polyperoxide structure.

The rate of decomposition of the polyperoxide increases with increasing temperature, addition of bases (amines) [36], or metal ions as radical initiators. Butadienyl polyperoxide is readily decomposed in the presence of metal ions of variable oxidation state. Therefore, the transition metal compounds participate as catalysts in the radical chain oxidation of BD with oxygen. The oxidation products are similar to those obtained under the decomposition of the polyperoxide. 3-Butene-1,2-diol and 2-butene-1,4-diol can be obtained with the selectivity sufficiently high for the chain radical process, especially if one considers the low stability of these products with respect to secondary oxidation. Thus, a mixture of 3-butene-1,2-diol and 2-butene-1,4-diol has been prepared by oxidative dihydroxylation of BD with oxygen in acetic acid solution of $Pd(OAc)_2$. From a practical point of view, the most valuable 2-butene-1,4-diol has been formed with selectivity of 25% [37].

We tested Pd and Au catalysts in the radical chain oxidation of BD in polar media. Both soluble palladium acetate and insoluble supported metals caused the formation of the products,

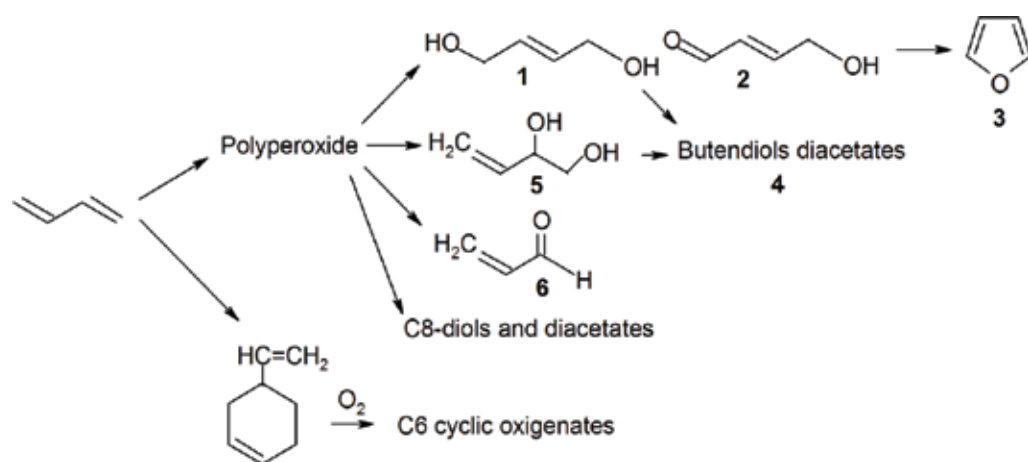


Scheme 1. Formation and reductive decomposition of the polyperoxide [30].

the most part of which appeared from decomposition of the intermediate butadienyl polyperoxide [32] (**Scheme 2**). The main products are 3-butene-1,2-diol and 2-butene-1,4-diol. 4-Hydroxybut-2-enal can be formed in the decomposition of polyperoxide and in oxidation of 2-butene-1,4-diol. Oxidative dehydration of 2-butene-1,4-diol produces furan. Both butane-diols can be esterified to form corresponding diacetates, but only 2-butene-1,4-diol diacetate has been found in the reaction solution. Acrolein occurs from breaking C–C bond under decomposition of polyperoxide or, possibly, from secondary conversion of 3-butene-1,2-diol. C8 oxygenates originate from polyperoxide fragments containing less than 1:1 ratio of butadiene to oxygen units. In addition, there are impurities of C6 cyclic oxygenates occurring from cyclodimerization of BD (Diels-Alder reaction) followed by oxidation of 4-vinylcyclohexene. The amount of the products is given in **Table 1**.

In addition to the stable compounds, a large amount of peroxide compounds have been iodometrically detected in acetic acid and acetic acid/dioxane solutions (**Table 1**). Peroxide oxygen refers to butadienyl polyperoxide since the addition of Ph_3P reducer to the solution results in disappearance of the peroxide and formation of 2-butene-1,4-diol together with minor amounts of furan and 3-butene-1,2-diol. The polyperoxide exhibited sufficient stability in several oxidation tests but almost completely decomposed with a large amount of Pd/C catalysts. As a result, enhanced formation of 2-butene-1,4-diol and 4-hydroxybut-2-enal is achieved in this case (fifth row in **Table 1**).

The addition of Te to Pd/C catalyst lowers the production of all oxidation products. Bottom row in **Table 1** shows the inhibitory effect of Te on the chain radical oxidation reaction. At the same time, more noticeable becomes formation of the oxidation products non typical for the chain radical mechanism. These are crotonaldehyde and methyl vinyl ketone, which show the possibility of a nonradical heterolytic mechanism of oxidation on the PdTe/C catalyst.



Scheme 2. GC-detected products of the radical chain oxidation of BD.

Catalyst (mg)	BD (mmol)	Solvent	T (°C)	Time (h)	Products (mmol)						
					1+2	3	4	5	6	Others ¹	Peroxide ²
Pd(OAc) ₂ 2.5	70	HOAc/H ₂ O 88/12	70	2	2.5	0.6	0.1	<0.1	1.3	0.2	8.5
Pd(OAc) ₂ 2.5	70	HOAc/dioxane/H ₂ O 19/75/6	80	2	4.6	3.1	<0.1	0.4	7.8	0.1	9.4
0.5%Au/SiO ₂ 120	70	HOAc/dioxane/H ₂ O 44/50/6	80	4	4.7	3.2	<0.1	0.1	8.9	2.0	9.1
0.5%Au/SiO ₂ 120	70	HOAc/dioxane/H ₂ O 44/50/6	80	6	8.5	5.3	0.4	1.3	10.7	7.1	7.0
5%Pd/C 3000	100	DMA/H ₂ O 94/6	90	3	10.3	0.4	0	4.8	2.2	0.7 ³	0.8
5%Pd0.5%Te/C 3000	100	DMA/H ₂ O 94/6	90	3	0.5	0.1	0	0.1	0.1	0.8 ⁴	0.2

¹C8 diols and acetates, and C6 cyclic oxygenates.

²Iodometric titration.

³0.1mmol crotonaldehyde and methyl vinyl ketone.

⁴0.4 mmol crotonaldehyde and methyl vinyl ketone.

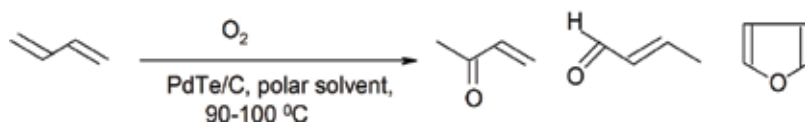
Table 1. GC detected products from oxidation of BD (70 mmol) by oxygen (O₂/N₂ = 10/90, 60 atm) in a solvent (100mL).

3. Oxidation of BD by a heterolytic mechanism involving palladium catalysts

Palladium catalysts are widely used in the liquid-phase heterolytic oxidation of olefins [38]. The most significant mechanisms for practice are acetoxylation of ethylene to vinyl acetate and Wacker oxidation of olefins converting ethylene to acetaldehyde and but-1-ene to methyl ethyl ketone. A mechanism of olefin oxygenation under the action of Pd(II) complexes established by Moiseev et al. and Henry et al. [39, 40] is now described in numerous publications (e.g., chapter by Reinhard Jira in book [24]). The mechanism includes the formation of Pd(II) complex with olefin and inner sphere transformations resulting in the reduction of Pd²⁺ to form carbonyl compound and Pd⁰ black. Assisted by Cu(II) chloride or other intermediate oxidant, reoxidation of Pd⁰ with oxygen closes the catalytic cycle, allowing the use of oxygen as a stoichiometric oxidant.

Analogous to light olefins, BD reacts under homogeneous conditions in an aqueous solution of PdCl₂ catalyst and CuCl₂ oxidant. The oxygenation is directed to one of the double bonds with the retention of the second double bond to produce crotonaldehyde [41, 42]. The oxidation conditions are identical to those applied for oxidation of ethylene to acetaldehyde and 1-butene to methyl ethyl ketone (Wacker-type oxidation), but the kinetics is different [43], in particular the order of reaction with respect to Cl⁻ and H⁺ ions. Unlike the oxidation of ethylene and other olefins, the oxidation of BD is zero-order with respect to the hydrocarbon. The kinetic parameters of BD oxidation are determined by high reactivity of the conjugated π -bonds, in particular by a strong BD to Pd²⁺ bonding in the intermediate complex. Unlike propylene, the oxygenation of the BD double bond is directed at the terminal rather than inner carbon atom to form crotonaldehyde. This is probably due to the stabilizing effect of the second double bond. In the presence of Pd²⁺ ions and another strong oxidizing agents of P-Mo-V heteropolyacids, BD is converted to furan in the similar conditions [44]. It seems like crotonaldehyde was initially formed and then converted under oxidizing conditions to furan, as in a similar homogeneous system [45]. Oxygen is a final stoichiometric oxidant, but the strong intermediate oxidant (Cu²⁺ or heteropolyacid) is necessary for easy regeneration of the ionic palladium in the oxidation of BD and olefins, as well.

We have observed catalysis by PdCl₂ when the radical chain oxidation of BD to diols, furan, and acrolein proceeds along with nonradical oxidation to form mainly crotonaldehyde together with small amounts of methyl vinyl ketone and furan (**Scheme 3**) (first row in **Table 2**). It is interesting that the system does not contain an oxidizing agent, except oxygen. There is no need of any intermediate oxidant since reoxidation of Pd⁰ to Pd²⁺ is provided by peroxide intermediates generated



Scheme 3. Nonradical reaction of BD on PdTe/C catalyst in polar solvents.

Catalyst (mg)	BD (mmol)	Time (h)	Products (mmol)						
			Furan	Acrolein	Methyl vinyl ketone	Crotonaldehyde	3-Butene-1,2-diol	2-Butene-1,4-diol, 4-hydroxybut-2-enal	Others
PdCl ₂ 120	43	3	0.4	1.1	0.3	1.6	3.2	3.9	0.2
PdCl ₂ 120, H ₆ TeO ₆ 800	43	3	0.2	0.5	<0.1	0.4	<0.1	0.5	0.1
5% Pd 2% Te/C 2000	22	6	0.1	<0.1	0.8	0.6	—	0.2	0.3

Table 2. GC detected products from oxidation of BD by oxygen (O₂/N₂ = 10/90, 60 atm) in DMA (30 mL, 3% H₂O), T 90°C.

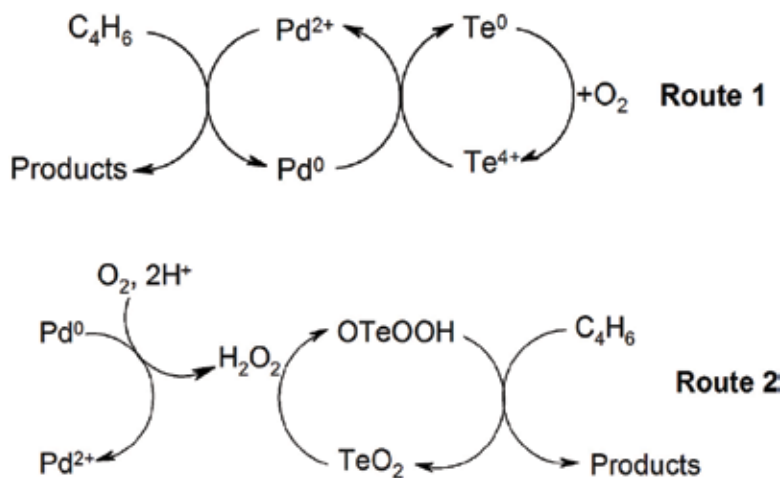
in a radical process. Telluric acid inhibits the radical process but does not operate as an oxidant for Pd⁰ to maintain the nonradical oxidation by Pd²⁺. As a result, the PdCl₂ with H₆TeO₆ solution is inactive in oxidation of BD (second row in **Table 2**). By contrast, the heterogeneous 5%Pd2%Te/C catalyst is able to provide nonradical oxidation, with the radical chain oxidation being inhibited by Te. As a result of inhibiting action of Te, the large amount of the catalyst and low concentration of BD appear unfavorable for the development of the chain process. The oxidation on the 5%Pd2%Te/C catalyst in aqueous dimethylacetamide (DMA) has been observed to give crotonaldehyde and methyl vinyl ketone as main products (third row in **Table 2**). Interestingly, crotonaldehyde is a predominant product of heterolytic oxidation with PdCl₂, but nearly equal amounts of crotonaldehyde and methyl vinyl ketone are produced on the 5%Pd2%Te/C catalyst in the same conditions.

Besides DMA, other polar solvents can be used in this oxidation. The presence of proton additive is required in the solvent (**Table 3**). No reaction has been observed in anhydrous acetonitrile.

Solvent (g)	Catalyst (g)	H ₂ O (%)	H ₂ SO ₄ (mmol/L)	Time (h)	Products (mmol)		
					Furan	Methyl vinyl ketone	Crotonaldehyde ¹
DMA	1	17	—	4	0.2	1.4	1.2
Dioxane	0.5	—	5	6	0.5	1.0	0.7
Acetonitrile	1	17	—	5	<0.1	1.0	0.8
Acetonitrile	1	17	8	5	0.3	1.7	0.9
Acetonitrile	0.5	—	2	4	0.8	2.0	1.2
Acetonitrile	0.5	—	—	3	0	0	0

¹Crotonaldehyde can be partly subjected to further oxidation to crotonic acid.

Table 3. GC detected products from oxidation of BD (4.5 mmol) by oxygen (O₂/N₂ = 10/90, 40 atm) on 5% Pd 2%Te/C catalyst in a solvent (35 mL), T 100°C.



Scheme 4. Tentative routes for nonradical oxidation of BD on PdTe/C catalyst.

According to XPS analysis, the 5%Pd2%Te/C catalyst contains both reduced Pd⁰ and ionic Pd²⁺, and two oxidation states of tellurium Te⁰ and Te⁴⁺ [46]. The Pd²⁺ to Pd⁰ ratio on the catalyst surface becomes larger with an increase in tellurium content that indicates an oxidizing influence of TeO₂. It can be expected that the oxidation state of the surface is enhanced under the reaction conditions. Nevertheless, dissolution of Pd and Te during reaction does not exceed 1% of the content of both components in the solid catalyst, the solution exhibiting no catalytic activity. Therefore, activity of the catalyst refers to the active components on the surface of carrier and is associated with their reversible redox transformations. Based on the known mechanisms of homogeneous oxidation of olefin, one can propose two possibilities for oxidation of BD by oxygen on the PdTe species, both assuming a nonradical heterolytic interaction. Perhaps the mechanism is in general similar to that postulated for the oxidation of BD and olefins in the presence of Pd²⁺ complexes, oxygen, and intermediate oxidant (**Scheme 4**, Route 1). It involves surface Pd²⁺ ions and TeO₂ oxidant providing regeneration of Pd²⁺.

However, there is a difference in products composition. Crotonaldehyde and furan are produced in above-mentioned oxidations of BD with homogeneous Pd²⁺ catalysts [41, 42], whereas methyl vinyl ketone is the second product formed in our oxidation on the PdTe catalyst. To explain this difference, one can consider an oxidation of BD by hydrogen peroxide as an alternative or parallel reaction (Route 2 in **Scheme 4**). Hydrogen peroxide is generated from oxygen on Pd⁰ species. The high reactivity of olefins with respect to peroxide compounds is known [47]. It is known that hydrogen peroxide does not accumulate during reaction. But it is found in trace amounts in the reaction solution and can form a reactive peroxide compound of Te⁴⁺ on the surface of the catalyst. In both mechanisms proposed, Te serves as a carrier of molecular or peroxide oxygen, and the surface of Pd²⁺/Pd⁰ activates reagents due to the adsorption of O₂ and BD. Thus, the PdTe/C catalyst opens the possibility of oxidation of BD by a nonradical heterolytic mechanism due to the combined effect of the two active components.

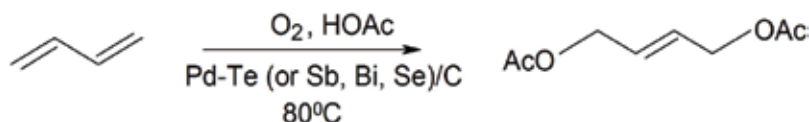
4. Heterolytic mechanism of 1,4-oxidative addition to BD

Wacker-type oxidation of olefins and analogous Pd-catalyzed nonradical oxidation of BD produce usually carbonyl compounds, but special additives are required for obtaining dioxygenates. Nevertheless, the oxidative 1,2-addition to olefins is known to occur under the action of Pd²⁺ complex and oxoanion strong oxidants, such as periodate [48] or nitrate anions, in acetic acid solution to form glycol derivatives [49–51]. Mechanism of the oxidation is based on a nonradical inner sphere interaction of olefin with oxidant in Pd²⁺ complex. Similar interaction is probably realized in oxidation of BD in the presence of palladium as the catalyst of nonradical heterolytic olefin oxidation and Sb, Bi, Te, or Se promoters. Heterogeneous catalysts containing these active components have shown unique catalytic properties in oxidation of BD selectively to 2-butene-1,4-diol diacetate (**Scheme 5**) [52, 53].

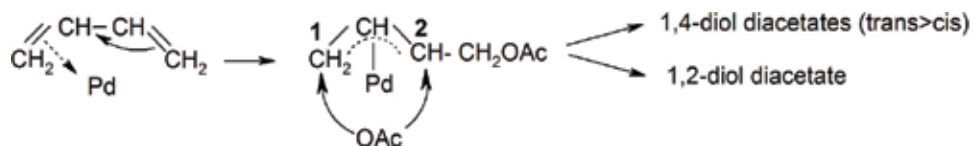
XPS analysis of the Pd and PdTe catalysts indicates that Te-oxide is able to increase positive charge on Pd surface [46], thus being an oxidation promoter for palladium. The ionic state of surface palladium is responsible for heterolytic oxidation. Acetic acid is used as a solvent for this reaction. The mechanism of formation of 2-butene-1,4-diol diacetate is proposed by Takehira et al. for PdTe catalyst (**Scheme 6**) [54], and fundamentally identical one is proposed for the RhTe catalyst [55]. The details in intermediate structures explain the preferential formation of trans-2-butene-1,4-diol in the case of Pd-containing catalyst and cis-isomer in the case of Rh.

Exceptionally high selectivity of BD to 2-butene-1,4-diol diacetate conversion is explained by a concert interaction of BD with surface Pd and with acetate anions. Adsorbed on Pd, BD forms π-allyl-type intermediate that undergoes acetoxylation on the terminal carbon atom. Resulting monoacetoxy reacts with the second acetate to give 2-butene-1,4-diol diacetates and 3-butene-1,2-diol diacetate in amounts proportional to the reactivity of carbon atoms 1 and 2 (**Scheme 6**). In fact, only 2-butene-1,4-diol diacetates are produced. Analogous mechanisms are realized in homogeneous oxidation of various dienes in the presence of Pd complexes and p-benzoquinone oxidizing agent, instead of Te. Oxidation of diene alcohols [56] and substituted conjugated diolefins [57] proceed effectively, but BD reacts with low yield and selectivity.

As noted earlier, Te-oxide is able to inhibit radical chain oxidation of BD, the selectivity of which is lower than the selectivity of the heterolytic process. Besides, Te operates as an inhibitor of radical polymerization of BD and oxidation products, thus preventing the formation of side high-boiling products. Acetic acid (possibly, other carboxylic acids) also contributes to the achievement of high selectivity in BD oxidation. Being not only solvent but also reagent (OAc⁻ anions), it is involved in an intermediate interaction with olefin to form the surface Pd



Scheme 5. Oxidative 1,4-addition to BD.



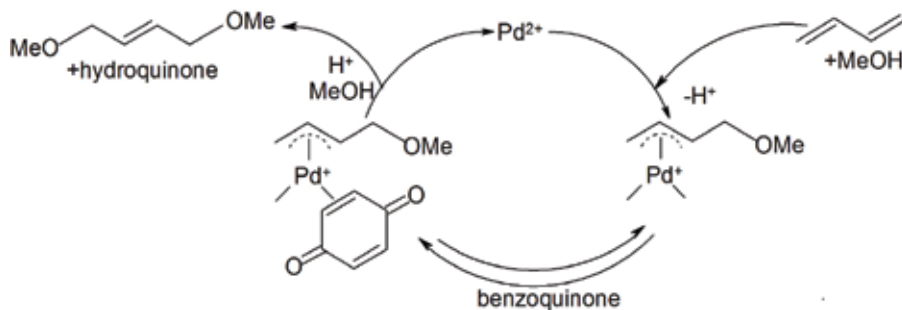
Scheme 6. Mechanism of 1,4-oxidative addition to BD [54].

intermediate, and finally stabilizes the product as ester, preventing its secondary transformations. Based on the unique properties of the PdTe/C-HOAc catalytic systems, the industrial process for the production of 2-butene-1,4-diol diacetate has been developed by Mitsubishi Chemical. BD is oxidized to 2-butene-1,4-diol diacetate with selectivity of 98%. Possible further improvements of the process can be connected with the application of other platinum metals (Pt, Rh, and Ir) combined with various promoters.

If acetic acid is replaced by alcohol, 1,4-dialkoxylation of conjugated dienes was developed in Pd(OAc)₂ solution. *p*-Benzoquinone was used as the oxidant and methanesulfonic acid as a promoter [58]. The oxidation is suggested to follow mechanism including the formation of the (π-allyl)palladium(benzoquinone) intermediate (**Scheme 7**).

In other case, dialkoxybutenes are prepared by reacting BD in the presence of carbon-supported Group VIII noble metals with Te or Se additives. Similar to diacetates, the formation of ethers in alcohol solvent increased the stability of dioxygenated products against secondary oxidation. However, the formation of 3,4-dimethoxy-1-butene and 1,4-dimethoxy-2-butene in comparable amounts is in contrast with **Scheme 6** and indicates a radical mechanism of BD oxidation, when 2-butene-1,4-diol and 3-butene-1,2-diol are formed as primary products and then converted to ethers in the alcohol medium [59].

We have prepared PdTe/C catalysts by hydrolytic deposition of palladium under the reductive conditions, followed by treatment with H₆TeO₆. The procedure is similar to one often described for the synthesis of PdTe catalysts. No evidences for the occurrence of binary Pd-Te phases have been provided by XRD, and XPS analysis evidences Pd⁰, PdO, Te⁰, and TeO₂ [60]. The absence of the Pd-Te phase and the partially oxidized state of the active metals have also been reported by Takehira [54] for Pd-Te-C catalysts. As assumed, Te is located in the

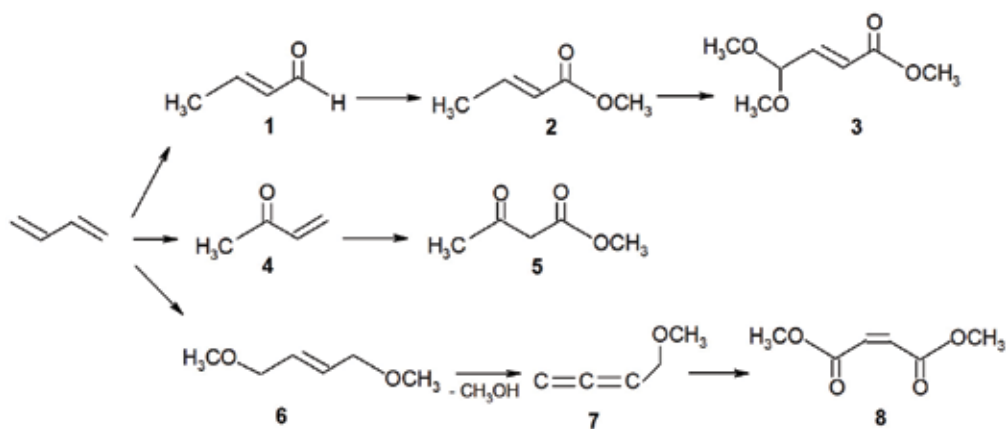


Scheme 7. 1,4-Dialkoxylation of conjugated dienes [38].

outer layer of supported particles. The characteristics of the PdTe/C catalysts were detailed by HAADF-STEM analysis of the surface and line EDX analysis of composition of the supported particles [60]. The results represent an unusual distribution of components on the surface, where Te does not form an individual crystalline phase but is located on the surface of Pd particles in a highly dispersed state. These data explain properties of the PdTe catalysts. In particular, the ability of Te to inhibit the radical reactions is in part due to the coverage of the palladium surface, which normally tends to initiate radical chains.

The primary products in BD oxidation on PdTe/C catalyst in methanol and further conversion of them under the oxidation conditions are shown in **Scheme 8**, and the amounts are given in **Table 4**.

As well as in DMA, nonradical heterolytic oxidation of BD in alcohol medium leads to the formation of crotonaldehyde (1) and methyl vinyl ketone (4). Besides, 1,4-dimethoxy-2-butene (6) is produced analogously to 2-butene-1,4-diol diacetate in acetic acid. The primary products undergo further transformations depending on the reaction conditions. Sulfuric acid promotes oxidation, especially toward 1,4-oxidative addition (comparison of first and second rows in **Table 4**). An increase in Te content lowers the reaction rate but increases proportion of products formed through 1,4-addition (third row in **Table 4**). Composition of oxidation products obtained in the presence of the Pd_{0.5}Te/C catalyst and H₂SO₄ is differed from the one in the radical chain oxidation (compare data given in **Tables 1** and **4**). 3,4-Dimethoxy-1-butene and acrolein that indicate nonradical oxidation do not appear. Peroxide compounds were also not detected in the solution after the reaction. The chain process does not develop due to the presence of Te and low concentration of BD used to eliminate the formation of the radical chains. Moreover, the radical products do not appear even at increased concentration of BD (fourth row in **Table 4**). Similarly to acetic acid, methyl alcohol in a mixture with sulfuric acid converts the oxidation products to methyl esters. However, oxidation in the alcohol medium is slower than in acetic acid, and further improvement of the selectivity of the formation of 1,4-addition products is required.



Scheme 8. Products of BD oxidation on PdTe/C catalyst in methyl alcohol.

Catalyst, conditions	Products (mmol)							
	1	2	3	4	5	6	7	8
5%Pd0.5%Te/C, 10 mmol BD, 100°C, 3 h	0.54	1.16	0.35	1.58	0.17	1.48	0	0.73
5%Pd0.5%Te/C, H ₂ SO ₄ , 10 mmol BD, 100°C, 3 h	0.45	2.02	0.08	0.12	1.42	2.30	0	1.81
5%Pd2.7Te/C, H ₂ SO ₄ , 10 mmol BD, 120°C, 2 h	0.24	0.06	0	0.06	0.66	2.80	2.0	0
5%Pd2.7Te/C, H ₂ SO ₄ , 40 mmol BD, 120°C, 2 h	0.23	0.06	0	0.07	0.78	6.70	3.90	0

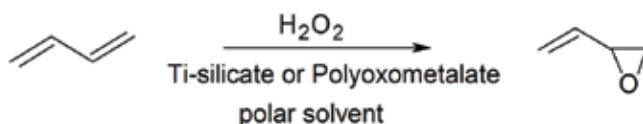
Table 4. Products of BD oxidation in solvent CH₃OH (10% H₂O) (30 mL), H₂SO₄ (0.1 mmol where indicated).

5. Synthesis of 3,4-epoxy-1-butene in liquid phase

Two competitive methods for direct epoxidation of olefins are gas-phase oxidation with oxygen over silver catalyst and liquid-phase reactions with organic hydroperoxides or hydrogen peroxide in the presence of soluble or supported W, Mo, Ti complexes. The gas-phase epoxidation is typical for obtaining light epoxides, whereas epoxidation with peroxide compounds in liquid is applicable for a wide range of substrates containing double bonds. Both type reactions are based on interaction of olefin with electrophilic oxygen species. Under liquid-phase epoxidation, catalytically active metal complexes react with peroxides to attach the reactive oxygen as ligand which attack the double bond of olefin. Hydrogen peroxide is effective oxygen donor and has an advantage of low-temperature reaction giving environmentally benign water as a by-product [61, 62].

The liquid-phase epoxidation of BD with H₂O₂ is known to occur over titanium silicates in CH₃OH [63] and in CH₃CN solution of heteropoly compounds [64, 65]. The data for these reactions are given in **Table 5**.

Both catalysts are activators of hydrogen peroxide, capable of forming peroxide complexes. Thoroughly investigated for various olefins, the mechanism of epoxidation is realized for the conversion of BD to 3,4-epoxy-1-butene. Coordinated on metal ion, the electrophilic oxygen interacts with one of the equivalent double bonds of BD leaving intact the second C=C bond. Oxygen transfer from peroxide ligand to double bond of olefin has been proved using isotopic reagents [64]. The addition of oxygen to the second bond of BD is more difficult; therefore, the formation of a diepoxide is not detected in reactions with hydrogen peroxide.



Lacunary polyoxotungstates are effective catalysts for epoxidation of olefins with H₂O₂ [66]. Besides olefins, [HPW₁₁O₃₉]⁶⁻ and [γ-SiW₁₀O₃₄(H₂O)₂]⁴⁻ anions catalyze epoxidation of BD with

Catalyst ¹	H ₂ O ₂ ¹ (mmol)	BD (bar)	Time (h)	Epoxide (mmol)	Sel.BD (%)	H ₂ O ₂ efficiency (%)	Reference
TS-1(6 mg) ²	0.5	1.5	1	0.25	n.d.	52	[63]
TBA4[γ-SiW ₁₀ O ₃₄ (H ₂ O) ₂] (3 μmol) ³	0.3	2.5	9	0.30	99	99	[64]
TBA-PW ₁₁ (10 μmol) ⁴	0.9	1	5.5	0.51	88	88	[65]
EMIm-PW ₁₁ (10 μmol) ⁴	0.9	1	5	0.65	91	90	[65]
EMIm-PW ₁₁ (2,3 μmol) ⁵	1.0	1	5	0.20	97	100	[65]

¹Catalyst, H₂O₂ and epoxide produced were normalized to 2 mL of the reaction mixture.

²CH₃OH solvent, room temperature.

³CH₃CN solvent, room temperature.

⁴CH₃CN solvent, 60 °C.

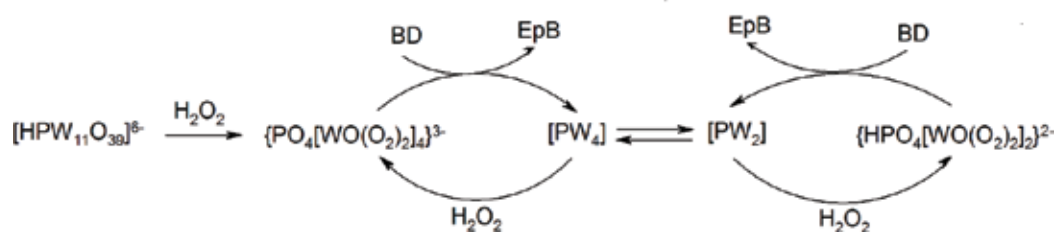
⁵CH₃CN solvent, 50 °C.

Table 5. Epoxidation of BD with H₂O₂ in solvents.

diluted aqueous H₂O₂ in acetonitrile solution. Epoxidation of BD has been shown to proceed with high selectivity for 3,4-epoxy-1-butene. Appearance of small admixtures of furan, 3-butene-1,2-diol, and 2-butene-1,4-oxygenates is associated with isomerization and hydrolysis of 3,4-epoxy-1-butene. The unproductive radical decomposition of H₂O₂ is minimal or absent when the reaction is carried out at a low temperature and at a low concentration of hydrogen peroxide. This is favorable for maintaining high selectivity for 3,4-epoxy-1-butene, because the secondary oxidation of 3,4-epoxy-1-butene by radical intermediates is prevented. As a result, only negligible amount of acrolein appears in the product. Moreover, small additives of EMImBr have been found to inhibit radical decomposition of H₂O₂, thus increasing the selectivity of BD to 3,4-epoxy-1-butene conversion and efficiency of H₂O₂ consumption. As a result, the efficiency of H₂O₂ consumption for producing 3,4-epoxy-1-butene is extremely high, it approaches to 100% under favorable conditions. Both Si- and P-centered heteropolytungstates exhibit equally effective catalysis.

Under reaction conditions, the catalytically active anions are generated from starting lacunary polyoxotungstate anion. It has been shown by NMR that [HPW₁₁O₃₉]⁶⁻ anion is a precursor of tungsten-depleted anions [PW₄] and [PW₂], which operate as the most effective activators of hydrogen peroxide and are responsible for epoxidation (**Scheme 9**) [65]. This is confirmed by the high reactivity of a specially synthesized anion {PO₄[WO(O₂)₂]₄}³⁻ in epoxidation of olefins [67].

Despite the limited use of 3,4-epoxy-1-butene itself, it is nevertheless a raw material for the synthesis of various C4-oxygenates such as 1,4-butanediol [68], 3-butene-1,2-diol and 2-butene-1,4-diol [69–71], and 2,5-dihydrofuran [72]. Therefore, low-temperature and selective epoxidation of BD can be considered as a principal stage of alternative synthesis of demanded and valuable chemicals.



Scheme 9. Transformations of heteropolytungstates in oxidation of BD to 3,4-epoxy-1-butene (EpB) [65].

6. Conclusion

Close nature of BD and light olefins is manifested in similar reaction properties, so that liquid-phase oxidation reactions of BD and olefins have similar mechanisms in many features. The oxidation of olefins and BD in liquid medium enables realization of several routes and obtaining a wide range of products, which are more diverse if compared with gas-phase oxidation. We have considered here the radical chain oxidative conversion of BD realized through the stable polyperoxide intermediate, the formation of which is, to a certain extent, inherent to many olefins. Palladium is able to catalyze homolytic (radical) and heterolytic (Wacker-type) oxidation of olefins. Very close to olefins, the properties of BD are manifested in reactions assisted by homogeneous and more often heterogeneous Pd-containing catalysts. (Note that the tendency to heterogenization of soluble catalysts is observed in liquid-phase reactions.) We observe an interesting phenomenon when the mechanism and products of the Pd-catalyzed oxidation are controlled by promoters. In dependence on other components, the catalytic action of Pd is switched from radical oxidation to nonradical oxygenation directed to one carbon atom or 1,4-position of BD when Pd is promoted with Te or related metals. The effect of Te as an oxidation promoter of palladium and a radical inhibitor allows PdTe catalysts to show substantial efficiency in the well-known industrial synthesis of 1,4-diacetoxybutene in acetic acid and also in other oxidations of BD such as formation of crotonaldehyde and methyl ethyl ketone in aqueous media. The reaction medium and concentration of reagents are also important factors to vary the mechanism of oxidation. Low concentration of BD in the reaction mixture reduces the development of the chain process and makes it possible to realize the oxidation by the heterolytic mechanism. Polar organics are conventional solvents for various oxidations, but acetic acid and methanol exhibit special properties creating conditions for preferable formation of esters of 1,4-butanediol. The identity in mechanisms is also observed in epoxidation of olefins and BD with hydrogen peroxide, where the same catalytically active Ti silicates and polyoxometalates are successfully used to attain highly selective conversion of hydrocarbon and H_2O_2 . All this shows that liquid-phase oxidation have a great potential in converting the BD into valuable oxygenates. To develop this area, extremely productive can be appeal to analogy in chemistry of BD and olefins. A large body of information relating to the oxidation of olefins can be productively applied to understand the mechanisms in oxidation of BD and to develop a strategy for synthesis of purposed oxidation products.

Acknowledgements

This work was conducted within the framework of budget project No 0303-2016-0006 for Boreskov Institute of Catalysis.

Author details

Nina I. Kuznetsova*, Lidia I. Kuznetsova, Olga A. Yakovina and Bair S. Bal'zhinimaev

*Address all correspondence to: kuznina@catalysis.ru

Boreskov Institute of Catalysis SB RAS, Novosibirsk, Russian Federation

References

- [1] Pedersen SE. Preparation of maleic anhydride using a crystalline vanadium(IV)bis (metaphosphate) catalyst. US4171316; 1979
- [2] Cavani F, Centi G, Trifiro F. Oxidation of I-butene and butadiene to maleic anhydride. 2. Kinetics and mechanism. Industrial and Engineering Chemistry Product Research and Development. 1983;**22**(4):570-577
- [3] Centi G, Trifiro F. Furan production by oxygen insertion in the 1-4 position of butadiene on V-P-O-based catalysts. Journal of Molecular Catalysis. 1986;**35**:255-265
- [4] Trifirò F, Jiru P. About some possibilities and causes of changes in selectivity of vanadium containing zeolitic catalysts in oxidation reactions. Catalysis Today. 1988;**3**(5):519-524
- [5] Hönicke D. Partial oxidation of 1,3-butadiene on $V_2O_5/Al_2O_3/Al$ -coated catalysts: Products and reaction routes. Journal of Catalysis. 1987;**105**:10-18
- [6] Schroeder WD, Fontenot CJ, Schrader GL. 1,3-Butadiene selective oxidation over VMoO catalysts: New insights into the reaction pathway. Journal of Catalysis. 2001;**203**:382-392
- [7] Monnier JR, Muehlbauer PJ. Epoxidation catalyst. US5081096; 1992
- [8] Barnicki SD, Monnier JR, Peters KT. Gas phase process for the epoxidation of non-allylic olefins. US5362890; 1999
- [9] Monnier JR, Peters KT. Selective epoxidation of conjugated diolefins. US6388106; 2002
- [10] Monnier JR. The direct epoxidation of higher olefins using molecular oxygen. Applied Catalysis A: General. 2001;**221**:73-91
- [11] Jin GJ, GZ L, Guo YL, Guo Y, Wang JS, Kong WY, Liu XH. Effect of preparation condition on performance of Ag-MoO₃/ZrO₂ catalyst for direct epoxidation of propylene by molecular oxygen. Journal of Molecular Catalysis A: Chemical. 2005;**232**(1-2):165

- [12] JQ L, Bravo-Suárez JJ, Takahashi A, Haruta M, Oyama ST. In situ UV–Vis studies of the effect of particle size on the epoxidation of ethylene and propylene on supported silver catalysts with molecular oxygen. *Journal of Catalysis*. 2005;**232**(1):85-95
- [13] Rao VNM. Oxidation catalyst. US4429055; 1984
- [14] Parthasarathy R, Hort EV. Solid catalysts for oxidative dehydrogenation of alkenes or alkadienes to furan compounds. US4293444; 1981
- [15] Parthasarathy R, Hort EV. Catalytic oxidative dehydrogenation of alkenes or alkadienes to furan compounds. US4309355; 1982
- [16] Bither Jr, TA. Vapor phase oxidation of n-butane to maleic anhydride. US4371702; 1983
- [17] Bither Jr, TA. Catalyst for vapor phase oxidation of n-butane to maleic anhydride. US4442226; 1984
- [18] Mailis PM. *The Organic Chemistry of Palladium*. New York and London: Academic Press; 1971
- [19] Niki E, Kamiya Y. The autoxidation of olefins in the liquid phase. *Sekiyu Gakkaishi*. 1967;**10**(4):248-254
- [20] Metelitsa DI. Mechanisms of the direct liquid-phase epoxidation of olefins. *Uspekhi Khimii*. 1972;**41**(10):1737-1765
- [21] Mill T, Hendry DG. Kinetics and mechanisms of free radical oxidation of alkanes and olefins in the liquid phase. *Comprehensive Chemical Kinetics*. 1980;**16**:1-87
- [22] Pritzkow W. Studies of liquid-phase oxidation of olefinic hydrocarbons with molecular oxygen. *Wissenschaftliche Zeitschrift der Technischen Hochschule Carl Schorlemmer Leuna-Merseburg*. 1987;**29**(1):25-47
- [23] Lyons JE. Selective oxidation of hydrocarbons via carbon-hydrogen bond activation by soluble and supported palladium catalysts. *Catalysis Today*. 1988;**3**(2-3):245-258
- [24] Stahl SS, Alsters PL, editors. *Liquid Phase Aerobic Oxidation Catalysis Industrial Applications and Academic Perspectives*. Weinheim, Germany: Wiley-VCH Verlag GmbH & Co. KGaA; 2016
- [25] Khatib SJ, Oyama ST. Catalytic oxidation of olefins. *Catalysis Reviews: Science and Engineering*. 2015;**57**(3):306-344
- [26] Brink G-J, Arends IWCE, Papadogianakis G, Sheldon RA. Catalytic conversions in water. Part 13. Aerobic oxidation of olefins to methyl ketones catalyzed by a water-soluble palladium complex—Mechanistic investigations. *Applied Catalysis A: General*. 2000;**194-195**:435-442
- [27] Zhang Y, You H. Direct oxidation of propylene to propylene oxide with molecular oxygen. *Open Fuels & Energy Science Journal*. 2011;**4**:9-11
- [28] Hudlicky M. *Oxidations in Organic Chemistry*. ACS Monograph Series. Washington, DC: American Chemical Society; 1990

- [29] Murphy EF, Mallat T, Baiker A. Allylic oxofunctionalization of cyclic olefins with homogeneous and heterogeneous catalysts. *Catalysis Today*. 2000;**57**:115-126
- [30] Handy CT, Rothrock HS. Polymeric peroxide of 1,3-butadiene. *Journal of the American Chemical Society*. 1958;**80**:5306-5308
- [31] Henry D, Mayo FR, Schuetzle D. Oxidation of 1,3-butadiene. *Industrial and Engineering Chemistry Product Research and Development*. 1968;**7**(2):136-145
- [32] Mabuchi S, Tsuzuki K, Matsunaga H, Shimizu S, Sumita M. Method of producing diol by hydrogenolysis of peroxide polymers with reactivation of Raney nickel catalyst. US3980720; 1976
- [33] Mabuchi S, Tsuzuki K. 1,4-Butanediol. DE 2232699; 1973
- [34] Tsuzuki K. Butan-1,4-diol production from butadiene via its polyperoxide and hydrogenolysis. DE2232699; 1973
- [35] Handy CT, Rothrock HS. Polymeric butadiene peroxide. US2898377; 1959
- [36] Henry DG, Mayo FR, Jones DA, Schuetzle D. Stability of butadiene polyperoxide. *Industrial and Engineering Chemistry Product Research and Development*. 1968;**7**(8):145-151
- [37] Nakanishi F, Inoue T, Omori Y, Harada A, Utsunomiya M. *Jpn Kokai Tokkyo Koho*. JP 2003238465 A 20030827; 2003
- [38] Henry PM. *Palladium Catalyzed Oxidation of Hydrocarbons*. Boston, MA: D. Reidel; 1980
- [39] Moiseev II, Vargaftik MN, Syrkin YK. Kinetic stages in the oxidation of ethylene by palladium chloride in aqueous solution. *Doklady Akademii Nauk SSSR*. 1963;**153**(1):140-143
- [40] Henry PM. Kinetics of the oxidation of ethylene by aqueous palladium(II) chloride. *Journal of the American Chemical Society*. 1964;**86**(16):3246-3250
- [41] Hotanahalli SS, Chandalia SB. Oxidation of butadiene to crotonaldehyde: Some aspects of process development. *Indian Chemical Journal*. 1970;**5**(1):187-193
- [42] Hotanahalli SS, Chandalia SB. Kinetics of oxidation of butadiene to crotonaldehyde. *Journal of Applied Chemistry*. 1970;**20**(10):323-325
- [43] Baiju TV, Gravel E, Doris E, Namboothiri INN. Recent developments in Tsuji-Wacker oxidation. *Tetrahedron Letters*. 2016;**57**:3993-4000
- [44] Lindsey RVJr, Prichard WW. Oxidation of butadiene to furan. US4298531 A 19811103; 1981
- [45] Lu L, Domen K, Maruya K, Ishimura Y, Yamagami I, Aoki T, Nagato N. Liquid phase oxidation of crotonaldehyde to furan by aqueous CuCl_2 . *Reaction Kinetics and Catalysis Letters*. 1998;**64**(1):15-20
- [46] Trebushat DV, Kuznetsova NI, Koshcheev SV, Kuznetsova LI. Oxidation of 1,3-butadiene over Pd/C and Pd-Te/C catalysts in polar media. *Kinetics and Catalysis*. 2013;**54**(2):233-242

- [47] Roussel M, Mimoun H. Palladium-catalyzed oxidation of terminal olefins to methyl Ketones by hydrogen peroxide. *The Journal of Organic Chemistry*. 1980;**45**:5387-5390
- [48] Kuznetsova NI, Fedotov MA, Likholobov VA, Yermakov YI. Mechanism of catalytic oxidation of olefins by periodic acid in acetic solution of palladium acetate. *Journal of Molecular Catalysis*. 1986;**38**:263-271
- [49] Henry PM. Oxidation of olefins by palladium(II). 111. Oxidation of olefins by a combination of palladium(II) chloride and copper(II) chloride in acetic acid. *The Journal of Organic Chemistry*. 1967;**32**:2575-2580
- [50] Tamura M, Yasui T. A novel synthesis of glycol mono-ester from an olefin. *Chemical Communications (London)*. 1968;**20**:1209
- [51] Kuznetsova N I, Likholobov VA, Fedotov MA, Yermakov YI. The mechanism of formation of ethylene glycol monoacetate from ethylene in the acetic acid-lithium nitrate-palladium acetate system. *Journal of the Chemical Society, Chemical Communications*. 1982;(17):973-974
- [52] Onoda T, Haji J. Process for preparing an unsaturated glycol diester. US3755423 (A); 1973
- [53] Onoda T, Yamura A, Ohno A, Haji J, Toriya J, Sato M, Ishizaki N. Process for preparing an unsaturated ester. US3922300 (A); 1975
- [54] Takehira K, Mimoun H, De Roch IS. Liquid-phase diacetoxylation of 1,3-butadiene with Pd-Te-C catalyst. *Journal of Catalysis*. 1979;**58**:155-169
- [55] Takehira K, Chena JAT, Niwa S, Hayakawa T, Ishikawa T. Liquid-phase diacetoxylation of 1,3-butadiene with Rh-Te-C catalyst. *Journal of Catalysis*. 1982;**76**:354-368
- [56] Backvall J-E, Andersson PG. Intramolecular palladium-catalyzed 1,4-addition to conjugated dienes. Stereoselective synthesis of fused tetrahydrofurans and tetrahydropyrans. *Journal of the American Chemical Society*. 1992;**114**:6374-6381
- [57] Backvall J-E, Byetrom SE, Nordberg RE. Stereo- and regioselective palladium-catalyzed 1,4-diacetoxylation of 1,3-dienes. *The Journal of Organic Chemistry*. 1984;**49**:4619-4631
- [58] Backvall J-E, Vagberg JO. Stereo- and regioselective palladium-catalyzed 1,4-dialkoxylation of conjugated dienes. *The Journal of Organic Chemistry*. 1988;**53**:5695-5699
- [59] Constantini M, Laucher D. Preparation of dialkoxybutenes. US5159120; 1992
- [60] Kuznetsova NI, Zudin VN, Kuznetsova LI, Zaikovskii VI, Kajitani H, Utsunomiya M, Takahashi K. Versatile PdTe/C catalyst for liquid-phase oxidations of 1,3-butadiene. *Applied Catalysis A: General*. 2016;**513**:30-38
- [61] Grigoropoulou G, Clark JH, Elings JA. Recent developments on the epoxidation of alkenes using hydrogen peroxide as an oxidant. *Green Chemistry*. 2003;**5**(1):1-7
- [62] Wojtowicz-Mlochowska H. Synthetic utility of metal catalyzed hydrogen peroxide oxidation of C-H, C-C and C=C bonds in alkanes, arenes and alkenes: Recent advances. *ARKIVOC (Gainesville, FL, United States)*. 2017;**2**:12-58

- [63] Zhang X, Zhang Z, Suo J, Li S. Catalytic monoepoxidation of butadiene over titanium silicate molecular sieves TS-1. *Catalysis Letters*. 2000;**66**:175-179
- [64] Kamata K, Kotani M, Yamaguchi K, Hikichi S, Mizuno N. Olefin epoxidation with hydrogen peroxide catalyzed by lacunary polyoxometalate $[\gamma\text{-SiW}_{10}\text{O}_{34}(\text{H}_2\text{O})_2]^{4-}$. *Chemistry: A European Journal*. 2007;**13**:639-648
- [65] Kuznetsova LI, Kuznetsova NI, Maksimovskaya RI, Aleshina GI, Koscheeva OS, Utkin VA. Epoxidation of butadiene with hydrogen peroxide catalyzed by the salts of Phosphotungstate anions: Relation between catalytic activity and composition of intermediate Peroxo complexes. *Catalysis Letters*. 2011;**141**:1442-1450
- [66] Al-Ajlouni AM, Saglama O, Diaflab T, Kuhn FE. Kinetic studies on phenylphosphopolyperoxotungstates catalyzed epoxidation of olefins with hydrogen peroxide. *Journal of Molecular Catalysis A: Chemical*. 2008;**287**:159-164
- [67] Venturello C, D'Aloisio R, Bart JCJ, Ricci M. A new peroxotungstate heteropoly anion with special oxidizing properties: Synthesis and structure of tetrahexylammonium tetra(diperoxotungsto) phosphate(-3). *Journal of Molecular Catalysis*. 1985;**32**:107-110
- [68] Mackenzie PB, Kanel JS, Falling SN, Wilson AK. Process for the preparation of 2-alkene-1,4-diols and 3-alkene-1,2-diols from gamma, delta-epoxyalkenes. US5959162; 1999
- [69] Cheeseman N, Fox M, Jakson M, Lennon IC, Meek G. An efficient, palladium-catalyzed, enantioselective synthesis of (2R)-3-butene-1,2-diol and its use in highly selective Heck reactions. *Proceedings of the National Academy of Sciences of the United States of America*. 2004;**101**:5396-5399
- [70] Remans TJ, van Oeffelen D, Steijns M, Martens JA, Jacobs PA. Iodide assisted zeolite catalyzed 1,4-addition of water to butadiene monoxide. *Journal of Catalysis* 1998;**175**:312-315
- [71] Musolino MG, Apa G, Donato A, Pietropaolo R. Cis-trans isomerization over solid acid catalyst. *Catalysis Today*. 2005;**100**:467-471
- [72] Matsuno H, Odaka K. Process for preparation of 2,5-dihydrofuran by cyclization of cis-2-butene-1,4-diol. *Jpn. Kokai Tokkyo Koho*. JP09110850; 1997

Polyolefins

Poly(olefin sulfone)s

Takeo Sasaki, Khoa Van Le and Yumiko Naka

Additional information is available at the end of the chapter

<http://dx.doi.org/10.5772/intechopen.69317>

Abstract

In this chapter, we introduce poly(olefin sulfone)s and review the recent progress on the photoinduced depolymerization of poly(olefin sulfone)s as well as their applications. Poly(olefin sulfone)s combined with photobase generators (PBGs) are depolymerized upon irradiation with light. A poly(olefin sulfone) is a 1:1 alternating copolymer of olefin monomer and sulfur dioxide in which the protons on the carbons adjacent to the sulfonyl groups can be readily abstracted by a base. This removal leads to a depolymerization chain reaction, resulting in incorporation of a photobase generating chromophore that can undergo a photoinduced unzipping reaction. During this reaction, the original olefin monomer and sulfur dioxide are regenerated from the primary chain of the poly(olefin sulfone). The photoinduced depolymerization of poly(olefin sulfone)s has been investigated for a wide variety of applications, including stereolithography, printable microcircuit fabrication, and removable adhesives.

Keywords: poly(olefin sulfone)s, depolymerization, photopolymers, dismantlable adhesives

1. Introduction

Photopolymers can change their physical and/or chemical properties through the absorption of light [1]. Although many studies on photopolymers have been reported, a few studies show photoinduced conversion to monomers under mild conditions. If a portion of the polymer is converted completely into monomers under light irradiation, the average molecular weight decreases, and this process has potential application to sophisticated device processing, including stereolithography without solvents. Such depolymerization under mild conditions is expected to yield recyclable (and, thus, environmentally friendly or “green”) polymers. However, most of the depolymerizable polymers reported require X-ray or electron-beam irradiation to trigger the depolymerization process [2, 3]. Only a few reports describe use

of low-energy irradiation for the depolymerization [4–10]. The unzipping degradation of a polymer main chain containing heteroatoms by X-ray or electron-beam irradiation has been achieved. For a poly(1-butene sulfone), only partial depolymerization occurs, and olefins are present in the gas produced by the irradiation [11, 12].

Degradation of a poly(olefin sulfone) doped with a photosensitizer has been investigated [13]. The degradation of poly(1-butene sulfone) doped with pyridine N-oxide was induced by irradiation with 300-nm light. In this system, however, a crosslinking reaction occurs in addition to degradation of the main chain. The number of photoinduced breaks in the main chain was 10–12. High-efficiency depolymerization to constituent monomers was achieved for poly(olefin sulfone)s containing photobase generators using low-energy light irradiation.

2. Poly(olefin sulfone)s

Poly(olefin sulfone)s are copolymers of olefin monomers and sulfur dioxide (**Figure 1**). They possess sulfonyl groups ($-\text{SO}_2-$) in the main chain and are easily synthesized by radical polymerization of an olefin monomer in a liquefied sulfur dioxide [14]. Peroxides, such as tert-butyl hydroperoxide, benzoyl peroxide, and diethyl ether peroxides, are used as polymerization initiators. The peroxide and sulfur dioxide act as a redox initiator and generate a radical species that reacts with an olefin monomer (**Figure 2**). While the sulfonyl radical is fairly stable, the olefin radical is unstable. The olefin radical generated in liquefied sulfur dioxide immediately reacts with a sulfur dioxide molecule to form an alkylated sulfonyl radical. The sulfonyl radicals then react with the olefin monomers to generate a polymer chain. Note that the sulfur atom of the sulfonyl radical is positively charged; therefore, it cannot react with the sulfur atom of sulfur dioxide, which is also positively charged. In addition, the olefin monomer and sulfur dioxide form a 1:1 charge-transfer complex in the liquefied SO_2 solution. The olefin- SO_2 complex reacts like a monomer unit in the radical polymerization process. Thus, the resulting poly(olefin sulfone) is a 1:1 alternating copolymer of olefin monomers and SO_2 [15].

2.1. Synthesis of poly(olefin sulfone)s

At ambient pressure, sulfur dioxide gas liquefies when cooled to temperatures below -10.2°C . The polarity of liquefied sulfur dioxide is comparable to that of dichloromethane, so liquefied sulfur dioxide dissolves a wide range of olefins. A high-pressure polymerization tube containing 1.0 g of an olefin monomer and 3.2×10^{-4} mol of t-butyl hydroperoxide (a redox initiator) was connected to a vacuum line and cooled in liquefied nitrogen. The tube was evacuated, and 6.0 g of sulfur dioxide was added by transfer through a vacuum line. The mixture was stirred for 24 h at -13°C . The resulting polymer was reprecipitated in methanol. Examples of chemical structures of simple poly(olefin sulfone)s are shown in **Figure 3**.

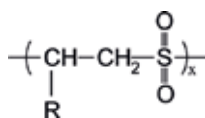


Figure 1. Structure of poly(olefin sulfone)s.

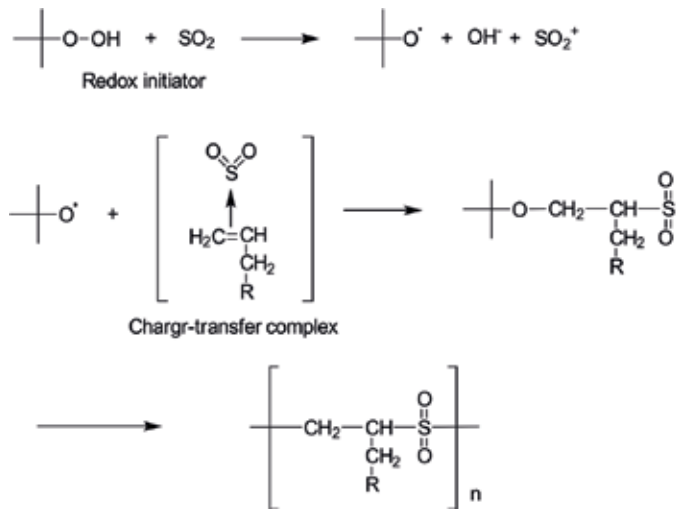


Figure 2. Polymerization of olefin monomers in liquefied sulfur dioxide.

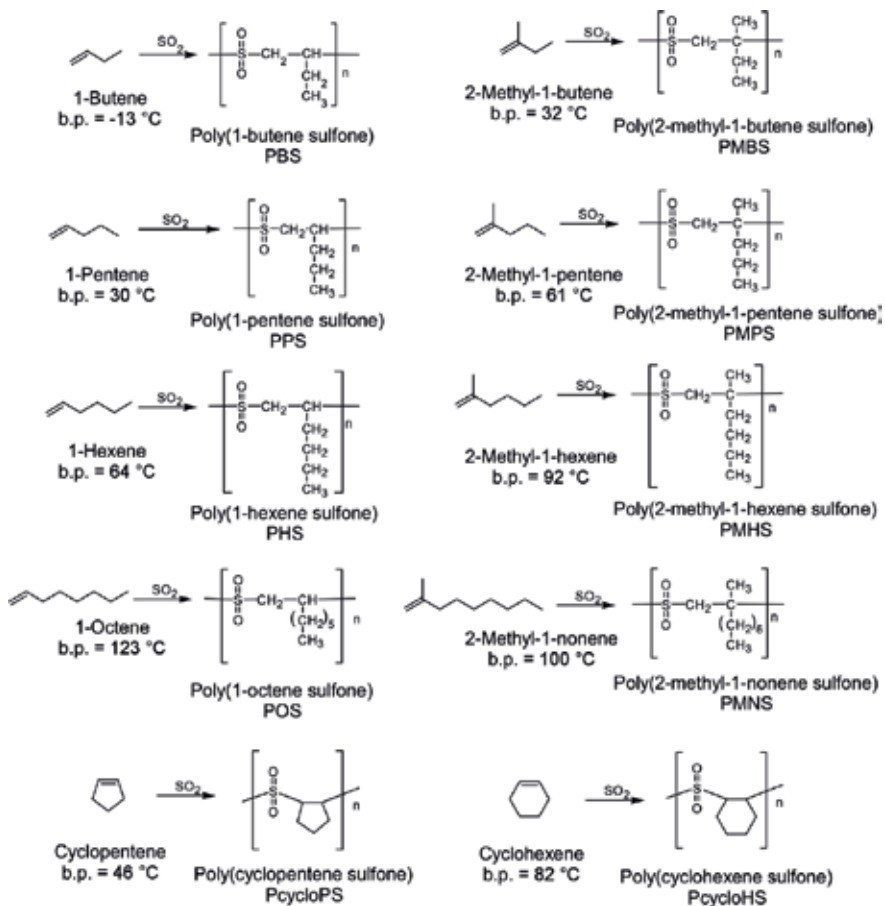


Figure 3. Examples of poly(olefin sulfone)s.

is shown in **Figure 5(b)**. Signals of the olefin protons are easily recognized. In contrast, no change was observed in the DEBA solution without the addition of base, indicating that the decomposition of DEBA was caused by the added base. The ^1H NMR spectrum of the olefin monomer (N, N-diethyl 3-butenoic amide) is shown in **Figure 5(c)**. A comparison of **Figure 5(b)** and (c) showed that the major product in the resulting solution can be attributed

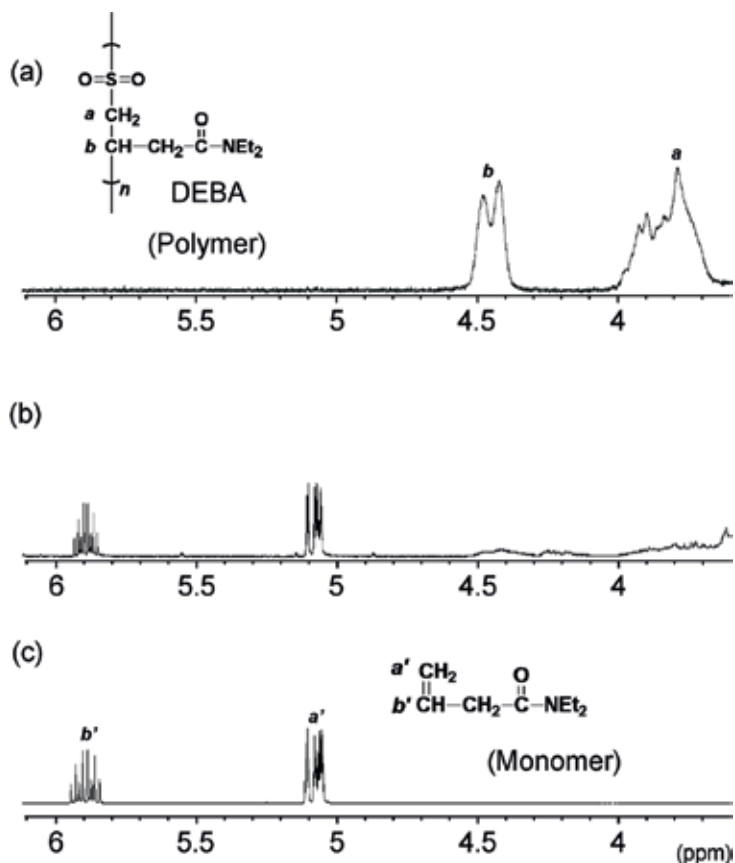


Figure 5. ^1H NMR spectra of DMSO-d_6 solutions of (a) DEBA, (b) DEBA mixed with 6.15 mmol/L 4,4'-trimethylenedipiperidine followed by heating at 100°C for 30 min, and (c) a monomer of DEBA.

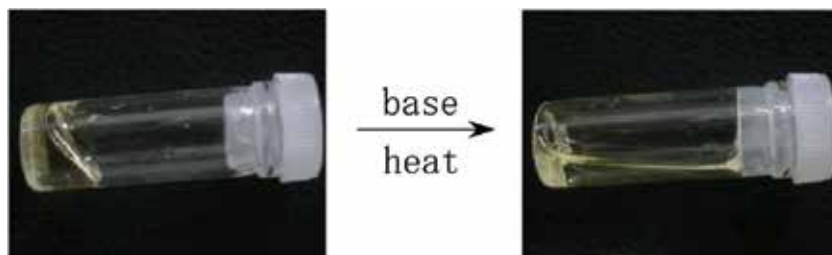


Figure 6. Photographs of the conc. solution of poly(olefin sulfone)s. The viscosity of the solution decreased rapidly when a trace of triethylamine was added to the solution.

to the DEBA monomer. **Figure 6** shows a picture of a concentrated solution of a poly(olefin sulfone). Although the viscosity of the solution was very high, when a trace of triethylamine vapor was added to the solution, the viscosity decreased immediately.

4. Photoinduced depolymerization of poly(olefin sulfone)s

A poly(olefin sulfone) possessing a photobase generating group depolymerizes upon photoirradiation and heating (**Figure 7**). Poly(olefin sulfone)s that possess photobase-generating groups were synthesized (**Figures 8 and 9**) [17]. The photobase-generating groups produce amine groups when irradiated with light. Photoinduced decomposition of the poly(olefin sulfone) was investigated using ^1H NMR. A poly(olefin sulfone) film was subjected to irradiation with 254-nm light, after which ^1H NMR spectra were recorded. **Figure 10(a)** and **(b)** show the ^1H NMR spectra of polymer 10 before and after irradiation, respectively, followed by heating. The progress of depolymerization was readily confirmed by the disappearance of the methylene and methine protons in the main chain (4.3–3.8 ppm), along with the appearance of signals near 5.1 and 5.8 ppm, which were assigned to protons on a vinyl group. The decomposition ratio of polymer 10 irradiated and heated under the conditions described above was estimated to be 95%. The decomposition ratio increased with the irradiation energy density (**Figure 11**). Conversion of the polymer to the olefin monomer (depolymerization ratio) was also estimated to be 50%. The irradiated film (polymer 10) after heating was dissolved in THF and the molecular weight measured by gel permeation chromatography (GPC) (**Figure 12**). The polymer completely disappeared and low-molecular-weight species appeared. The retention time of the lowest molecular weight species was coincident with that of the olefin monomer. The number average molecular weight decreased from 130,000 to 300.

As shown in **Figure 13**, a lithographic image with clear positive tone of alternating 40- μm wide lines and gaps on a film of polymer 10 could be developed with 0.012 M aq. HCl.

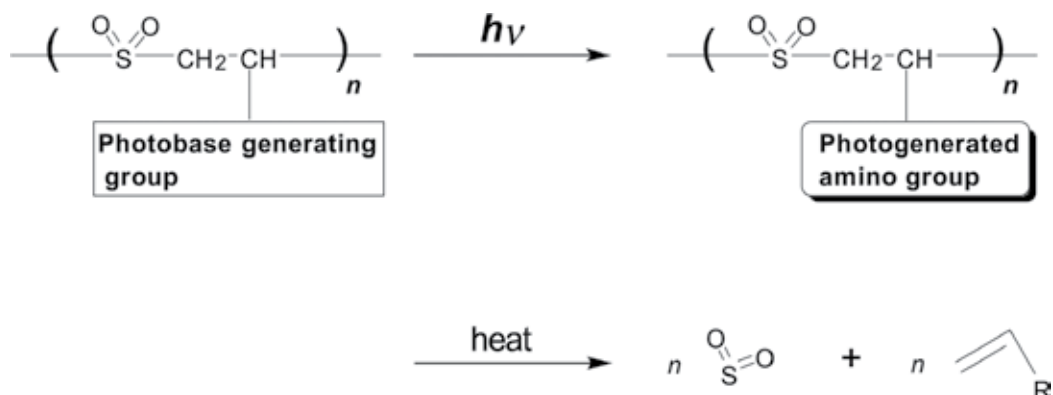


Figure 7. Proposed mechanism of base-catalyzed thermal depolymerization of 1:1 alternating poly(olefin sulfone)s.

Irradiation with 254-nm light triggered the generation of a base along with creation of a latent image. The visible image could be developed after heating the exposed polymer film.

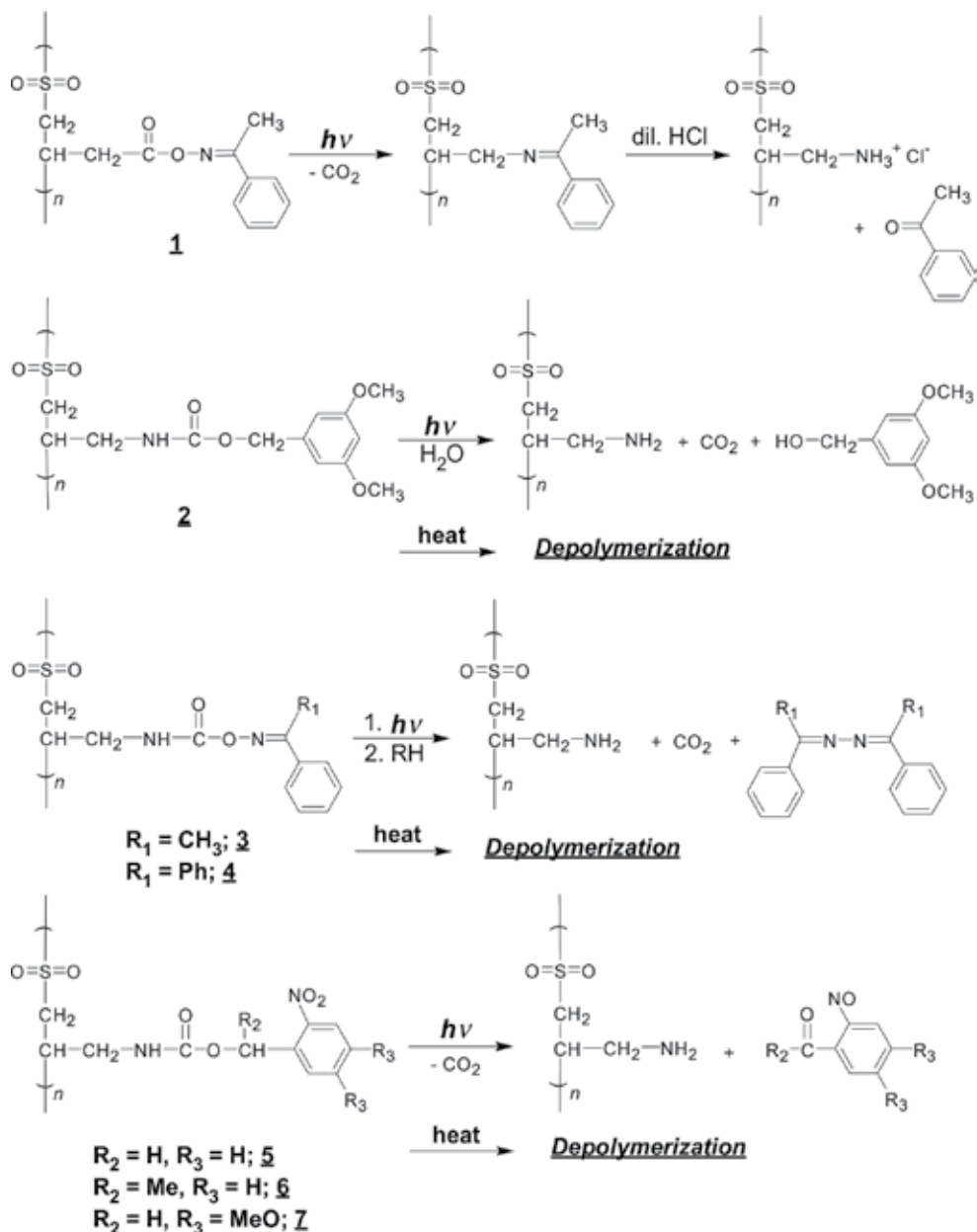


Figure 8. Structures of poly(olefin sulfone)s that generates primary amine by photo irradiation and the photochemical reactions of the pendant group.

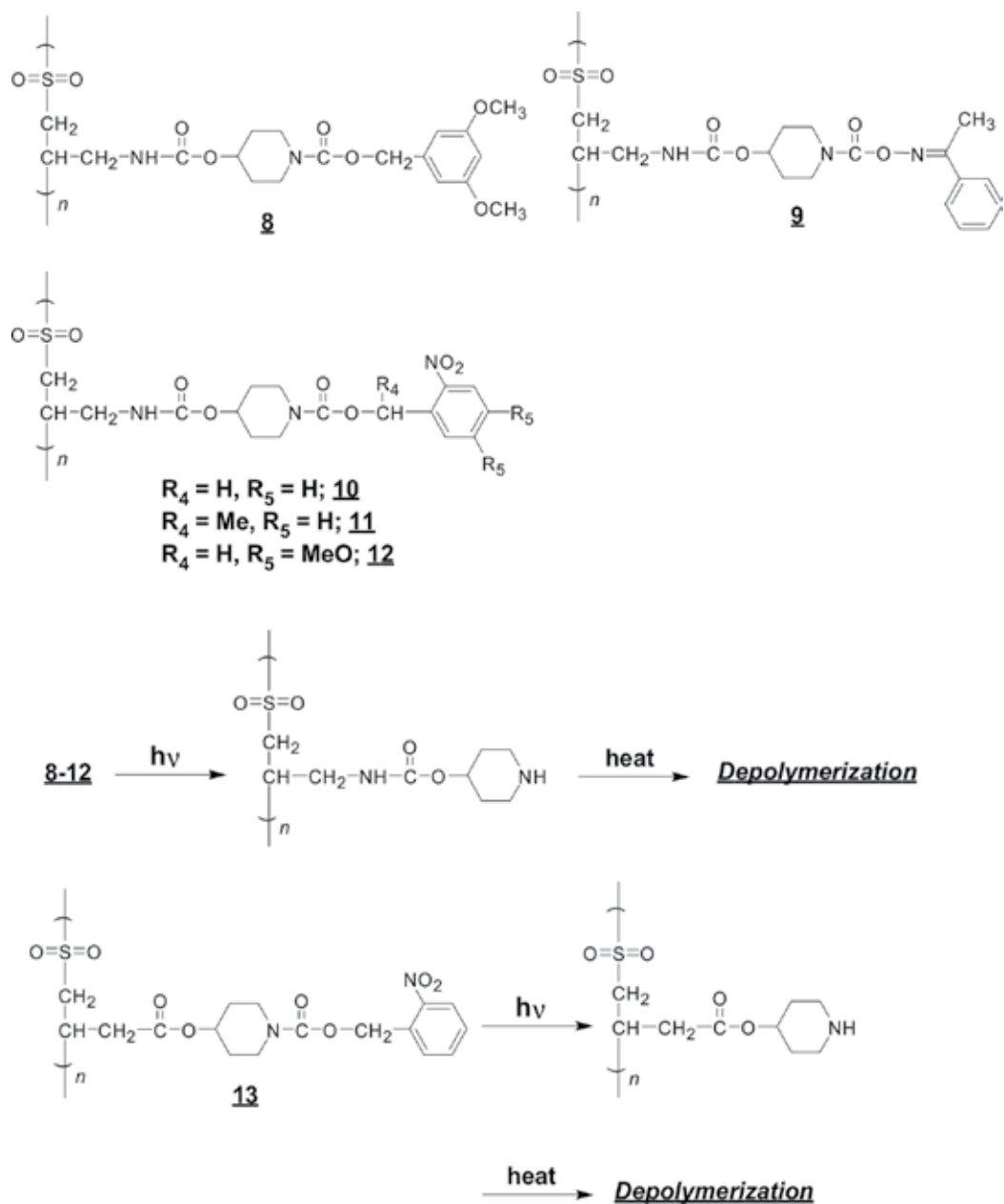


Figure 9. Structures of poly(olefin sulfone)s that generates secondary amine by photo irradiation and the photochemical reactions of the pendant group.

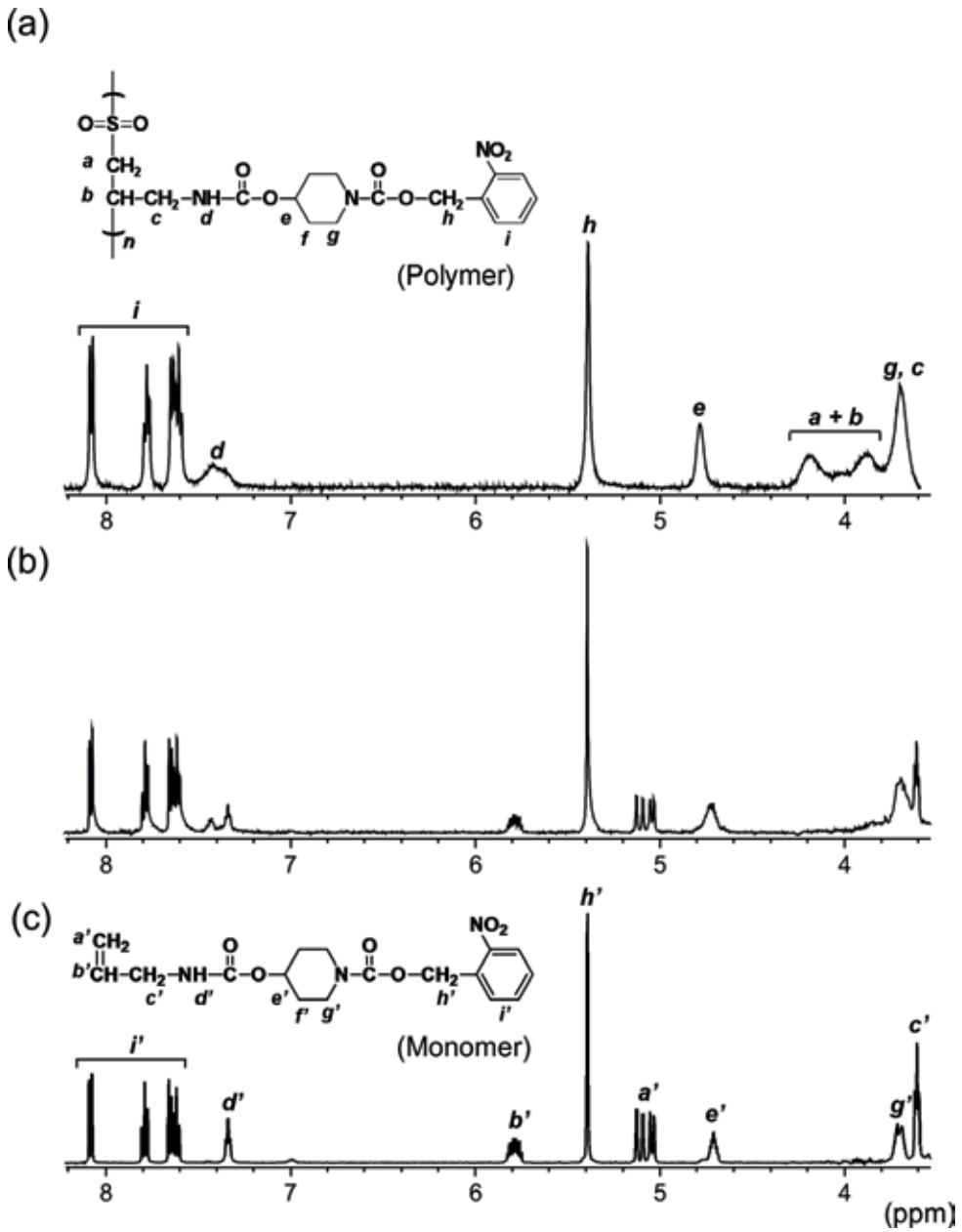


Figure 10. ^1H NMR spectra of polymer 10 in DMSO-d_6 , (a) before UV irradiation, (b) after 254-nm irradiation of 600 mJ/cm^2 followed by heating at 150°C for 15 min, and (c) monomer 10.

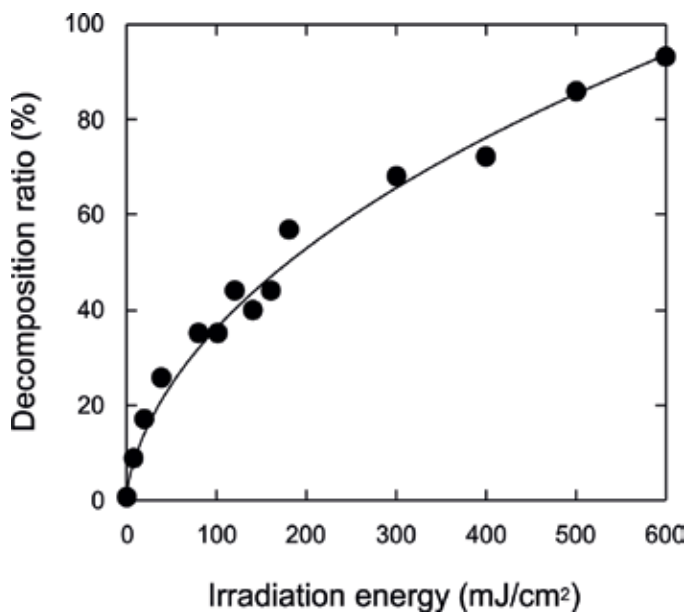


Figure 11. Decomposition ratio of polymer 10 heated at 150°C for 15 min after UV irradiation as a function of irradiation energy.

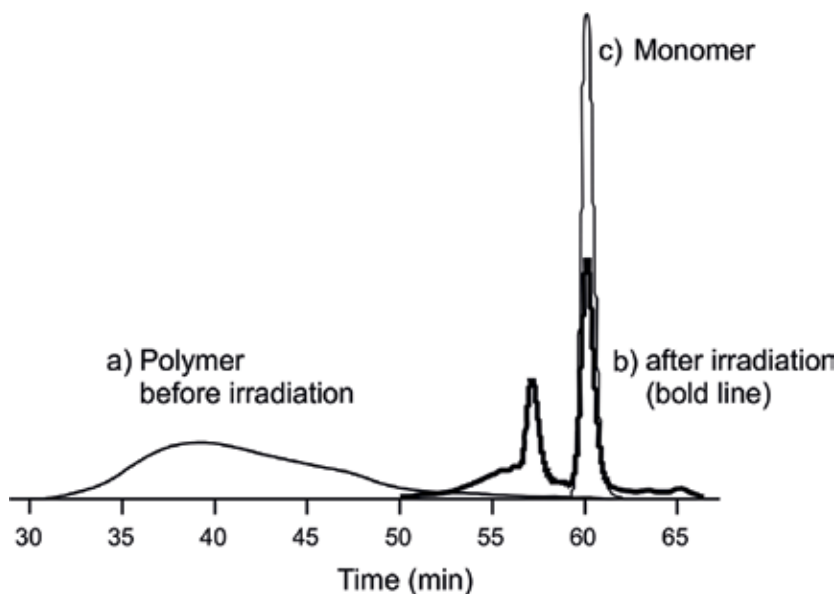


Figure 12. GPC curves of polymer 10 (a) before UV irradiation, (b) after UV irradiation at 600 mJ/cm², followed by heating at 150°C for 15 min, and (c) the corresponding olefin monomer.

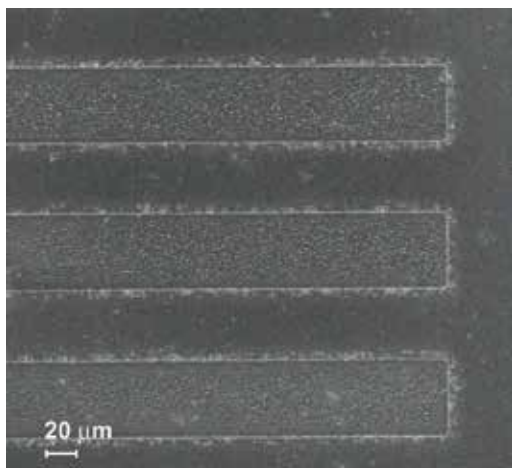


Figure 13. SEM image of polymer 10 film after UV irradiation at 100 mJ/cm^2 , followed by heating at 130°C for 60 sec and washed with 0.012 M HCl(aq) .

5. Effect of main chain structure on depolymerization of poly(olefin sulfone)s

Photoinduced depolymerization of the polymers shown in **Figure 3** mixed with a low-molecular-weight photo-base generator (ANC2) was investigated [18]. **Figure 14(a)** shows the change in the IR spectrum of PMPS film coated on a KBr plate without light irradiation, and **Figure 14(b)** shows the corresponding spectrum after light irradiation during heating (post-exposure heat treatment). The absorption spectrum of the nonirradiated film was independent of the heating time, whereas the sulfonyl stretching bands (1311 and 1130 cm^{-1}) decreased with the heating time after film irradiation, which indicates decomposition of the polymer main chain. The extent of decomposition increased with the irradiation energy density (**Figure 14(c)**), and the extent of PMPS decomposition was estimated to be 95%. Conversion of the polymer to the olefin monomer (extent of depolymerization) was estimated by $^1\text{H NMR}$ as 92%. Therefore, the polymer was converted to monomers with very high efficiency. **Figure 15(a)** shows the residual ratio of the PBS sulfonyl group as a function of heating time after photoirradiation. The change in residual ratio (decomposition of the main-chain) was slow compared to that for PMPS. In contrast, the change in the residual ratio of PMBS was as fast as that for PMPS (**Figure 15(b)**). The only structural difference between PBS and PMBS is the number of substituents on the main chain. Thus, the decomposition characteristics must be dependent on the structure of the main chain. **Figure 16** shows the residual ratios for all polymers as a function of heating time after photoirradiation. The results show that the decomposition characteristics of the polymers can be divided into two groups: poly(olefin sulfone)s that possess only one type of proton on the main chain (branched 1-olefins such as PMBS, PMPS, PMHS, and PMNS), and poly(olefin sulfone)s that possess two types of protons

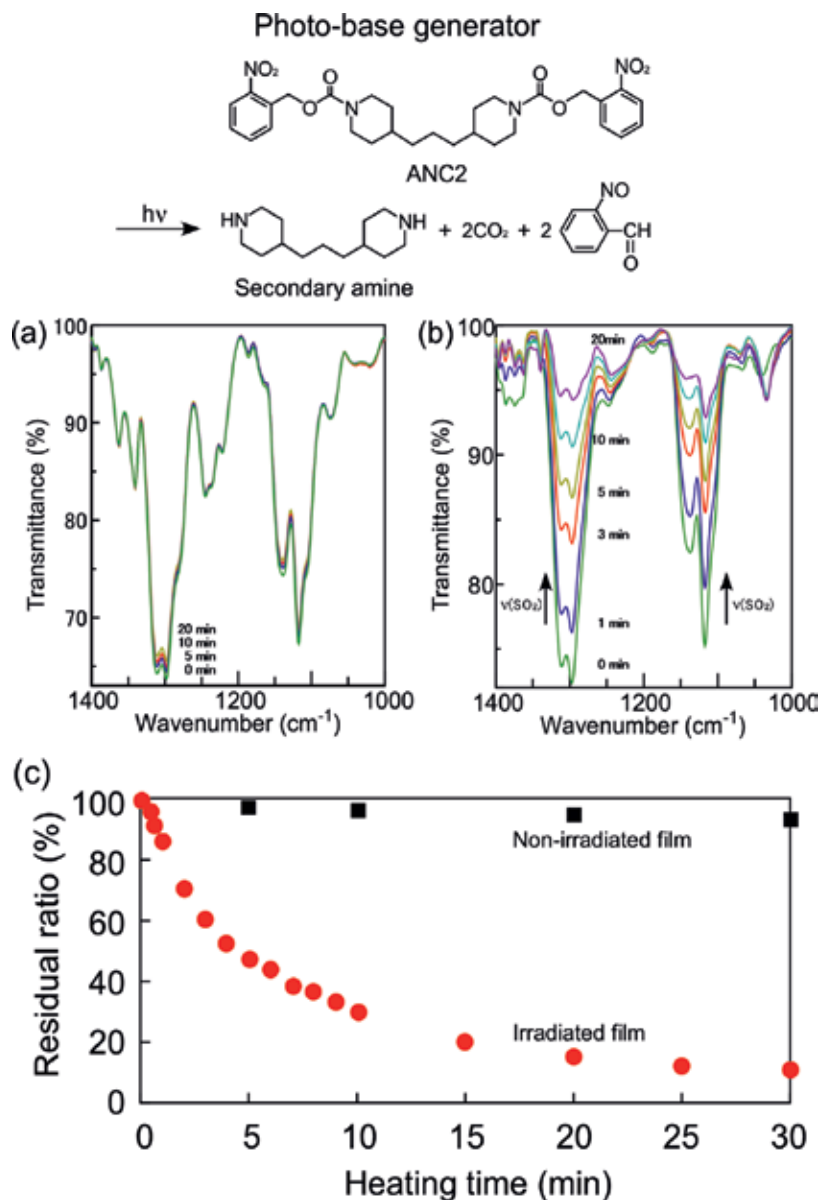


Figure 14. Changes in the IR absorption spectra of the sulfonyl group in PMPs coated on a KBr plate (a) without irradiation and (b) after light irradiation at 254-nm and $180 \text{ mJ}/\text{cm}^2$. The thickness of the film was $2 \mu\text{m}$. The post-exposure heat treatment time was varied from 0–15 min at 150°C . (c) Residual ratio of the PMPs main-chain as a function of heating time after irradiation, as estimated by IR absorption. The concentration of the L-ANC2 (photo-base generator) was 30 wt%. The heating temperature was 120°C and the irradiation energy was $3.15 \text{ J}/\text{cm}^2$.

on the main chain (straight chain 1-olefins and cycloolefins such as PBS, PPS, PHS, PycloPS, and PycloHS). The poly(olefin sulfone)s possessing only one type of proton on the main chain can undergo extensive decomposition, whereas the poly(olefin sulfone)s possessing

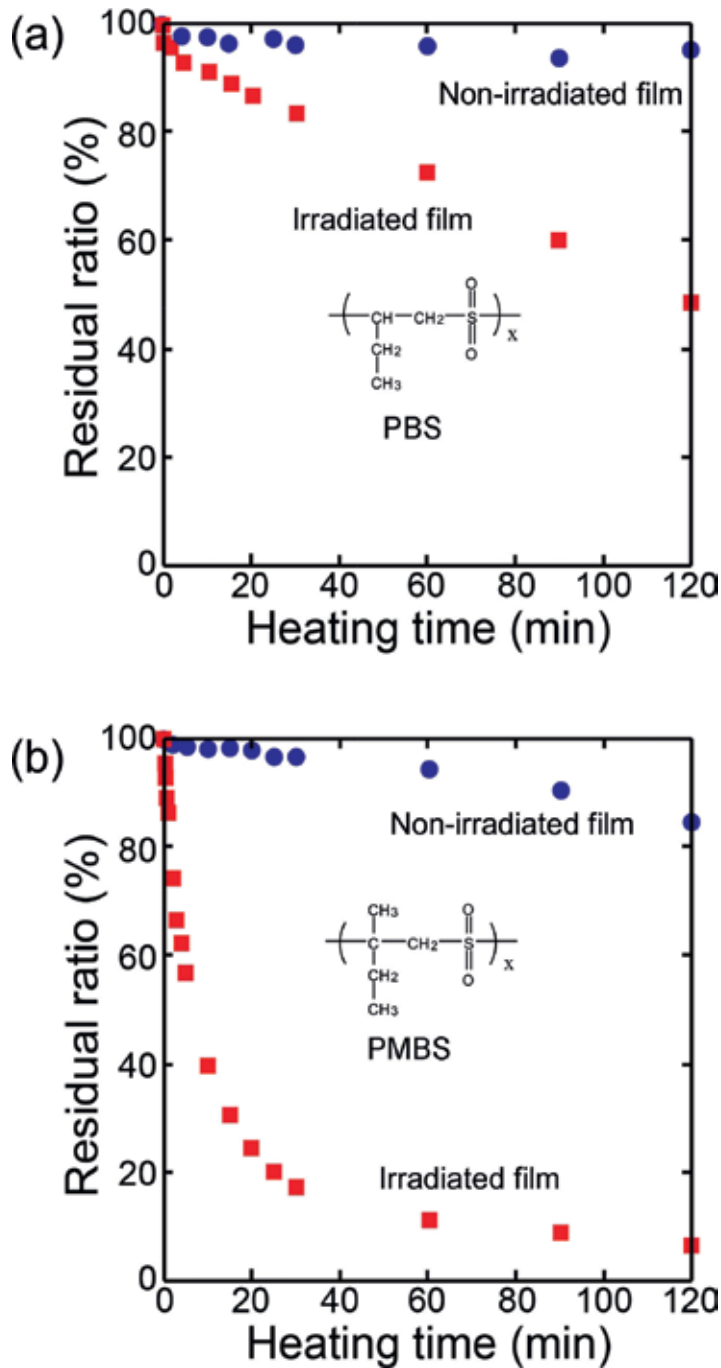


Figure 15. Residual ratios of the main-chain of poly(olefin sulfone)s in films estimated by IR absorption as a function of heating time after irradiation. (a) PBS film without irradiation (●) and after irradiation (■). (b) PMBS film without irradiation (●) and after irradiation (■). The concentration of the PBG was 30 wt%. The heating temperature was 120°C and the irradiation energy was 3.15 J/cm².

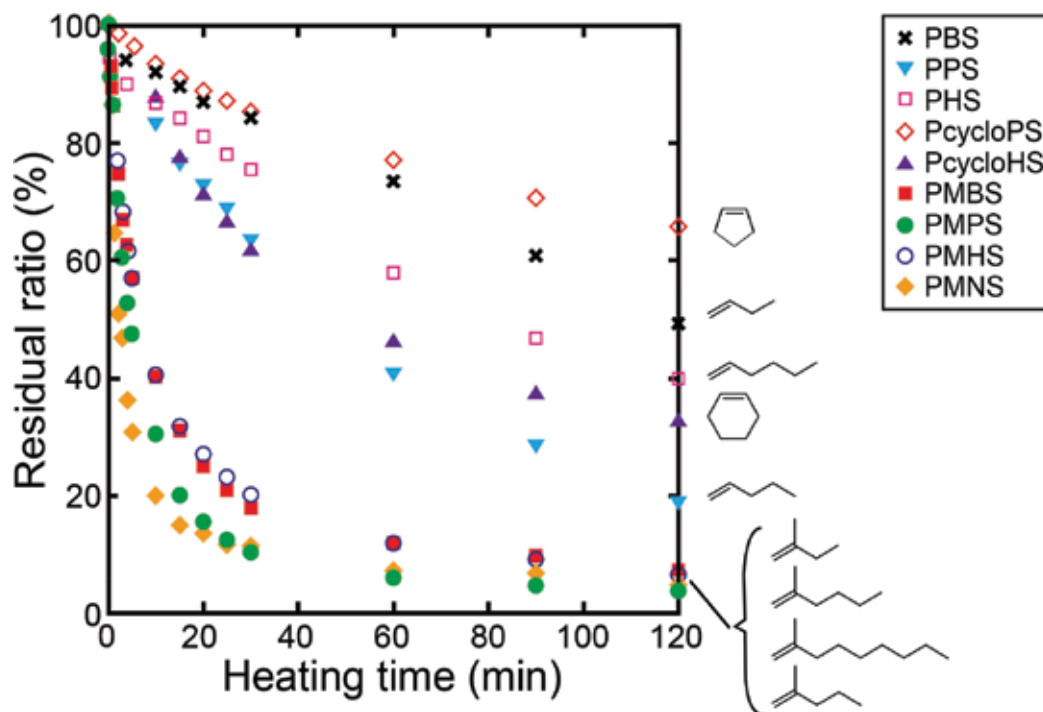


Figure 16. Residual ratios of the main-chains of poly(olefin sulfone)s in films as a function of heating time after irradiation. The concentration of the PBG was 30 wt%. The heating temperature was 120°C and the irradiation energy was 3.15 J/cm².

two types of protons on the main chain undergo only a low extent of decomposition. The number of protons that can be abstracted appears to affect the extent of depolymerization. When many protons existing on a single main chain are abstracted, the yield of monomers was reduced, as shown in the reaction mechanism in **Figure 4**.

6. Poly(olefin sulfone)s possessing a photobase generator and base amplifier

Photoinduced depolymerization of poly(olefin sulfone)s possessing a base-amplifying moiety in the side chain has been investigated using a film doped with a photobase-generating compound [19]. Poly(olefin sulfone)s that possess the 9-fluorenylmethoxycarbonyl (Fmoc) group as a base-labile N-protecting group have been synthesized (**Figure 17**). The Fmoc group can undergo amine-catalyzed thermolysis to an amino group with the evolution of carbon dioxide and dibenzofulvene [20, 21]. Therefore, the number of amino groups increased in the irradiated poly(olefin sulfone) films containing the Fmoc group and doped with PBGs during the subsequent heating step. Even though the irradiation produced few amino groups, their concentration could be amplified by the amine-catalyzed thermal degradation of the Fmoc group.

Figure 18 shows the decomposition ratio of P4 and P5 plotted as a function of irradiation energy density. The decomposition ratio of copolymer P4 was greater than that of P5. For P4, a decomposition ratio of 98% was obtained at an energy density of 900 mJ/cm². Thus, the presence of a base-amplifying group in the side-chain enhanced the amount of base generated in the P4 film.

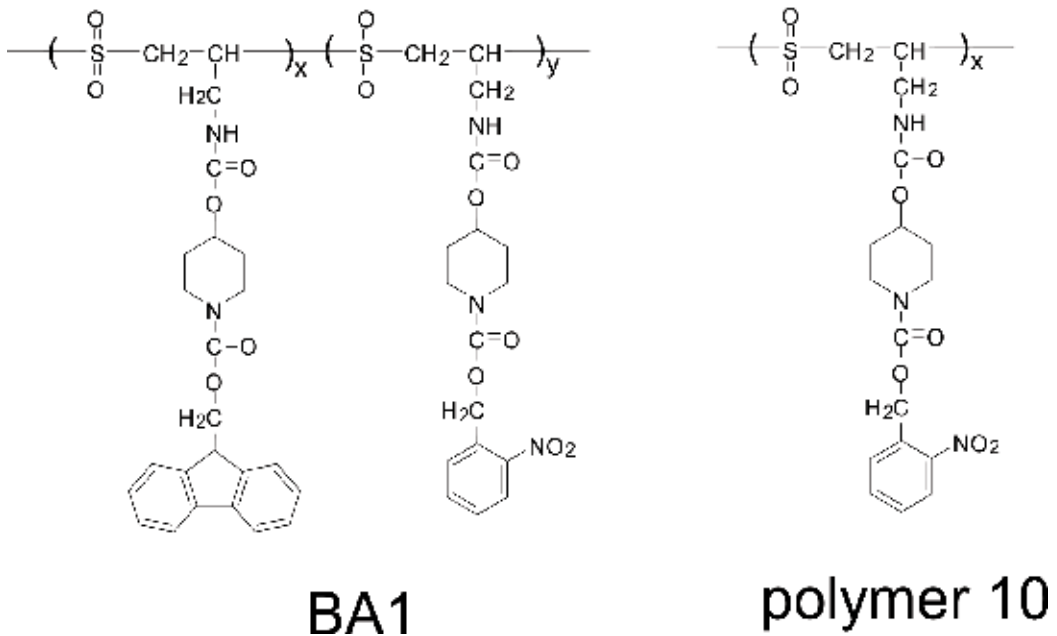
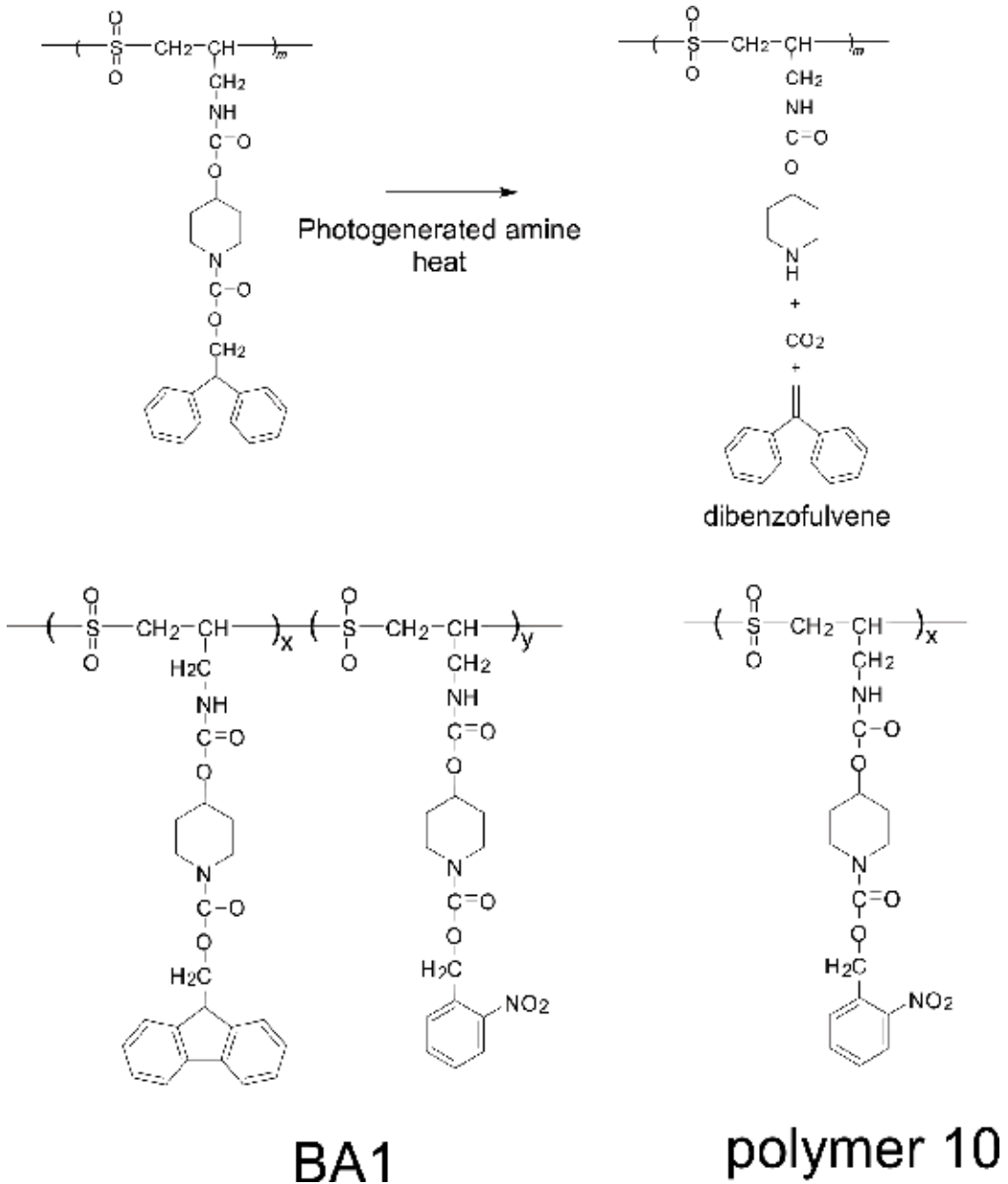


Figure 17. Base amplification mechanism and structures of copolymer BA1 and polymer 10.

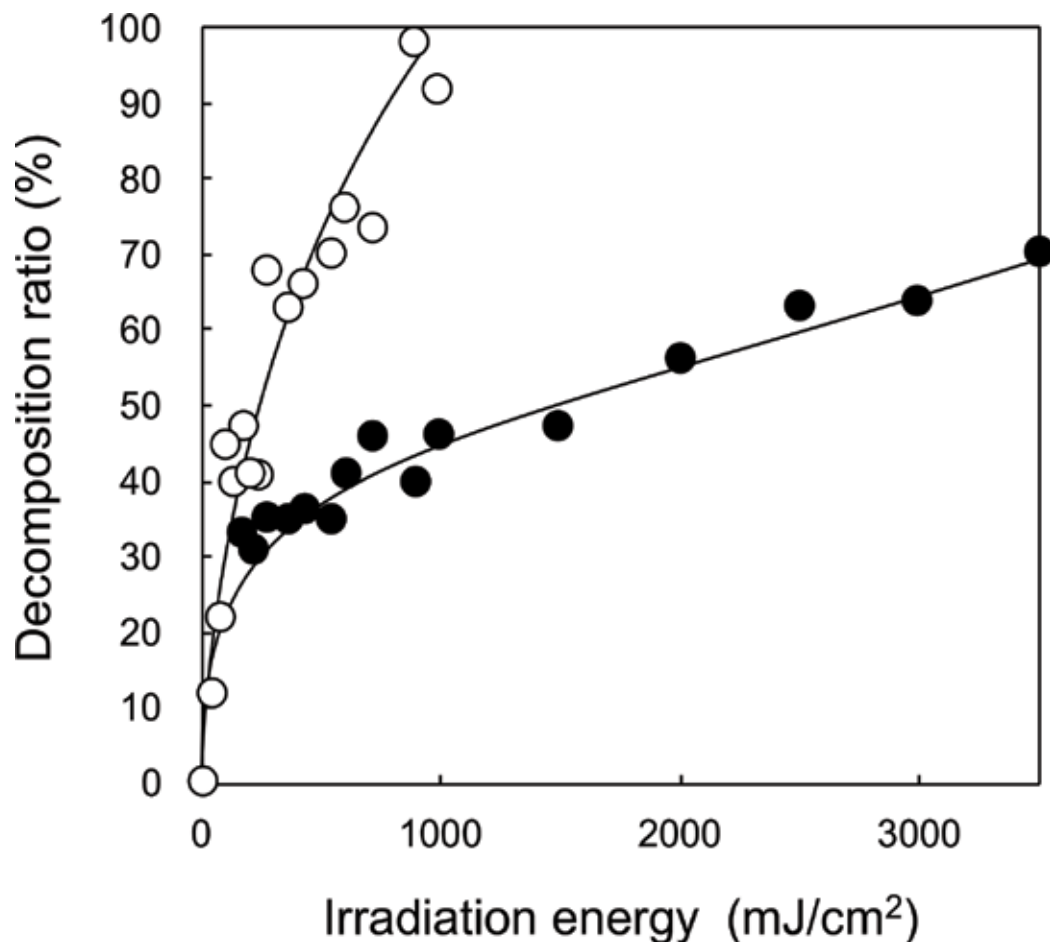


Figure 18. Decomposition ratio of BA1 (○) and polymer 10 (●) as a function of the irradiation energy.

7. Poly(olefin sulfone)s composed of volatile monomers

The photoinduced depolymerization of poly(olefin sulfone)s composed of volatile olefins was investigated [18]. The polymers were converted into volatile compounds by photoinduced depolymerization. A poly(olefin sulfone) film containing a photobase generator (ANC2) was irradiated with 254-nm light at ambient temperature through a photomask. While very little change occurred in the film just after irradiation, the irradiated area of the film vaporized upon heating to 110°C, forming a mask pattern on the film (**Figure 19**). The surface of the film was also observed by AFM after heat treatment. The results confirmed that the irradiated area was removed, leaving a bare surface. This enables a wide variety of applications, such as stereolithography without the use of solvents, photo-detachable adhesives, and printable nanocircuit fabrication.

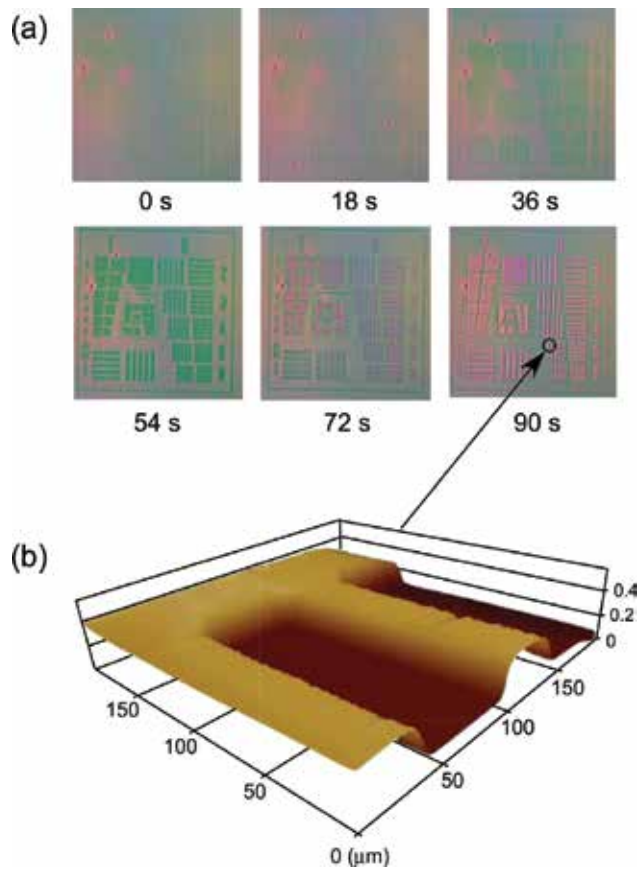


Figure 19. (a) Changes in a photomask pattern irradiated film during heating at 110°C. (b) AFM image of the photomask pattern irradiated area of the PMPs film after heating at 110°C for 15 min.

8. Application of photo-depolymerizable poly (olefin sulfone)s to photo-detachable adhesives

Detachable adhesives have attracted great interest due to their potential applications in reusable products and reworkable systems [22–26]. Adhesives used in many applications, and a variety of strong adhesives that can be employed in extreme environments have been developed [27]. However, most high-performance adhesives are strongly adhesive, making them difficult to remove and therefore cannot be used in recyclable materials or in reworking processes. Therefore, a need exists for glues that provide firm bonding but also can be easily detached. The strength of an adhesive bond essentially depends on surface interactions between the adhesive material and the substrate. Therefore, if the chemical structure of the adhesive material can be changed after adhesion, the adhesion strength may also change. Studies have been reported on the adhesive strength of substrates fastened using degradable polymers [23, 24, 26]. The results showed that depolymerizable polymers can act as detachable adhesives.

The adhesive strength of a poly(olefin sulfone) composed of a volatile olefin monomer and a second olefin monomer possessing a crosslinkable moiety has been evaluated [28]. This polymer was expected to act as a detachable adhesive, as illustrated in **Figure 20**. When a mixture of this poly(olefin sulfone) and a crosslinking reagent was embedded between two glass plates and cured, the plates remained glued together. Subsequently, the glued plates could be separated upon irradiation with UV light and heating. For further investigation, a mixture of the poly(olefin sulfone), a cross-linking agent, and a photobase generator were prepared, and the adhesive strengths before and after photoirradiation were examined. **Figure 21** shows the chemical structures of the samples. The bond strength of the test samples was measured using a cross-tensile test apparatus, shown in **Figure 22**. **Figure 23(a)** shows the tensile strengths obtained from plates bonded with various adhesives: cross-linked TPAS-11, PMPS, a commercially available epoxy adhesive (Araldite Rapid), and polypropylene. The polypropylene did not result in adhesion between the quartz plates, while the cross-linked TPAS-11 clearly possessed a tensile strength greater than those obtained either with the Araldite Rapid or PMPS. The superior bonding strength of the cross-linked TPAS-11 was thought to be due to the highly polar poly(olefin sulfone) main chain and hydrogen bond-

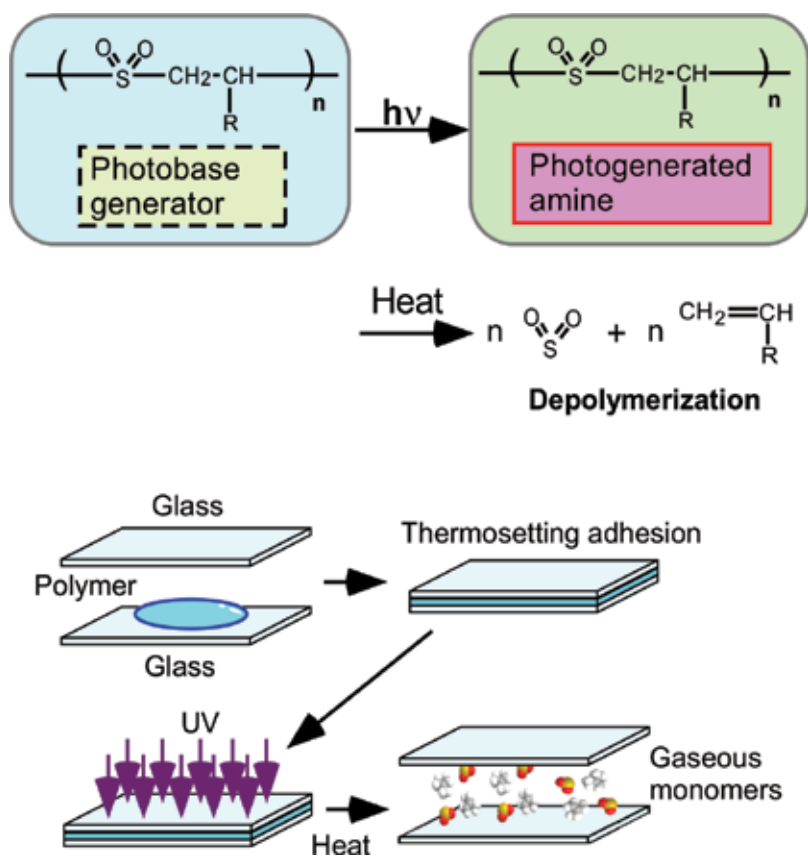


Figure 20. Photoinduced depolymerization of poly(olefin sulfone)s containing photobase generators and a sequence showing a photodetachable thermosetting adhesive.

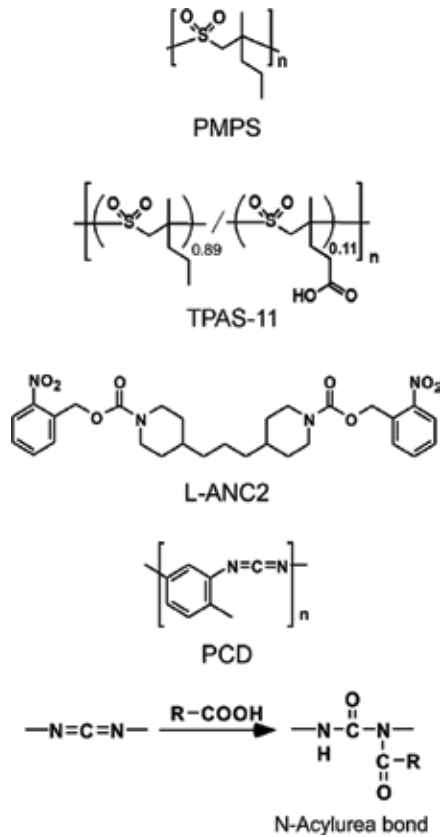


Figure 21. Structures of the poly(olefin sulfone)s (PMPS and TPAS-11), photobase generator (L-ANC2) and crosslinker (PCD) employed in the present study and crosslinking reaction of the carbodiimide PCD and a carboxylic acid.

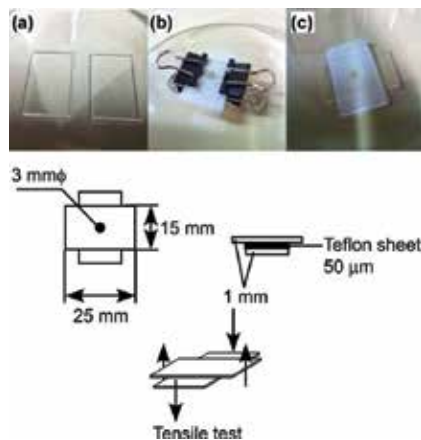


Figure 22. Preparation of samples for adhesion strength measurements: (a) a mixture of TPAS-11, PCD (5 wt%) and L-ANC2 (20 wt%) is placed on quartz plates, (b) the plates are sandwiched on either side of a 50 μm Teflon sheet with a 3 mm diameter hole and the assembly heated to 100°C for 10 min, and (c) a finished sample ready for adhesive strength measurements (cross tensile test).

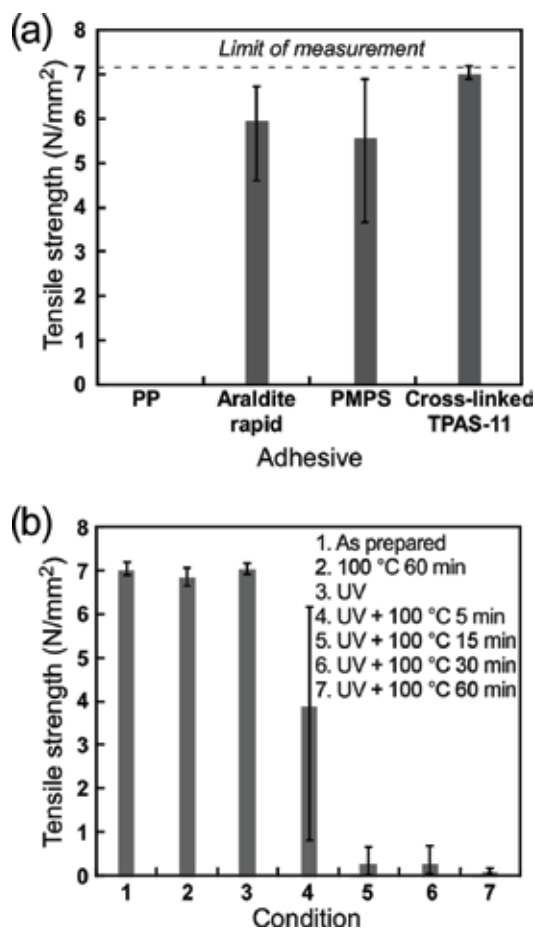


Figure 23. (a) Adhesive strengths of quartz plates bonded with polypropylene (PP), Araldite rapid, PMPS and cross-linked TPAS-11 (with 5 wt% of PCD). Both the PMPS and cross-linked TPAS contained 20 wt% L-ANC2. The maximum tensile strength that could be measured (7.2 N/mm²) is indicated by a dashed line. The tensile test was conducted for 5 times in each measurement. (b) Adhesive strengths of quartz plates bonded with a mixture of TPAS-11, PCD (5 wt%) and L-ANC2 (20 wt%): (1) immediately after sample preparation, (2) after heating at 100°C for 60 min, (3) after irradiation with 254-nm UV light (3.0 J/cm²), (4) after irradiation with UV and heating at 100°C for 5 min, (5) after irradiation with UV and heating at 100°C for 15 min, (6) after irradiation with UV and heating at 100°C for 30 min, and (7) after irradiation with UV and heating at 100°C for 60 min. The tensile test was conducted for 5 times in each measurement.

ing between the carboxylic acid groups and the N-acylurea groups at the cross-linking sites (**Figure 21**). Note that PMPS-glued plates detached upon heating to temperatures above the glass transition temperature of PMPS because it is a thermoplastic resin. In contrast, cross-linked TPAS acted as a thermoset resin and resulted in stable adhesion. The change in the adhesive strength of the cross-linked TPAS-11 upon light irradiation and/or heating was also investigated. **Figure 23(b)** shows the tensile strength of the cross-linked TPAS-11 sample as prepared and after heating at 100°C for 60 min, and upon irradiation with 254-nm UV

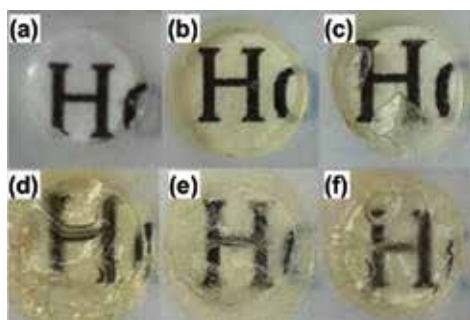


Figure 24. Photographs of a mixture of TPAS-11, PCD (5 wt%) and L-ANC2 (20 wt%): (a) after heating at 100°C for 30 min without UV irradiation, (b) after irradiation with 254-nm UV light (3.0 J/cm²), (c) after UV irradiation and heating at 100°C for 5 min, (d) after UV irradiation and heating at 100°C for 15 min, (e) after UV irradiation and heating at 100°C for 30 min, and (f) after UV irradiation and heating at 100°C for 60 min.

light at 3.0 J/cm², with or without heating for different durations. The results demonstrate that heating before UV irradiation did not weaken the bond strength, while heating after UV irradiation caused the adhesive strength to decrease to nearly zero. **Figure 24** shows photographs of the adhered samples, indicating that the cross-linked TPAS-11 was both colorless and transparent. Following irradiation with UV light, the resin became slightly yellow because of the production of nitrosobenzaldehyde via photodecomposition of L-ANC2. Heating the sample to 100°C also generated gaseous products because of depolymerization of the poly(olefin sulfone), allowing the quartz plates to detach.

9. Conclusions

Photoinduced depolymerization of poly(olefin sulfone)s containing photobase generators was summarized. Since poly(olefin sulfone)s are copolymers of olefins and sulfur dioxide, the sulfur dioxide produced through the depolymerization evaporates from the system. Thus, the depolymerization reaction proceeds only in one direction, and the polymer is converted into consistent olefins. The photoinduced depolymerization of poly(olefin sulfone)s has been investigated for a wide variety of applications, including stereolithography, printable micro-circuit fabrication, and detachable adhesives.

Author details

Takeo Sasaki*, Khoa Van Le and Yumiko Naka

*Address all correspondence to: sasaki@rs.kagu.tus.ac.jp

Tokyo University of Science, Shinjuku-ku, Tokyo, Japan

References

- [1] Sarker MA, Mejiritski A, Wheaton RB, Neckers CD. Novel imaging materials: Synthesis and characterization of Poly[N,N-dimethyl-N-(p-benzoylbenzyl)-N-(2-methacryloyl-ethyl)ammonium triphenylbutylborate] as a single-component photoimaging system. *Macromolecules*. 1997;**30**:2268-2273. DOI: 10.1021/ma961249x
- [2] Shaw MJ, Hatzakis M, Paraszczak J, Liutkus J, Babich E. Organosilicon polymers for lithographic applications. *Polymer Engineering & Science*. 1983;**23**:1054. DOI: 10.1002/pen.760231816
- [3] Roberts, DE J. The preparation and properties of a polysiloxane electron resist. *Journal of the Electrochemical Society*. 1973;**120**:1716. DOI: 10.1149/1.2403351
- [4] Wilkins Jr. WC, Reichmanis E, Chandross A EJ. Preliminary evaluation of copolymers of Methyl Methacrylate and acyloximino methacrylate as deep U.V. resists. *The ECS Journal of Solid State Science and Technology*. 1980;**127**:2510-2513. DOI: 10.1149/1.2129505
- [5] Hartless LR, Chandross AE. Deep-UV photoresists: Poly(methyl methacrylate-co-indenone). *Journal of Vacuum Science and Technology*. 1981;**19**:1333-1337. DOI: 10.1116/1.571271
- [6] Ito H, Ueda M, Schwalm R. Highly sensitive thermally developable positive resist systems. *Journal of Vacuum Science and Technology*. 1988;**6**:2259-2263. DOI: 10.1116/1.584093
- [7] Ito H, England PW, Ueda M. Chemical amplification based on acid-catalized depolymerization. *Journal of Photopolymer Science and Technology*. 1990;**3**:219-233. DOI: 10.2494/photopolymer.3.219
- [8] Fréchet JMJ, Bouchard F, Houlihan MF, Kryczka B, Eichler E, Clecak N, Willson GC. New approach to imaging systems incorporating chemical amplification: Synthesis and preliminary evaluation of novel resists based on tertiary copolycarbonates. *Journal of Imaging Science and Technology* 1986;**30**:59-64
- [9] Fréchet JMJ, Bouchard F, Eichler Eva, Houlihan MF, Iizawa T, Kryczka B, Willson GC. Thermally depolymerizable polycarbonates V. Acid catalyzed thermolysis of allylic and benzylic polycarbonates: A new route to resist imaging. *Polymer Journal*. 1987;**19**:31-49. DOI: 10.1295/polymj.19.31
- [10] Fréchet JMJ, Eichler E, Stanculescu M, Iizawa T, Bouchard F, Houlihan MF, Willson GC. Acid-catalyzed thermolytic depolymerization of polycarbonates: A new approach to dry-developing resist materials. *ACS Symposium Series: Polymers for High Technology*. 1987;**346**:138-148. DOI: 10.1021/bk-1987-0346.ch012
- [11] Brown RJ, O'Donnell HJ. The degradation of poly (butene-1 sulfone) during γ irradiation. *Macromolecules*. 1970;**3**:265-267. DOI: 10.1021/ma60014a029
- [12] Watanabe A, Sakakibara T, Ito S, Ono H, Yoshida Y, Tagawa S, Matsuda M. Photodegradation and electron-beam-induced degradation of poly[(pentamethyldisilyl)styrene sulfones]. *Macromolecules*. 1992;**25**:692-697. DOI: 10.1021/ma00028a030

- [13] Hiraoka H, Welsh WL Jr. Deep UV photolithography with composite photoresists made of Poly(olefin sulfones). ACS Symposium Series Polymers in Electronics. 1984;55-64. DOI: 10.1021/bk-1984-0242.ch005
- [14] Ito O, Matsuda M. A new dual-parameter for reactivities of vinyl monomers toward free-radicals. Journal of Polymer Science Part A: Polymer Chemistry. 1990;28:1947-1963. DOI: 10.1002/pola.1990.080280725
- [15] Cais ER, O'Donnell HJ, Bovey AF. Copolymerization of styrene with sulfur dioxide. Determination of the monomer sequence distribution by carbon-13 NMR. Macromolecules. 1977;10:254-260. DOI: 10.1021/ma60056a008
- [16] Shinoda T, Nishiwaki T, Inoue H. Decomposition of poly(4-hydroxystyrene sulfone) in alkaline aqueous solutions. Journal of Polymer Science Part A: Polymer Chemistry. 2000;38:2760-2766. DOI: 10.1002/1099-0518(20000801)38:15<2760::AID-POLA160>3.0.CO;2-J
- [17] Yaguchi H, Sasaki T. Photoinduced depolymerization of poly(olefin sulfone)s possessing photo-base generating groups in the side-chain. Macromolecules. 2007;40:9332-9338. DOI: 10.1021/ma702001h
- [18] Sasaki T, Kondo T, Noro M, Saida K, Yaguchi H, Naka Y. Photoinduced depolymerization in poly(olefin sulfone) films composed of volatile monomers doped with a photobase generator. Journal of Polymer Science Part A: Polymer Chemistry. 2012;50:1462-1468. DOI: 10.1002/pola.25898
- [19] Sasaki T, Yaguchi H. Photoinduced depolymerization of poly(olefin sulfone)s possessing base amplifying groups. Journal of Polymer Science Part A: Polymer Chemistry. 2009;47:602-613. DOI: 10.1002/pola.23179
- [20] Ichimura K. Nonlinear organic reactions to proliferate acidic and basic molecules and their applications. The Chemical Record. 2002;2:46-55. DOI: 10.1002/tcr.10013
- [21] Arimitsu K, Ichimura K. Nonlinear organic reaction of 9-fluorenylmethyl carbamates as base amplifiers to proliferate aliphatic amines and their application to a novel photopolymer system. Journal of Materials Chemistry. 2004;14:336-343. DOI: 10.1039/B311358B
- [22] Malik J, Clarson SJ. A thermally reworkable UV curable acrylic adhesive prototype. The International Journal of Adhesion and Adhesives. 2002;22:283-289. DOI: 10.1016/S0143-7496(02)00005-2
- [23] Sato E, Hagihara T, Matsumoto A. Cohesive force change induced by polyperoxide degradation for application to dismantlable adhesion. ACS Applied Materials & Interfaces. 2010;2:2594-2601. DOI: 10.1021/am1004392
- [24] Sato E, Hagihara T, Matsumoto A. Facile synthesis of main-chain degradable block copolymers for performance enhanced dismantlable adhesion. ACS Applied Materials & Interfaces. 2012;4:2057-2064. DOI: 10.1021/am300028f

- [25] Inui T, Yamanishi K, Sato E, Matsumoto A. Organotellurium-mediated living radical polymerization (TERP) of acrylates using ditelluride compounds and binary Azo initiators for the synthesis of high-performance adhesive block copolymers for on-demand dismantlable adhesion. *Macromolecules*. 2013;**46**:8111-8120. DOI: 10.1021/ma401595w
- [26] Wang YZ, Li L, Du FS, Li ZC. A facile approach to catechol containing UV dismantlable adhesives. *Polymer*. 2015;**68**:270-278. DOI: 10.1016/j.polymer.2015.05.032
- [27] Possart W. Adhesion: Current research and applications. Wiley-VCH Weinheim. 2005. DOI: 10.1016/j.carbpol.2005.10.011
- [28] Sasaki T, Hashimoto S, Nogami N, Sugiyama Y, Mori M, Naka Y, Khoa V. Le dismantlable thermosetting adhesives composed of a cross-linkable poly(olefin sulfone) with a photobase generator. *ACS Applied Materials & Interfaces*. 2016;**8**:5580-5585. DOI: 10.1021/acsami.5b10110

Polyolefin Fibres for the Reinforcement of Concrete

Marcos G. Alberti, Alejandro Enfedaque and
Jaime C. Gálvez

Additional information is available at the end of the chapter

<http://dx.doi.org/10.5772/intechopen.69318>

Abstract

Given that concrete has limited tensile strength, it has been necessary to combine its properties with the use of steel bars. This resulted in the arrival of reinforced concrete which was the main solution used in structures in the last century. Partial or even full substitution of steel bars for fibres would not only allow the cost of a structure to be reduced but also provide certain improved properties. Modern fibre-reinforced concrete (FRC) now permits reduction or substitution of steel bars that has given rise to the commonly named structural FRC. Advances in the plastic industry during the last three decades have allowed the production of macro-polymer fibres as an alternative to steel fibres due to their chemical stability and lower weights for analogous residual strengths. After 30 years of research and practice, polyolefin-based macro-fibres have offered additional advantages such as safe handling, low pump wear and reduction in weight when transported and stored. This chapter provides an overview of the properties and structural capacities of polyolefin fibre-reinforced concrete (PFRC). Furthermore, the respective codes and test methods are examined. Moreover, the results obtained for structural design and the mechanical properties, found both in the literature and in practice, are supplied and discussed.

Keywords: self-compacting concrete, fibre-reinforced concrete, polyolefin fibres, steel fibres, fracture behaviour

1. Why polyolefin fibres?

The recent advances made in polymer science, chemical composition and engineering have increased the importance of polyolefins in day-to-day applications. Polyethylene and polypropylene are widespread polyolefins and the fastest growing polymer family due to the

lower cost of production compared with the plastics and materials they replace [1]. Polyolefin fibres encompass a spectrum of uses in modern societies. The associated low costs, good resistance to chemicals, and high strength and toughness have encouraged the use. Their commercial advantages and disadvantages are listed in **Table 1**, although it should be noted that not all are applicable to the case of reinforcing concrete. In general, polyolefin fibres have good tensile properties, good abrasion resistance and excellent resistance to chemicals.

Regarding their use in concrete, the development of polyolefin-based synthetic macro-fibres with improved mechanical properties has extended the use of such plastic fibres beyond a conventional use in shrinkage-cracking control. Such synthetic macro-fibres have become an alternative to the traditional use of steel fibres in fibre-reinforced concrete (FRC) [3], forming what has been termed steel fibre-reinforced concrete (SFRC). The addition of randomly distributed steel fibres to concrete improves its low tensile strength and its brittleness enabling its use in industrial pavements or tunnels [4–6] among others. Based on the existing codes and standards [7–9], the contribution of the steel fibres has been considered in the structural design in recent years [10–12]. However, the recent concern of society regarding the environmental cost of materials, building processes and infrastructure refurbishment and rehabilitation has given rise to certain structures having a lifespan of up to 100 years. Therefore, the durability of materials has emerged as a key factor in the choice of materials. In such a sense, the potentially corrodible nature of steel fibres has aroused an interest in fibres that are not only chemically stable but also increase the mechanical performance of concrete. In addition, steel fibres are expensive for both purchase and in terms of storing and handling. Plastic industry in recent years has solved the aforementioned disadvantages allowing the production of a new generation of polyolefin-based synthetic macro-fibres that are inert in an alkaline environment and provide concrete with structural capacities to substitute steel reinforcement. Therefore, polyolefin fibres, which have good tensile properties, abrasion resistance, excellent

Advantages	Disadvantages
Low density (0.90–0.96 g/cm ³)	Low melting point (120–125°C for PE;
Good tensile properties	160–165°C for PP)
Good abrasion resistance	Prone to photolytic degradation
Excellent resistance to chemicals	Inferior shrink resistance above
Excellent resistance to mildew,	100°C
Micro-organisms and insects	Poor dyeability
Almost negligible moisture regain	High flammability
Good wicking action	Inferior resilience
High insulation	Significant degree of creep
Avoidance of dermatological problems	

Table 1. Commercial advantages and disadvantages associated with the use of polyolefin fibres [2].

resistance to chemical attack, and a reduced moisture regain, have emerged as an alternative to corrosive steel solutions that use steel-reinforcing mesh or steel fibres.

In order to consider these newly developed applications, in 2006 the European Committee for Standardization (CEN) approved the European Standard 14889 [13] which classifies the types of fibres that can be added to concrete. Such a recommendation divides the fibres into two groups: the first one deals with steel fibres and the second one polymer fibres. However, not all the characteristics that may be relevant in examining the performance of FRC were addressed. The recommendation defines the possible geometrical shapes and physical parameters of the fibres and establishes the procedures for the measurement of the fibre mechanical properties such as tensile strength or modulus of elasticity. In the case of polymer fibres, they are divided into two groups: non-structural micro-fibres and structural macro-fibres. The criterion used is their equivalent diameter, with it being classified into two types depending on whether its diameter is greater or smaller than 0.30 mm. **Figure 1** shows the classification of the fibres made by such a reference [13]. Polyolefin fibres with surface bulges and grooves along the fibre surface are produced from homo-polymeric resin into a mono-filament form [14] and, according to EN-14889, are classified as Class II macro-fibres.

Among the synthetic macro-fibres that can be employed in concrete, those made of high-density polyethylene (HDPE) boast a density of 0.95 g/cm³ and a reduced tensile strength between

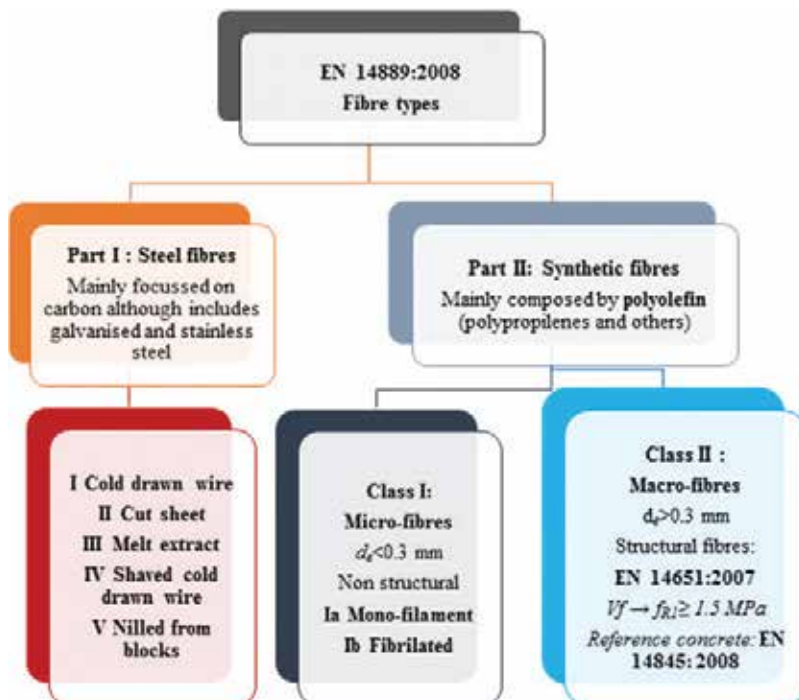


Figure 1. Fibre classification following EN-14889 [13].

25 and 40 MPa. These reduced mechanical properties hamper their use as a way to improve concrete mechanical properties. Nevertheless, other types that have been recently employed, which are manufactured with polyethylene terephthalate (PET), boast remarkable mechanical properties. Their tensile strength above 400 MPa might enable a successful use in concrete reinforcement but there are several issues reported [15]. Some that have been thoroughly studied are the difficulties found in their manufacturing process as well as their reduced resistance to alkaline environments [16, 17]. These two difficulties prevent their widespread use as a concrete reinforcement. Other types of macro-fibres that deserve being cited are those obtained from virgin and recycled polypropylene (PP). PP fibres have been widely used in the concrete industry, due to its ease of production, high alkaline resistance [18], and high tensile strength and Young's modulus [19].

Polyolefin fibres, which are among those considered PP fibres, enjoy an outstanding mechanical behaviour, their modulus of elasticity being of great relevance. The common value of such modulus is 9 GPa or even up to 15–20 GPa, which is much higher than certain other plastics that offer around 2–3 GPa. In addition, polyolefin fibres boast a tensile strength above 400 MPa. These remarkable properties have been obtained by using a bi-component fabrication strategy that combines two polymers: a core of high modulus and a sheath of low modulus [20, 21].

Another reason behind the remarkable performance of polyolefin fibres is the notable bond generated between the fibres and the concrete matrix due to their rough surface. This is provided for both the shape of the fibres and the mechanical interaction that takes place when the fibres are loaded. In such a sense, the interface fibre-matrix becomes rougher due to the damage of the fibre surface produced during the mixing process. Such roughening forms a mechanical interlock opposite to the relative movement of fibres after the cracks are initiated [22–24]. Concerning the fibre shape, the optimum macro-synthetic fibre geometry has also been sought. This involved exploiting the matrix anchorage fully without fracturing the fibres, and reaching the maximum pull-out resistance. In terms of bond, the crimped ones were the best among several deformed synthetic structural fibres [25, 26].

2. Fibre pull-out response of polyolefin fibres when added to concrete

Regardless of the type of fibre used, reinforcement is effective in concrete when the tensile strength of the fibre is significantly higher than that of concrete (two or three times), when the fibre-matrix bond strength is in the same order of magnitude of the tensile strength of the matrix, and the fibre modulus of elasticity in tension is significantly higher than that of the concrete [27, 28]. **Figure 2** shows the failure mechanisms of the fibres in PFRC.

At the optimum situation, the crack opening is controlled by 'fibre bridging' which has a portion of fibre on each side of the crack with enough embedded length and allows fibres to work at 100% without any slipping (number 3 in **Figure 2**). In such a situation, if the crack-growing process continues it is possible to make full use of the potential of the fibre up to its failure. On the contrary, if fibres slip during the opening processes, the debonding process may occur

and the fibre may be pulled out. If one fibre is mobilized by friction shear stresses, it is possible that such stresses cause matrix cracking.

In order to determine which of the cases shown in **Figure 2** might emerge, the critical length (l_c) of the fibres used requires examination. Such a critical length has been defined as the length that allows the tensile strength of the fibre to be used without pulling it out of the matrix. In an ideal situation, when the fibre is being pulled out from the concrete matrix, two types of forces are applied to the fibre, preventing it from being extracted: the chemical adhesion in the inner part of the fibre and the frictional bond in the part of the fibre closer to the crack. A sketch of this can be seen in **Figure 3**.

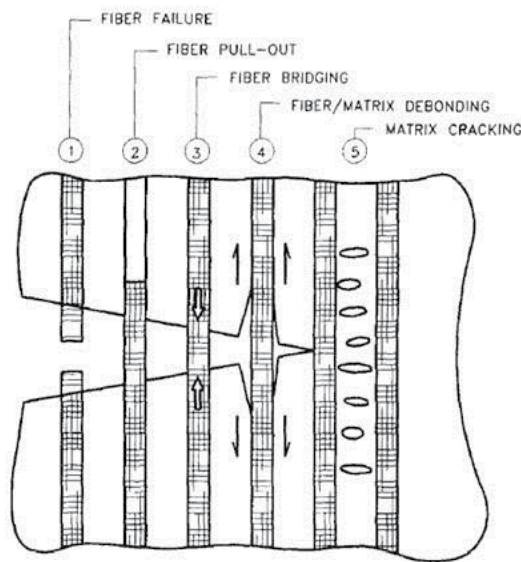


Figure 2. Energy absorbing the fibre matrix mechanisms [29].

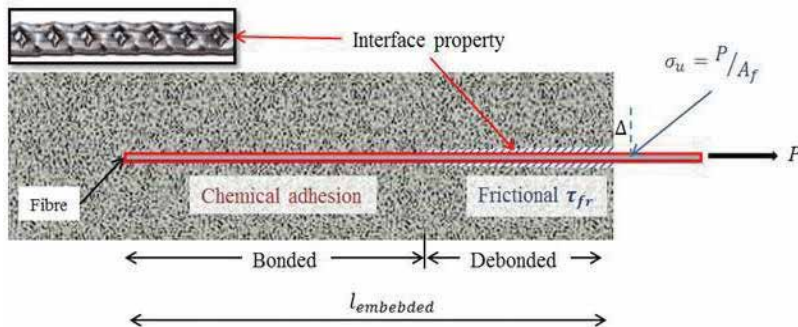


Figure 3. Pull-out mechanisms [8, 28].

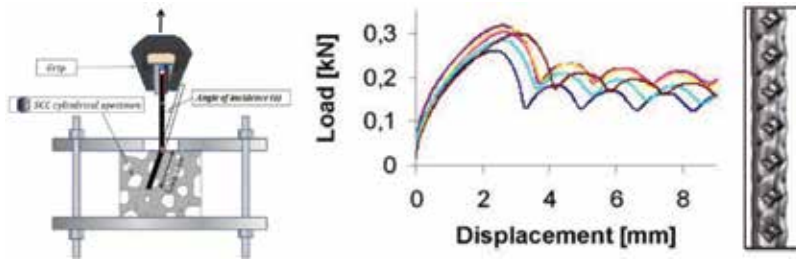


Figure 4. Set-up of pull-out test of a polyolefin-based macro-fibre made by [8] (left); pull-out test result (centre), typical embossed surface of a polyolefin fibre (right) [28, 30].

In the case of a certain type of polyolefin fibre, the test setup and the pull-out response obtained in the test can be seen in **Figure 4**. The results obtained depend on two variables: the embedded length and the angle formed between the fibre and the free surface of the sample. The amount of energy absorbed while pulling out of the fibre increases as the embedded length does. However, the effect of the angle between the free surface and the fibre has a minor effect in the total response of the system [8]. Apart from these two factors, the test results showed that the geometry of the embossed surface of the fibre has a major impact on the results. **Figure 4** shows how the load-displacement curves swing at a certain load level as a result of the fibre surface geometry.

The results obtained in the pull-out tests show that polyolefin fibres are apt for concrete reinforcement. How these micro-mechanisms are transferred into the macro-scale material behaviour will be explained in the next sections. Similarly, both the influence that the fibres have on the manufacturing process and the fresh state of the material will be shown in too.

3. Manufacturing of polyolefin fibre-reinforced concrete

Macro-fibre volumes currently used in FRC range from 0.3 to 1.5%. With such volume fractions, the procedure for mix proportioning can be essentially the same as that used for plain concrete [31]. While the addition of fibres does not affect the nature of the components of the mix, it does affect the mix workability. There are no limitations as regards the types of cement employed, although the most common one is a Portland cement without additions. Regarding the type of aggregates chosen, those rounded and crushed have been successfully used without encountering any disadvantage caused by interaction of the fibres and the aggregates [28]. The reduction of the concrete workability can be compensated with slight variations of the aggregate distribution, increasing the amount of fine fractions or even by adding or increasing the amount of admixtures. In any case, it is advisable to prepare trial mixes to achieve the final proportions. FRC can be manufactured, in general, with the same equipment and similar procedures merely by carefully studying the best mixing sequence to ensure that a good uniform dispersion of each type of fibres avoids segregations and balling of the fibres.

The cement content and the water/cement ratio are as decisive as in plain concrete. However, and in contrast to the cement content for SFRC, there is no general recommendation to increase the amount of cement weight used [32]. Such a difference is based on the bendable nature of polyolefin fibre in contrast to the stiffness of the steel fibres that result in a remarkable reduction of the concrete workability.

Regarding the fine/total aggregates relation, although there are no general recommendations it would be advisable to increase such a relation and limit the maximum aggregate size. For SFRC, it is usually accepted that the maximum aggregate size should not surpass $2/3$ of the fibre length (the use of fibres two to five times longer than the maximum aggregate size is frequent) [33, 34]. Such guidelines should be followed and can be considered a valuable rule of thumb given that they enhance workability without affecting the hardened state properties. Moreover, if PFRC is placed by pumping it is recommended (as in the case of SFRC) that the amount of coarse aggregates employed be reduced by 10% [34]. While in the case of a steel fibre addition the possible effects between the proportion of fine aggregates and the fibre content for a given aspect ratio (l/d) have been clearly reported, in the case of polyolefin fibre such relations have not yet been clearly established due to the flexible nature of the fibres [35]. However, the use of between 40 and 60% of fine aggregates seems to be a fair option in obtaining satisfactory results. Above all, it should be noted that these recommendations are considered for fibre volumetric fractions below 2%. Above such values, in all probability the number of fibres added would severely change the fresh-state properties and obtain a heterogeneous distribution of fibres that would lead to a reduction of the properties of the concrete obtained. These precautions should not give the impression of a great modification of the fresh-concrete properties or even of a limited applicability of polyolefin fibres to high-performance concretes, such as high-strength concrete or self-compacting concrete (SCC) [36].

In the case of combining an SCC with an addition of polyolefin fibres, certain changes should be added to the proportions of the concrete constituents. Some design criteria [28, 37] focus on targeting a slump-flow diameter of 600 mm, with a recommended reference mixture being about 700 mm of diameter of the patty without fibres. Such rheology characteristics can be obtained by increasing the amount of cement and/or the proportion of fine aggregates by adding a fine material such as lime powder and using superplasticizer proportions of over 1% of the cement weight. In any case, due to the difficulty of obtaining an SCC, the aforementioned changes should be tested in laboratory preliminary mixes before in situ production. As may be easily understood, such changes in the concrete formulation have a remarkable impact on the final cost of the material. Similar to what happens in the case of a conventional concrete, the slump flow of SCC decreases with the addition of fibres depending on the type of fibre and its geometry. The addition of fibres in all cases alters the results of the fresh-state tests. If an excessive amount of fibres is added, obstruction of the flow and clustering of the fibres and/or aggregates may occur.

The mixing sequence employed for a vibrated conventional concrete (VCC) PFRC starts by carrying out a homogenization of the aggregates. The cement and the other fine components, if used, are then added to the mixer. Later, water and additives are added to the mix. In such

a sense, some of the most common additives are superplasticizer and viscosity modifiers. Once the plain concrete is prepared, fibres are added to the mix and a thorough mixing is carried out in order to obtain a homogeneous distribution of fibres within the fresh concrete. This sequence has been altered on some occasions by adding the fibres directly after the aggregate homogenization with satisfactory results being obtained.

In the case of SCC with an addition of polyolefin fibres, due to the difficulty of obtaining such a type of concrete some changes should be made in the aforementioned procedure for obtaining satisfactory results. It is advised that fibres be added gradually during the mixing process. A third of the fibres should be added after the aggregate homogenization, another after adding the cement and lime powder, and the last one after pouring the water with the additives. It should be noted that the influence that the fibres have on the fresh properties of concrete might require supporting a final addition of superplasticizer to obtain the desired results in the fresh-state tests. Lastly, enough time should be left for the chemical additive to act which would mean that on some occasions the mix should rest for a few minutes in the mixer before emptying. **Figure 5** shows the procedure.

Regarding the placing method, if the mix is properly designed PFRC can be placed by external vibration, pumped or projected to pass through obstacles and with a good performance in hardened state. It is true that compacting FRC might be more difficult to achieve with high fibre contents if at least a descent of 9 cm in the slump test is recommended [28]. On another note, the placing conditions and the formwork geometries clearly affect the final properties of the hardened FRC because they influence the final positioning of the fibres [9]. Therefore, it is important to highlight that VCC and SCC moulds are not usually filled with FRC in the same manner. In such a sense, at the placing stage SCC improves the positioning of fibres in the pouring direction. Conversely, external vibration tends to align the fibres perpendicularly to the direction of vibration. Several test recommendations [38, 39] have fixed the procedure for casting the specimens and filling the moulds. Additionally, the standards establish that in the case of self-compacting concrete the mould should be filled in a single pour and levelled

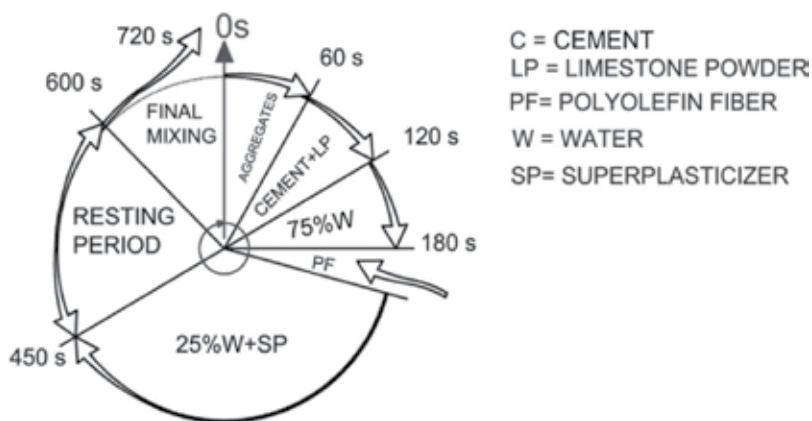


Figure 5. Mixing sequence of a polyolefin fibre-reinforced concrete.

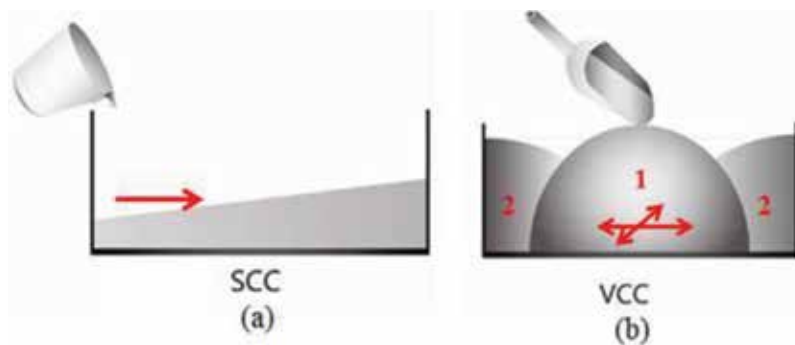


Figure 6. Filling methods for FRC: (a) flow method for SCC; (b) RILEM and EN-14651 Vibrated Concrete [38].

off without any compaction. The capacity of SCC to level itself enables the mould to be filled from one end to the other [30, 40]. **Figure 6** shows the procedures.

Once demoulded, as in the case of a conventional concrete, elements should be properly cured. In the case of laboratory specimens, they should be cured at 20°C and with a relative humidity above 95% until the age of testing.

4. Fresh and hardened concrete properties of polyolefin fibre-reinforced concrete

In the case of a VCC, the fresh-state properties are usually assessed by means of the slump test. It is clear that the presence of fibres hampers a normal behaviour of the material. Although it is true that as the amount of fibres grows, the viscosity of the PFRC increases it cannot be overlooked that the influence of the fibres is reduced when compared with that of steel fibres. In such a sense, it has been found that with an increment of around 15% of the superplasticizer added to the mix, it is possible to maintain at similar values the slump even when adding 10 kg/m³ of polyolefin fibres [41, 28].

Similar to the case of a vibrated conventional concrete, the presence of fibres harms the self-compatibility that SCC has. However, the flexible nature of the polyolefin fibres significantly reduces such a decrease. In the case of an SCC, the fresh-state properties of the concrete are frequently determined by using tests such as the slump-flow test, the L-box test and the V-funnel tests. **Figure 7** shows the influence of the presence of fibres even if an SCC is limited, in both the slump test and the V-funnel test. This phenomenon underlines the versatile nature of polyolefin fibre if compared with rigid steel fibres of any kind. In addition, even in the case of a 10-kg/m³ addition of fibres, no hint of balling was noticed. Moreover, there is evidence that concrete discharged from using polyolefin fibres in ready-mix trucks maintains a regular distribution of fibre along the concrete mass [7].

Compressive and tensile strengths of fibre-reinforced concrete have been thoroughly studied in the last decades with regard to steel and synthetic fibres [42, 43]. Fibres typically enhance

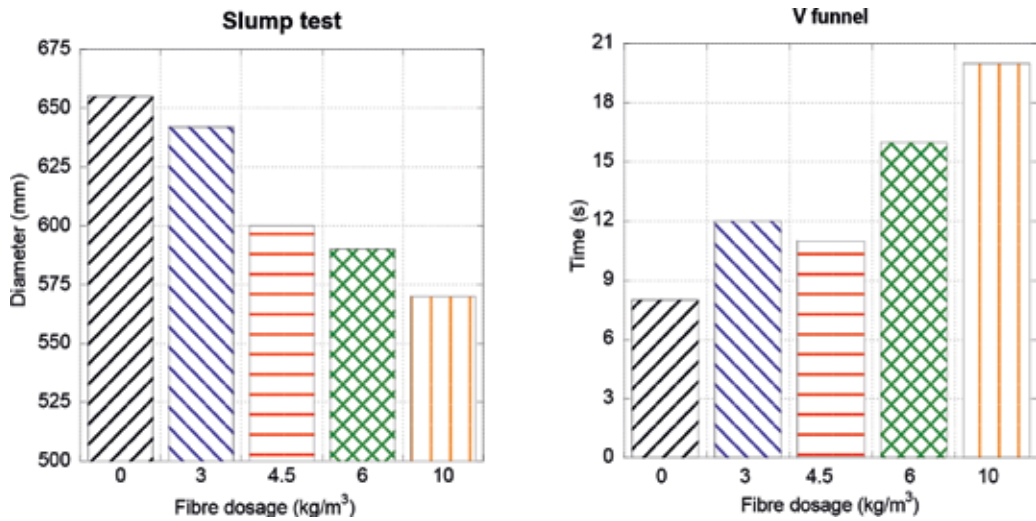


Figure 7. Slump test in an SCC PFRC [28].

the tensile properties of the plain concrete. However, their influence on other mechanical properties is varied depending on the type and shapes of the fibres.

Compressive strength, which is the most representative parameter to characterize concrete, provides essential information. The test is performed in a similar way to that of plain concrete [44]. In a conventional concrete, strength is not significantly affected when regular amounts of fibres are added. Nevertheless, the failure is usually less brittle due to the enhancement of the ductility and toughness provided by the fibres. Even a reduced amount of fibres produces remarkable changes in the failure mode, with it losing scarcely any mass (as **Figure 8** shows).

Nonetheless, it should be pointed out that there seems to be a threshold of volume fraction from which compressive strength is reduced even below values typical of plain concrete. This might have taken place due to a worsening of workability and compaction that causes heterogeneities in the concrete bulk and reduces its mechanical properties.

The mechanical explanation of this change in the failure mode is based on the reduction of lateral deformations above stress values 75% of its compressive strength. Such a change prevents the typical shear bands of plain concrete failure mode from appearing, avoiding the explosive failure of the material without fibres.

In order to assess tensile strength (as is accepted for plain concrete assessments), the indirect tensile-splitting tests—also named Brazilian tests—can be carried out. It should be clarified that in this subsection, tensile properties refer to initial tensile strength assessed by tensile-splitting tests. The residual post-cracking tensile strength is the keystone of the use of structural fibres and deserves a specific subsection focussed on fracture behaviour in tension or under tensile-flexural tests.

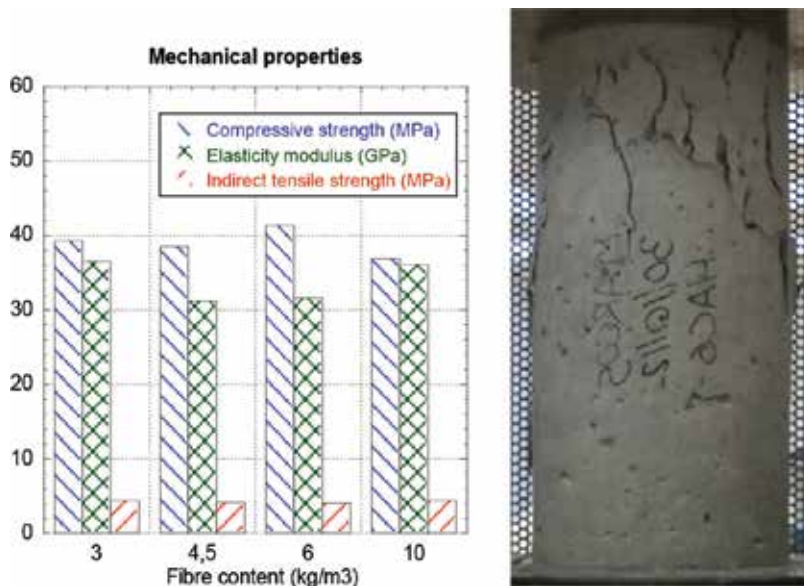


Figure 8. Mechanical properties and compressive strength sample after testing.

The tests and procedures are easy to perform. In the test, a concrete cylinder similar to the type used for compression tests is placed with its axis horizontal and between the platens of a testing machine. When the load is evenly applied along a generatrix, a near-constant tensile stress occurs in the central part of the vertical diameter [45]. The indirect tensile strength is related with the load at the first crack corresponding to peak load for plain concrete with brittle behaviour. However, this type of test is not suitable for assessing the residual strength of the materials provided by the fibres due to second-order effects that add bending stresses to the sample. Even though such second-order effects do not enable accurate residual strength values to be obtained, these indirect tests provide interesting values for the initial tensile strength. As regards the influence of the fibre content in the indirect tensile strength, as in the case of the compressive strength it could be considered that the influence of the fibre volume is negligible if the amount of fibres remains within the regular ranges (as **Figure 8** shows).

Regarding the modulus of elasticity (E) of the composite material, although theoretically its value should be related with the proportions of concrete and fibres, some other parameters have to be considered such as the fibre orientation and fibre length. Even in that case, the influence of the fibres in the modulus of elasticity is not clear as can be seen in **Figure 8**. In some cases, even when adding fibres with higher elasticity modulus than the matrix, a lower value of the composite material has been obtained.

All the features that were mentioned for the case of conventional vibrated concrete are also valid without performing major changes in the case of an SCC.

Another point that is worth considering is the durability of the PFRC when placed in potentially hazardous environments. The capacity of the PFRC to maintain its properties even in

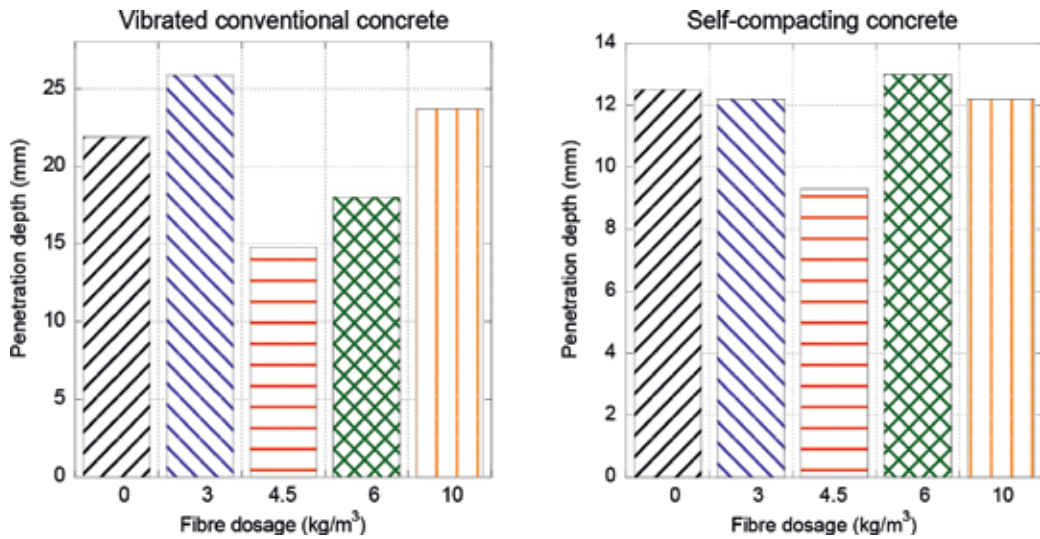


Figure 9. Permeability under pressure of water of VCC and SCC PFRC.

such environments depends on the action of the chemical compounds that ingress in the concrete bulk through the connected network of pores. In that sense, it should be underlined that the presence of fibres might offer preferential ways for such ingress. As can be seen in **Figure 9**, the permeability of the material under pressure of water is uninfluenced by the presence of fibres as there is no dependency of the penetration depth and the fibre content. Therefore, as happens with plain concretes, permeability is related to parameters such as the paste aggregate ratio and the size distribution of the aggregates used. If the type of aggregates and their proportion in the concrete mix are adequate, PFRC may be a material that bears the most hazardous of environments considered in some recommendations [12] such as those in direct contact with marine water, erosive materials, freeze-thaw conditions or even chemical industries.

5. Fracture behaviour and residual load-bearing capacity of polyolefin fibre-reinforced concrete

As previously mentioned, the main reason for adding fibres to a concrete formulation lies in the improvement of the flexural and tensile behaviour of plain concrete. The description of the fracture behaviour of plain concrete has significant differences due to the fibre-reinforcement nature, first and foremost, as regards the post-peak behaviour of the material. The response of concrete-reinforced with polyolefin fibres is conventionally characterized by testing specimens in the mesoscale under direct or flexural tensile stresses.

The uniaxial tension test, as described in several recommendations [30], can be used to determine the tensile strength and the softening parameters and define the stress-crack-opening curve in FRC. The test uses a notched cylindrical specimen with both ends fixed with respect to rotation. It is conducted under controlled tensile displacements. The test setup, as shown in

Figure 10, is rather complex and demands highly trained and experienced personnel. Therefore, as it is somewhat expensive and time-consuming, it is not considered an appropriate method for practical material testing (only being suitable for research purposes in specialized laboratories).

The most economical and practical tests available to determine the post-crack behaviour and assess the influence of conditions such as fibre types and dosage are bending tests. The three-point bending (TPB) test uses beams with a cross section of 150×150 mm and a span of 500 mm loaded in the middle of the upper face. A transverse notch of standard dimensions is made in the middle of the lower specimen face, in the same cross section where the load is applied. This setup, as shown in **Figure 11**, ensures that the crack is formed in this predefined position, making crack control simpler than in un-notched beams [30, 39].

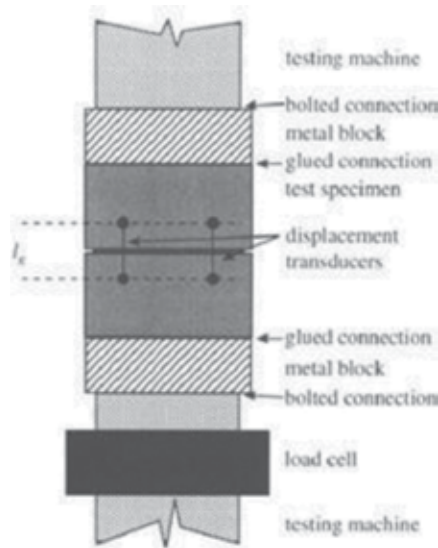


Figure 10. Uni-axial tension testing for concrete [30].

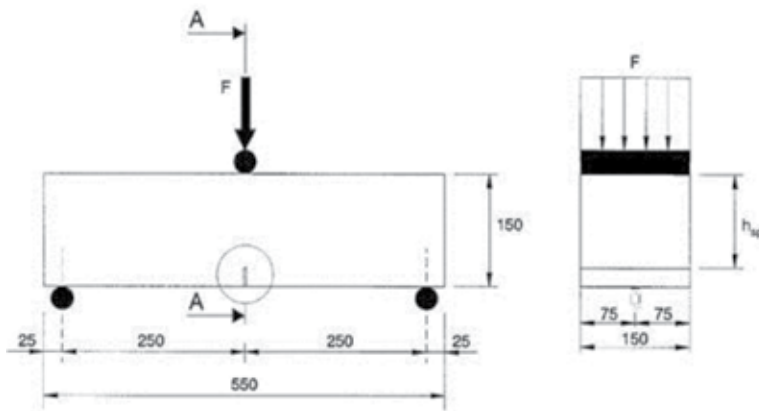


Figure 11. Test set-up in [38]. Measures in mm.

Four-point bending tests have also been adopted by some country national recommendations. The cross section of 150×150 mm has two equal loads applied in both sides of the middle third of the span [41, 45]. A typical setup is shown in **Figure 12**. The advantage of the four-point un-notched test is that the first crack will appear at the weakest section, therefore providing for the effect of a variation of material strength. The disadvantage is that the measuring of the crack opening is harder because the crack position cannot be predicted. Therefore, obtaining a complete characterization of the material is not always possible.

Regardless of the testing method employed, the curves obtained show the enhancement of the mechanical properties provided by the fibres. Furthermore, the behaviour or the composite material could be examined by taking into account the main effects regarding the plain concrete behaviour added to the contribution of the fibre reinforcement. Such a contribution depends on the crack opening and appears in the form of fibre bridging, fibre debonding and even fibre tensile failure. A theoretical scheme can be seen in **Figure 13**.

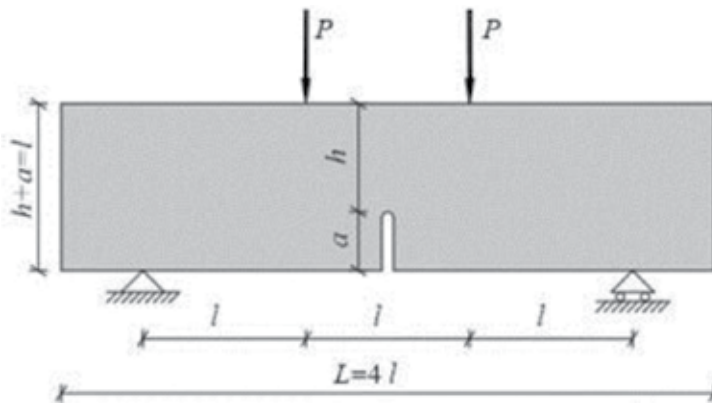


Figure 12. Four-point bending test [38, 46].

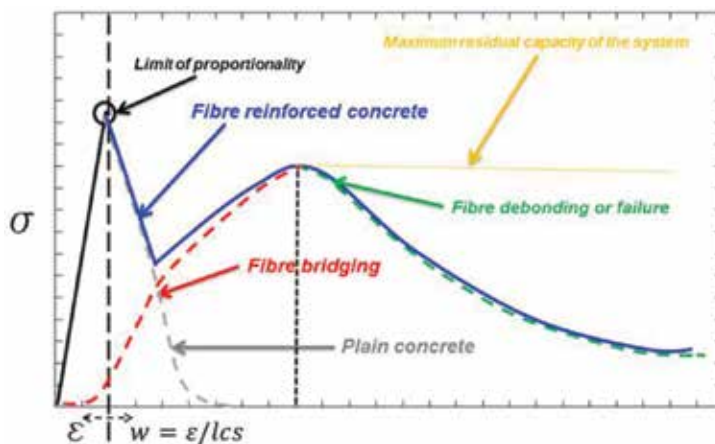


Figure 13. Conceptual bases of the discrete entities contribution to FRC constitutive relation [28].

Evidently, there are certain characteristics of the curves shown in **Figure 13** that depend not only on the amount of fibres used but also on the geometrical and mechanical properties of the fibres, the orientation and distribution of the fibres within the concrete element, the fresh properties of the concrete, the pouring process and, among others, the consolidation method. It is worth noting that predictive models and tools to consider such differences can be consulted in detail in references [28] and [47]. In any case, the main factor is the amount of fibres added. **Figure 14** shows how the amount of fibres changes the post-peak mechanical behaviour of PFRC.

The curves depicted in **Figure 14** have several common characteristics that should be mentioned. The behaviour of each curve is defined by the presence of three turning points. The first turning point took place when the loading process reached the maximum value and only a few inelastic processes were apparent (the behaviour of concrete is mostly linear if compared with subsequent stages). The turning point where the load reaches the maximum is commonly known as the load at the limit of proportionality (L_{LOP}), with it being the overall maximum load in plain concrete. A softening behaviour may also be

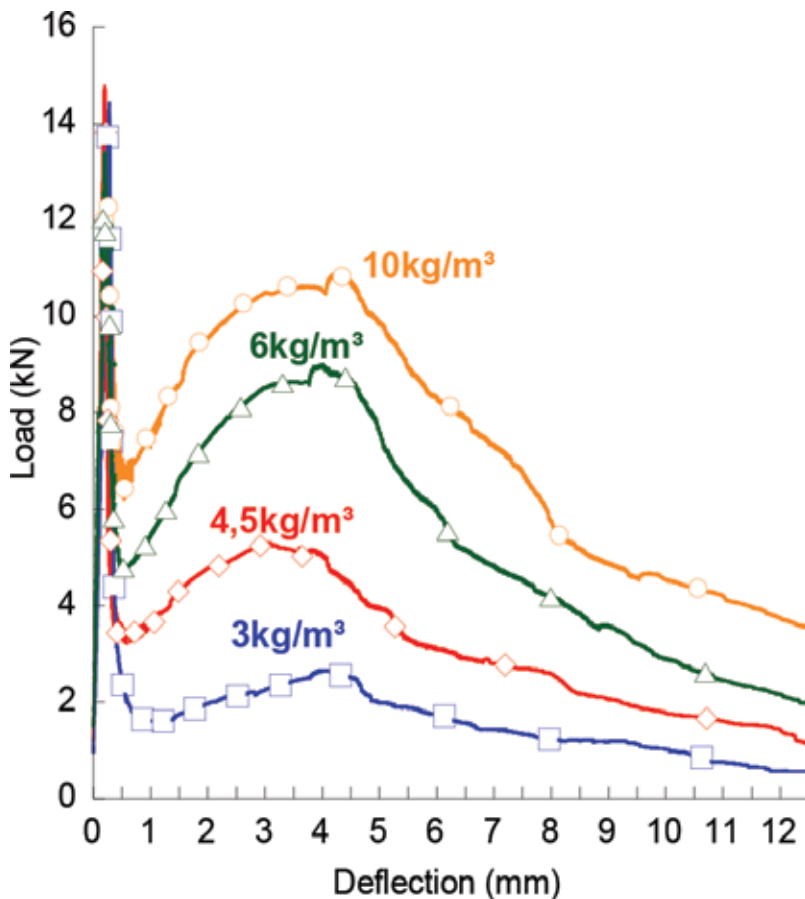


Figure 14. Fracture behaviour of PFRC with several amounts of fibres.

identified that governs the branch after L_{LOP} as reported in many FRC types and especially for PFRC [3]. The softening behaviour is a distinctive characteristic in plain concrete fracture and, in such a case a steep unloading process leads to the specimen failure and collapse. Nonetheless, the polyolefin fibres are able to absorb the energy released by the concrete in the fracture processes by the so-called fibre bridging and change the loading tendency. At such a point, the curve reaches the minimum post-cracking load (L_{MIN}) while another uploading process starts again. The end of the load-increasing ramp is the third remarkable point of the curve. The descending slope drawn after L_{REM} continues until the end of the test. It should be noted that even at great deformation states, PFRC does not fail or collapse and that it shows remarkable improvements in ductility and toughness with respect to plain concrete.

Based on the previous description, it is easier to perceive the influence that the changes have on the behaviour that can appear when varying the amounts of polyolefin fibres added. The amount of fibres has a negligible influence on the peak load recorded in the fracture tests, and therefore L_{LOP} does not change with fibre dosage. The value of L_{LOP} is mainly determined by the tensile strength of the plain concrete. After reaching the peak load, the unloading part of the curve appears and such a part ends at L_{MIN} that is related with the amount of fibres added. The higher volumetric fraction of fibres the greater is the value of L_{MIN} obtained. It should be highlighted that, in contrast with the behaviour of an SFRC, even with volumetric fractions around 1% the value of L_{MIN} greatly differs from L_{LOP} . The slope of the curve between L_{MIN} and L_{REM} is greater as the amount of fibres added increases. In this case, it is important to note that the deflection value where L_{MIN} takes place does not depend remarkably on the dosage of fibres. Nevertheless, the maximum post-peak value L_{REM} is greatly modified by the amount of fibres added.

The number of fibres present in the fracture surface generated during the tests greatly influences the values of L_{MIN} and L_{REM} alike. However, not all the fibres that appear in the fracture surface influence the value of L_{MIN} . Due to the limited deformation state that the sample is bearing when L_{MIN} occurs, which is commonly used for service limit state (SLS) design, the contribution of fibres placed in the tensioned part of the section is more important than the rest of fibres. This corresponds to the lower third of the fracture surface generated. For high deformations, almost the whole cross section is in tension and, due to the quasi-brittle nature of the material, would already be almost fully cracked. Therefore, the total number of fibres would bear the final load obtained in the tests. These advanced deformations would correspond to ultimate limit state design (ULS). The situations that take place in the case of SLS and ULS are shown in **Figure 15**.

In order to relate the presence and distribution of fibres to the mechanical behaviour of the material, the values of L_{MIN} and L_{REM} versus the amount of fibres in the lower third of the fracture surface and the total amount of fibres in the fracture surface are plotted in **Figure 16**. This figure shows that there is a linear relation between the presence of fibres both in the lower third and the complete fracture surface with the values of L_{MIN} and L_{REM} in both conventional and self-compacting PFRC. It is also worth noting that the presence of fibres in the fracture surfaces does not correspond directly to the amount of fibres added. In such a sense, it should be noted that in not all cases higher dosages of fibres result in a greater number of

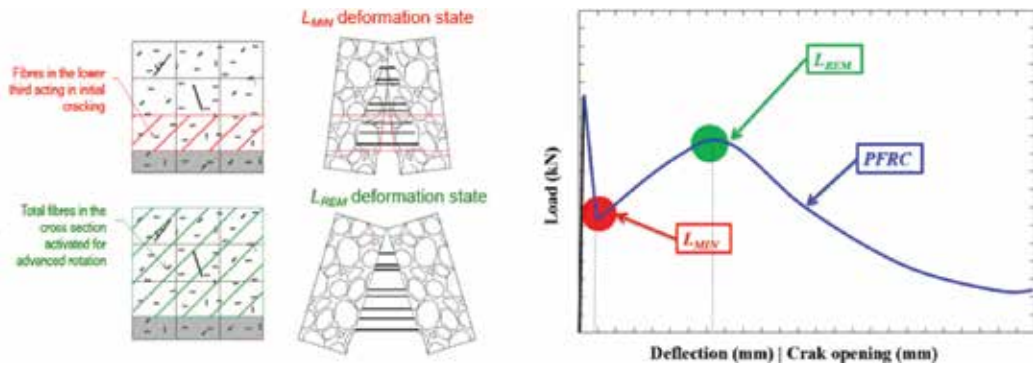


Figure 15. Deformation states of SLS or ULS.

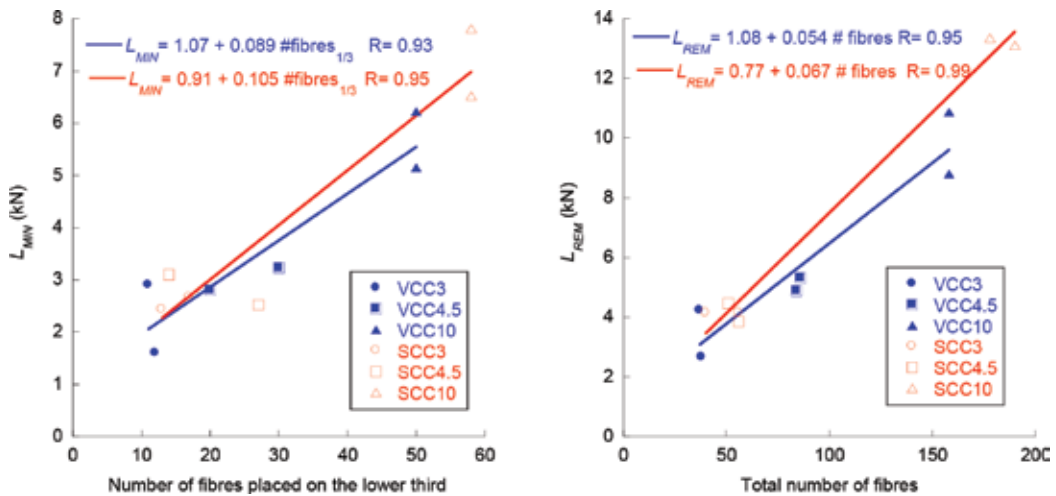


Figure 16. Relation between the number of fibres present in the fracture surfaces and the residual loads L_{MIN} and L_{REM} for vibrated conventional PFRC (VCC) and self-compacting PFRC (SCC). Tests performed following EN-14651 in reference [5].

fibres present in the fracture surfaces. Therefore, there are certain variations in the mechanical properties of the material that rely on other parameters unrelated with the amount of fibres added, such as the material rheology, pouring method and, among others, size of the element manufactured.

6. PFRC properties and their relation with the standards and recommendations

In previous sections, the improvement of properties provided by the fibres in PFRC has been shown. In order to take advantage of these benefits in the structural design of concrete

elements, the mechanical properties of PFRC should fulfil certain requirements established in several standards and recommendations. Conventionally, as the most widespread structural fibres have been steel fibres almost all regulations have considered some of the requirements and borne in mind the properties of SFRC. However, if the fracture behaviours of SFRC and PFRC are compared, it can be noted that there are certain differences that should be underlined. If the fracture behaviours of a certain SFRC and PFRC are sketched as they are in **Figure 17**, such differences are perceived. As regards the peak load, there are no remarkable differences because this value both in SFRC and in PFRC is directly related with the properties of the bulk concrete due to the low volume fractions of fibres used. Nevertheless, once the unloading process that takes place after reaching the peak load starts, the first differences appear. Where SFRC is concerned, the decrement of the load-bearing capacity of the material is more reduced than in the case of the PFRC. This phenomenon appears even in the case of using high dosages of polyolefin fibres, which might be related, with the comparatively lower modulus of elasticity of these fibres if compared with steel fibres. Another difference that can be perceived is that the maximum post-peak load in the case of a PFRC takes place at higher deformation states than in the case of SFRC. Moreover, when L_{REM} is reached, the final unloading branch of SFRC will have been progressing for a while. Taking into account the aforementioned characteristics, it can be stated that for limited deformation states, such as those that correspond to SLS, SFRC might be more suitable than PFRC. On the contrary, if ULS is considered, then the most suitable option would be PFRC.

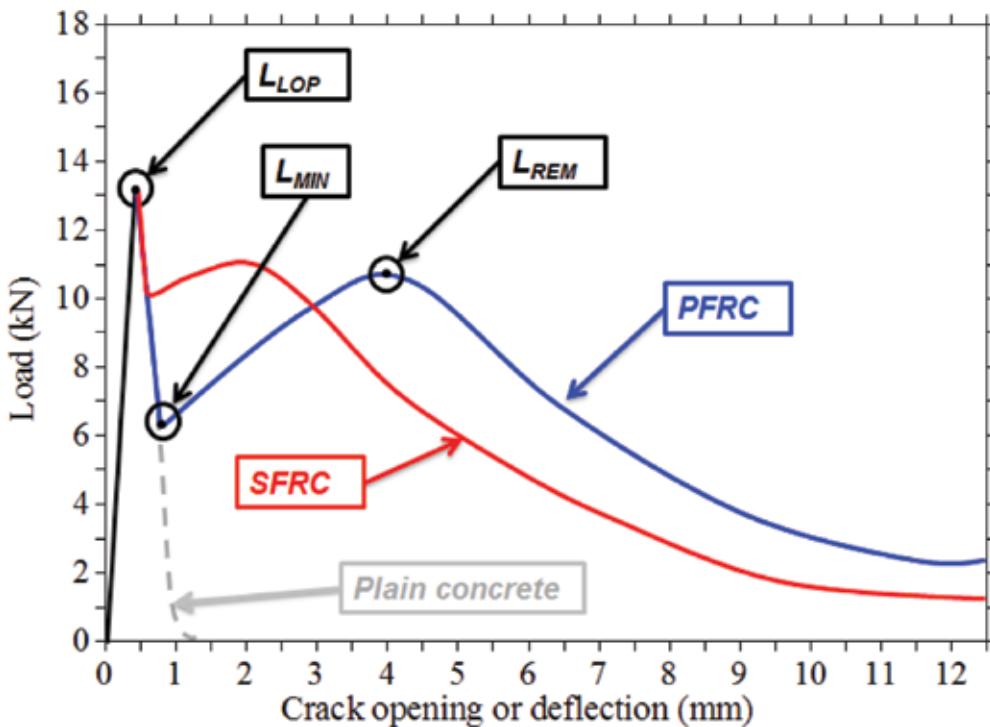



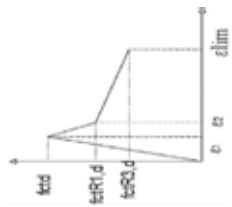

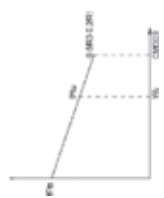
Figure 17. Schematic shape of the typical load-deflection curve obtained in a fracture test of PFRC compared with SFRC.

In any case and in order to supply structural requirements to design engineers, some national codes have offered several tests and guidelines. In 1992, the German Code [40, 45] proposed a σ - ε relationship for the structural design of tunnel linings that use steel fibres in concrete. In the last 15 years, many European countries, as well as Japan and the United States, have published codes and guidelines that allow the practical design of structures by considering fracture mechanics concepts aimed at taking into account the post-cracking residual strength under tension stress. Responding to their own internal demands, Germany [46], Italy [41] and Spain [12] have produced and even revised their codes and design guidelines. A complete review of the European codes can be seen in [11, 48, 49]. A summary of the types of tests and requirements can be seen in **Table 2**. At the time of writing, CEB-FIB Model Code 2010, MC2010 [50] is considered as a reference for newer revisions of Eurocode 2 and the guidelines of various European nation-states. Model Code 2010 establishes a material classification based on the results obtained by the earlier mentioned three-point bending tests as per EN 14651 [38] or [39, 51]. Model Code considers that the contribution of the fibres can be considered in the structural design if the following conditions are met. The value of the load at a crack mouth-opening displacement (CMOD) of 0.5 mm should be greater than 40% of the peak load, and when a CMOD reaches 2.5 mm the value of the load should be at least 20% of the peak load. Those values in terms of strength are known as f_{R1} and f_{R3} at 0.5 and 2.5 mm of CMOD, as can be better understood by consulting **Figure 18**. The first requirement is set for avoiding brittle failures of the structure and the second one seeks to set a minimum contribution of the fibres to the ultimate failure of the concrete element.

Although in some cases the requirements set by the standards are based on load values, in some others it is necessary to transform the load obtained from the fracture tests performed into residual strength values. This task can be accomplished in accordance with EHE-08 [12] and the Model Code [50] by Eq. (1) that transforms load values into strength, with L being the distance between the supporting cylinders, f_j the force registered by the load cell, b the width of the sample and h_{sp} the length of the ligament, is as follows:

$$f_{ct,j} = \frac{3}{2} \frac{f_j L}{b h_{sp}} \quad (1)$$

When comparing **Figure 18** with **Figures 14** and **17**, the shapes of the curves are remarkably different. The fracture curves obtained in the PFRC of material after reaching the minimum post-peak load value (L_{MIN}) are capable of sustaining higher loads and reaching a maximum post-peak value (L_{REM}). As previously mentioned, structural requirements are related to the most representative residual strengths f_{R1} and f_{R3} at crack openings of 0.5 and 2.5 mm. Consequently, the brittleness limitation stated by the strength value at f_{R1} might be of relative significance when these regulations are used to assess the performance of PFRC. However, the analysis of **Table 3** reveals that an SCC and a VCC with 10 kg/m³ of fibres (VCC10 and SCC10) met the aforementioned requirements. By contrast, when a VCC or an SCC with 6 or 4.5 kg/m³ (VCC6, SCC6, VCC4.5 and SCC4.5) was studied, although it is clear that these mixes did not fulfil the requirements, such mixes were able to avoid brittleness. The latter is shown by the increment of the load that takes place in all mixes, after reaching L_{MIN} . Regarding a PFRC with 3 kg/m³ of fibres (VCC4.5 and SCC3), although brittleness is avoided due to the

Test	Standard	Parameters	Constitutive models for structural design
Three point bending	EHE	f_{R1}, f_{R3}, f_L	<p>Rectangular</p>  <p> $f_{ctR,d} = 0.33 f_{R3,d}$ $\epsilon_{lim} = 20\%$ (flexural) $\epsilon_{lim} = 10\%$ (tensile) </p>
			<p>Trilinear</p>  <p> $f_{ct,d} = 0.6 f_{ctR1,d}$ $f_{ctR1,d} = 0.45 f_{R1,d}$ $f_{ctR3,d} = k (0.5 f_{R3,d} - 0.2 f_{R1,d})$, con $k=1$ (flexural) ò $k=0.7$ (tensile) $\epsilon_1 = 0,1 + 1000 \cdot f_{ct,d} / E_{c0}$ $\epsilon_2 = 2,5 / \epsilon_{cs}$ $\epsilon_{lim} = 20\%$ (flexural) ò 10% (tensile) </p>
	FIB model code	$f_{R1}, f_{R3}, f_{Fu}, f_{Fs}$	<p>Rigid-Plàstic</p>  <p> $f_{Fu} = \frac{f_{R3}}{3}$ $\epsilon 1 = \epsilon_{lim} = 10\%$ hardening; 20% softening </p>
			<p>Lineal</p>  <p> $f_{Fu} = 0.45 f_{R1}$ $f_{Fu} = f_{Fs} \frac{WU}{CMOD3} (f_{Fs} - 0.5 f_{R3} + 0.2 f_{R1})$ $\epsilon_{EHL} = CMOD1 / l_{cs}$; $\epsilon_{S1,U} = WU / l_{cs} = \min(\epsilon_{Fu}, 2.5 / l_{cs}, 2.5 / Y)$; $\epsilon_{Fu} = 10\%$ end; 20% ablan $f_{R1} / f_{R3} / f_{R1} (CMOD=0.5) \geq 1.5$ MPa $f_{R1} (CMOD=3.5 \text{ mm}) \geq 1$ MPa </p>

UNE 14889





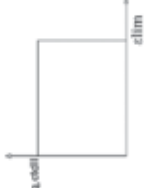
Test	Standard	Parameters	Constitutive models for structural design
Four point bending	CNR-DT204	$f_{Ftu}, f_{Ftu}, f_{eq1}, f_{eq2}$	<p>Lineal-Elastic</p>  $f_{Fts} = 0.45 \cdot f_{eq1}$ $f_{Ftu} = k \left[f_{Fts} - \frac{Wu}{WZ} \cdot (Fts - 0.5 f_{eq2} + 0.2 f_{eq1}) \right]$ $k = 1 \text{ (flexural) } \text{ or } k = 0.7 \text{ (tensile)}$ $\epsilon_2 = \epsilon_u \text{ (20\% softening; 10\% hardening)}$ $f_{Ftu} = \frac{f_{eq2}}{3}$ $\epsilon 1 = \epsilon_{lim} = 10\% \text{ hardening; 20\% softening}$
			<p>Rigid-PLASTIC</p> 
	DBV	$f_{ctb,II}, f_{eq,ctb,I}, f_{eq,ctb,II}$	<p>Trilineal</p>  $\sigma_1 = f_{ctd} = \alpha'_c \cdot f_{ctb,II} / \gamma'_{ct}$ $\sigma_2 = f_{eq,ctd,I} = \alpha'_c \cdot \alpha'_c / \gamma'_{ct}$ $\sigma_3 = f_{eq,ctd,II} = \alpha'_c \cdot \alpha'_c / \gamma'_{ct} \leq f_{eq,ctd,I}$ $\epsilon 1 = \sigma_1 / E_{HRF}; \epsilon 2 = \epsilon 1 + 0.1\%; \epsilon 3 = \epsilon u = 25\%$
			<p>Bilinear</p>  $\sigma_1 = f_{eq,ctd,I} = \alpha'_c \cdot \alpha'_c / \gamma'_{ct}$ $\sigma_2 = f_{eq,ctd,II} = \alpha'_c \cdot \alpha'_c / \gamma'_{ct} \leq f_{eq,ctd,I}$ $\epsilon u = \epsilon 2 = 10\%$
			<p>Rectangular</p>  $\sigma_1 = f_{eq,ctd,II} = f_{eq,ctb,II} \cdot \alpha'_c / \gamma'_{ct} \leq f_{eq,ctd,I}$ $\epsilon 1 = \epsilon u = 10\%$

Table 2. Comparison of some of the recommendations and standards.

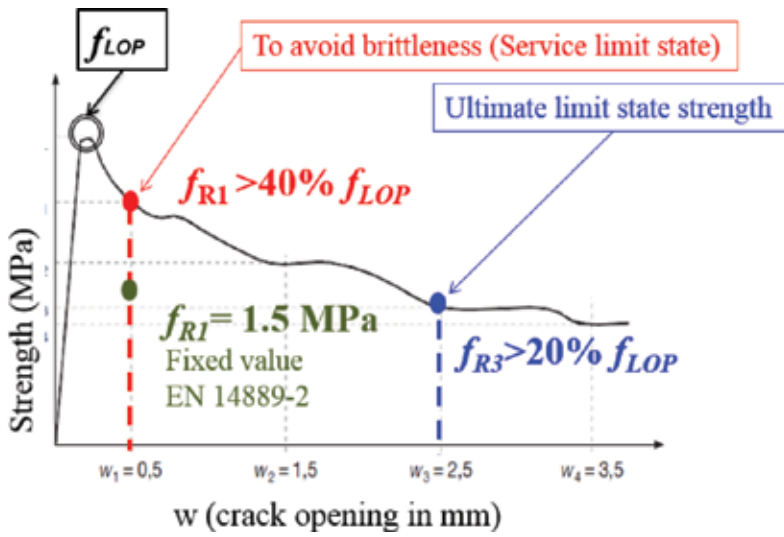


Figure 18. Load-CMOD curve of a FRC as stated in [12] with structural requirements.

	f_{LOP} (MPa)	f_{R1} (MPa)	$\% f_{LOP}$	f_{R3} (MPa)	$\% f_{LOP}$
VCC3	4.81	0.93	19%	0.96	20%
SCC3	5.21	0.93	19%	1.15	22%
VCC4.5	4.74	1.06	22%	1.40	29%
SCC4.5	5.23	0.95	18%	1.25	24%
VCC6	4.41	1.57	36%	2.38	54%
SCC6	5.09	1.39	27%	2.03	40%
VCC10	4.21	1.98	47%	2.87	68%
SCC10	5.22	2.41	46%	3.87	74%

Table 3. Residual strength of concrete.

increment of load that the material can bear at f_{R3} , there is only a 10% improvement of the strength between f_{R1} and f_{R3} . A wider view and detailed results with additional tools to consider fibre positioning as a function of the influencing parameters can be seen in Ref. [28].

Acknowledgements

The authors gratefully acknowledge the financial support provided by the Ministry of Economy and Competitiveness of Spain by means of the Research Fund Project BIA 2016-78742-C2-2-R. They also offer their gratitude to SIKA SAU for supporting the Enterprise University Chair: Cátedra Sika-UPM.

Author details

Marcos G. Alberti, Alejandro Enfedaque and Jaime C. Gálvez*

*Address all correspondence to: jaime.galvez@upm.es

Civil Engineering Department, Construction, E.T.S de Ingenieros de Caminos, Canales y Puertos, Technical University of Madrid, Madrid, Spain

References

- [1] Ugbolue SC. Polyolefin Fibres: Industrial and Medical Applications. CRC Press; 2009
- [2] McIntyre JE. Synthetic Fibres: Nylon, Polyester, Acrylic, Polyolefin. Elsevier; 2004
- [3] Alberti MG, Enfedaque A, Gálvez JC, Agrawal V. Reliability of polyolefin fibre reinforced concrete beyond laboratory sizes and construction procedures. *Composite Structures*. 15 April 2016;**140**:506-524. ISSN 0263-8223. DOI: <http://dx.doi.org/10.1016/j.compstruct.2015.12.068>
- [4] Alberti MG, Enfedaque A, Gálvez JC. On the mechanical properties and fracture behavior of polyolefin fiber-reinforced self-compacting concrete. *Construction and Building Materials*. 31 March 2014;**55**:274-288. ISSN 0950-0618. DOI: <http://dx.doi.org/10.1016/j.conbuildmat.2014.01.024>
- [5] Alberti MG, Enfedaque A, Gálvez JC. Comparison between polyolefin fibre reinforced vibrated conventional concrete and self-compacting concrete. *Construction and Building Materials*. 15 June 2015;**85**:182-194. ISSN 0950-0618. DOI: <http://dx.doi.org/10.1016/j.conbuildmat.2015.03.007>
- [6] Alberti MG, Enfedaque A, Gálvez JC. Fracture mechanics of polyolefin fibre reinforced concrete: Study of the influence of the concrete properties, casting procedures, the fibre length and specimen size. *Engineering Fracture Mechanics*. March 2016;**154**:225-244. ISSN 0013-7944. DOI: <http://dx.doi.org/10.1016/j.engfracmech.2015.12.032>
- [7] Sorensen C, Berge E, Nikolaisen EB. Investigation of fiber distribution in concrete batches discharged from ready-mix truck. *International Journal of Concrete Structures and Materials*. 2014;**8**(4):279-287
- [8] Alberti MG, Enfedaque A, Gálvez JC, Ferreras A. Pull-out behaviour and interface critical parameters of polyolefin fibres embedded in mortar and self-compacting concrete matrixes. *Construction and Building Materials*. 2016;**112**:607-622. ISSN 0950-0618
- [9] Torrijos MC, Barragán BE, Zerbino RL. Placing conditions, mesostructural characteristics and post-cracking response of fibre reinforced self-compacting concretes. *Construction and Building Materials*. 2010;**24**(6):1078-1085

- [10] Alberti MG, Enfedaque A, Gálvez JC, Agrawal V. Fibre distribution and orientation of macro-synthetic polyolefin fibre reinforced concrete elements. *Construction and Building Materials*. 30 September 2016;**122**:505-517. ISSN 0950-0618. DOI: <http://dx.doi.org/10.1016/j.conbuildmat.2016.06.083>
- [11] Di Prisco M, Colombo M, Dozio D. Fibre-reinforced concrete in fib Model Code 2010: Principles, models and test validation. *Structural Concrete*. 2013;**14**(4):342-361
- [12] EHE-08. Spanish Structural Concrete Code. Spanish Minister of Public Works; 2008
- [13] EN 14889-2. Fibres for Concrete. Polymer Fibres. Definitions, Specifications and Conformity; 2008
- [14] Bentur A, Mindess S. *Fibre Reinforced Cementitious Composites*. Taylor & Francis; 2006
- [15] Ochi T, Okubo S, Fukui K. Development of recycled PET fiber and its application as concrete-reinforcing fiber. *Cement and Concrete Composites*. 2007;**29**(6):448-455
- [16] Silva DA, Betioli AM, Gleize PJP, Roman HR, Gomez LA, Ribeiro JLD. Degradation of recycled PET fibers in Portland cement-based materials. *Cement and Concrete Research*. 2005;**35**(9):1741-1746
- [17] EPC. Advanced alkalinity testing. *Elasto Plastic Concrete*; 2012, www.elastoplastic.com
- [18] Santos ASF, Teixeira BAN, Agnelli JAM, Manrich S. Characterization of effluents through a typical plastic recycling process: An evaluation of cleaning performance and environmental pollution. *Resources, Conservation and Recycling*. 2005;**45**(2):159-171
- [19] Yin S, Tuladhar R, Combe M, Collister T, Jacob M, Shanks R. Mechanical properties of recycled plastic fibres for reinforcing concrete. In: *Proceedings of the 7th international conference fibre concrete, From: 7th International Conference Fibre Concrete, September 12-13, 2013, Prague, Czech Technical University, Prague. Czech Republic; 2013*. pp. 1-10
- [20] Akers S, Kaufmann J, Lübben J, Schwitter E. Reinforcement of concrete and shotcrete using bi-component polyolefin fibres. In: *Concrete Solutions 2009 Conference, Sydney; Concrete Institute of Australia, 2009*
- [21] Kaufmann J, Lübben J, Schwitter E. Mechanical reinforcement of concrete with bi-component fibers. *Composites Part A: Applied Science And Manufacturing*. 2007;**38**(9): 1975-1984
- [22] Yan L, Pendleton RL, Jenkins CH. Interface morphologies in polyolefin fiber reinforced concrete composites. *Composites Part A: Applied Science and Manufacturing. Cement and Concrete Research*. 1998;**29**(5-6):643-650
- [23] Wang Y, Backer S, Li VC. An experimental study of synthetic fibre reinforced cementitious composites. *Journal of Materials Science*. 1987;**22**(12):4281-4291
- [24] Li VC, Wang, Y., & Backer, S. (1990). Effect of inclining angle, bundling and surface treatment on synthetic fibre pull-out from a cement matrix. *Composites*. **21**(2):132-140.

- [25] Won JP, Lim DH, Park CG. Bond behaviour and flexural performance of structural synthetic fibre-reinforced concrete. *Magazine of Concrete Research*. 2006;**58**(6):401-410
- [26] Trottier BY, Mahoney M, Forgeron D. Can synthetic fibers replace in slabs-on-ground? *Concrete International*. 2002;**24**(11):59-68
- [27] Naaman AE. Engineered steel fibers with optimal properties for reinforcement of cement composites. *Journal of Advanced Concrete Technology*. 2003;**1**(3):241-252
- [28] Alberti MG. Polyolefin fiber-reinforced concrete: From material behavior to numerical and design considerations [Doctoral dissertation, Ph. D. Thesis]. Madrid, Spain: Technical University Madrid; 2015
- [29] Zollo R. Fiber-reinforced concrete: an overview after 30 years of development. *Cement & Concrete Composites*. 1997;**19**:107-122
- [30] Døssland ÅL. Fibre reinforcement in load carrying concrete structures [Doctoral dissertation, PhD thesis]. The Norwegian Institute of Technology; 2008
- [31] Mindess S, Young J, Darwin D. *Concrete*. 2nd ed. Upper Saddle River, NJ: Pearson Education; 2003
- [32] Kooiman AG. *Modelling Steel Fibre Reinforced Concrete for Structural Design*. Delft, The Netherlands: TU Delft, Delft University of Technology; 2000
- [33] Johnston D. Proportioning, mixing and placement of fibre-reinforced cements and concretes. In: Bartos MA, editor. *Production Methods and Workability of Concrete*. London: E & FN Spon; 1996
- [34] Grünewald S. *Performance-based design of self-compacting fibre reinforced concrete*. Delft, The Netherlands: Delft University Press; 2004
- [35] Martinie L, Rossi P, Roussel N. Rheology of fiber reinforced cementitious materials: Classification and prediction. *Cement and Concrete Research*. 2010;**40**(2):226-234
- [36] Yang J-M, Min K-H, Shin H-O, Yoon Y-S. Effect of steel and synthetic fibers on flexural behavior of high-strength concrete beams reinforced with FRP bars. *Composites Part B: Engineering*. April 2012;**43**(3):1077-1086. ISSN 1359-8368. DOI: <http://dx.doi.org/10.1016/j.compositesb.2012.01.044>
- [37] Grünewald S, Walraven JC. Rheological measurements on self-compacting fibre reinforced concrete. In: PRO 33: 3rd International RILEM Symposium on Self-Compacting Concrete. RILEM Publications; 2003. pp. 49-58
- [38] EN 14651:2007+A1. Test Method for Metallic Fibre Concrete. Measuring the Flexural Tensile Strength (limit of proportionality (LOP), residual); European Committee for Standardization (CEN), Brussels. 2007
- [39] RILEM TC162-TDF. Test and design methods for steel fibre reinforced concrete: Bending test (final recommendation). *Materials and Structures*. 2002;**35**:579-582

- [40] Grünewald S. 9 - Fibre reinforcement and the rheology of concrete. In: Roussel N, editor. *Understanding the Rheology of Concrete*. Woodhead Publishing Series in Civil and Structural Engineering. Woodhead Publishing; 2012. pp. 229-256. ISBN 9780857090287
- [41] CNR-DT 204. *Guide for the design and construction of fiber-reinforced concrete structures*. Rome: Consiglio Nazionale delle Ricerche; 2006
- [42] Song PS, Hwang S, Sheu BC. Strength properties of nylon- and polypropylene-fiber-reinforced concretes. *Cement and Concrete Research*. 2005;**35**(8):1546-1550
- [43] Wafa FF, Ashour SA. Mechanical properties of high-strength fiber reinforced concrete. *ACI Materials Journal*. 1992;**89**(5):449-455
- [44] EN 12390-3. *Testing Hardened Concrete. Part 3: Compressive Strength of Test Specimens*; European Committee for Standardization (CEN), Brussels. 2009
- [45] EN 12390-6. *Testing Hardened Concrete. Part 6. Tensile Splitting Strength of Test Specimens*; European Committee for Standardization (CEN), Brussels. 2009
- [46] DBV. *Merkblatt Stahlfaserbeton*, Deutsche Beton Vereins, 2001
- [47] Alberti MG, Enfedaque A, Gálvez JC. On the prediction of the orientation factor and fibre distribution of steel and macro-synthetic fibres for fibre-reinforced concrete. *Cement and Concrete Composites*. 2016;**77**:29-48, 2017
- [48] Blanco A, Pujadas P, de la Fuente A, Cavalaro S, Aguado A. Application of constitutive models in European codes to RC-FRC. *Construction and Building Materials*. 2013;**40**:246-259
- [49] Di Prisco M, Plizzari G, Vandewalle L. Fiber reinforced concrete: New design perspective. *Materials and Structures*. 2009;**42**:1261-1281
- [50] fib Model Code. *Model Code*. Paris: Fédération Internationale du Béton fib/International Federation for Structural Concrete; 2010
- [51] ASTM C 1609/C 1690M-07. *Standard Test Method for Flexural Performance of Fiber Reinforced Concrete (using beam with third-point loading)*. 2007. pp. 1-8

Edited by Reza Davarnejad and Baharak Sajjadi

In organic chemistry, Alkenes, also known as olefins, are the unsaturated hydrocarbons with the general formula of C_nH_{2n} that contains one or more carbon-carbon double bonds in their chemical structures ($RC=CR'$). The presence of this double bond allows alkenes to react in ways that alkanes cannot. Hence, alkenes find many diverse applications in industry. These compounds are widely used as initial materials in the synthesis of alcohols, plastics, lacquers, detergents, and fuels. The current book includes all knowledge and novel data according to the structure of alkenes, their novel synthesis methods, and their applications. In addition, manufacture, properties, and the use of polyalkenes are the other important topics that are covered in this book. These data are collected by the efforts and contributions of many authors and scientists from all over the globe, and all of us are ready to further improve the contents of this book as per the readers' comments.

Photo by StationaryTraveller / iStock

IntechOpen

